

Second-Order Effects in Reinforced Concrete Columns Exposed to Fire

Tweede-orde-effecten in gewapendbetonkolommen blootgesteld aan brand

Lijie Wang

Promotoren: prof. dr. ir. L. Taerwe, prof. dr. ir. R. Caspeele
Proefschrift ingediend tot het behalen van de graad van
Doctor in de ingenieurswetenschappen: bouwkunde



UNIVERSITEIT
GENT

Vakgroep Bouwkundige Constructies
Voorzitter: prof. dr. ir. L. Taerwe
Faculteit Ingenieurswetenschappen en Architectuur
Academiejaar 2016 - 2017

ISBN 978-90-8578-988-8

NUR 955, 956

Wettelijk depot: D/2017/10.500/23

Supervisor

Prof. dr. ir. Luc Taerwe

EA14, UGent, Belgium

Prof. dr. ir. Robby Caspeele

EA14, UGent, Belgium

Examination committee

Prof. dr. ir. Patrick De Baets

EA08, UGent, Belgium

(chairman)

Prof. dr. ir. Geert De Schutter

EA14, UGent, Belgium

(secretary)

Prof. dr. ir. Luc Taerwe

EA14, UGent, Belgium

(supervisor)

Prof. dr. ir. Robby Caspeele

EA14, UGent, Belgium

(supervisor)

Prof. dr. ir. Bart Merci

EA03, UGent, Belgium

Prof. dr. ir. Joost Walraven

TU Delft, The Netherlands

**Prof. dr. ir. -arch. Emmanuel
Annerel**

EA14, UGent, Belgium

Dr. ir. Thomas Gernay
Université de Liège, Belgium

Dr. ir. Ruben Van Coile

The University of Edinburgh, UK

Research institute

Ghent University, Department of Structural Engineering

Magnel Laboratory for Concrete Research

Technologiepark-Zwijnaarde 904, B-9052 Ghent, Belgium

This research was supported through the CSC (China Scholarship Council)

Research Foundation.



Copyright © Lijie Wang 2017

All rights reserved. No part of this publication may be reproduced, stored in a retrieval system or transmitted in any form or by any means electronic, mechanical, photocopying, recording or otherwise, without the prior written permission of the author and his supervisor.

ACKNOWLEDGEMENTS

This research was performed in the Magnel Lab of Ghent University and with the financial support of CSC (China Scholarship Council), so the support of Ghent University and the CSC is gratefully acknowledged and appreciated.

First of all, I would like to give my sincerely thanks to my supervisors prof. Luc Taerwe and prof. Robby Caspeele. They always gave me valuable suggestions and supports throughout the research work. Without their kind supervision, I would not be able to have reached this milestone.

The Magnel Lab gave me a good opportunity to meet nice colleagues and make friends. The first good friend and colleague that comes to my mind is Ruben Van Coile. He does not only showed his friendship and invited me for visits, but also gave me many good ideas and proposals for my research work. I would like to thank him explicitly for the tour guide in London city together with Karolina, as well as for his guidance for my PhD research on fire. Furthermore, I would like to give my thanks to Farid Van Der Vurst. He is the most warm-hearted person I have ever met. As a native speaker, he helped me a lot with the translation work of the Dutch documents and solved many problems. Besides, he taught me Dutch for two months and introduced his friends and family to me. As a consequence, we are now friends and family.

Special thanks are given to my old and new officemates and friends — Ioan Pop, Hai Dang Le, Kai Wu, Benoît Hilloulin, Julia García-González, Desirée Rodríguez-Robles, Pieterjan Criel, Natalia Mariel Alderete, Zhiqiang Dong and Cheng Xing. They showed not only their scientific spirit, but also their kind warmth in non-profession activities. My daily life would have been dull and boring without them. As a precious memory, I will always remember the fun we had during coffee breaks and our spare time.

I further show my greatest appreciation to friends who have filled my life with joy from travelling — Florent Forest, Thomas Autissier, Raul Zagon, Darius Zagon, Teodora Salcudean, Ioan Pop, Corina Şoşdean, Wenhao Xiao, Benjin Wang, Hugo Eguez Alava, João Luis Garcia Feiteira, Koichi Matsuzawa, Yury Villagrán, Alessandro Proia and Yang Lv. Florent and Thomas have showed me almost entire

France, including the fantastic French food, amazing sight-seeing locations as well as the elegant wine culture. Raul and Darius have invited me for Christmas twice. Because of them, I have had a chance to celebrate my first and second Christmas and I was treated like one of the family members. Ioan and Teodora have met me every other weekend for small road trips and food parties. Hugo has made trips with me to Spain and Florida to meet his family. I have enjoyed the South American culture and the stay with his family (special thanks go to his wife, Cecilia, who always considered me as her son).

I wish to thank my other colleagues and friends who always do me favours and share their happiness — Didier Droogné, Kenny Martens, Kunpeng Zheng, Nicky Reybrouck, Wouter Botte, Yihua Zeng, Dirk Gouverneur, Jonas Dispersyn, Bert Van Lancker, Jianyun Wang, Yu Liang, Xiang Hu, Limin Lu, Yun Gao, Zhijun Tan, Borjn Van Belleghem, Didier Snoeck, Philip Van den Heede, Cornelia Baera, Rosaida Dolce, Adelaide Araújo, Yusuf Cagatay Ersan, Robin De Schryver, and our lovely secretaries Marijke Reunes and Christel Malfait, as well as SANACON for their nice Friday afternoon treats.

A very special mention goes to my family. My parents always respect every decision that I have made and give me the largest supports. I would like to thank them. Without their support, I would not have been here for the abroad journey. I would like to thank my step-sister Shuqing Nie for her encouragement and I give my best wishes to her baby who is going to be born in April. Furthermore, I would like to thank my uncle who is running a construction materials business. He always gave me support for my current stay, motivations for my life as well as information about the current situation and future developments on the market.

Finally, I wish to thank everybody who has been a part of my life: family, friends and all the colleagues from the Magnel Lab. Thanks for meeting all of you.

Lijie Wang
March 27th, 2017

TABLE OF CONTENTS

LIST OF SYMBOLS	III
Introduction	III
Roman symbols.....	III
Greek symbols	VI
Other symbols.....	VIII
Abbreviations.....	VIII
SAMENVATTING	XI
SUMMARY	XVII
CHAPTER I GENERAL INTRODUCTION & RESEARCH SCOPE	2
I.1. Background and context of the research topic.....	3
I.2. Material properties at elevated temperatures	4
I.3. Mechanical properties and spalling at elevated temperatures	7
I.4. Real fires, standard fires and parametric fires	11
I.5. Available experimental results and analytical methods	13
I.6. Simplified methods provided by standards and provisions in order to determine the load bearing capacity of concrete elements.....	15
I.7. Contemporary research challenges	18
I.8. The outlines and objectives of this thesis	19
CHAPTER II SIMPLIFIED METHODS PROVIDED IN EUROCODE 2 FOR COLUMNS EXPOSED TO FIRE TAKING INTO ACCOUNT SECOND-ORDER EFFECTS	22
II.1. Simplified methods for columns at ambient temperature	23
II.2. Simplified design methods for columns at elevated temperatures	31
II.3. Examples	34
II.4. Conclusions	38
CHAPTER III NUMERICAL METHODS FOR SLENDER COLUMNS EXPOSED TO FIRE TAKING INTO ACCOUNT SECOND-ORDER EFFECTS	40
III.1. Material models.....	41
III.2. Transient thermal model	48
III.3. Structural model	52
III.4. Validation of interaction curves.....	62
III.5. A parameter study	69
III.6. Conclusions	74

CHAPTER IV DESIGN OF REINFORCED CONCRETE COLUMNS EXPOSED TO FIRE IN CASE OF UNIAXIAL BENDING USING TABULATED DATA.....	76
IV.1. Influence of the fire exposed faces on the temperature distribution	77
IV.2. Comparison of calculated ISO834 standard fire resistance times of rectangular concrete columns with EN 1992-1-2 tabulated values for different slenderness ratios and eccentricities	81
IV.3. Extension of the tabulated data for concrete columns exposed to hydrocarbon fires and natural fires	92
IV.4. Conclusions.....	106
CHAPTER V EVALUATION OF SIMPLIFIED CALCULATION METHODS FOR SECOND-ORDER EFFECTS IN CASE OF UNIAXIAL BENDING AND AN ISO 834 STANDARD FIRE.....	108
V.1. Parametric study on applicability of the 500°C isotherm method.....	109
V.2. Parametric study on buckling of concrete columns exposed to fire.....	114
V.3. Effect of imperfections	120
V.4. Improved curvature approximation based on interaction diagrams.....	127
V.5. Conclusions.....	140
CHAPTER VI SIMPLIFIED METHOD AND PROBABILISTIC ANALYSIS FOR EVALUATING THE BIAXIAL CAPACITY OF RECTANGULAR REINFORCED CONCRETE COLUMNS DURING FIRE.....	142
VI.1. Introduction	143
VI.2. Basic calculation methods	144
VI.3. Assumptions and calculation models for biaxial bending during fire exposure	148
VI.4. Validation of the calculation model.....	150
VI.5. Calculation of $\gamma(v)$ and parametric study.....	154
VI.6. Values of $\gamma(v)$ for different reinforcement ratios	164
VI.7. Uncertainty quantification of columns subjected to biaxial bending combined with fire in the framework of structural reliability-based design	169
VI.8. Conclusions.....	180
CHAPTER VII GENERAL DISCUSSIONS , CONCLUSIONS & FUTURE RESEARCH.....	182
VII.1. General discussions	183
VII.2. Conclusions.....	187
VII.3. Future work	190
REFERENCES	194
LIST OF PUBLICATIONS	206

LIST OF SYMBOLS

Introduction

Common symbols and abbreviations used throughout the dissertation are listed below. Specific symbols which are not listed may be used locally and in a specific context. It is worth mentioning that some symbols may be used for a different meaning in a specific context. This local use of the same symbol has been accepted in case of conventions in literature.

Roman symbols

A	cross-sectional area [mm ²]
A _c	area of the concrete cross-section [mm ²]
A _f	floor area of fire compartment [m ²]
A _s	total area of the reinforcement [mm ²]
A _t	total area of enclosure (walls, ceiling and floor, including openings) [m ²]
A _w	total area of vertical openings on all walls [m ²]
a _z	width of the damaged zone [mm]
b	width [mm]
c	concrete cover thickness [mm]
	factor depending on the curvature distribution (chapter II)
	[-]
	specific heat of boundary of enclosure (section IV.3.2)
	[J/kgK]
c ₀	integration factor [-]
c _i	coefficient which depends on the distribution of the first-order moment [-]
c _p (θ)	specific heat at temperature θ [J/kgK]
d	effective depth [mm]
E	load effect [kN] [kN·m]
e	eccentricity [mm]

e_0	initial eccentricity [mm]
e_2	second-order deflection [mm]
e_{1d}	first-order eccentricity [mm]
e_{2d}	eccentricity due to the deformation of the compression member [mm]
E_{cd}	design value of modulus of elasticity of concrete [N/mm ²]
E_{cm}	secant modulus of elasticity of concrete [N/mm ²]
e_d	maximum permitted eccentricity [mm]
E_f	fictive modulus of elasticity [N/mm ²]
EI	bending stiffness [N·mm ²]
e_i	eccentricity taking into account imperfections [mm]
EI_d	design value of bending stiffness [N·mm ²]
E_s	design value of modulus of elasticity of reinforcement at ambient temperature [N/mm ²]
$E_s(\theta)$	elastic modulus of the reinforcement at temperature θ [N/mm ²]
e_{tot}	maximum permitted eccentricity to the centroid [mm]
e_x	maximum permitted eccentricity along the x axis [mm]
e_y	maximum permitted eccentricity along the y axis [mm]
$f_{0.2k}$	characteristic 0.2% proof-stress of reinforcement [N/mm ²]
f_{cd}	design value of concrete compressive strength [N/mm ²]
f_{ck}	characteristic compressive cylinder strength of concrete at 28 days [N/mm ²]
f_{cm}	mean value of concrete cylinder compressive strength [N/mm ²]
f_{ctd}	design value of concrete tensile strength [N/mm ²]
f_{ctk}	characteristic axial tensile strength of concrete [N/mm ²]
$f_{c,\theta}$	compressive strength of concrete at temperature θ [N/mm ²]
f_{tk}	characteristic tensile strength of reinforcement [N/mm ²]
f_{yd}	design yield strength of reinforcement [N/mm ²]
f_{yk}	characteristic yield strength of reinforcement [N/mm ²]
H	heat [J]
h	height [mm]
	height of the occupancy (chapter IV) [m]
h_w	weighted average of window heights on all walls [m]
I_c	second moment of area of concrete cross-section [mm ⁴]
I_s	second moment of area of the reinforcement [mm ⁴]
i_s	radius of gyration of the total reinforcement area [mm]

I_{Zc}	moment of inertia of the reduced concrete section [mm ⁴]
I_{Zs}	moment of inertia of the reinforcing bars [mm ⁴]
K	effective length factor [-]
k	moisture content by weight (%) [-] coefficient in function of concrete compressive stress and shortening strain (chapter II) [-]
k_1	factor which depends on the concrete strength class [-]
k_2	factor which depends on the axial force and the slenderness [-]
K_c	factor for effects of cracking, creep etc. [-]
$k_{c,p}$	mean reduction coefficient [-]
$k_c(\theta_M)$	reduction coefficient for concrete strength as a function of the temperature at point M [-]
K_E	model uncertainty for the load effect [-]
K_R	model uncertainty for the resistance effect [-]
K_F	correction factor depending on the axial load [-]
K_s	factor for the contribution of the reinforcement [-]
K_φ	factor for taking account of creep [-]
l	length [m]
l_0	effective length at ambient temperature [m]
$l_{0,fi}$	effective length at elevated temperatures [m]
M	bending moment [kN·m]
m	dimensionless bending moment of a column at normal temperature conditions [-]
M_{01}, M_{02}	first-order end moments [kN·m]
M_{0Ed}	first-order moment, including the effect of imperfections [kN·m]
M_2	second-order moment [kN·m]
M_c	design value of bending moment for concrete [kN·m]
M_{Ed}	design moment [kN·m]
M_s	design value of bending moment for reinforcing bars [kN·m]
M_x	design value of bending moment along the x axis [kN·m]
M_y	design value of bending moment along the y axis [kN·m]
m_x	relative design moment [-]
N	axial load [kN]
n	load level of a column at normal temperature conditions [-]
n'	relative axial load [-]
N_B	buckling load [kN]

n_{bal}	value of n at the maximum moment of resistance [-]
N_c	design value of normal force for concrete [kN]
n_d	design value of relative axial force [-]
N_{Ed}	design value of the axial force [kN]
N_s	design value of normal force for reinforcing bars [kN]
n_u	relative load capacity [-]
O	opening factor [-]
p	number of segments [-]
P_f	probability of failure [-]
q	number of parallel zones in the width w [-]
R	resistance effect [kN] [kN·m]
r_m	moment ratio [-]
1/R	curvature [1/m]
1/R ₀	maximum curvature [1/m]
s	distance between nodes [m]
t	time [sec/min/h]
V	coefficient of variation [-]
v	displacement [m]
y	distance to neutral axis [mm]

Greek symbols

α_c	convection coefficient [W/m ² K]
α_{cc}	coefficient taking into account long term effects on the compressive strength and unfavourable effects resulting from the way the load is applied [-]
α_{ct}	coefficient taking account of long-term effects on the tensile strength and of unfavourable effects [-]
α_R	value of sensitivity factor of resistances [-]
α_μ	angle of the bending axis [degree]
β	coefficient taking into account creep (section II.1.2) [-] factor which depends on the distribution of 1 st and 2 nd order moments (section II.1.3) [-]
Γ	target reliability (chapter VI) [-]
$\gamma, \gamma_1, \gamma_2$	coefficients depending on the column dimensions, reinforcement ratio, effective depth and material properties

γ_c	partial factor for concrete [-]
γ_{Ec}	partial factor for modulus of elasticity of concrete [-]
γ_s	partial factor for reinforcement [-]
Δ	difference [-]
ε	strain [-]
	ratio of the maximum permitted eccentricity (chapter VI) [-]
ε_{c1}	compressive strain in the concrete at the peak stress f_c [-]
$\varepsilon_{c1,\theta}$	compressive strain in the concrete at the peak stress $f_{c,\theta}$ at temperature θ [-]
$\varepsilon_{c,cr}(\sigma, \theta)$	creep strain of concrete at temperature θ [-]
$\varepsilon_{c,th}(\theta)$	thermal strain of concrete at temperature θ [-]
$\varepsilon_{c,tr}(\sigma, \theta)$	stress dependent strain of concrete at temperature θ [-]
$\varepsilon_{c,tot}(\theta)$	total strain of concrete at temperature θ [-]
ε_{cu1}	ultimate compressive strain in the concrete [-]
$\varepsilon_{cu1,\theta}$	ultimate compressive strain in the concrete at temperature θ
ε_f	emissivity of the fire [-]
ε_m	surface emissivity of the member [-]
$\varepsilon_{mech}(\xi, \eta)$	mechanical strain [-]
ε_{sd}	strain of the reinforcing bars at the top layer [-]
ε'_{sd}	strain of the reinforcing bars at the bottom layer [-]
$\varepsilon_s(\theta)$	thermal strain of the reinforcing steel at temperature θ [-]
ε_{uk}	characteristic strain of reinforcement or prestressing steel at maximum load [-]
ε_x	total strain due to bending along the vertical axis [-]
ε_y	total strain due to bending along the horizontal axis [-]
ε_{yd}	design value of yield strain of reinforcement [-]
η	ratio of concrete strain to concrete strain at peak stress (section II.1.1) [-]
	distance between the calculated point and the centroid point [mm]
η_{fi}	reduction factor for the design load level [-]
θ	temperature [°C]
θ_g	gas temperature [°C]
θ_m	surface temperature of the member [°C]
θ_r	effective radiation temperature of the fire environment [°C]
$\kappa_{0.8MEd}$	the curvature of a cross-section subjected to a load effect of $0.8 M_{Ed}$ [1/m]
κ_d	maximum design curvature [1/m]

μ	mean value [-]
μ_x	dimensionless bending moment capacities along the x axis [-]
μ_y	dimensionless bending moment capacities along the x axis [-]
λ	slenderness ratio [-]
λ_c	thermal conductivity [W/mK]
λ_{lim}	limit of slenderness ratio [-]
ν	dimensionless axial load [-]
$\rho(\theta)$	density at elevated temperature θ [kg/ m ³]
σ	stress [N/mm ²]
	Stephan Boltzmann constant (section III.2) [-]
	standard deviation (chapter VI) [-]
σ_c	compressive stress in the concrete [N/mm ²]
σ_s	steel stress [N/mm ²]
$\Phi(\cdot)$	cumulative normal distribution function [-]
ϕ	configuration factor which measures the fraction of the total radiative heat leaving a given radiating surface that arrives at a given receiving surface [-]
φ_{ef}	effective creep ratio [-]
χ	curvature [1/m]
χ_0	curvature at the reference point [1/m]
χ_{bal}	curvature at the maximum moment of resistance [1/m]
ω	mechanical reinforcement ratio [-]

Other symbols

\emptyset	reinforcing bar diameter [mm]
-------------	-------------------------------

Abbreviations

FEM	finite element method
fi	fire
FORM	first-order reliability method
HSC	high strength concrete
KLE	quasi-linear theory of elasticity
NSC	normal strength concrete

SCC	self-compacting concrete
SLS	serviceability limit states
ULS	ultimate limit state

SAMENVATTING

Brand is een van de strengste ontwerpsituaties en speelt bijgevolg een belangrijke rol in het ontwerp van betonconstructies en betonelementen. Brand heeft niet alleen een effect op de betonsterkte, maar ook op de structurele stijfheid en stabiliteit van betonelementen. Daar een betonkolom meestal onderworpen is aan zowel verticale krachten als aan buigmomenten afkomstig van platen en balken, is het ontwerp met betrekking tot brandwerendheid niet eenvoudig.

Het mechanisch gedrag van betonkolommen in geval van brand kan ingeschat worden met de vereenvoudigde methoden of tabellen uit EN 1992-1-2 (2004). Sommige bepalingen en voorspellingen blijken echter onveilig te zijn voor sommige gevallen in vergelijking met experimentele gegevens. Bovendien zijn sommige vereenvoudigde methodes, die gebaseerd zijn op een ontwerp bij gewone omgevingstemperaturen en nog moeten gevalideerd worden in brandomstandigheden, te conservatief. Vanuit zowel de veiligheid als economisch oogpunt, dienen de getabelleerde waarden die opgenomen zijn in Eurocode 2 (2004), te worden herzien. De huidige vereenvoudigde methoden voor het concreet ontwerp van betonkolommen moeten worden aangepast voor toepassing onder brandomstandigheden.

Tweede-orde-effecten spelen een belangrijke rol bij het ontwerp van kolommen onderworpen aan axiale belastingen en buigende momenten. De norm EN 1992-1-1 (2004) verduidelijkt de voorwaarden waarbij de tweede-orde-effecten getoetst moeten worden. Er wordt gesuggereerd dat tweede-orde-effecten verwaarloosd kunnen worden wanneer de slankheid onder een bepaalde grenswaarde ligt. Echter, bij brand is deze grenswaarde voor de slankheid niet meer dezelfde omwille van de schade veroorzaakt door de hoge temperaturen. Bijgevolg moet het toepassingsgebied van de tweede-orde-effecten voor betonnen kolommen worden herbekeken.

In dit proefschrift wordt een numerieke rekentool gepresenteerd, gebaseerd op een discretisatie van de doorsnede rekening houdend met tweede-orde-effecten. De basis van deze berekening is het $M-\chi$ diagram, dat een iteratieve berekening toelaat van de tweede-orde-effecten voor elk van de beschouwde knooppunten, in

plaats van gebruik te maken van een maximale kromming (zoals aangenomen bij de vereenvoudigde methoden) om het maximum buigmoment voor een gegeven axiale belasting te berekenen. Hierdoor kan het maximum buigmoment nauwkeuriger berekend worden dan met de vereenvoudigde methoden. Om de voorgestelde rekentool te valideren zijn een reeks vergelijkende simulaties gedaan op basis van de experimentele resultaten van de Technische Universiteit van Braunschweig (Hass, 1986), van de Universiteit van Luik (Dotreppe, 1993), en van Lie (1993).

Op basis van de fundamentele theorie en de validatie van de rekentool zijn de tabelwaarden gegeven in Eurocode 2 (2004) herberekend met de numerieke tool. Uit de berekeningen blijkt dat de bepalingen in de Eurocode enerzijds niet veilig zijn voor het geval van een mechanische wapeningsverhouding gelijk aan 0,1 en 0,5 indien de axiale last groot is. Bij hoge mechanische wapeningsverhoudingen ($\omega = 1.0$) zijn de tabelgegevens dan weer te conservatief, wat resulteert in inefficiënt en oneconomisch materiaalgebruik. De voorgestelde tabelwaarden in dit proefschrift laten een nauwkeuriger berekening van het ontwerp van betonnen kolommen in brandomstandigheden toe.

Op basis van kwantitatieve simulaties met de rekentool zijn ook sommige van de bestaande vereenvoudigde methoden nagezien, hetgeen leidt tot de volgende vaststellingen:

(1) Er wordt vastgesteld dat de 500 ° C isotherme methode een efficiënte en eenvoudig te gebruiken methode is om de interactiekrommen van kolommen bij brand te voorspellen. Echter, voor kleine dwarsdoorsneden (minder dan 200 mm x 200 mm) of kolommen die langer dan 90 minuten aan een standaardbrand volgens de norm ISO 834 blootgesteld worden, is de voorspelling met deze vereenvoudigde methode zeer conservatief. Voor deze gevallen wordt aangeraden om een isotherme met een hogere kritieke temperatuur te hanteren tijdens het brandwerendheidsontwerp.

(2) Om de tweede-orde-effecten te berekenen wordt vaak gewerkt met de nominalestijfheidsmethode bij normale temperaturen. Deze methode is een vereenvoudiging die bewezen heeft, veilig genoeg te zijn bij het ontwerp van kolommen. Echter, de interactiecurves verkregen met de nominalestijfheidsmethode zijn te conservatief in het geval van slanke kolommen. Hoewel de capaciteit berekend met de KLE- methode gegeven in de Nederlandse

norm NEN 1995 een lichte overschatting oplevert bij omgevingstemperaturen, liggen de interactiecurves berekend op basis van de KLE-methode dichter bij de numerieke resultaten dan deze berekend met de nominalestijfheidsmethode. Bij hogere temperaturen is de aanname van de stijfheid van de kolom verkregen met de helling van het moment-kromming curve op $0,8M_{Ed}$ volgens de Nederlandse voorschriften (NEN, 1995) niet meer van toepassing. Een waarde die overeenkomt met een hoger buigmoment wordt aanbevolen voor de aangenomen stijfheid bij brand.

(3) Imperfecties kunnen niet verwaarloosd worden bij slanke kolommen bij in acht name van tweede-orde-effecten. Op basis van een parameterstudie bleek dat de brandduur en de excentriciteit een belangrijke invloed hebben op de impact van imperfecties. De slankheid, evenals de afmetingen van de doorsnede hebben een significant effect op de imperfecties onder een aantal specifieke voorwaarden.

(4) De toepassing van de methode gebaseerd op de nominale kromming zoals gegeven in de *fib Model Code 2010* (2013) werd uitgebreid voor toepassing bij brand, op basis van een parameterstudie. Het besluit is dat enkel de slankheid een belangrijke invloed heeft op de voorspelling van de tweede-orde-effecten met de voorgestelde vereenvoudigde formule. Bij dezelfde axiale belasting nemen de verschillen tussen de doorbuigingen verkregen met de vereenvoudigde methode en de numerieke resultaten toe naarmate de slankheid stijgt. Echter, de vereenvoudigde formule heeft reeds bewezen gemakkelijk bruikbaar en veilig te zijn voor de voorspelling van tweede-orde-effecten in kolommen blootgesteld aan brand.

Eurocode 2 (2004) voorziet enkel minimale afmetingen met betrekking tot een ISO 834 standaard brand, maar bevat geen informatie over hoe structurele elementen en samenstellen van elementen zich zullen gedragen in een echte brand of bij blootstelling aan een koolwaterstofbrand. Omdat de weerstand tegen een koolwaterstofbrand vereist is in sommige specifieke situaties en slechts weinig data beschikbaar is voor het ontwerp van betonkolommen blootgesteld aan koolwaterstofbranden, is een aanvulling van de tabellen uit EN 1992-1-2 (2004) belangrijk. In dit proefschrift zijn koolwaterstofbranden verder onderzocht en getabelleerde waarden zijn voorzien. De rekentool is aangepast aan een case study waarin kolommen werden blootgesteld aan natuurlijke branden.

Na vergelijking van de resultaten op basis van de koolwaterstofbrand met de tabellen voor een ISO 834 standaardbrand, wordt opgemerkt dat de brandwerendheid tegen een koolwaterstofbrand kan leiden tot zeer hoge eisen. Verder zijn enkele specifieke voorbeelden van kolommen onderworpen aan natuurlijke branden onderzocht. Zowel boven- als ondergrenscurven zijn ingevoerd om de brandwerendheid van kolommen te onderzoeken wanneer de temperatuur begint te dalen. De resultaten tonen aan dat de tweede-orde-effecten niet significant zijn wanneer de axiale kracht laag is. Bij grote excentrische belastingen, daalt het maximum opneembaar buigmoment van de kolom eerst continu tijdens de brand, waarna een lichte stijging optreedt tijdens de afkoelingsfase. Bijgevolg kan de waarde gebaseerd op de ondergrenscurve bepalend zijn voor de minimumafmetingen voor deze specifieke brand.

Zoals eerder vermeld, zijn tweede-orde-effecten meer uitgesproken wanneer de axiale belasting aangrijpt met een zekere excentriciteit. Dit verschijnsel komt niet alleen voor bij éénassige buiging maar ook bij scheve buiging. Ook kolommen onderworpen aan scheve buiging moeten dus onderzocht worden. In ontwerpsituaties bij gewone omgevingstemperaturen bevatten zowel EN1992-1-1 als ACI318 richtlijnen voor het ontwerp van kolommen onderworpen aan scheve buiging. Echter, het effect van brand op kolommen onderworpen aan scheve buiging is niet in de bepalingen vermeld. Het is belangrijk om het mechanisch gedrag van kolommen bij scheve buiging gecombineerd met brand te evalueren en dus extra onderzoek te verrichten naar richtlijnen voor het brandwerendheidsontwerp.

De toepasselijkheid van de meest gebruikte vereenvoudigde formule voor scheve buiging, namelijk de Bresler benadering, wordt met behulp van de ontwikkelde rekentool onderzocht voor betonkolommen onderworpen aan een ISO 834 standaard brand.

Op basis van de simulaties met de ontwikkelde rekentool wordt aangetoond dat de door Bresler (1960) voorgestelde waarde 1,0 voor de coëfficiënt $\gamma(v)$ een goede benadering is wanneer de dimensieloze axiale kracht $v > 0,4$ bij normale omgevingstemperaturen. In een conservatieve benadering kan deze waarde (1,0) gebruikt worden voor alle axiale krachten bij normale temperaturen. Deze coëfficiënt is meestal gelegen tussen 1,00 ~ 2,00 bij hoge temperaturen. Echter, net zoals bij normale omgevingstemperaturen is de range van 1,00 ~ 1,50 ook aanbevolen voor $\gamma(v)$ in het geval van brand als $v = 0,15 \sim 0,4$. De

conservatieve waarde 1.00 kan ook gebruikt worden voor $\gamma(v)$, terwijl een grotere waarde alleen aanvaardbaar is voor specifieke situaties in geval van brand die verder zijn toegelicht in hoofdstuk VI. Op basis van parametrische studies bij normale omgevingstemperatuur en in geval van brand kan $\gamma(v) = 1.0$ worden voorgesteld voor andere kolomdimensies, wapeningschikkingen, en wapeningsverhoudingen als een conservatieve vereenvoudiging. Maar, zoals gezegd bevat dit werk ook enkele minder conservatieve resultaten voor een aantal specifieke situaties.

Omdat variaties van de geometrische configuraties, de betondekking en de betondruksterkte significante verschillen in interactiediagrammen kunnen veroorzaken, kan een probabilistische evaluatie gebruikt worden om het veiligheidsniveau van betonkolommen bij brand te evalueren. De rekentool werd aangepast om rekening te houden met onzekerheden omtrent essentiële parameters zoals betondruksterkte, vloeispanning van de wapening en betondekking. Op basis van “ruwe” Monte Carlo simulaties en rekening houdend met het door Van Coile (2015) voorgestelde model voor balken en platen, zijn de probabilistische evaluaties verkregen door het bepalen van de kansdichtheidsfunctie voor de weerstand van betonkolommen bij brand. Op basis van de interactiecurves bepaald bij het onderzoek naar scheve buiging, is een parameterstudie over het gedrag van betonkolommen rekening houdend met onzekerheden uitgevoerd.

Uit de vergelijking van het referentie interactiediagram met de probabilistische evaluatie bij normale omgevingstemperaturen blijkt dat er een goede overeenkomst is. Omdat er geen streefwaarde van de betrouwbaarheid beschikbaar is voor het geval van brand, zijn de probabilistische berekeningen een belangrijk instrument om de betrouwbaarheid van de voorgestelde ontwerpregels te evalueren bij brand. De tweede-orde-effecten zijn meer uitgesproken bij toenemende brandduur en bij toenemende slankheid.

Samengevat kunnen we stellen dat de voorgestelde numerieke rekentool eenvoudig te gebruiken is en zeer efficiënt is om de brandwerendheid van betonkolommen te evalueren. Bovendien verschaft de rekentool meer inzicht dan de vereenvoudigde werkwijzen voor het brandwerendheidsontwerp die beschikbaar zijn in de literatuur.

SUMMARY

Fire, as one of the most severe design situations, has an important influence on concrete structures and structural members. It does not only affect the strength of concrete, but also the structural stiffness and stability. A concrete column, compared to other structural members, has most often to cope with vertical forces and bending moments from slabs and beams. The fire resistance design of concrete columns turns out to be rather complicated.

In order to find out the mechanical behavior of concrete columns in case of fire, simplified methods as well as tabulated values are provided in EN 1992-1-2 (2004). However, the provisions and predictions, on the one hand, are considered unsafe for some cases when compared to experimental data. On the other hand, simplified methods which are adopted at ambient temperature still need to be validated for fire conditions while some others which have been already widely accepted in case of fire are considered sometimes over-conservative. From both the safety and economical point of view, the tabulated values provided in Eurocode 2 (2004) should be reconsidered and the current simplified methods for concrete column design at ambient temperature should be adjusted to be applicable for fire conditions.

Further, second-order effects play an important role for columns subjected to axial loads and bending moments. In EN 1992-1-1 (2004) the conditions where the second-order effects need to be considered are explained. Furthermore, it suggests that the second-order effects can be neglected when the slenderness ratio is below a certain limiting value. However, with respect to fire, the limit of slenderness ratio is not suitable anymore due to the damage caused by the high temperatures. Hence, the application area of adopting second-order effects for concrete columns needs to be reconsidered.

In this dissertation, a numerical calculation tool is presented. This tool is based on a discretization of the cross-section taking into account second-order effects. The basis of this calculation tool is depending on a $M-\chi$ relationship which allows an iterative calculation respectively for each of the calculated nodes considering second-order effects instead of adopting the maximum curvature for each nodes

(assumed by the simplified methods) to obtain the bending moment capacity for a given axial load. As a result, the corresponding bending moment capacity is more precise than that obtained with the simplified methods. Furthermore, a number of comparisons have been done with experimental results from the Technical University of Braunschweig (Hass, 1986) and the University of Liège (Dotreppe, 1993) as well as Lie (1993) in order to validate the proposed calculation tool.

Based on the fundamental theory and the validation of the tool, the tabulated values provided in Eurocode 2 (2004) are recalculated with the numerical tool. It is found that Eurocode provisions on the one hand are not safe for the case of a mechanical reinforcement ratio equal to 0.1 as well as a mechanical reinforcement ratio equal to 0.5 when the axial load is large. On the other hand, tabulated data is found to be too conservative for high mechanical reinforcement ratios ($\omega = 1.0$), which results in inefficient and uneconomical solutions for practice. Considering structural safety, the tabulated data obtained in the current work provide more precise proposals for the design of concrete columns exposed to fire.

Furthermore, some of the existing simplified methods are discussed based on quantitative simulations with the calculation tool, which leads to the following observations.

(1) The 500°C isotherm method is proven to be an efficient and easy-to-use method to predict the interaction curves of columns in case of fire. With respect to small cross-sections (less than 200 mm × 200 mm) or columns with fire exposure times of more than 90 minutes to the standard ISO 834 fire however, the prediction with this simplified method is very conservative. Hence, for these cases, a higher critical isotherm temperature is recommended for the fire resistance design.

(2) Considering second-order effects, the nominal stiffness method is widely used at ambient temperature. This method, as a simplification, is proven to be safe enough for the design of columns. However, the interaction curves obtained with the nominal stiffness method are too conservative in case of slender columns. The capacity calculated with the KLE-method provided by the Dutch code (NEN, 1995) is slightly on the unsafe side at ambient temperature. However, interaction curves with the KLE-method are closer to the numerical results than those from the nominal stiffness method. Regarding elevated temperatures, the stiffness of the column obtained with the slope of the moment-curvature curve assumed at $0.8M_{Ed}$ in the Dutch guidelines (NEN, 1995) is not applicable anymore. A value

corresponding to a higher bending moment is recommended for the assumed stiffness in case of fire.

(3) Imperfections cannot be neglected for slender columns considering second-order effects. Based on the parametric study, fire duration and eccentricity have an important influence on the effect of imperfections. The slenderness ratios as well as dimensions of the cross-section have a significant effect on imperfections under some specific conditions.

(4) The application of the curvature approximation method provided by the *fib* Model Code 2010 (2013) is extended to the application of fires, based on a parametric study. Furthermore, it is concluded that only the slenderness ratio has a significant influence on the prediction of the second-order effects with the proposed simplified formula. The difference between the deflections obtained with the simplified method and the numerical values increases in function of the slenderness ratio in case of the same axial load. However, the simplified formula is proven to be easy-to-use and safe for the prediction of second-order effects of columns exposed to fire.

Moreover, Eurocode 2 (2004) only provides minimum dimensions with respect to an ISO 834 standard fire, but this standard fire does not provide information on how structural members and assemblies will behave in an actual fire or when exposed to a hydrocarbon fire. As resistance to hydrocarbon fires may be required in specific situations and little data is available on the design of concrete columns exposed to hydrocarbon fires, extending the tables from EN 1992-1-2 (2004) with respect to this more severe design fire is important. Therefore, hydrocarbon fires are investigated in the dissertation and tabulated values are provided. Further, the calculation tool is also adapted for a case study when columns are subjected to natural fires.

Comparing the results for the hydrocarbon fire with the tables obtained for the ISO 834 standard fire, it is noted that fire resistance to the hydrocarbon fire may result in very stringent requirements. Furthermore, some specific examples are given in case of columns subjected to natural fires. Both the upper limit and lower limit curves are introduced to investigate the fire resistance of columns when the fire temperature begins to decrease. The results prove that second-order effects are insignificant when the normal force is low. When the eccentric loads are large, the maximum bending moment of the column firstly decreases continuously during the

fire, and then shows a slight increase during the cooling phase. As a result, this value based on the lower limit curve could be considered when determining minimum dimensions for this specific fire.

As it is mentioned before, second-order effects are more pronounced in case an eccentricity is associated with the axial load. This phenomenon of loaded columns does not only occur in case of uniaxial bending but also in case of biaxial bending. Therefore, it is important to investigate columns subjected to biaxial bending as well. For design situations in case of ambient temperature, both EN1992-1-1 and ACI318 provide guidelines for the design of columns in case of biaxial bending. However, the effect of fire on these columns subjected to biaxial bending is not mentioned in the provisions. It is important to evaluate the mechanical behaviour of columns in case of biaxial bending combined with fire and, hence, to perform additional research in order to provide guidelines for their fire resistance design.

The applicability of the classic Bresler approximation which is the most used simplified formula in case of biaxial bending, is investigated for concrete columns subjected to an ISO 834 standard fire in case of biaxial bending, using the developed calculation tool.

Based on the simulations with the developed calculation tool, it is shown that 1.0 for the coefficient $\gamma(v)$ proposed by Bresler (1960) is an acceptable approximate value when the relative axial force $v > 0.4$ at ambient temperature. As a conservative consideration, this value 1.0 can be adopted for all the axial forces at ambient temperature. Further, this coefficient $\gamma(v)$ is mainly situated between 1.00 ~ 2.00 at elevated temperatures. However, as at ambient temperature, a range of 1.00 ~ 1.50 is also recommended for $\gamma(v)$ in case of fire when $v = 0.15 \sim 0.4$. Furthermore, a conservative value 1.00 can be used for $\gamma(v)$ while a larger value is only possible for specific situations in case of fire, for which some guidance however can be found in the results reported in chapter VI. Based on parametric studies at ambient temperature as well as in case of fire, $\gamma(v) = 1.0$ can be suggested for other column dimensions, reinforcement arrangements and reinforcement ratios as a conservative simplification. However, as mentioned this work also presents less conservative results for several specific situations.

Since variations of the geometric configurations, the cover thickness, as well as the concrete compressive strength might cause significant differences to interaction diagrams, a probabilistic evaluation can be considered to evaluate the safety level

of concrete columns during fire exposure. For this purpose, the calculation tool was adapted to take into account uncertainties which may exist with respect to basic parameters such as the concrete compressive strength, the reinforcement yield stress and the concrete cover. Based on crude Monte Carlo simulations and considering the model proposed by Van Coile (2015) for beams and slabs, the probabilistic evaluations are obtained by determining the probability density function of the resistance of concrete columns during fire exposure. Further, based on the interaction curves obtained for the investigation of the case of biaxial bending, a parametric study on the behaviour of concrete columns taking into account uncertainties is performed.

Comparing the reference interaction diagram with the probabilistic evaluation at ambient temperature, it is seen that they are in a good agreement. Since there is no explicit target reliability available for the case of fire, the probabilistic calculations provide an important tool to evaluate the reliability of proposed design guidelines during fire. Furthermore, it is observed that the second-order effects are more pronounced with increasing fire duration and with increasing slenderness ratio.

In conclusion, the proposed numerical calculation tool is easy-to-use and very efficient to evaluate the fire resistance of concrete columns and provides more insight than the simplified methods for the fire resistance design available in literature.

CHAPTER I

GENERAL INTRODUCTION & RESEARCH SCOPE

I.1. Background and context of the research topic

Although fire on the one hand was a keystone in the development of civilization, on the other hand, it is a threat to life, property and environment. Fire disasters already happened in times of early civilization. With respect to severe fires recorded in the history, the first one was dated back to 64 A.D. as an urban fire spread to the entire city of Rome and lasted for five days (Flemmer et al., 1999). Fire disasters still occur nowadays due to the inadequate use of chemicals, gases, electrical equipment and consumer electronics, household products or as a result of lighting fires, etc. As a result, it has mostly a direct effect on the buildings and hence it is important to study the fire influence on structures.

Fire, as one of the most severe conditions, has an important impact on concrete elements and structures. It does not only affect the strength of concrete, but also the structural stiffness and stability. A concrete column, compared to other structural members, has most often to cope with vertical forces and bending moments from slabs and beams. Consequently, it is essential to find a reliable and practical way to establish interaction curves for the overall structural behaviour of concrete columns subjected to fire. The structural European Standard EN 1992-1-1 (Eurocode 2, 2004) provides a simplified calculation method for second-order effects in case of ambient temperatures. However, Eurocode 2 (2004) refers only briefly to the second-order effects in case of fire. As such, the necessity was formulated to find a coherent analytical methodology for second-order effects under fire, preferably verified using FEM simulations and experimental data. Hence, an analytical calculation tool is presented in this dissertation in order to investigate second-order effects of columns in case of fire.

This Ph.D. research consists of five parts: firstly, the simplified methods provided by Eurocodes as well as some other codes are briefly discussed; secondly, an analytical calculation tool is presented and validated with the experimental data; further, based on the analytical tool, tabulated tables for the fire resistance are given for interaction curves of columns taking into account different parameters and optimizations are proposed for the current simplified methods; further, the calculation tool is extended towards biaxial bending combined with fire; finally, a probabilistic analysis is performed.

I.2. Material properties at elevated temperatures

I.2.1. Thermal and physical properties of concrete

Thermal conductivity is the property of a material to conduct heat. Harmathy (1970) proposed that the thermal conductivity would have a linear decrease with increasing temperature when the temperature is below 700°C. Further, Lie (1993) found out that the major influencing factors are moisture content, type of aggregate and mix proportions. As such, the thermal conductivity for both siliceous and carbonate aggregate high strength concrete (HSC) were compared and the tests indicated that the thermal conductivity of siliceous aggregate concrete is higher than that of the carbonate concrete in the temperature range of 200°C to 800°C. This is due to the higher crystallinity of the siliceous aggregates as compared to that of the carbonate aggregates. The higher the crystallinity, the higher the thermal conductivity and its rate of decrease with temperature (Lie, 1993). The effect of aggregate type on the thermal conductivity of high strength concrete (HSC) is similar to that of normal strength concrete (NSC) (Harmathy, 1970).

Specific heat is the amount of heat per unit mass, required to change the temperature of a material by one degree and is generally expressed in terms of thermal capacity which is the product of specific heat and density (Kodur, 2014). Lie (1972) figured out that the specific heat increases with increasing temperature — the first increase of specific heat at 150°C is caused by evaporation of free water and the second one is caused by the removal of crystal water from the cement paste. Considering the moisture content is the determining factor on specific heat below temperatures of 200°C, Schneider (1982) found out that around 100°C initially wet concrete shows an apparent specific heat nearly twice high as the oven dried concrete. Further, Kodur and Sultan (2003) investigated the influence of aggregate type on the specific heat. For calcareous aggregate concrete, the specific heat shows a peak at temperatures near 150 and 400°C, while there is a small peak at 500°C for siliceous aggregate concrete. When the temperature is above 600°C, the specific heat of the calcareous aggregate concrete is generally higher than that of the siliceous aggregate concrete. In EN 1992-1-2 (Eurocode 2, 2004), an estimated value of the specific heat as a function of temperature at 3 different moisture contents of 0%, 1.5% and 3% is provided.

The thermal diffusivity of material is defined as the ratio of the thermal conductivity to the volumetric weight specific of the material (Harmathy, 1970). It

measures the heat from an exposed surface of a material to inner layers. The larger the diffusivity, the faster the temperature rises at a certain depth in the material (Kodur, 2014). Kodur and Sultan (2003) studied high strength concrete in this regard and concluded that the type of aggregate has a significant influence on the thermal diffusivity. For siliceous aggregate concrete, the thermal diffusivity increases with temperatures up to 700°C and then remains constant. The increase in thermal expansion near 550°C can be attributed to the transformation of quartz in siliceous aggregate. This could contribute to spalling (Harmathy 1970). For carbonate aggregate, the thermal expansion increases sharply with temperatures above 500°C. This can be partly attributed to the dissociation of dolomite, which is present in carbonate aggregate. Above 800°C, the thermal expansion of the HSC has a slight decrease, due to further dehydration and shrinkage of the concrete (Lie, 1972). In EN 1992-1-2 (Eurocode 2, 2004), functions for the thermal diffusivity coefficient (thermal elongation) are provided for normal concrete with siliceous and calcareous aggregates (Fig. I.1).

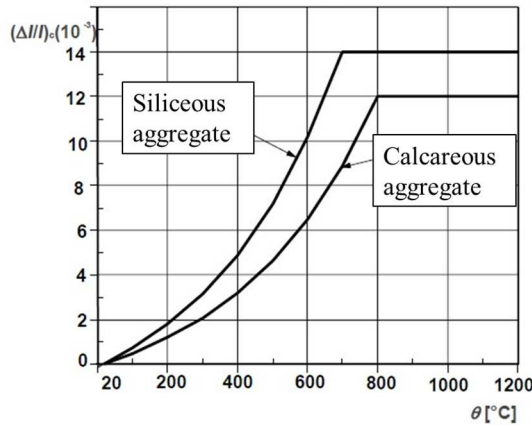


Fig. I.1: Total thermal elongation of concrete

With respect to mass loss, Lie and Kodur (1995, 1996) indicated that the type of aggregate also has an influence. The mass loss for both concrete types is hardly observed until about 600°C (about 3% of the original mass). Between 600°C and 700°C, the mass of carbonate aggregate concrete drops considerably with increasing temperature. Above 750°C, the mass loss again decreases slowly with temperature. The substantial mass loss and decrease in density for carbonate aggregate concrete is caused by the dissociation of the dolomite in the concrete. This endothermic chemical reaction is expected to be beneficial in preventing spalling of concrete (Lie, 1993). In the case of siliceous aggregate concrete, the

mass loss remains insignificant even above 600°C. In Eurocode 2 (2004), the density as a function of temperature is defined.

The constitutive model of heated and loaded concrete consists of four parts: thermal elongation, stress dependent strain, transient strain and creep strain (Anderberg et al., 1976). The expression of the total strain is written as:

$$\varepsilon_{c,tot}(\theta) = \varepsilon_{c,th}(\theta) + \varepsilon_{c,\sigma}(\sigma, \theta) + \varepsilon_{c,tr}(\sigma, \theta) + \varepsilon_{c,cr}(\sigma, \theta, t) \quad (I.1)$$

- where $\varepsilon_{c,tot}$ is the total strain of concrete at elevated temperature θ ;
 $\varepsilon_{c,th}$ is the thermal elongation of concrete at elevated temperature θ ;
 $\varepsilon_{c,\sigma}$ is the stress dependent strain of concrete at elevated temperature θ ;
 $\varepsilon_{c,tr}$ is the transient strain of concrete at elevated temperature θ ;
 $\varepsilon_{c,cr}$ is the creep strain of concrete at elevated temperature θ ;
 σ is the stress in the concrete;
 t is the time (related to the creep dependent deformations).

The transient strain and creep strain are often considered together and then form the so-called transient creep strain. The transient creep strain is consisting of the implicit model and the explicit model. The most commonly used implicit transient creep strain material model is given by EN 1992-1-2 (Eurocode 2, 2004). The thermal elongation of concrete is increasing with temperature. The main influencing factors are the type of aggregates, the water content, the heating rate, etc. The model provided in Eurocode is proven to be applicable for the heating phase during a fire (Gernay & Franssen, 2010). However, concrete can lose an additional part of its strength during cooling. Therefore, Annex C of EN 1994-1-2 (2005) recommends an additional reduction of 10% on the residual strength after cooling down.

Regarding the explicit material model, the total strain is actually— as previously mentioned— a sum of four parts: thermal strain, instantaneous stress-related strain, transient strain and creep strain. Tao (2008) compared the explicit material model given by Anderberg & Thelandersson (1976), Diederichs (reported by Youssef, 2007), Terro (1998) and Guo (2003) for the normal strength concrete and also presented formulations for the transient strain of self-compacting concrete. Later, Lu (2015) compared the explicit material model proposed by Tao (2003) with Eurocode 2 (2004), it showed that the total strain from Tao's model was slightly

lower than that of the EC2 model (2004) for the same stress level and that the difference was increasing with increasing compressive stress.

I.2.2. Thermal elongation of reinforcing and prestressing steel

In EN 1992-1-2 (Eurocode 2, 2004), the thermal elongation of reinforcing steel and prestressing steel are shown in Fig. I.2, respectively. The thermal elongation of reinforcing steel increases with temperature up to 750°C and then remains constant till 860°C. When the temperature reaches values above 860°C, the thermal elongation increases again. The thermal elongation of prestressing steel has an almost linear increase with temperature.

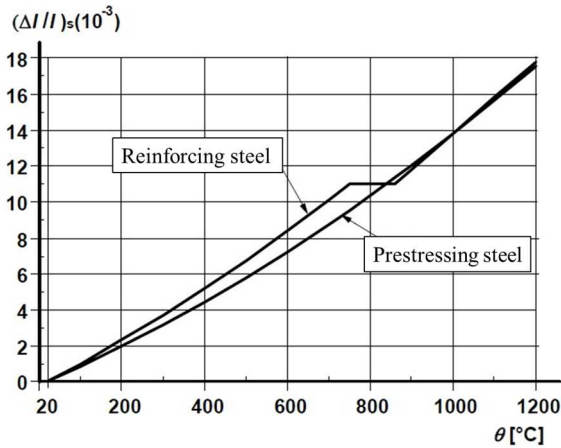


Fig. I.2: Total thermal elongation of steel

I.3. Mechanical properties and spalling at elevated temperatures

With respect to reinforced concrete columns, mechanical properties of concrete and steel need to be specified. In EN 1992-1-1 (Eurocode 2, 2004), the mechanical properties of concrete, reinforcing and prestressing steel at ambient temperature (20°C) are provided. The behaviour of concrete and steel material properties at elevated temperatures are readily available in literature.

I.3.1. Concrete under compression

Regarding the strength of concrete at elevated temperatures, Malhotra (1956) found out that a predominant influencing factor is the aggregate-cement ratio. Concrete with high aggregate-cement ratio undergoes a smaller proportional reduction in strength compared to concrete with low aggregate-cement ratio. In 1985, Schneider (1985) reported that the type of aggregate and applied load also have significant influence on the compressive strength of concrete at elevated temperature. Concrete with siliceous aggregates exhibits the largest amount of strength reduction compared with that of calcareous or lightweight aggregates. However, the strength of concrete in the stressed state is apparently higher than that of in the unstressed state during the heating process. Based on the experimental data, the stress-strain relationships of normal weight concrete with siliceous or calcareous aggregate concrete at elevated temperatures are provided in EN 1992-1-2 (Eurocode 2, 2004), see **chapter III**. Eurocode shows the relationship of the compressive strength of concrete in function of temperature and indicates that the reduction of compressive strength is low when the temperature is below 400°C. However, the compressive strength of concrete decreases significantly above 800°C.

Based on the experimental results of compressive tests performed on concrete specimens heated to pre-specified temperatures, a number of models exist in literature. Anderberg and Thelandersson (1976) firstly carried out tests in order to determine stresses as well as deformations of concrete specimens under torsional loading in case of high temperatures and then proposed a model for the mechanical behaviour of concrete in compression under transient temperature conditions. Afterwards, the model of Lie et al. (1986) was used by Lin et al. (1995) to investigate the behaviour of repaired concrete columns after fire. Later, Meda et al. (2002) compared the mechanical decay of high-performance/high-strength (HPC/HSC) concrete and normal concrete and investigated the influence of temperature on interaction curves for these two types of concrete columns. Moreover, in order to develop the stress-strain relationship of high-performance concrete, Cheng et al. (2004) tested four types of HSC for different temperatures considering different concrete strength, type of aggregate as well as the addition of steel fibers. Later, Li and Purkiss (2005) made comparisons between the existing available models for the mechanical behaviour of concrete at elevated temperatures and gave recommendations on the use of these models. Finally, Youssef and Moftah (2007) compared the predictions of Lie (1992) and Eurocode 2 (2004) with the experimental results of Abrams (1978), Pettersson (reported by Lie, 1992) and

Khoury (1985). The results showed to be closely correlated for concrete with light weight and carbonate aggregates. For concrete with siliceous aggregates, the predictions of the Eurocode model (2004) matched better with the experimental results.

I.3.2. Tensile strength of concrete

In EN 1992-1-2 (Eurocode 2, 2004), the reduction of the characteristic tensile strength of concrete is given if the tensile strength needs to be taken into account when using the simplified or advanced calculation. The tensile strength of concrete normally is to be ignored.

Only very few research have been performed on the tensile strength of concrete at elevated temperatures. Bazant and Chern (1987) proposed a model based on the experimental data from Anderberg and Thelandersson (1976) to calculate the tensile resistance of concrete at elevated temperature. Li and Guo (1993) suggested a simplified formula for the tensile strength of concrete at elevated temperature. A linear relationship is widely used to represent the pre-cracking behaviour. Terro (1998) suggested using for the part after cracking, a linear degrading branch that joints the point of cracking and a point on the horizontal axis with a strain of 0.004. Finally, Youssef and Moftah (2007) compared all the models above and gave some recommendations.

I.3.3. Reinforcing steel and prestressing steel

In order to investigate the reduction on the strength of steel at elevated temperatures, tests and numerical analyses on mechanical properties of structural steel have been carried out since the last century (Cooke, 1988). Woolman and Mottram (1964) firstly tested the tensile properties of steel up to 800°C. Later, Crook (1980) examined the tensile strength properties of hot rolled mild reinforcing bars up to 700°C under isothermal test conditions. The experimental data showed that the variation of the elastic modulus at 550°C had reduced to about 65% of that at ambient temperature. Further, Anderberg (1978) made a comparison between four different types of reinforcing steel at 400°C and 600°C. The results indicated that all these reinforcing steels had a similar stress-strain relationship at 400°C and 600°C. Based on tests, Anderberg (1988) proposed an analytical behaviour model to simulate the mechanical behaviour of steel. In EN 1992-1-2 (Eurocode 2, 2004),

the stress-strain relationships of reinforcing steel as well as prestressing steel are provided based on the results of the research proposed by Anderberg (1988).

Moreover, Topcu and Karakurt (2008) tested the residual mechanical properties of two types of reinforcing bars (ribbed and plain reinforcing bars with diameters between 10 mm and 16 mm) subjected to 20, 100, 200, 300, 500, 800, and 950°C for 3 hours. Comparing splitting tensile strength, elongation and toughness values, the plain reinforcing bar is less affected than the ribbed reinforcing bar at elevated temperatures. Finally, the behaviour of both ribbed and plain reinforcing bars of relatively small diameter at elevated temperature as well as in terms of post-fire residual properties have been investigated by Elghazouli et al. (2009). The results show that the post-cooling residual properties of both hot-rolled and cold-worked reinforcing bars remain almost the same until the temperature reaches 400°C. However, when the temperature reaches 600°C, the residual ultimate mechanical strain is shown to be about 50% in hot-rolled bars and about 150% in case of cold-worked bars.

I.3.4. Spalling

Spalling of concrete structural members can occur in case of fire. However, it is still complicated to predict the spalling due to its random occurrence. Connolly (1995) carried out an experimental investigation on the spalling of concrete at elevated temperatures and categorized spalling into four distinct types: aggregate spalling, corner spalling, surface spalling and explosive spalling. Eurocode 2 (2004) states that explosive spalling is unlikely to occur when the moisture content of the concrete is less than $k\%$ by weight. If the moisture content is above $k\%$, type of aggregate, permeability of concrete and heating rate should be considered. A value $k = 3$ is recommended. Annerel (2010) summarized that the main factors affecting spalling are the heating rate (especially above 3°C/min), the permeability of the material (a denser concrete is more sensitive for pore pressure built up, for example HPC and SCC), pore saturation level (especially above 2-3% moisture content by weight of concrete), the presence of reinforcement and the level of externally applied load.

I.4. Real fires, standard fires and parametric fires

A real fire in a compartment with adequate ventilation normally consists of three stages: pre-flashover, post-flashover and the decay period. Flashover occurs when the majority of the exposed surfaces in a space are heated to their auto-ignition temperature and emit flammable gases. In case of fire developing into flashover, the whole compartment will be engulfed by flames and smoke. After the flashover, the fire enters a fully developed stage with the maximum heat release rate and a steady burning rate. Subsequently, the rate of burning decreases as the combustible materials is consumed and the fire goes to the decay phase. Hence, the structural fire safety issue is depending on different fire scenarios and behaviours when determining the available safe evacuation time as well as the structural bearing capacity.

The nominal curves are idealized simplified fires represented by a temperature-time relationship (*fib* bulletin 38, 2007). These nominal fire curves define the gas temperature Θ_g in the compartment as a function of the exposure time t and are used for fire resistance testing of components in accordance with European legislation (Van Coile, 2015). In order to investigate the temperature distribution of structural members in case of fire, the heat transfer is obtained from the given gas temperature by considering radiation, convection and conduction.

In EN 1991-1-2 (2002), the standard temperature-time curve (ISO 834 standard fire) and the hydrocarbon curve are expressed as Eq.(I.2) and Eq.(I.3), respectively.

$$\Theta_g = 20 + 345 \log_{10}^{(8t+1)} \quad (\text{I.2})$$

$$\Theta_g = 20 + 1080 (1 - 0.325 e^{-0.167 t} - 0.675 e^{-2.5 t}) \quad (\text{I.3})$$

where Θ_g is the gas temperature in the fire compartment [$^{\circ}\text{C}$]

t is the time [min]

The convection coefficient of the standard fire is:

$$\alpha_c = 25 \text{W/m}^2\text{K} \quad (\text{I.4})$$

The standard temperature-time curve ISO 834 (Fig. I.3), also known as the cellulosic curve is used for standard fire tests for most structures and the

hydrocarbon curve is used for specific structures with a risk of hydrocarbon fires (EN 1991-1-2, 2002).

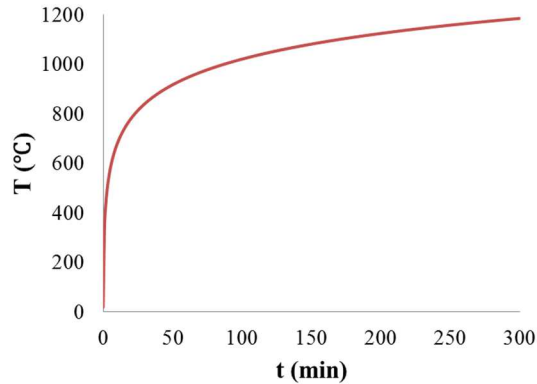


Fig. I.3: The standard ISO 834 temperature-time curve

In addition, considering a more realistic fire scenario, a highly recommended fire curve to adopt is that of the parametric fire curve as outlined in EN 1991-1-2 (2002). Unlike a standard fire, the parametric curve reaches a post flash-over phase where the fire-load density is completely burned-out and a cooling phase occurs contributed by the ventilation.

A number of large-scale standard fire resistance tests have been performed on reinforced concrete structural elements in standard fire testing furnaces (e.g. ASTM 2011, ISO 1999) since the mid-1990s (Bisby et al., 2013). Regarding to concrete columns, fully restrained reinforced concrete columns were tested in case of a standard fire at the Technical University of Braunschweig in the 1970s (Klingsch et al., 1977, Haß and Klingsch, 1980). Furthermore, a summary is given in the Ph.D. thesis from Haß reporting on 47 reinforced concrete columns (1986). Later, a total number of 25 tests have been carried out in Belgium in case of an ISO 834 standard fire (Dotreppe et al., 1996).

Compared to a standard fire, hydrocarbon fires can cause violent explosive spalling in concrete structures, especially in HSC due to the fact that hydrocarbon fire has a significant increase in temperature in the initial period of fire (i.e. it reaches 1000°C in only 8 minutes) (Ta et al., 2011). Ta (2009) carried out tests to compare the behaviour of normal strength concrete and high-strength concrete walls subjected to both an ISO 834 fire and hydrocarbon fire curves. Further, Ngo et al.

(2013) investigated two polypropylene fibres added HSC walls under hydrocarbon fire conditions. Furthermore, a number of tests have been done for the fire resistance of high strength concrete columns in case of hydrocarbon fire exposures and guidelines are proposed by Kodur (2003). Finally, critical factors governing the fire performance of high-strength concrete systems are given in (Kodur and Phan, 2007).

According to the reviews on concrete structures exposed to parametric fires (Bisby et al., 2013), only one large-scale natural fire test of a ‘real’ multi-storey concrete building appears to have ever been performed. Bailey (2002) presented the results of a natural fire test on a full-scale, seven-storey cast in-place concrete building that was performed at the UK Building Research Establishment (BRE) Cardington test site. Due to the fact that there is no reliable experimental data, mathematical models or design specifications for predicting the fire resistance of reinforced concrete structural members under realistic fire scenarios, numerical studies are mostly adopted (Sadaoui et al., 2013). Gernay and Dimia (2011) adopted SAFIR software to study the structural behaviour of concrete columns in case of natural fires including the cooling down phase. At the same time, Dimia et al. (2011) studied on the collapse of reinforced concrete columns subjected to natural fire conditions during and after the cooling phase of the fire. Further, a parametric study on concrete columns subjected to natural fires considering different fire load density was investigated in (Wang et al., 2014) and reported in **chapter IV**. Finally, optimum design solutions for a concrete slab exposed to natural fires are given by Van Coile et al. (2014).

I.5. Available experimental results and analytical methods

With respect to concrete columns exposed to fire, Lie et al. (1984) carried out tests to study the influences of concentric loads, cross-section, moisture and aggregate type on the structural fire resistance. At the same time, experiments were done at the Technical University of Braunschweig, Ghent University and the University of Liège on the fire resistance of columns with different slenderness ratios (Dotreppe et al., 1999). Haß (1986) tested the fire resistance of 47 columns with different cross-sectional sizes, steel sections, concrete strengths and load ratios. The main parameters affecting the behaviour of reinforced concrete columns at elevated temperatures and their influence on the fire endurance have been examined by the

experimental tests executed at Ghent University and the University of Liège (Franssen and Dotreppe, 2003).

Meanwhile, based on other experimental data, a mathematical approach to predict the fire resistance of circular reinforced concrete columns was developed in (Lie and Celikkol, 1991). This method was further developed in order to include rectangular cross-section columns (Lie and Irwin, 1993). Dotreppe et al. (1999) developed a computer code to simulate the structural behaviour under fire conditions. Meda and Gambarova (2002) made comparisons between the M-N interaction curves for normal-strength concrete and high-performance concrete. Most recently, Kodur and Raut (2012) proposed a simplified approach to predict the fire resistance of reinforced concrete columns under biaxial bending. Van Coile et al. (2013) developed a cross-sectional calculation model in order to calculate the bending moment capacity for a concrete beam exposed to fire in the framework of reliability calculations. This model was further used as a basis for the lifetime cost optimization of the structural fire resistance of concrete slabs (2013).

It is common that columns are subjected to bending moments. Whitney (1947) proposed an approximate formula for the design of uniaxially loaded columns. This formula is applicable to columns with reinforcement symmetrically placed in single layers parallel to the axis of bending. However, it was pointed out by Nawy (1986) that Whitney's formula is not safe enough under some loading conditions. In the ACI design handbook (1978), design charts are presented in case of uniaxially loaded columns.

Regarding columns subjected to fire, it is reported that uniaxial bending and axial restraint are the two most important factors for the fire resistance analysis of column elements (Tan and Nguyen, 2013). Benmarce and Guenfoud (2005) tested twelve high-strength columns in fire under two heating rates at different load ratios and restraining levels. It was found that the maximum deformation is independent of the rate of heating and the load that has been applied during the tests. Furthermore, Wu and Li (2009) presented the fire performance of eight axially restrained reinforced concrete columns under a combination of two different ratios and two different axial restraint ratios. It was observed that the maximum deformations during the expanding phase were influenced mostly by the load ratio and hardly by the axial restraint ratio. For a given load ratio, the axial restraint ratio had an influence on the development of axial deformations during the contraction phase beyond the initial equilibrium state. More recently, Tan and Nguyen (2013) tested six full-scale axially-restrained reinforced concrete columns subjected to

different levels of uniaxial bending and initial applied load. The lateral deflection of columns at elevated temperatures is affected by both eccentricity and initial load level. The development of thermal-induced restraint increases with increasing eccentricity but decreases with initial load level.

Considering columns commonly subjected to biaxial bending, Bresler (1960) first proposed a design formula for columns subjected both to compression and biaxial bending based on numerical simulations as well as test results. Parme et al. (1966) further developed the formula proposed in (Bresler, 1960) and adapted it to determine the required size for the columns. Chen and Shoraka (1972) computed moment-thrust-curvature relations for reinforced concrete short columns in biaxial bending at different load levels. For the case of long columns, ACI Building Code (1971) provided the moment magnification factors for the design of columns with the magnified biaxial moments according to a given axial compressive load. Further, Bousias et al. (1992) investigated the experimental behaviour of slender flexure-dominated reinforced concrete columns in eight biaxial load paths under constant axial load. The results showed strong coupling between the two orthogonal directions of bending, which increased energy dissipation. Regarding the fire condition, Raut and Kodur (2011) presented a macroscopic finite element approach for modeling the fire response of concrete columns under biaxial bending. Recently, Tan and Nguyen (2013, 2014) investigated the effects of symmetrical biaxial bending, restraint ratio and concrete strength on the structural behaviour of reinforced concrete columns at elevated temperatures and proposed a simplified model to determine the thermal-induced restraint forces.

I.6. Simplified methods provided by standards and provisions in order to determine the load bearing capacity of concrete elements

EN 1992-1-2 (Eurocode 2, 2004) allows two methods for determining section resistance in case of fire: the 500°C isotherm method (Anderberg, 1978) and the zone method proposed by Hertz (1981).

The 500°C isotherm method is based on the analysis of a number of fire tests carried out on flexural reinforced concrete elements. This method is applicable to a standard fire exposure or any other fire scenarios with an opening factor $O \geq 0.14 \text{ m}^{1/2}$. The method of 500°C isotherm is relatively simple and may be applied

for all cross-section shapes and different heating scenarios, but it also has some limitations (Chudyba & Seręga, 2013). It was experimentally verified for structural members made of normal strength concrete (NSC) that were subjected to failure due to exceeding the capacity of tensile reinforcement and usually not heated from the compressive side. For compressed members, especially when the eccentricity of the axial force is small, the load bearing capacity may be overestimated with the 500°C isotherm method in case of fire for members made of high strength concrete (HSC) (Meda & Gambarova, 2002) (Bamonte & Meda, 2005) (Seręga, 2008). The differences in results obtained from the 500°C method for HSC members may to some extent be reduced by assuming a lower than 500°C level of limit temperature (as high strength concretes are characterized with faster reduction in compressive strength with increasing temperature in comparison with normal strength concrete) (Meda & Gambarova, 2002).

The zone method retains the philosophy of the 500°C isotherm method, but considers a more complex and realistic reduced section, whose dimensions depend on the temperature distribution. Also, the characteristics of the concrete in the reduced section (compressive strength and Young's modulus) depend on the temperature distribution (*fib* bulletin 46, 2008). Cyllok and Achenbach (2009) considered the effect of the hindered thermal strains on the compressed reinforcement by a reduced strength of the reinforcing steel. Zilch et al. (2010) introduced the thermal strains in their proposal for the use of the zone method. Finally, Achenbach and Morgenthal (2015) developed the zone method to an enhanced method, to consider the effect of the hindered thermal strains of the reinforcement.

With respect to second-order effects, a general method and two simplified methods— the general method, the curvature method and the stiffness method— are introduced in Eurocode 2 (2004).

The general method is based on non-linear analysis, including both material and geometric non-linearity. This method was introduced and was verified with experimental data for predicting the behaviour of slender columns by Westerberg (1971). Furthermore, it was proven to be valid also for high strength concrete (Claeson, 1998). For non-linear analysis as a design tool, the safety design format has been the subject of various proposals (CEB/FIP bulletin 239, 1997). In the commentary to Eurocode 2 (2008), the design should satisfy two basic criteria: 1) it should be possible to use the same set of material parameters in all parts of the

member in order to avoid discontinuities and computational problems; 2) it should be compatible with the general design format based on partial safety factors. As currently used in the Eurocodes, the general method can be used for direct design applications, but its main application is probably to serve as a basis for developing simplified methods (*fib* bulletin 16, 2002).

The curvature method, also named as model column method (CEB/FIP bulletin 123, 1977), is based on the effective length l_0 and an estimated maximum curvature and is primarily suitable for isolated members with constant normal force and a defined effective length (Eurocode 2, 2004). Robinson et al. (1975) provided a more fundamental basis than curvature method, so-called curvature-based approach in line with the major steps of the “sinusoidal total eccentricity method”. This method is also described by Marí and Hellesland (2003) with some explanations and application conditions.

The stiffness method is based on nominal values of the flexural stiffness, taking into account the effects of cracking, material non-linearity and creep on the overall behaviour (Eurocode 2, 2004). In this method, the nominal second-order moment is determined by linear analysis and the design moment can be expressed by means of a magnification factor (*fib* bulletin 16, 2002). For design purposes, a simple formulation of stiffness, with correction factors for the concrete term but not on the reinforcement term, is provided by the Swedish code BBK 94 (1995). In EN 1992-1-1 (Eurocode 2, 2004), a correction factor is also proposed on the reinforcement term. Furthermore, a quasi-linear theory of elasticity (KLE) method is illustrated in the Dutch concrete code NEN 6720 (NEN, 1995). The KLE-method makes it possible to determine the physical non-linear behaviour for a concrete structure while using the linear theory of elasticity.

Considering second-order effects, imperfections have an influence on the moment capacity of columns, especially for slender columns. EN 1992-1-1 (Eurocode 2, 2004) points out that allowance should be made in the design for uncertainties associated with the prediction of second-order effects. Lie et al. (1984, 1996) firstly considered an estimated eccentricity as the effect of imperfections to compare with the experimental data of concrete columns exposed to fire and combined with concentrated axial loads and later in case of steel columns filled with reinforced concrete. Then, Becque and Rasmussen (2007) investigated the interaction of local and overall buckling of stainless steel I-shaped columns with experimental and numerical methods. Further, Schillinger et al. (2010) developed a finite element

based methodology for the stochastic buckling analysis of imperfect I-section beam-columns. Karmazinova and Melcher (2013) expanded the research to steel-concrete composite columns.

As the general method, the curvature method and the stiffness method are often used for the design of structural members, they are also discussed in **chapter II**. The two simplified methods show a wide deviation when compared to the general method and they are not suitable for all the columns. Therefore, one of the main aims of the Ph.D. research is to give suggestions for the application of these simplified methods as well as the use in case of fire.

I.7. Contemporary research challenges

With respect to concrete columns subjected to fire, most research efforts have been focusing on experimental analysis, numerical analysis and the application of simplified methods. Experiments can indicate the performance of columns in case of fire precisely. However, they are time and cost consuming as well as they are labour-intensive. Besides, a number of tests are required to conclude the fire resistance of columns taking into account parameter variations and considering uncertainties. Therefore, analytical approaches and simplified methods are more used (sometimes after calibration based on the existing experimental data).

Considering second-order effects of columns, the general method, the curvature method as well as the stiffness method are mostly used. The general method is good for its accuracy and flexibility. However, it requires the use of a computer to find solutions (CEB/FIP Bulletin 123, 1977). Regarding the curvature method and the stiffness method, they are proven sometimes to be over-conservative (see **chapter II**).

In order to investigate the performance of columns in fire conditions, in EN 1992-1-2 (Eurocode 2, 2004), on the one hand, tabulated tables of the required minimum dimensions and the axis distances are provided in case of an ISO 834 standard fire of different fire durations. As guidelines for the design, however, they are proven to be sometimes on the unsafe side compared to experimental data (see **chapter IV**). On the other hand, simplified methods provided by Eurocode 2 (2004), the 500°C isotherm method for example are often considered too conservative (see

chapter V). Moreover, in EN 1992-1-2 (Eurocode 2, 2004), no tabulated data is available for design on the basis of a more realistic fire scenario.

Further, columns are not always subject to the pure uniaxial bending. The influence of biaxial bending is also very important. This effect on columns could be more significant in case of fire. In EN 1992-1-1 (Eurocode 2, 2004) and *fib* Model Code 2010 (2012), a simplified criterion proposed by Bresler (1960) is introduced to evaluate the biaxial bending capacity of columns. However, this so-called Bresler approximation has not been validated to be used in case of fire yet. Furthermore, the parameters which determine the application of this approximation in case of fire should be discussed.

The fire resistance of a structural member is known if its material properties, geometrical properties and actions can be precisely known. However, uncertainties always exist due to randomness inherent in nature and the limit of human knowledge (Ayyub and Mc Cuen, 2003). To the best acknowledgement we have been now on the fire resistance of a structural member, however, one should realise that the material or geometrical properties and actions on the structure are of a stochastic nature and hence the response of the structure cannot be determined with certainty (Benjamin and Cornell, 1970). Therefore, a probabilistic treatment is preferential to come to design proposals.

I.8. The outlines and objectives of this thesis

The main goal of the expected research is to investigate the second-order effects of columns in case of fire. As the first step of the investigation, a literature review has briefly been provided in **chapter I**. The developments in the field of thermal properties (radiation, conductivity and convection) and mechanical properties of concrete as well as steel in case of fire has been introduced. Further, different types of fire curves have been presented. The application of standard curves, hydrocarbon curves and parametric curves was discussed. Furthermore, the current simplified methods provided by standards and literature as well as experimental and numerical simulations have been explained. Finally, based on all the studies on the second-order effects of concrete columns exposed to fire, drawbacks and applications of the existing methods have been pointed out.

With respect to simplified methods for columns at ambient temperature, a general method and two simplified methods (curvature method and stiffness method) provided in Eurocode 2 (2004) are presented in **chapter II**. Meanwhile, a nominal stiffness based method— KLE method— provided by the Dutch standard NEN 6720 (1995) is introduced. Considering columns at elevated temperatures, two simplified methods— the 500°C isotherm method and the zone method— as well as an equation for the equivalent stiffness of the reduced concrete section are proposed in EN 1992-1-2 (Eurocode 2, 2004). Finally, an example is given to quantify differences on interaction curves of columns at ambient temperature comparing the curvature method and stiffness method with the general method, taking into account different slenderness ratios. The same columns are investigated in case of an ISO 834 fire using the equivalent stiffness provided by Eurocode 2 (2004).

In **chapter III**, a cross-sectional calculation tool is presented to investigate the combination of axial force and bending moments in columns exposed to fire. Firstly, the material model and thermal transient model for the calculation tool are introduced. The temperature distribution obtained with the tool is compared with Eurocode 2 (2004). Further, the structural model is presented taking into account second-order effects. In order to have an idea of the number of iterations needed to obtain convergence, a parametric study is investigated for different fire durations in case of an ISO 834 standard fire, slenderness ratios and axial loads. Finally, interaction curves calculated with the tool are validated on the basis of experimental data from Meda et al. (2002), background documents of Eurocode 2 (2008), Lie et al. (1984), and experimental data from the Technical University of Braunschweig (Hass, 1986) and the University of Liège (Dotreppe, 1993).

As the calculation tool has been verified with experimental data, the influence of fire parameters such as different fire scenarios, exposed faces as well as fire durations on the load bearing capacity of columns in case of uniaxial bending are presented in **chapter IV**. Firstly, the thermal analysis is illustrated for both a circular cross-section and a square cross-section. Then, a square cross-sectional column with different exposed faces is investigated. Temperature distributions as well as interaction curves are illustrated. Further, the upper limit and the lower limit of the thermal conductivity are adopted, respectively. The differences on the temperature distribution and interaction curves are discussed. Finally, the effects of three types of fire curves are analysed: an ISO 834 standard fire, a hydrocarbon

fire and natural fires provided in Eurocode 2 (2004), taking into account different configurations, reinforcement ratios, axial loads and slenderness ratios.

Tabulated design guidelines provided by Eurocode 2 (2004) for the fire resistance of columns in case of an ISO 834 standard fire are compared with the results obtained with the calculation tool.

The existing simplified methods provided in codes and literature such as the 500°C isotherm method (Eurocode 2, 2004), KLE method (NEN 6720, 1995) are not explicitly mentioning their application areas. What is more, the parameters which might have significant influences are not introduced. Therefore, a parametric study adopting the numerical calculation tool is presented in **chapter V**. Simplified methods and formulas—the 500°C isotherm method (Eurocode 2, 2004), the KLE method (NEN 6720, 1995)— a simplified formula taking into account imperfections as well as a curvature-based method are discussed. Finally, some suggestions and references are proposed for the application of these simplified methods and formulas.

For standard design requirements, both EN 1992-1-1 (Eurocode 2, 2004) and ACI 318 (2011) provide guidelines for the capacity design of columns, as well as the design criterion in case of biaxial bending. For biaxial bending capacity of columns, a simplified method (the so-called Bresler approximation) is proposed by Bresler (1960) and is adopted in many standards (i.e. EN 1992-1-1, ACI 318, *fib* Model Code and etc.). However, the effect of fire on these columns subjected to biaxial bending is not mentioned in the provisions. In order to validate the application of that approach for columns subjected to fire, the basic assumptions and the calculation models adopted in the tool in case of biaxial bending are firstly presented in **chapter VI**. Furthermore, the results obtained with the calculation tool are validated with experimental data from Tan (2013). Then, the applicability of the Bresler approximation is discussed considering a parametric study executed by using the developed calculation tool. Furthermore, suggestions are given for adopting the Bresler approximation in case of fire. Finally, a probabilistic evaluation is made to investigate the effect of the variability of the basic model parameters.

Finally, **chapter VII** gives an overview of the main conclusions and general discussions, summarizes advantages and drawbacks of the developed calculation tool and methods and also proposes possibilities for further research.

CHAPTER II

SIMPLIFIED METHODS PROVIDED IN EUROCODE 2 FOR COLUMNS EXPOSED TO FIRE TAKING INTO ACCOUNT SECOND-ORDER EFFECTS

II.1. Simplified methods for columns at ambient temperature

Concrete columns not only bear vertical loads, but also forces induced by the connection with beams and slabs. As it is complicated to simulate the real structural behaviour of beam-columns, simplifications are usually made. In EN 1992-1-1 (Eurocode 2, 2004), a general method and two simplified methods, the curvature method and the stiffness method, are introduced. Conditions of equilibrium and strain compatibility need to be satisfied at the level of cross-sections. As a simplification of these simplified methods, the critical cross-section as well as a relevant variation of the curvature over the column length is taken into account for the calculation of interaction curves for columns. Furthermore, a quasi-linear theory of elasticity (KLE) method has been introduced in the Dutch concrete code NEN 6720 (NEN, 1995).

II.1.1. General method

The general method is based on a non-linear second-order effects analysis. “General” here refers to the fact that the method can be used for any cross-section of any shape, any axial load and first order moment, any boundary conditions, any stress-strain relations, uniaxial or biaxial bending etc. The general rules for applying such non-linear methods are (Eurocode 2, 2004):

- (1) The non-linear analysis can be used for both ULS (ultimate limit states) and SLS (serviceability limit states), assuming an adequate non-linear behaviour for materials;
- (2) Any inelastic deformation implied by the analysis should be checked for the ultimate limit state;
- (3) The influence of previous load applications may generally be neglected in case of static loads and a monotonic increase of the intensity of actions is assumed;
- (4) The material characteristics which represent the stiffness in a realistic way shall be considered taking into account uncertainties.

For slender structures, where second-order effects cannot be neglected, stress-strain curves for concrete and steel shall be used for the overall analysis.

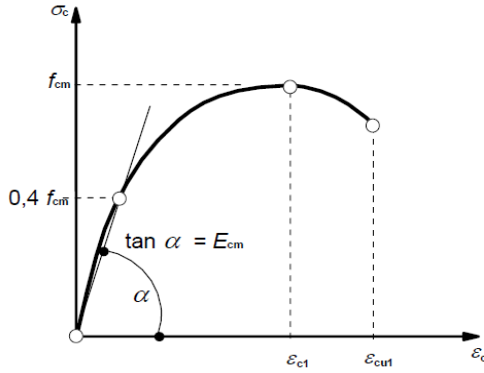


Fig. II.1: Stress-strain relation for structural analysis presented in Eurocode 2 (2004)

The stress-strain curve for concrete under short term uniaxial loading shown in Fig. II.1 is given by:

$$\frac{\sigma_c}{f_{cm}} = \frac{k\eta - \eta^2}{1 + (k-2)\eta} \quad (\text{II.1})$$

where $\eta = \frac{\epsilon_c}{\epsilon_{c1}}$

ϵ_{c1} is the strain at peak stress

$$k = 1.05 E_{cm} \times |\epsilon_{c1}| / f_{cm}$$

Eq. (II.1) is valid for $0 < |\epsilon_c| < |\epsilon_{cu1}|$ where ϵ_{cu1} is the nominal ultimate strain.

Stress-strain diagrams of typical reinforcing steel provided in Eurocode 2 (2004) are shown in Fig. II.2.

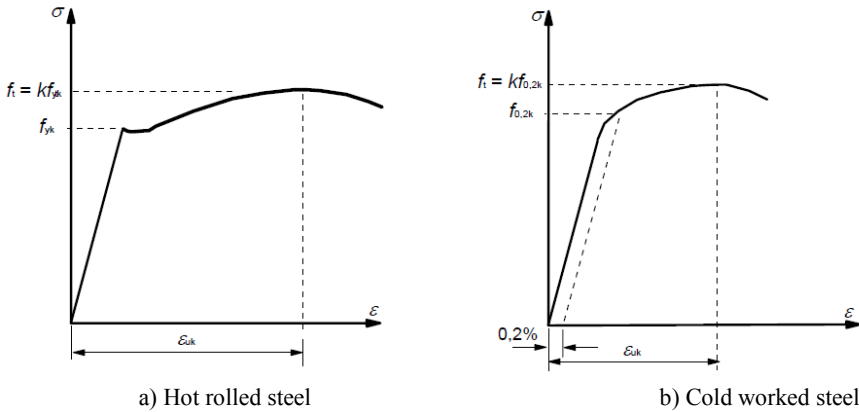


Fig. II.2: Stress-strain diagrams of typical reinforcing steel presented in Eurocode 2 (2004)

The yield stress f_{yk} (or the 0.2% proof stress $f_{0.2k}$) and the tensile strength f_{tk} are obtained as the characteristic value of the yield load and the characteristic maximum load, respectively, in direct axial tension, each divided by the nominal cross-sectional area. The elongation at maximum force ϵ_{uk} for Class A, B and C is given in Annex C of EN 1992-1-1 (Eurocode 2, 2004).

Further, considering the imperfections of a column in case of an eccentric load N (see Fig. II.3), a general homogeneous solution for the sideways displacement $v(x)$ expressed as Eq. (II.2) is given by Archer (1978).

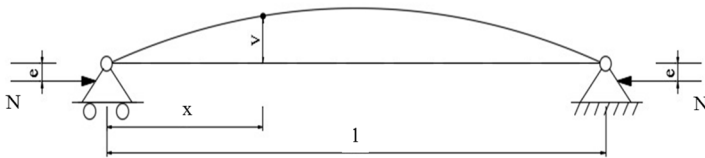


Fig. II.3: Basic calculation model

$$v(x) = A \sin \sqrt{\frac{N}{EI}} x + B \cos \sqrt{\frac{N}{EI}} x + Cx + D \quad (\text{II.2})$$

The boundary condition $v = 0$ at $x = 0$ and $x = l$, and

$$M = EI \frac{d^2 v}{dx^2} = Ne \quad (\text{II.3})$$

enable to find the following solution for the sideway displacement

$$v(x) = -e \left(\frac{1 - \cos \sqrt{\frac{N}{EI}} x}{\sin \sqrt{\frac{N}{EI}}} \sin \sqrt{\frac{N}{EI}} x + \cos \sqrt{\frac{N}{EI}} x - 1 \right) \quad (\text{II.4})$$

In Eq. (II.4), e is the eccentricity of the external load. Based on EN 1992-1-1 (Eurocode 2, 2004), the stiffness of the column can be evaluated as $0.4E_{cd}I_c$ in case of a cracked section while $0.8E_{cd}I_c$ can be considered in case of an uncracked section, where E_{cd} is the design value of the modulus of elasticity of concrete ($E_{cd} = E_{cm} / \gamma_{Ec}$, the recommended value of $\gamma_{Ec} = 1.2$ as well as the modulus of elasticity E_{cm} are provided in Eurocode 2 (2004)) and I_c is second moment of area of the column. Members that are not expected to be loaded above the level which would cause the tensile strength of the concrete to be exceeded anywhere within the member, should be considered to be uncracked. The value of the design tensile strength f_{ctd} is defined as $f_{ctd} = \alpha_{ct} f_{ctk,0.05} / \gamma_c$, where γ_c is the partial factor for concrete ($\gamma_c = 1.5$) and α_{ct} is a coefficient taking account of long-term effects on the tensile strength and of unfavourable effects, resulting from the way the load is applied (the recommended value is 1.0).

In Eurocode 2 (2004), creep is taken into account by multiplying all strain values in the concrete stress-strain diagram with a factor $(1 + \varphi_{ef})$, where φ_{ef} is the effective creep ratio.

II.1.2. Curvature method

The curvature method is based on a lateral deflection v (shown in Fig. II.3), which is determined by the effective length and an estimated maximum curvature of the column. The design moment is:

$$M_{Ed} = M_{0Ed} + M_2 \quad (\text{II.5})$$

where M_{0Ed} is the first-order moment, including the effect of imperfections
 M_2 is the nominal second-order moment

$$M_2 = N_{Ed} \cdot e_2 \quad (\text{II.6})$$

where N_{Ed} is the design value of the axial force

e_2 is the deflection of the calculated point of the structural member
(expressed as v in Fig. II.3)

$$e_2 = (1/R)l_0^2/c \quad (\text{II.7})$$

where $1/R$ is the curvature

l_0 is the effective length

c is a factor depending on the curvature distribution; $c = 10$ is normally used.

$$1/R = K_r \cdot K_\varphi \cdot 1/R_0 \quad (\text{II.8})$$

where K_r is a correction factor depending on the axial load

K_φ is a factor for taking account of creep

$$K_r = \frac{n_u - n_d}{n_u - n_{bal}} \leq 1 \quad (\text{II.9})$$

where $n_d = \frac{N_{Ed}}{A_c f_{cd}}$, the relative axial force

N_{Ed} is the design value of the axial force

$$n_u = 1 + \omega, \quad \omega = \frac{A_s f_{yd}}{A_c f_{cd}}$$

n_{bal} is the value of n at the maximum moment of resistance; the value 0.4 may be used

A_s is the total area of the reinforcement

A_c is the area of the concrete cross-section

$$K_\varphi = 1 + \beta \varphi_{ef} \geq 1 \quad (\text{II.10})$$

where φ_{ef} is the effective creep ratio

$$\beta = 0.35 + \frac{f_{ck}}{200} - \frac{\lambda}{150}; \quad \lambda \text{ is the slenderness ratio}$$

$$1/R_0 = \frac{\varepsilon_{yd}}{0.45d} \quad (\text{II.11})$$

where $\varepsilon_{yd} = \frac{f_{yd}}{E_s}$

d is the effective depth, $d = \frac{h}{2} + i_s$; i_s is the radius of gyration of the total reinforcement area

II.1.3. Stiffness method

This method is based on the nominal stiffness of slender compression members with an arbitrary cross-section, which is estimated by the expression (II.12):

$$EI = K_c E_{cd} I_c + K_s E_s I_s \quad (\text{II.12})$$

where E_{cd} is the design value of the modulus of elasticity of concrete

I_c is the moment of inertia of the concrete cross-section

E_s is the design value of the modulus of elasticity of the reinforcement

I_s is the second moment of area of the reinforcement, about the centre of gravity of the concrete

K_c is a factor for effects of cracking, creep etc.

K_s is a factor for the contribution of the reinforcement

The factors listed in (II.13) can be adopted in Eq. (II.12) when the geometric reinforcement ratio $\frac{A_s}{A_c} \geq 0.002$

$$K_s = 1$$

$$K_c = k_1 k_2 / (1 + \varphi_{ef}) \quad (\text{II.13})$$

where φ_{ef} is the effective creep ratio

k_1 is a factor which depends on the concrete strength class, $k_1 = \sqrt{f_{ck}/20}$ [MPa]

k_2 is a factor which depends on the axial force and the slenderness, $k_2 = n' \cdot \frac{\lambda}{170} \leq 0.20$; $n' = \frac{N_{Ed}}{A_c f_{cd}}$, the relative axial force; λ is the slenderness ratio

As a simplified alternative, the following factors may be used in (II.12) when $\frac{A_s}{A_c} \geq 0.01$:

$$K_s = 0$$

$$K_c = 0.3 / (1 + 0.5\varphi_{ef}) \quad (\text{II.14})$$

Considering the second-order moment, the total design moment may be expressed as (II.15) resulting from a linear analysis:

$$M_{Ed} = M_{0Ed} \left(1 + \frac{\beta}{(N_B/N_{Ed}) - 1} \right) \quad (\text{II.15})$$

where M_{0Ed} is the first-order moment
 N_{Ed} is the design value of the axial load
 N_B is the buckling load based on the nominal stiffness
 β is a factor which depends on the distribution of 1st and 2nd order moments. For isolated members with constant cross-section and axial load, the second-order moment may be assumed to have a sine-shaped distribution.

$$\beta = \pi^2 / c_0 \quad (\text{II.16})$$

where c_0 is a coefficient which depends on the distribution of the first-order moment (for instance, $c_0 = 8$ for a constant first-order moment, $c_0 = 9.6$ for a parabolic and 12 for a symmetric triangular distribution etc.).

II.1.4. KLE-method

The KLE-method is based on the quasi-linear theory of elasticity. In clause 7.2.3 of the Dutch standard NEN 6720 (NEN, 1995), it is stated that the stiffness of the concrete column equals the stiffness of the same structure subjected to a load of $0.8M_{Ed}$. This is based on the assumption that $0.8M_{Ed}$ is an average between the bending moment in the ultimate limit state (ULS) and the serviceability limit state (SLS). In Fig. II.4, a quasi-linear model for the stiffness is presented.

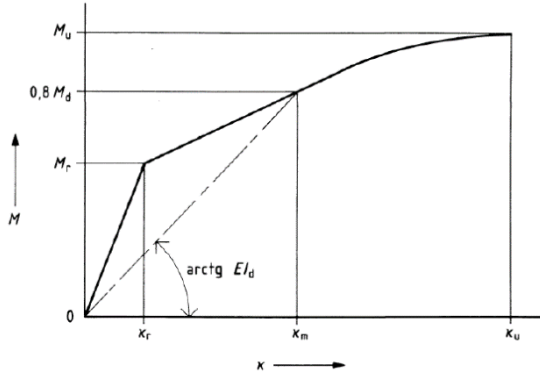


Fig. II.4: Quasi linear stiffness according to Figure 21 of NEN 6720

The stiffness of the structure can be acquired by determining the curvature of a cross-section subjected to a load effect of $0.8 M_{Ed}$. The resulting stiffness equals to:

$$EI_d = \frac{0.8M_{Ed}}{\kappa_{0.8M_{Ed}}} \quad (II.17)$$

where $\kappa_{0.8M_{Ed}}$ is the curvature of a cross-section subjected to a load effect of $0.8 M_{Ed}$

The fictive modulus of elasticity E_f is subsequently determined by dividing EI_d with the second moment of inertia of the uncracked cross-section.

Once the stiffness is estimated, the buckling load can be calculated as:

$$N_B = \frac{\pi^2 EI_d}{l_0^2} \quad (II.18)$$

where EI_d is a representative bending stiffness
 N_B is the buckling load
 l_0 is the effective length of the column

Considering the buckling load of columns subjected to fire, this method will be discussed in **chapter V** more extensively.

II.2. Simplified design methods for columns at elevated temperatures

With respect to the fire in a compartment, estimation of the temperature of gases is of importance. Enclosure gas temperature resulting from fire can vary greatly depending on the position in the enclosure. Since we are concerned mainly with that period of the fire during which structural damage would occur, the pre-flashover stage may be neglected as average temperatures are relatively low. Further, as the time frame at the post-flashover stage is relatively long (often 0.5 to 3 hours), the fire is assumed to have caused flashover at a very early stage and the design fire is usually given as a temperature-time curve (Drysdale, 1999). In order to simplify the fire to a temperature-time curve, the most commonly used assumption is the one-zone model, where the entire compartment is assumed to be filled with fire gases of uniform temperature. The calculations have a basis in the energy and mass balance of the compartment and the objective is to arrive at a temperature-time curve covering the whole process of fire development (Karlsson & Quintiere, 2000). Based on the assumption, temperature-time curves are adopted to investigate the fire resistance of concrete columns in the current research.

Furthermore, buckling of concrete columns is a major issue in fire design, since heating of the columns will result in damage of the outer layers of the member as well as a decrease of the modulus of elasticity at the inner layers. Due to the combination of a decrease of the material strengths and a reduction of the stiffness, second-order effects can be significant in case of fire although their effect is sometimes negligible at ambient temperature. Moreover, the second-order effects become even more explicit when considering non-uniform heating along the height and perimeter of a column, as it would appear in reality. Hence, an easy-to-use method is required to study the behaviour of columns in case of fire. In EN 1992-1-2 (Eurocode 2, 2004), two simplified methods — the 500°C isotherm method and the zone method — and an equation for the equivalent stiffness of the reduced concrete section are proposed.

II.2.1. 500°C isotherm method

The 500°C isotherm method is applicable to a standard fire exposure as well as any other time-heating regimes which cause similar temperature fields in the structural member exposed to fire. The hypothesis of the 500°C isotherm method is that concrete at a temperature of more than 500°C is neglected in the calculation of the load bearing capacity, while concrete at a temperature below 500°C is assumed to retain its full strength (Eurocode 2, 2004). However, the temperature of the individual reinforcing bars is taken as the real temperature in the center of the bar. It is worth pointing out that the reinforcing bar whose temperature is in excess of 500°C is included in the calculation of the ultimate load-bearing capacity of the fire exposed cross-section.

II.2.2. Zone method

The zone method is only applicable to the standard temperature-time curve. However, this method is more accurate than the 500°C isotherm method especially for columns. The basic principle of this method is that the fire damaged cross-section is represented by a reduced cross-section ignoring a damaged zone of thickness a_z at the fire exposed sides (Eurocode 2, 2004). The reduction of strength and cross-section for sections exposed to fire is shown in Fig. II.5, where a_z is the thickness of a damaged zone of the cross-section at the fire exposed sides, $k_c(\theta_M)$ is a reduction coefficient for concrete strength at point M.

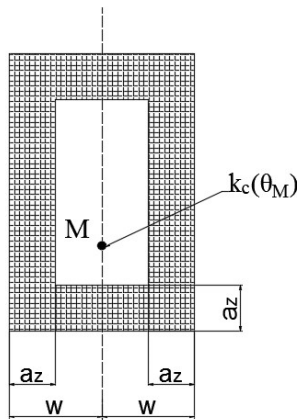


Fig. II.5: Reduction of strength and cross-section for sections exposed to fire

Take a column with two opposite sides exposed to fire for instance, the division into zones for use in calculation of strength reduction is shown in Fig. II.6, where

the half thickness of the column is divided into q ($q \geq 3$) parallel zones of equal thickness.

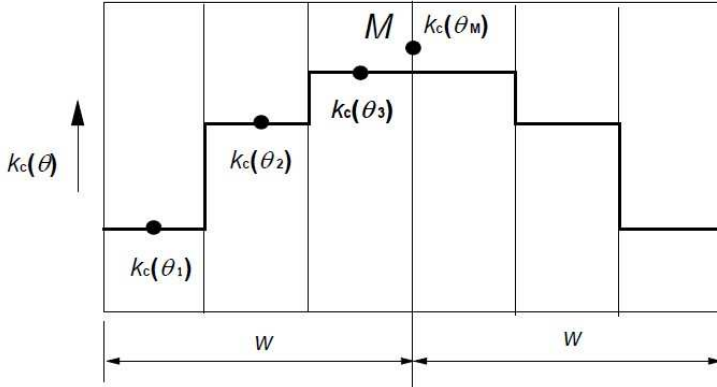


Fig. II.6: Division of a column, with the opposite sides exposed to fire, into zones for use in calculation of strength reduction and a_z values

As it is shown in Fig. II.6, the mean reduction coefficient $k_{c,p}$ is expressed as:

$$k_{c,p} = \frac{(1 - \frac{0.2}{q})}{q} \sum_{i=1}^q k_c(\theta_i) \quad (\text{II.19})$$

where q is the number of parallel zones in the width w

w is half the total width

p is the number of segments

The width of the damaged zone may be calculated as:

$$a_z = w \left[1 - \frac{k_{c,p}}{k_c(\theta_M)} \right] \quad (\text{II.20})$$

where $k_c(\theta_M)$ denotes the reduction coefficient for concrete at point M (see Fig. II.5)

II.2.3. Equivalent stiffness of columns

According to EN 1992-1-2 (Eurocode 2, 2004), the effective length of the column in case of fire $l_{o, fi}$ may be taken as equal to l_0 at ambient temperature as a safe simplification. In order to obtain a more accurate estimation of the second-order effects of columns in case of fire, the decrease of its stiffness should be taken into account. A reduced cross-section of a column presented in Annex B.2 of Eurocode 2 (2004) may be used. The equation of the equivalent stiffness of the reduced concrete section is given by:

$$(EI)_Z = [k_c(\theta_M)]^2 \cdot E_c \cdot I_{Zc} + E_s(\theta) \cdot I_{Zs} \quad (II.21)$$

where $k_c(\theta_M)$ is a reduction coefficient for concrete at point M (see EN1992-1-2 B.2)

E_c is the elastic modulus of the concrete at normal temperature

I_{Zc} is the moment of inertia of the reduced concrete section

$E_s(\theta)$ is the elastic modulus of reinforcement at elevated temperatures

I_{Zs} is the moment of inertia of the reinforcing bars

II.3. Examples

In order to show the differences between these methods on interaction curves of columns, a comparison is made between the curvature method, the stiffness method and the general method based on Eq. (II.4). First, a simply supported column is chosen as a basic model. The properties of this column are: cross-section 300 mm × 300 mm, 4 bars of diameter 25 mm and concrete cover 30 mm; 20°C concrete compressive strength $f_{ck} = 80$ MPa, mechanical reinforcement ratio $\omega = 0.2$ and Young's modulus of steel $E_s = 2 \times 10^5$ N/mm². Considering second-order effects of columns for different slenderness ratios $\lambda = 0, 35, 70, 105$ and 140, interaction curves are shown in Fig. II.7, where $n' = \frac{N_{Ed}}{A_c f_{cd}}$ and $m_x = \frac{M_{Ed}}{A_c f_{cd} h}$, A_c is the cross sectional area of concrete, A_s is the cross sectional area of the reinforcing bars, f_{cd} is the design value of concrete compressive strength, f_{yd} is the design yield stress of the reinforcement, N_{Ed} is the design value of the applied axial force and M_{Ed} is the design value of the bending moment. It is worth mentioning that $0.4E_{cd}I_c$ is adopted in case of a cracked section (see Fig. II.7) while $0.8E_{cd}I_c$ is taken for an uncracked section when the general method is considered.

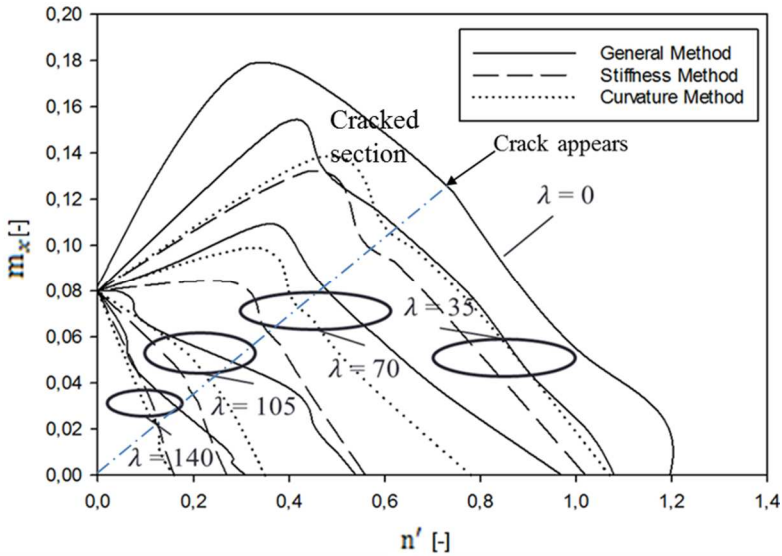


Fig. II.7: Comparison of interaction curves of columns for different slenderness ratios adopting the general method, the stiffness method and the curvature method

As it can be seen in Fig. II.7, both simplified methods show a rather wide deviation when compared to the general method. However, the curvature method predicts comparatively reasonable results for low to moderate slenderness, although the prediction is too conservative in case of high slenderness ratios. This is because the factor K_r defined by Eq. (II.9) gives no reduction of the curvature at all in case $n' < 0.4$, and in case of high slenderness ratios this parameter is always less than 0.4. The same holds for the stiffness method. The prediction from the stiffness method is always more conservative than the one from the curvature method. It is worth pointing out that the prediction of the bending moment capacity from these two simplified methods in case of $\lambda = 35$ is sometimes on the unsafe side.

Further, the equivalent stiffness given by Eq. (II.21) is adopted to calculate the columns shown in Fig. II.7 exposed to an ISO 834 fire. Interaction curves of columns for different slenderness ratios in case of fire durations equal to 30 minutes, 60 minutes and 90 minutes are presented in Figs. II.8, II.9 and II.10, respectively.

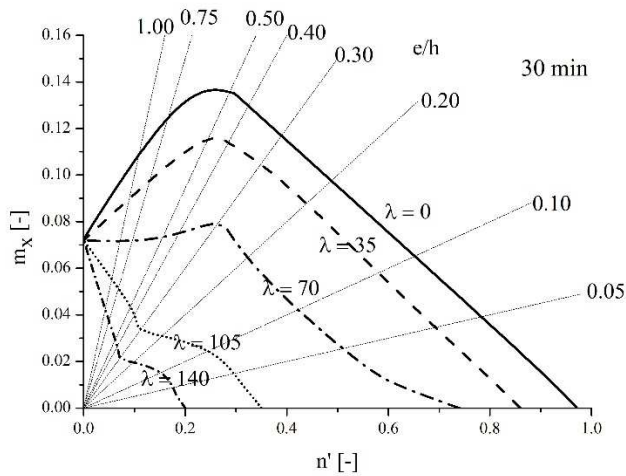


Fig. II.8: Interaction curves for columns of different slenderness in case of an ISO 834 fire for a fire duration of 30 minutes

The dotted lines in Fig. II.8 represent the first-order relationship between normal force and bending moment for different eccentricities e/h and a slenderness ratio $\lambda = 0$. The intersections of the dotted lines with the interaction curve for $\lambda = 0$ indicate the maximum resisting normal force for the different eccentricities considering first-order effects. In Fig. II.9, both a first-order relationship (solid line) between n' and m_x and a second-order relationship (dashed line) are visualized. From Fig. II.9, we can see that second-order effects are significant in case of slender columns. It shows the first-order effects of bending moments $M_1 = Ne$ and the second-order effects of bending moments $M_2 = N\Delta$. Further, as it is shown in Fig II.9, based on the slenderness ratio there are three modes of failure of reinforced concrete columns, i.e. short columns which consider the column failure mode due to pure compression, material failure which happens when the stresses in steel and concrete reach their yield stress and stability failure for which the reinforcement steel and concrete reach their yield stress even for small loads and fail due to lateral elastic buckling.

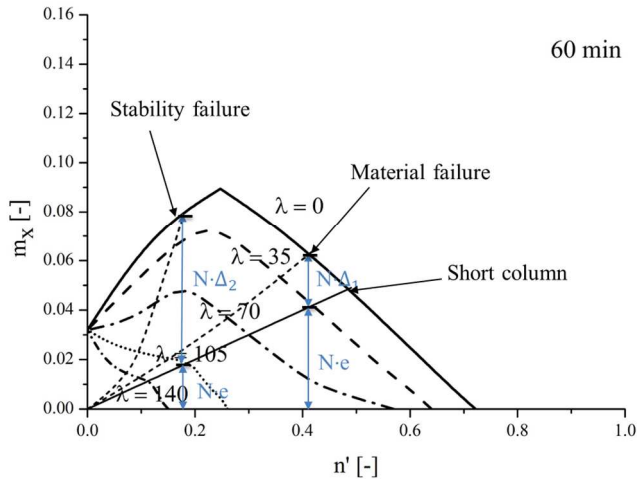


Fig. II.9: Interaction curves for columns of different slenderness in case of an ISO 834 fire for a fire duration of 60 minutes

In Fig. II.9, second-order effects in the case of columns of $\lambda = 140$ are much larger than first-order effects, while for the case of $\lambda = 35$ the second-order effects are smaller. Therefore, second-order effects need to be considered in case of slender columns. In addition, comparing the cases at 0 min, 30 min and 60 min fire duration, it is found that the load bearing capacity of columns decreases slightly during the fire from 0 min to 30 min, while there is a significant reduction from 30 min to 60 min.

Finally, Interaction curves of columns for different slenderness in case of an ISO 834 fire for a fire duration of 90 minutes are presented in Fig. II.10.

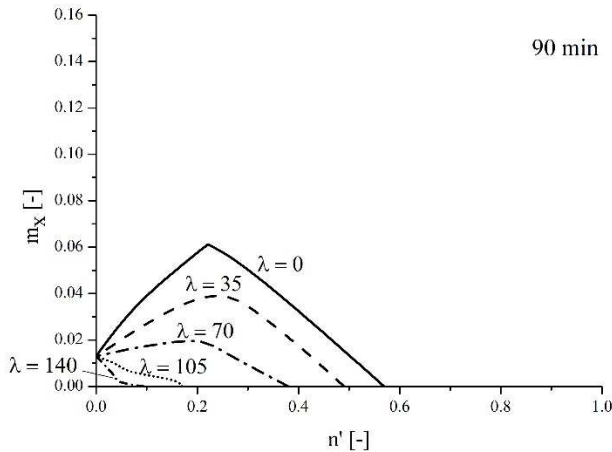


Fig. II.10: Interaction curves for columns of different slenderness in case of an ISO 834 fire for a fire duration of 90 minutes

In Fig. II.10, it is seen that the maximum bending moment capacity of the cross-section in case of 90 minutes fire is about two third as that in case of 60 minutes fire and 45% as that in case of 30 minutes. Considering second-order effects of columns exposed to fire, the decrease on the moment capacity is more significant. Therefore, it is important to investigate the behaviour of columns in case of fire.

II.4. Conclusions

The curvature method and the stiffness method are mostly used to obtain the capacity of columns at ambient temperature. It is proven that these two simplified methods are applicable at elevated temperatures. Compared with the general method, the curvature method predicts comparatively reasonable results for low to moderate slenderness, although the prediction is too conservative in case of high slenderness ratios while the stiffness method always gives conservative results for the given example. As a simplification, both these methods can be used for evaluating the fire resistance of columns. However, the results obtained with the simplified methods are not precise enough to be taken for the fire resistance design. Therefore, it is significant to investigate the parametric influence of these methods and to adapt them for the application in case of fire.

Furthermore, with respect to 500°C isotherm method and the zone method, they are often adopted for calculating the capacity of the structural members exposed to fire. However, the results obtained with the 500°C isotherm method are over conservative (**chapter V**) and the zone method can be only used in case of a standard fire. Hence, it is necessary to find an efficient calculation tool which can be adopted for all kinds of time-heating regimes and fire scenarios.

Above all, simplified methods may be adopted to predict interaction curves of columns in case of ambient temperature and fire. However, these predictions are sometimes either not safe or too conservative. Hence, it is essential to find and validate an easy-to-use design tool to analyze the fire resistance of columns.

CHAPTER III

NUMERICAL METHODS FOR SLENDER COLUMNS EXPOSED TO FIRE TAKING INTO ACCOUNT SECOND-ORDER EFFECTS

Structural fire analysis consists of an integrated approach of both transient thermal analysis and structural analysis. Transient thermal analysis, on the one hand, is a procedure to obtain the temperature distribution by considering fire effects and its influence on the material density, the thermal conductivity, the specific heat capacity and the convection coefficient. On the other hand, the structural deformations as well as the stress and strain increase in the case of fire are quantified using a structural analysis. In this chapter, a numerical tool which includes both the thermal and the structural analysis is elaborated.

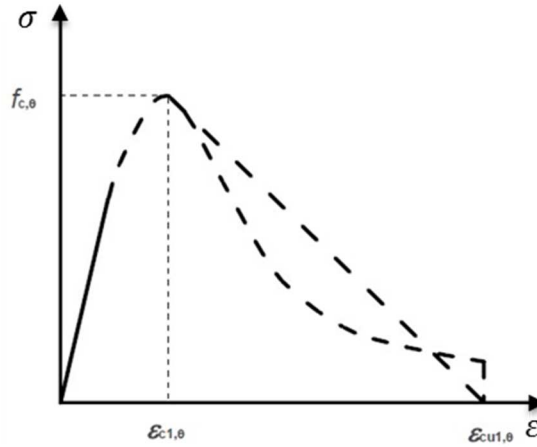
III.1. Material models

In order to study the combination of axial force (N) and bending moments (M) in columns subjected to fire, a numerical method is introduced, based on cross-section calculations and the material models of EN 1992-1-2 (Eurocode 2, 2004).

III.1.1. Concrete

III.1.1.1. Stress-strain relationship for concrete

The stress-strain relationship shown in Fig. III.1 is defined by two parameters: the compressive strength $f_{c,\theta}$ and the strain $\varepsilon_{c1,\theta}$ corresponding to $f_{c,\theta}$. The values of these parameters are a function of the concrete temperature. As a conservative approach, the tensile strength of concrete is normally neglected (Eurocode 2, 2004).



Range	Stress $\sigma(\theta)$
$\varepsilon \leq \varepsilon_{c1,\theta}$	$\frac{3\varepsilon f_{c,\theta}}{\varepsilon_{c1,\theta} \left[2 + \left(\frac{\varepsilon}{\varepsilon_{c1,\theta}} \right)^3 \right]}$
$\varepsilon_{c1,\theta} < \varepsilon \leq \varepsilon_{cu1,\theta}$	For numerical purposes a descending branch should be adopted. Linear or non-linear models are permitted. In this Ph.D., a linear model is adopted in our calculation tool.

Fig. III.1: Mathematical model for stress-strain relationship of concrete under compression at elevated temperatures

III.1.1.2. Thermal and physical properties of concrete

(1) Thermal elongation

In EN 1992-1-2 (Eurocode 2, 2004), the thermal strain $\varepsilon_{c,th}(\theta)$ of concrete is determined with reference to the length of concrete elements at 20 °C:

Siliceous aggregates:

$$\varepsilon_{c,th}(\theta) = -1.8 \times 10^{-4} + 9 \times 10^{-6}\theta + 2.3 \times 10^{-11}\theta^3 \quad \text{for } 20^\circ\text{C} \leq \theta \leq 700^\circ\text{C}$$

$$\varepsilon_{c,th}(\theta) = 14 \times 10^{-3} \quad \text{for } 700^\circ\text{C} < \theta \leq 1200^\circ\text{C}$$

Calcareous aggregates:

$$\varepsilon_{c,th}(\theta) = -1.2 \times 10^{-4} + 6 \times 10^{-6}\theta + 1.4 \times 10^{-11}\theta^3 \quad \text{for } 20^\circ\text{C} \leq \theta \leq 805^\circ\text{C}$$

$$\varepsilon_{c,th}(\theta) = 12 \times 10^{-3} \quad \text{for } 805^\circ\text{C} < \theta \leq 1200^\circ\text{C}$$

(2) Specific heat

The specific heat $c_p(\theta)$ of dry concrete (moisture content 0%) is determined as follows:

Siliceous and calcareous aggregates:

$$c_p(\theta) = 900 \text{ (J/kg K)} \quad \text{for } 20^\circ\text{C} \leq \theta \leq 100^\circ\text{C}$$

$$c_p(\theta) = 900 + (\theta - 100) \text{ (J/kg K)} \quad \text{for } 100^\circ\text{C} < \theta \leq 200^\circ\text{C}$$

$$c_p(\theta) = 1000 + (\theta - 200)/2 \text{ (J/kg K)} \quad \text{for } 200^\circ\text{C} < \theta \leq 400^\circ\text{C}$$

$$c_p(\theta) = 1100 \text{ (J/kg K)} \quad \text{for } 400^\circ\text{C} < \theta \leq 1200^\circ\text{C}$$

where θ is the concrete temperature ($^\circ\text{C}$)

In Fig. III.2, $c_p(\theta)$ (J/kg K) is illustrated for different moisture contents of 0%, 1.5% and 3%.

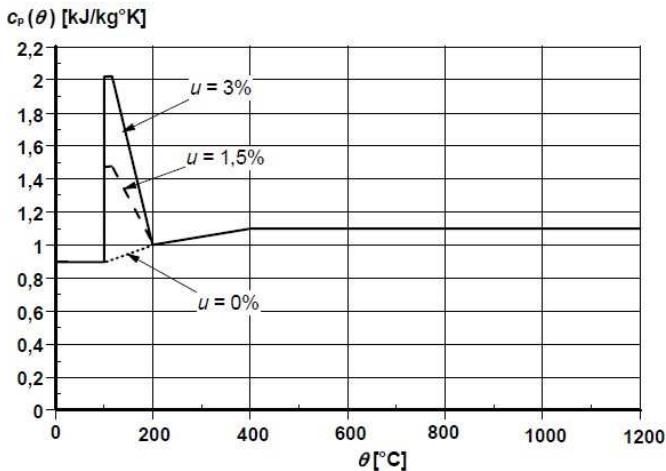


Fig. III.2: Specific heat in case of moisture contents of 0%, 1.5% and 3% by weight for siliceous and calcareous concrete

As shown in Fig. III.2, for concrete that is not fully dry, the specific heat $c_p(\theta)$ starts to show a local peak at 100 °C, then it remains constant between 100°C and 115°C and finally it decreases between 115°C and 200 °C; for dry concrete, it is assumed that $c_p(\theta)$ increases linearly from 900 J/kg K at 100°C to 1000 J/kg K at 200°C. For other moisture contents, a linear interpolation is acceptable (Eurocode 2, 2004).

Considering water loss, the variation of density with temperature is defined as:

$$\begin{aligned} \rho(\theta) &= \rho(20^\circ\text{C}) && \text{for } 20^\circ\text{C} \leq \theta \leq 115^\circ\text{C} \\ \rho(\theta) &= \rho(20^\circ\text{C}) \cdot (1 - 0.02(\theta - 115)/85) && \text{for } 115^\circ\text{C} \leq \theta \leq 200^\circ\text{C} \\ \rho(\theta) &= \rho(20^\circ\text{C}) \cdot (0.98 - 0.03(\theta - 200)/200) && \text{for } 200^\circ\text{C} \leq \theta \leq 400^\circ\text{C} \\ \rho(\theta) &= \rho(20^\circ\text{C}) \cdot (0.95 - 0.07(\theta - 400)/800) && \text{for } 400^\circ\text{C} \leq \theta \leq 1200^\circ\text{C} \end{aligned}$$

(3) Thermal conductivity

The thermal conductivity λ_c of concrete is given between lower and upper limit values in EN 1992-1-2 (Eurocode 2, 2004).

The upper limit of the thermal conductivity λ_c of normal weight concrete is calculated by:

$$\lambda_c = 2 - 0.2451(\theta/100) + 0.0107(\theta/100)^2 \text{ [W/m K]} \quad \text{for } 20^\circ\text{C} \leq \theta \leq 1200^\circ\text{C}$$

where θ is the concrete temperature (°C)

The lower limit of the thermal conductivity λ_c of normal weight concrete is determined by:

$$\lambda_c = 1.36 - 0.136(\theta/100) + 0.0057(\theta/100)^2 \text{ [W/m K]} \quad \text{for } 20^\circ\text{C} \leq \theta \leq 1200^\circ\text{C}$$

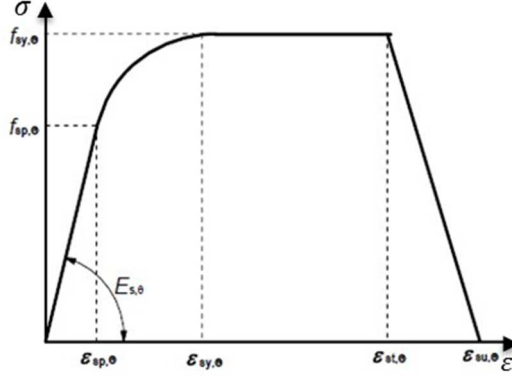
where θ is the concrete temperature (°C)

Temperature profiles in Annex A of EN 1992-1-2 are based on the lower limit of thermal conductivity.

III.1.2. Reinforcing steel

III.1.2.1. Stress-strain relationship of reinforcing steel

The stress-strain relationship of reinforcing steel shown in Fig. III.3 is defined by three parameters: the slope of the linear elastic range $E_{s,\theta}$, the proportional limit $f_{sp,\theta}$ and the maximum stress level $f_{sy,\theta}$.



Range	Stress $\sigma(\theta)$	Tangent modulus
$\varepsilon_{sp,\theta}$	$\varepsilon E_{s,\theta}$	$E_{s,\theta}$
$\varepsilon_{sp,\theta} \leq \varepsilon \leq \varepsilon_{sy,\theta}$	$f_{sp,\theta} - c + \frac{b}{a} [a^2 - (\varepsilon_{sy,\theta} - \varepsilon)^2]^{0.5}$	$\frac{b(\varepsilon_{sy,\theta} - \varepsilon)}{a[a^2 - (\varepsilon - \varepsilon_{sy,\theta})^2]^{0.5}}$
$\varepsilon_{sy,\theta} \leq \varepsilon \leq \varepsilon_{st,\theta}$	$f_{sy,\theta}$	0
$\varepsilon_{sy,\theta} \leq \varepsilon \leq \varepsilon_{su,\theta}$	$f_{sy,\theta} [1 - \frac{\varepsilon - \varepsilon_{st,\theta}}{\varepsilon_{su,\theta} - \varepsilon_{st,\theta}}]$	-
$\varepsilon = \varepsilon_{su,\theta}$	0	-
Parameter	$\varepsilon_{sy,\theta} = \frac{f_{sp,\theta}}{E_{s,\theta}} f_{sy,\theta} = 0.02 \quad \varepsilon_{st,\theta} = 0.15 \quad \varepsilon_{su,\theta} = 0.2$	
Functions	$a^2 = (\varepsilon_{sy,\theta} - \varepsilon_{sp,\theta})(\varepsilon_{sy,\theta} - \varepsilon_{sp,\theta} + \frac{c}{E_{s,\theta}})$ $b^2 = c(\varepsilon_{sy,\theta} - \varepsilon_{sp,\theta})E_{s,\theta} + c^2$ $c = \frac{(f_{sy,\theta} - f_{sp,\theta})^2}{(\varepsilon_{sy,\theta} - \varepsilon_{sp,\theta})E_{s,\theta} - 2(f_{sy,\theta} - f_{sp,\theta})}$	

Fig. III.3: Mathematical model for stress-strain relationships of reinforcing steel at elevated temperatures

III.1.2.2. Thermal elongation of reinforcing steel

In EN 1992-1-2 (Eurocode 2, 2004), the thermal strain $\varepsilon_{s,\theta}$ of steel is determined with reference to the length at 20 °C:

$$\varepsilon_s(\theta) = -2.416 \times 10^{-4} + 1.2 \times 10^{-5}\theta + 0.4 \times 10^{-8}\theta^2 \text{ for } 20^\circ\text{C} \leq \theta \leq 750^\circ\text{C}$$

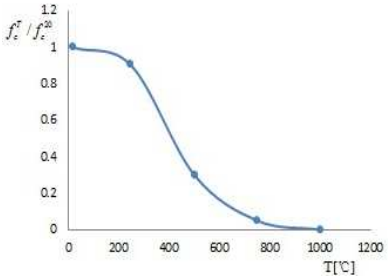
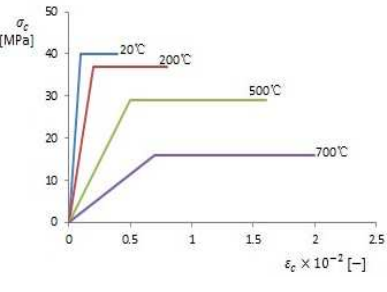
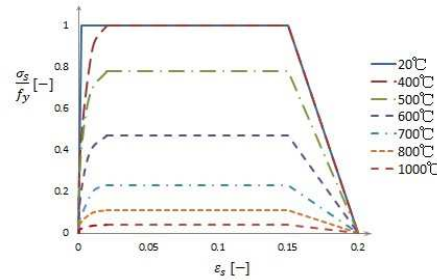
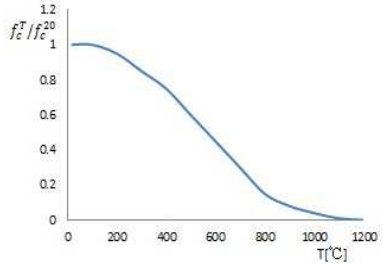
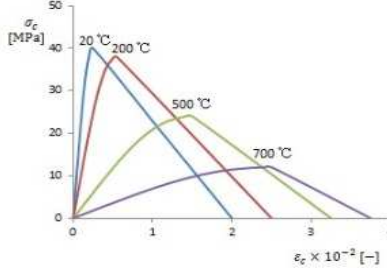
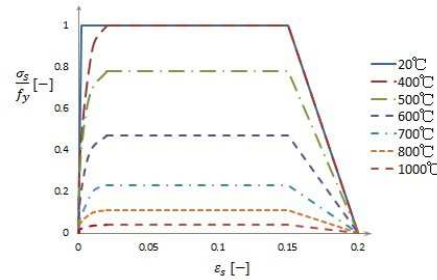
$$\varepsilon_s(\theta) = 11 \times 10^{-3} \text{ for } 750^\circ\text{C} \leq \theta \leq 860^\circ\text{C}$$

$$\varepsilon_s(\theta) = -6.2 \times 10^{-3} + 2 \times 10^{-5}\theta \text{ for } 860^\circ\text{C} \leq \theta \leq 1200^\circ\text{C}$$

III.1.3. Comparison of material models

In order to verify the numerical tool, a comparison of the material model adopted in our numerical tool and the model based on tests from Meda et al. (2002) is shown in Table III.1. Further on in this chapter, interaction curves based on these two material models are compared and discussed.

Table III.1: Comparison of material models

	The ratio of the concrete compressive strength at elevated temperatures to the 20 °C concrete compressive strength	Stress-strain laws of concrete in compression at elevated temperatures	Stress-strain relationships of reinforcing steel in tension at elevated temperatures
<p>Meda's model (2002)</p>			
<p>Material model as implemented in this Ph.D. in accordance to EN 1992-1-2</p>			

III.2. Transient thermal model

The heat transfer and temperature calculation is based on Fourier's law for conduction, Newton's law for convection and Stefan-Boltzmann's law for radiation. Consequently, the heat flow between nodes of a cross-section can be calculated by setting up relationships within a time-dependent matrix. For the transient heat calculation, we need to distinguish between two cases: elements which are directly exposed to the surroundings and elements located in the interior of the column. The heat flow of the external surface area directly exposed to the fire is governed by (Eurocode 2, 2004):

$$\Delta H = \alpha_c \cdot (\theta_g - \theta_m) + \phi \cdot \varepsilon_m \cdot \varepsilon_f \cdot \sigma \cdot [(\theta_r + 273)^4 - (\theta_m + 273)^4] \quad (\text{III.1})$$

where α_c is the coefficient of heat transfer by convection [W/ m²K]
 ϕ is the configuration factor which measures the fraction of the total radiative heat leaving a given radiating surface that arrives at a given receiving surface
 ε_m is the concrete surface emissivity of the member, $\varepsilon_m = 0.7$
 ε_f is the emissivity of the fire, generally taken as 1.0
 σ is the Stephan Boltzmann constant ($= 5.67 \times 10^{-8}$ W / m²K⁴)
 θ_g is the gas temperature in the vicinity of the fire exposed member [°C]
 θ_r is the effective radiation temperature of the fire environment [°C]
 θ_m is the surface temperature of the member [°C]

The heat flow between internal surfaces in one direction (shown in Fig. III.4) is calculated as Eq. (III.2) which is derived from Fourier's law (Eurocode 2, 2004):

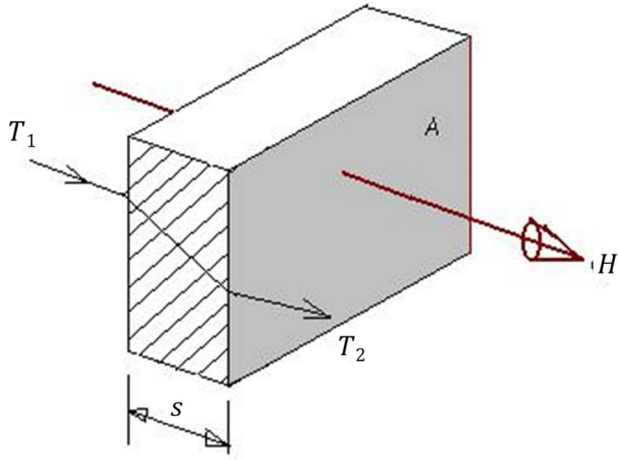


Fig. III.4: The heat flow between internal surfaces

$$\Delta H = \lambda_c \cdot A \cdot \frac{T_1 - T_2}{s} \quad [\text{W/m}^2] \quad (\text{III.2})$$

where λ_c is the thermal conductivity

A is the surface area

T_1, T_2 are the temperatures of the internal surfaces [$^{\circ}\text{C}$]

s is the distance between nodes [m]

As the first step for the node temperature calculation, the cross-section under consideration is discretized into small elements. A 1 mm×1 mm square is selected as a basic calculation element. Considering different boundary conditions (fire duration, exposed surface, heat transfer direction, etc.), a program implemented in (Matlab, 2013) has been developed in the current work to calculate the temperature distribution for different fire exposed surfaces.

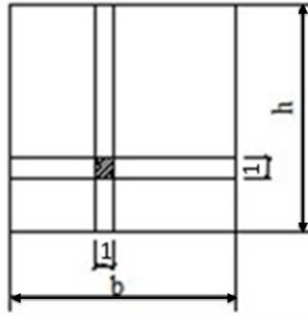
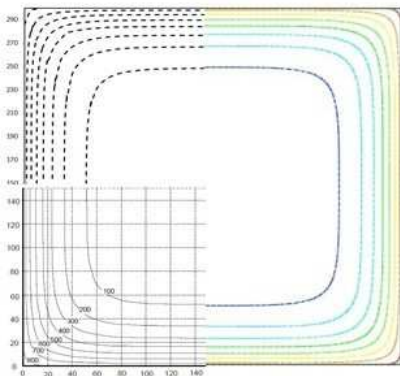


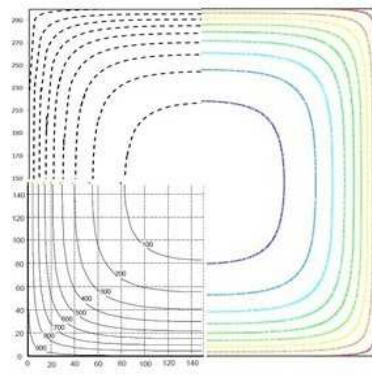
Fig. III.5: Cross-section discretization

The temperature distribution of the cross-section is first calculated with the proposed methodology and validated by a comparison with the finite element program (DIANA, 2012) and Eurocode 2 provisions (Fig. III.6). For the temperature simulation, the lower limit of the thermal conductivity, a concrete moisture content of 1.5% and a concrete density of 2300 kg/m³ are considered.



Black dashed line - MATLAB
 Colorful dashed line - DIANA
 Black solid line - Eurocode 2

(a)



Black dashed line - MATLAB
 Colorful dashed line - DIANA
 Black solid line - Eurocode 2

(b)

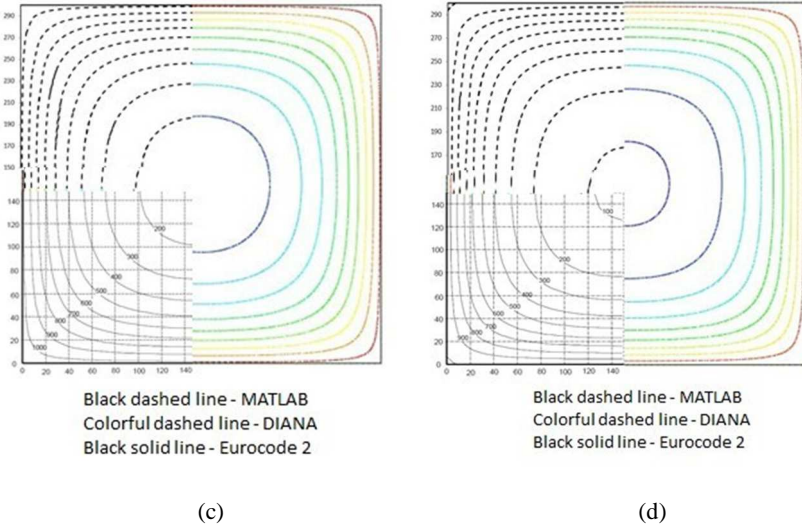


Fig. III.6: Comparison of the temperature distribution calculated using the proposed methodology implemented in a Matlab routine, with graphs given in EN 1992-1-2 and results obtained with the finite element program DIANA at (a) 30 min, (b) 60 min, (c) 90 min, (d) 120 min

From Fig. III.6, it becomes clear that the temperature distribution prediction from the newly developed routine (Matlab, 2013) is in good agreement with EN 1992-1-2 Annex A (Eurocode 2, 2004) and the results obtained from the finite element software analysis (DIANA, 2012).

Consequently, node temperatures from this temperature calculation will be implemented into the cross-sectional structural analysis model (also implemented in a routine (Matlab, 2013)) to calculate interaction curves of columns exposed to fire.

The thermal strain of concrete can be considered for different types of aggregates. Taking siliceous aggregates for instance, a formula of the thermal strain presented in EN 1992-1-2 (Eurocode 2, 2004) is adopted in the calculation performed within this Ph.D.:

$$\varepsilon_{c,th}(\theta) = \min\{-1.8 \times 10^{-4} + 9 \times 10^{-6}\theta + 2.3 \times 10^{-11}\theta^3, 14 \times 10^{-3}\} \quad (\text{III.3})$$

with θ the node temperature

III.3. Structural model

The same cross-sectional discretization as used for the temperature calculation is used for the structural analysis. The mechanical strain is expressed as follows (*fib* Bulletin 46, 2008):

$$\varepsilon_{\text{mech}(\xi,\eta)} = \varepsilon_{\text{tot}} - \varepsilon_{\text{th}} = \varepsilon_0 + \chi_0 \eta - \varepsilon_{\text{th}} \quad (\text{III.4})$$

where ε_{tot} is the total strain

ε_{th} is the thermal strain

ε_0 is the strain at the centroid

χ_0 is the curvature

η is the distance between the calculated point and the centroid point

In EN 1992-1-2 (Eurocode 2, 2004), the transient strain is implicitly considered in the mechanical strain term. The stress-strain curves of concrete and reinforcing bars given in Eurocode 2 (2004) are adopted in this paper.

In Fig. III.7, the relationship between the total strain, the thermal strain and the mechanical strain is illustrated.

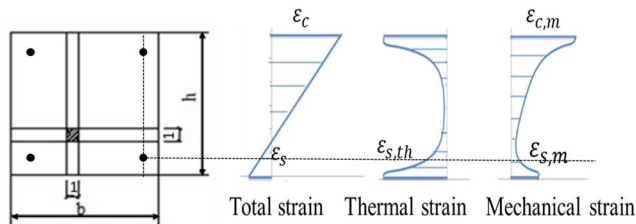


Fig. III.7: Total, thermal and mechanical strain

In order to obtain the cross-sectional structural resistance, various possibilities of limit state design are explained in (Caldas et al., 2010) and shown in Fig. III.8—a limit state is conventionally attained whenever $\varepsilon_{\text{mech}(\xi,\eta)}$ in any fiber of the cross-section or reinforcement reaches its temperature-dependent compressive strain limit value ε_{cu} taken from a stress-strain curve. Compression strains are considered to be positive.

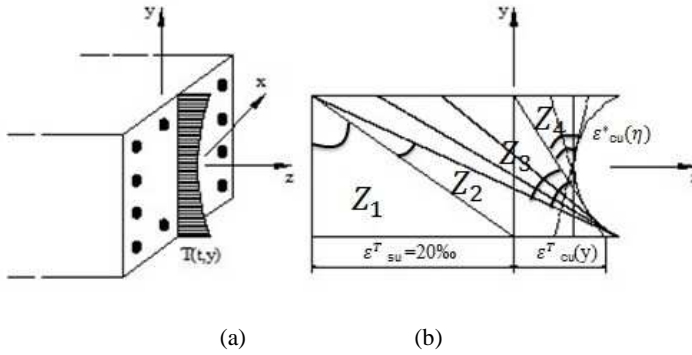


Fig. III.8: (a) Temperature distribution along the height direction; (b) strain profiles and strain limits (Caldas et al., 2010)

Assuming the geometry and temperature profiles in all cross-sections identical to the critical one, deflections along the column are obtained taking into account second-order effects.

EN 1992-1-1 (Eurocode 2, 2004) states that second-order effects may be ignored if the slenderness λ is below a certain value λ_{lim} .

$$\lambda = \frac{l_0}{\sqrt{I/A}} \quad (III.5)$$

$$\lambda_{lim} = 20 \cdot A \cdot B \cdot C \quad (III.6)$$

where

l_0 is the effective column length

I is the second moment of area

A is the cross-sectional area

$$A = 1 / (1 + 0.2\varphi_{ef})$$

$$B = \sqrt{(1 + 2\omega) / \eta'}$$

$$C = 1.7 - r_m$$

φ_{ef} is the effective creep ratio; if φ_{ef} is not known, $A = 0.7$

$\omega = A_s f_{yd} / (A_c f_{cd})$ is the mechanical reinforcement ratio; if ω is not known, $B = 1.2$

A_s is the total area of longitudinal reinforcement

$n' = N_{Ed} / (A_c f_{cd})$ is the relative normal force

$r_m = M_{01} / M_{02}$ is the moment ratio

M_{01}, M_{02} are the first-order end moments, $|M_{02}| \geq |M_{01}|$

For slender columns, second-order effects will need to be considered. In order to solve the problem, the cross-sectional calculation tool is further extended to take into account second-order effects and different slenderness ratios. In this paper, a basic column model with two hinged ends and loaded by an eccentric load at each end is investigated.

As Fig. III.9 shows, bending moments m in the case of a transverse force $N = 1$ can easily be obtained and the deflection v is calculated as:

$$v = \sum \int m \cdot \frac{M}{EI} dx \quad (III.7)$$

with M the bending moment at the local cross-section

EI the stiffness of the cross-section

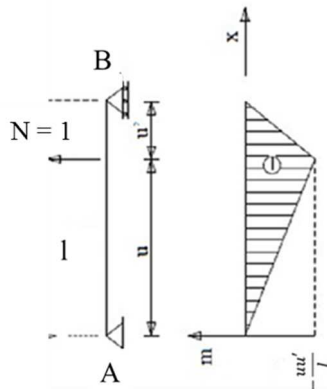


Fig. III.9: The bending moment diagram in the case of a transverse force $N = 1$

Further, the bending moment M , in a loaded column (shown in Fig. III.10) can be written in the form:

$$M = \int y \sigma dA \quad (III.8)$$

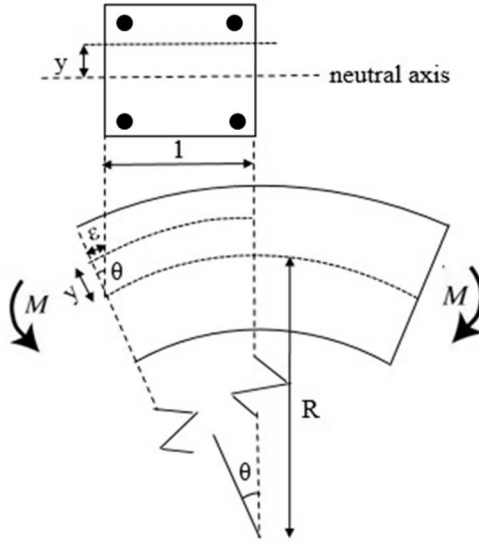


Fig. III.10: The relationship between the strain ϵ and the curvature χ

Fig. III.10 shows that $\theta = \frac{1}{R} = \frac{\epsilon}{y}$, and hence the axial strain ϵ is given by the ratio y/R . Equivalently, $1/R$ (the curvature χ) is equal to the through-thickness gradient of axial strain. It follows that the axial stress at a distance y from the neutral axis of the column is given by

$$\sigma = E\chi y \quad (\text{III.9})$$

where χ is the local curvature of the column

Thus, Eq. (III.8) can be expressed as:

$$M = \int y(E\chi y dA) = \chi E \int y^2 dA \quad (\text{III.10})$$

Considering the second moment of area $I = \int y^2 dA$, Eq. (III.10) can be written as:

$$M = \chi EI \quad (\text{III.11})$$

Hence, $\frac{M}{EI}$ in Eq. (III.7) can be replaced by χ and the equation can be expressed as:

$$v = \sum \int m. \chi dx \quad (III.12)$$

From Eq. (III.12), it is seen that the M- χ relationship is required in order to obtain the deflection along the column. For a first-order analysis, the bending moment is considered to be constant along the column when one considers the column subjects to two equal moments (with opposite signs) at the end of the column. However, second-order effects always occur and these play a predominant role in case of column subjected to fire. Hence, the column along the height is divided into segments to consider the deflection at different nodes. Further, based on the cross-sectional analysis, a calculation tool is developed to obtain M- χ curves as well as interaction curves of columns based on a second-order analysis.

As the first step of the calculations, the curvature χ in case of the first order bending moment can be obtained based on the cross-sectional calculation. Deflections at any position of the column are calculated according to Eq. (III.12). Then, additional bending moments caused by deflections under the eccentric loads (or equivalent end moments) are obtained. Next, a new χ corresponding to the new bending moment can be found from the cross-sectional calculation. This procedure is repeated until the bending moment converges and further iterations do not alter the bending moment significantly.

In order to have an idea of the number of iterations needed to obtain convergence taking into account second-order effects, a simply supported column with a cross-section of $b \times h = 300 \text{ mm} \times 300 \text{ mm}$, 20°C concrete compressive strength $f_{ck} = 55 \text{ MPa}$, reinforcement yield strength $f_y = 500 \text{ MPa}$ and Young's modulus of steel $E_s = 2 \times 10^5 \text{ N/mm}^2$ is investigated for different fire durations (in case of an ISO 834 standard fire), slenderness ratios as well as axial loads.

(1) Fire duration

First, the bending moments M in function of the number of iterations (performed for the second-order analysis) are shown in Figs. III.11 to III.13 for a column with a height of $l = 3 \text{ m}$ (slenderness ratio $\lambda = 35$, $l/b = 10$) in case of fire durations of 0 min, 60 min, 90 min, respectively and an axial load $N = 495 \text{ kN}$ ($n = 0.1$) at an eccentricity of 0.026 m.

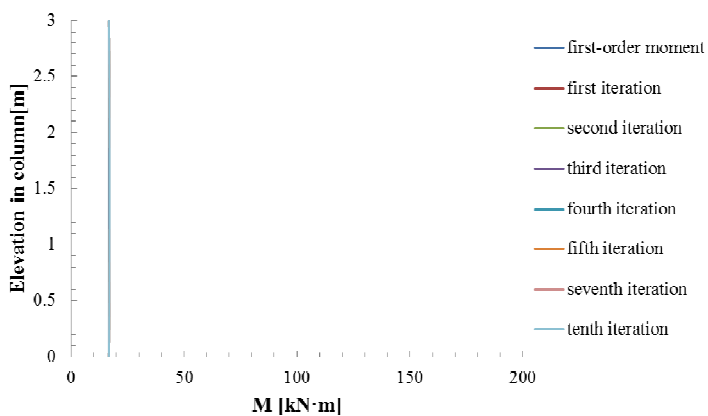


Fig. III.11: Relationship between the bending moment and the number of iterations performed for the second-order analysis in case of a fire duration of 0 min

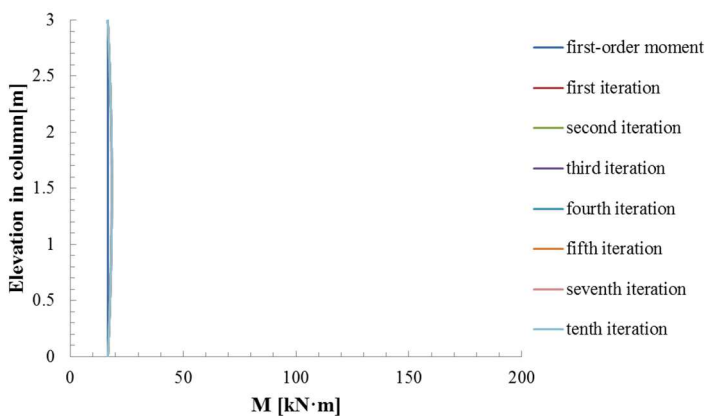


Fig. III.12: Relationship between the bending moment and the number of iterations performed for the second-order analysis in case of a fire duration of 60 min

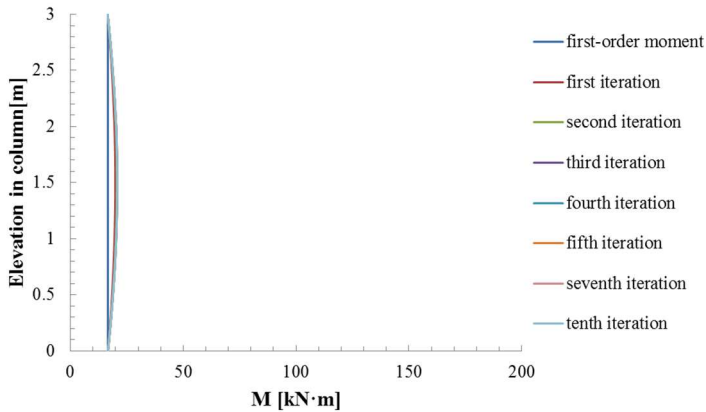


Fig. III.13: Relationship between the bending moment and the number of iterations performed for the second-order analysis in case of a fire duration of 90 min

From Figs. III.11 to III.13, it can be seen that for such a given eccentricity, the second-order effects are not very significant. As a result, the bending moment converges very soon at ambient temperature (less than 3 iterations) while it takes more iterations to find the solution at elevated temperatures ($\Delta \leq 1\%$ is used as a convergence criterion). It is observed that for longer exposure times, more iterations are needed. However, for most of the short columns ($l/b \leq 10$) the calculations can converge with less than 7 iterations.

(2) Slenderness ratio

For analysing the influence of the slenderness ratio on the number of iterations performed for the second-order analysis, a fairly long fire duration of 90 minutes is chosen. The bending moments M in function of the number of iterations are shown in Fig. III.14 for a column with height $l = 6$ m (slenderness ratio $\lambda = 70$, $l/b = 20$) in case of an axial load $N = 495$ kN ($n = 0.1$) at an eccentricity of 0.026 m.

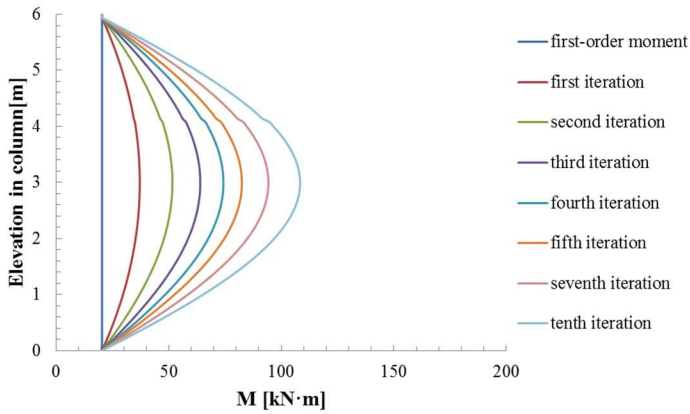


Fig. III.14: Relationship between the bending moment and the number of iterations (up to 10) in case of a slenderness ratio of 70 and a fire duration of 90 min

Unlike short columns, the increments of the bending moment for slender columns are not always getting smaller with the number of iterations (shown in Fig. III.14).

In order to investigate the relationship of the bending moment capacity and iterative times for this column, the number of iterations (7, 10 and 13) are compared in Fig. III.15, Fig. III.16 and Fig. III.17, respectively.

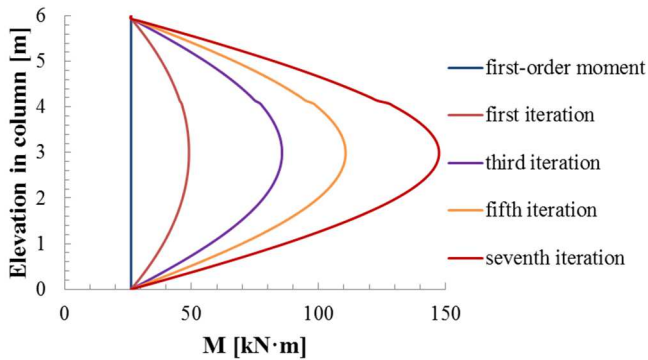


Fig. III.15: Relationship between the bending moment and the number of 7 iterations in case of a slenderness ratio of 70 and a fire duration of 90 min

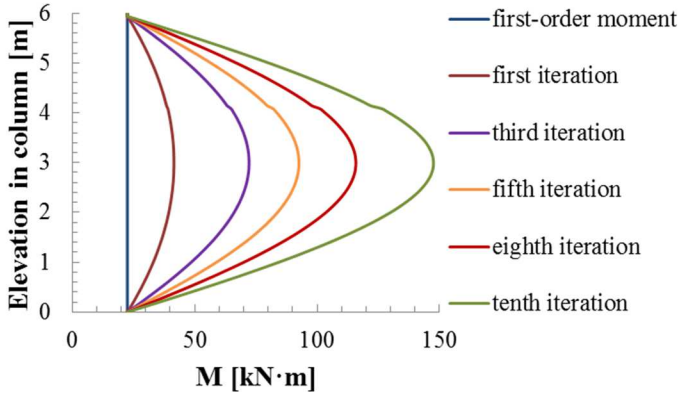


Fig. III.16: Relationship between the bending moment and the number of 10 iterations in case of a slenderness ratio of 70 and a fire duration of 90 min

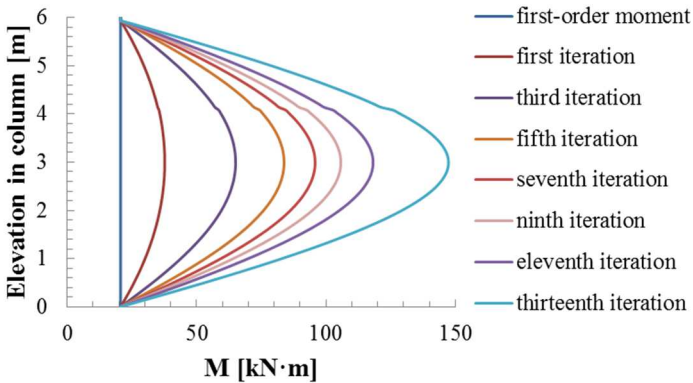


Fig. III.17: Relationship between the bending moment and the number of 13 iterations in case of a slenderness ratio of 70 and a fire duration of 90 min

Figs. III.15 to III.17 show the relationship of the bending moments along the height of the column and the number of iterations. The first-order moments in case of an axial load $N = 495 \text{ kN}$ are obtained with the calculation tool as $20.6 \text{ kN}\cdot\text{m}$ (after 13 iterations), $22.5 \text{ kN}\cdot\text{m}$ (after 10 iterations) and $26.2 \text{ kN}\cdot\text{m}$ (after 7 iterations),

respectively. From Figs. III.15 to III.17, it can be seen that the calculation cannot get convergence with only a few iterations in case of slender columns. In the following, a difference between consecutive steps $\Delta \leq 1\%$ is used as a convergence criterion and the number of iterations is limited to at maximum 50 for slender columns in case of fire. If the difference between consecutive steps cannot reach $\Delta \leq 1\%$ after 50 iterations, the column is considered to fail.

(3) Axial load

Finally, an axial load of 1485 kN ($n = 0.3$) at an eccentricity of 0.026 m is applied on a column with height $l = 3$ m (slenderness ratio $\lambda = 35$, $l/b = 10$) in case of a fire duration of 60 min. The bending moments M in function of the number of iterations are given in Fig. III.18.

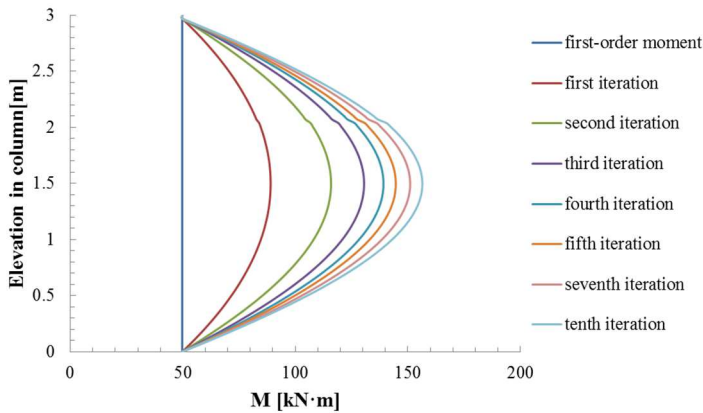


Fig. III.18: Relationship between the bending moment and the number of iterations in case of a fire duration of 90 min and an axial load of 1485 kN

For the same given eccentricity, the first-order moments (shown in Fig. III.18) are three times as indicated in Fig. III.13. However, as for the case of an axial load of $F = 495$ kN, convergence is obtained (difference between consecutive steps $\Delta \leq 1\%$ in this case) after 7 iterations when the axial load is 1485 kN.

Based on the investigated cases, the slenderness ratio has the most significant influence on the number of iterations. In order to obtain reliable interaction curves, the difference between consecutive steps $\Delta \leq 1\%$ is used as a convergence criterion and the number of iterations is limited to at maximum 50. It is worth mentioning

that due to the finite precision of the computations performed, the interaction curves might show a few minor jump points.

III.4. Validation of interaction curves

III.4.1. Validation of interaction curves based on cross-sectional calculations

In order to verify the calculation method, the results obtained for the specific case of a square column with a cross-section of 600 mm × 600 mm, 24 bars with diameter 20 mm and a concrete cover of 50 mm, 20°C concrete compressive strength $f_{ck} = 40$ MPa, reinforcement yield stress $f_y = 430$ MPa and Young's modulus of steel $E_s = 2 \times 10^5$ N/mm² are compared to the results from Meda et al. (2002), where the same dimension of columns, reinforcement, strength and Young's modulus of concrete and reinforcement at ambient temperature were used for the analysis. There are two differences between the calculation model from Meda et al. (2002) and the current calculation: first, the compressive strength of concrete at elevated temperatures in (Meda et al., 2002) is based on experimental data (Meda et al., 2002), while the current method is based on EN 1992-1-2 provisions (2004). Secondly, stress-strain laws of concrete in compression at elevated temperatures used in (Meda et al., 2002) are different (see Table III.1) from the EN 1992-1-2 (2004) prescriptions.

The results of the interaction curves in the case of fire exposure at all sides are visualized in Fig. III.19 considering $n' = \frac{N_c + N_s}{f_c b h}$ and $m_x = \frac{M_c + M_s}{f_c b h^2}$, where N_c , M_c , N_s , M_s are design values of normal forces and bending moments about the x-axis (see Fig. III.8) respectively for concrete and steel reinforcement, b is the width of the cross-section and h is the height of the cross-section.

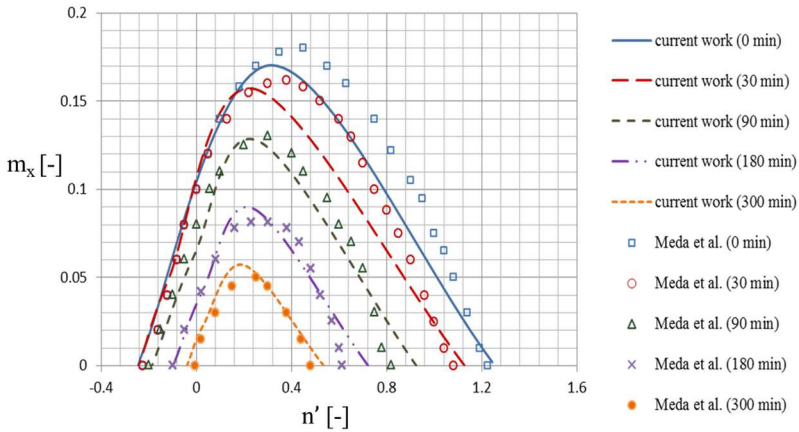


Fig. III.19: Comparison of calculated interaction curves with results available in (Meda et al., 2002)

Fig. III.19 indicates that interaction curves at 0 min and 30 min obtained from the proposed numerical method are more conservative than results presented in (Meda et al., 2002). The origin of the differences are related to the different material models that have been chosen. For stress-strain laws of concrete in compression, elastic and perfectly-plastic stress-strain curves are adopted in (Meda et al., 2002), whereas decreasing branches in the stress-strain laws are considered in the proposed method. As a result, the corresponding maximum bending moments are a little smaller than those in (Meda et al., 2002). The differences are largest when the temperatures of the column are low.

Subsequently, also cases of columns with 1 to 4 exposed surfaces are compared to the data from Caldas et al. (2010) who used the same input parameters as Meda et al. (2002). The cases of columns with different exposed surfaces subjected to the ISO standard fire at 90 minutes and 300 minutes have been illustrated in Fig. III.20 and Fig. III.21, respectively.

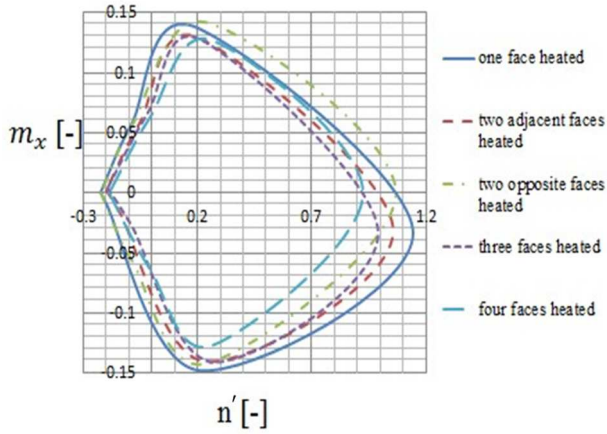


Fig. III.20: The effects of different exposed surfaces on M-N interaction curves in case of an ISO 834 standard fire and a fire duration of 90 minutes

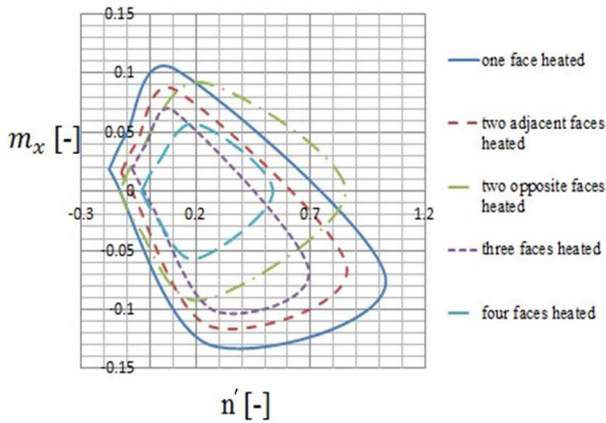


Fig. III.21: The effects of different exposed surfaces on M-N interaction curves in case of an ISO 834 standard fire and a fire duration of 300 minutes

From these two diagrams shown in Fig. III.20 and Fig. III.21, it can be seen that the effects of different exposed surfaces subjected to fire are not significant at the beginning of fire. As the fire duration increases, the difference of the interaction curves between different considered cases becomes more significant. After 300 minutes fire, the load capacity in case of 4 faces exposure can be only half as that in case of 1 face exposure.

Based on comparisons, the results obtained with the developed calculation tool prove to be very close to results found in (Meda et al., 2002) and (Caldas et al., 2010).

III.4.2. Validation of interaction curves based on theoretical and experimental data considering second-order effects

In this section, interaction curves that consider second-order effects are respectively compared with results obtained from the background document of Eurocode 2 (2008) and experimental data (Lie et al., 1984).

First, a basic column model with two pinned ends and the same material parameters as in the background document (2008) of Eurocode 2 (i.e. concrete grade C80/95, $\omega = 0.2$, $\varphi_{ef} = 0$) was chosen in order to validate once again the accuracy of the calculation tool. The interaction curves are shown in Fig. III.22, where e_0 is the eccentricity of the axial load and e_2 is the deflection at the mid-height of the column caused by the eccentric load. As a first step of the calculation, the interaction curve for $\lambda = 0$ at normal temperature is obtained with the general method provided in the background document (2008) of Eurocode 2 and shown in blue dots. Further, the deflection e_2 caused by the eccentric load is calculated with Eq. (III.12). In order to obtain the interaction curve taking into account second-order effects, an example is given for $\lambda = 35$. Since the initial eccentricity e_0 and the deflection e_2 are calculated, the first-order moment and the second-order moment are indicated with a light blue line and a light red line in Fig. III.22, respectively. The intersection between the red line and the blue dots predicts the design value of the axial load. Hence, the design value of the bending moment taking into account second-order effects is a corresponding moment to the design load value, which is located on the blue straight line. The same calculations are performed for the slenderness ratios of 70, 105 and 140. Finally, interaction curves (solid lines) calculated with the analytical tool are compared with interaction curves (in dots) obtained with the general method and provided in the background document (2008) of Eurocode 2.

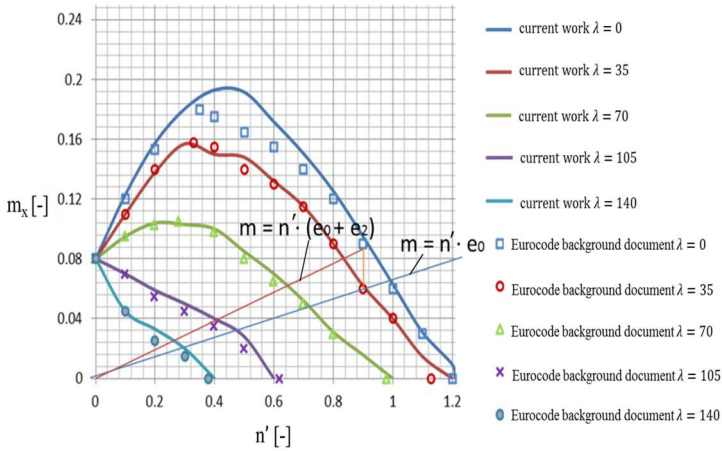


Fig. III.22: Interaction curves for columns of different slenderness: comparison with background documents of Eurocode 2 (2008)

From Fig. III.22, it can be seen that results obtained with our calculation tool are in agreement with results provided in the background document (2008) of Eurocode 2.

Subsequently, this method is adopted to study the second-order effects of columns exposed to fire. A series of twelve reinforced concrete columns were fabricated and tested by Lie et al. (1984). In order to validate the performance of the developed cross-sectional calculation tool, two of the clamped reinforced concrete columns with siliceous aggregates were chosen to compare. The geometry and material properties of these two columns are as follows: cross-section of 305 mm \times 305 mm, length of 3810 mm (measured from end plate to end plate), 4 bars with diameter 25 mm and a concrete cover of 48 mm; 20°C concrete compressive strength $f_{ck} = 35$ MPa, reinforcement yield strength $f_y = 415$ MPa and Young's modulus of steel $E_s = 2 \times 10^5$ N/mm². The same experimental fire curve as well as geometric and material properties as in the experimental test setup are taken into account. The calculation model as well as the deflection shape is illustrated in Fig. III.23, where L is the length of the column, K is the effective length factor, v is the lateral deflection of the column at mid-height and χ is the curvature of the column at mid-height.

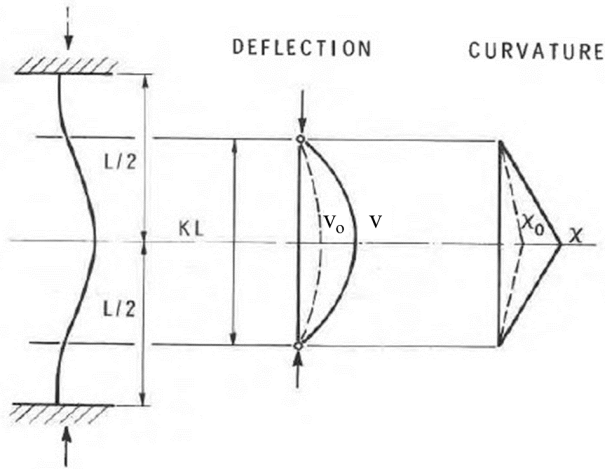


Fig. III.23: Basic column model and deflection shape (Lie et al., 1984)

Considering the clamped end conditions, a factor $K = 0.6$ was used to calculate the effective length of the columns as it was recommended in (Lie et al., 1984).

In the standard fire test, concentric axial loads of 1333 kN and 1778 kN were applied to the columns (A and B, see Table III.2), respectively, whereas in practice there is always some eccentricity of the load. A minimum eccentricity is specified for structural design in ACI (1977), CSA (1977) codes and also in Eurocode 2 (2004). Hence, in the calculation model proposed by Lie et al. (1984), the axial load is assumed to have an eccentricity of 2.5 mm in order to compare with experimental data. Finally, the columns failed in compression after 2 hours 50 minutes and 2 hours and 26 minutes of the ASTM-E119 standard fire, respectively. Considering the same failure time, calculations for different axial loads are performed. The maximum allowable eccentricities are obtained for different axial loads and are given in Table III.2.

Table III.2: Comparison of fire resistance of columns subjected to second-order effects with experimental test observations (Lie, 1984)

Test case	A		B	
Fire duration (hr : min)	2:50		2:26	
Current calculation model	Eccentricity (mm)	Load (kN)	Eccentricity (mm)	Load (kN)
	0	1603	0	1887
	1.1	1335	1.8	1790
	1.9	1237	2.3	1778
	2.7	1172	3.1	1758
Experimental results (Lie et al., 1984)	0 ~ 2.5 mm (assumed)	1333	0 ~ 2.5 mm (assumed)	1778

It can be seen that maximum eccentricities of 1.1 mm and 2.3 mm are obtained with the calculation tool for Column A and Column B under the given experimental loading conditions. Hence, the results are in good agreement with experimental data obtained by Lie et al. (1984).

Further, two more comparisons have been performed with respect to tests from the Technical University of Braunschweig (Hass, 1986) and the University of Liège (Dotreppe, 1993), respectively.

The first group of tests are from the Technical University of Braunschweig (Hass, 1986). 39 reinforced concrete columns were tested in case of the ISO 834 standard fire. Among them, 7 simply supported columns with a cross-section of 200 mm × 200 mm are chosen for comparison. The configuration of the columns as well as the material properties are shown in Table III.3. The results from experiments and analytical calculations are also given.

Table III.3: Comparison of fire resistance of columns subjected to second-order effects with test data from the Technical University of Braunschweig (Hass, 1986)

No.	Cover thickness (mm)	Reinf. (mm)	f_c (N/mm^2)	f_y (N/mm^2)	Height (m)	Eccentricity (mm)	Fire duration (min)	F (kN)		Cal/Exp
								Exp.	Cal.	
1	20	4Φ20	29.0	487	3.76	0	58	420	371	0.88
2	20	4Φ20	29.0	487	4.76	0	48	340	325	0.96
3	20	4Φ20	37.0	487	4.76	10	49	280	281	1.00
4	20	4Φ20	37.0	462	4.76	20	36	240	311	1.30
5	20	4Φ20	37.0	462	4.76	60	49	170	178	1.05
6	20	4Φ20	37.0	418	4.76	100	53	130	126	0.97
7	20	4Φ20	39.0	443	5.76	10	40	208	250	1.20

The simulation is based on the failure time provided by the tests. It is seen in Table III.3 that there are some differences between the results of the numerical tool and the test results. However, for most cases, the numerical values are in reasonable agreement with the experimental results.

Furthermore, 16 simply supported columns subjected to fire were investigated by the University of Liège and Ghent University (Dotreppe, 1993). An ISO 834 standard fire was adopted. 6 columns with cross-section of 300 mm × 300 mm are compared.

The configurations and the material properties of the columns as well as the maximum axial loads are listed in Table III.4.

Table III.4: Comparison of fire resistance of columns subjected to second-order effects with test data from the University of Liège (Dotreppe, 1993)

No.	Cover thickness (mm)	Reinf. (mm)	f_c (N/mm^2)	f_y (N/mm^2)	Height (m)	Eccentricity (mm)	Fire duration (min)	F (kN)		Cal/Exp
								Exp.	Cal.	
1	25	4Φ16	31.6	576	3.9	20	0	2000	2161	1.08
2	25	4Φ16	32.3	576	3.9	0	61	950	1221	1.29
3	25	4Φ16	32.8	576	3.9	0	120	622	561	0.90
4	25	4Φ16	32.7	576	3.9	20	125	220	221	1.00
5	40	4Φ16	31.8	576	3.9	20	123	349	372	1.07
6	25	4Φ25	27.9	591	3.9	20	120	475	364	0.77

It can be seen that the maximum axial loads calculated with the numerical tool are in good agreement with the experimental data.

From Tables III.2, III.3 and III.4, it is observed that the experimental results are in close agreement with the predictions by the calculation method developed in this thesis. Hence, this tool is further adopted for practical applications.

III.5. A parameter study

Since the numerical calculation tool has been validated with experimental data, a parametric study is discussed. Simple examples are given taking into account the influences of fire durations, dimensions, reinforcement ratios, axial compression ratios and eccentricities, concrete cover thickness and slenderness ratios.

III.5.1. Influence of fire duration on the cross-sectional capacity

Similarly as Fig. III.6 has shown the temperature distribution of a column with a cross-section of 300 mm × 300 mm in case of an ISO 834 standard fire of fire durations of 30 min, 60 min, 90 min and 120 min, the same column and fire durations is used here to perform a parameter study. The interaction curves of the column with reinforcement ratio of $\omega = \frac{A_s f_{yd}}{A_c f_{cd}} = 0.5$ and a cover thickness $c = 25$ mm are given in Fig. III.24, where $n = \frac{N_c + N_s}{0.7(A_c f_{cd} + A_s f_{yd})}$, $m = \frac{M_c + M_s}{0.7(A_c f_{cd} + A_s f_{yd})h}$, N_c , M_c , N_s , M_s are the maximum axial forces and bending moments for concrete and reinforcement respectively, b is the width of the column and h is the height of the cross-section. The parameter $f_{cd} = \alpha_{cc} f_{ck} / \gamma_c$ is the design value of concrete compressive strength with γ_c the partial factor for concrete and α_{cc} a coefficient taking into account long term effects on the compressive strength and unfavourable effects resulting from the way the load is applied ($\gamma_c = 1.5$ and $\alpha_{cc} = 0.85$ as recommended by Eurocode 2 are adopted). The parameter $f_{yd} = f_{yk} / \gamma_s$ is the design yield stress of the reinforcement with $\gamma_s = 1.15$ as recommended by Eurocode 2. A_c is the cross-sectional area of concrete and A_s is the cross-sectional area of the reinforcement.

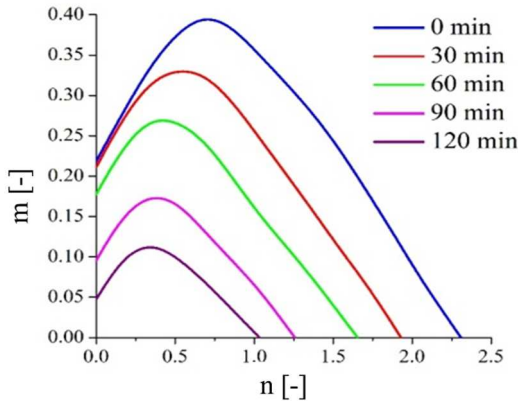


Fig. III.24: Interaction diagrams of the investigated column in case of an ISO 834 fire with fire durations of 0 min, 30 min, 60 min, 90 min and 120 min

Fig. III.24 indicates the influence of fire durations on the interaction curves of a column. It is seen that the decrease of the moment capacity in case of a small axial load is barely observed at the first 30 minutes. However, the load capacity in case of a fire duration of 2 hours is less than half of the load capacity at ambient

temperature. Further, the axial compression ratio corresponding to the peak moment decreases with increasing fire duration.

III.5.2. Influence of column dimensions on the cross-sectional capacity

In order to investigate the influence of the column dimensions on the resistance in case of fire, a cross-section of 500 mm × 500 mm, but the same reinforcement ratio of $\omega = 0.5$ and the cover thickness $c = 25$ mm as the cross-section of 300 mm × 300 mm analysed previously. The interaction curves of these two columns subjected to an ISO 834 fire in case of a fire duration of 120 min are shown in Fig. III.25.

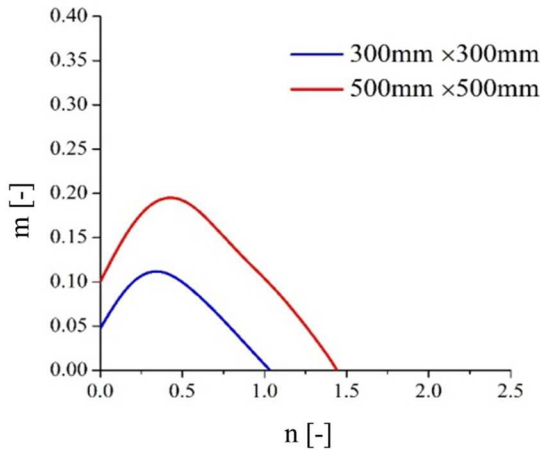


Fig. III.25: Interaction diagrams of two different size of columns subjected to an ISO 834 fire and a fire duration of 120 min

Fig. III.25 shows interaction curves of two different sizes of columns subjected to an ISO 834 fire and a fire duration of 120 min. The maximum moment capacity of the 500 mm × 500 mm column is about twice that of the 300 mm × 300 mm column while the pure axial load capacity is 1.4 times higher compared to that of the 300 mm × 300 mm column. It is worth mentioning that the axial compression ratio corresponding to the peak moment is about the same.

III.5.3. Influence of the reinforcement ratio on the cross-sectional capacity

Columns with a cross-section of 300 mm × 300 mm and three different reinforcement ratios of 0.1, 0.5 and 1.1 are compared. The interaction curves in case of an ISO 834 fire and a fire duration of 120 min are given in Fig. III.26.

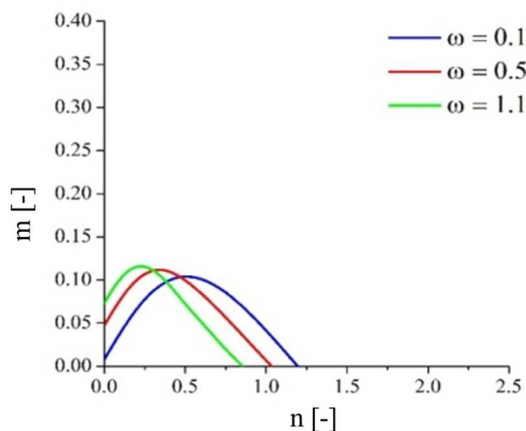


Fig. III.26: Interaction diagrams of columns with different reinforcement ratios in case of an ISO 834 fire and a fire duration of 120 min

Fig. III.26 indicates that the load capacity decreases with the decreasing concrete characteristic compressive strength (the increasing reinforcement ratio) in case of a same cross-section. The difference between the maximum moment capacity is not significant for these three columns after 2 hours fire. However, the axial compression ratio corresponding to the peak moment decreases with increasing reinforcement ratio in case of a same cross-section.

III.5.4. Influence of axial compression ratio and eccentricity on the cross-sectional capacity

From the previous results, it is already clear that the moment capacity increases first and then decreases with increasing compression ratio. The maximum permitted eccentricity decreases with increasing compression ratio. The value of the axial compression ratio corresponding to the peak moment is influenced by the fire duration and the reinforcement ratio of columns. The difference of the axial compression ratio corresponding to the peak moment in case of the same

reinforcement ratio and the same fire duration but with different sizes of cross-section is not so significant.

III.5.5. Influence of the cover thickness on the cross-sectional capacity

A comparison in case of a fire duration of 120 min is given between two columns with the same cross-section of 300 mm × 300 mm and a reinforcement ratio of $\omega = 0.5$, but with different concrete cover thickness $c = 25$ mm and $c = 45$ mm, respectively (Fig. III.27).

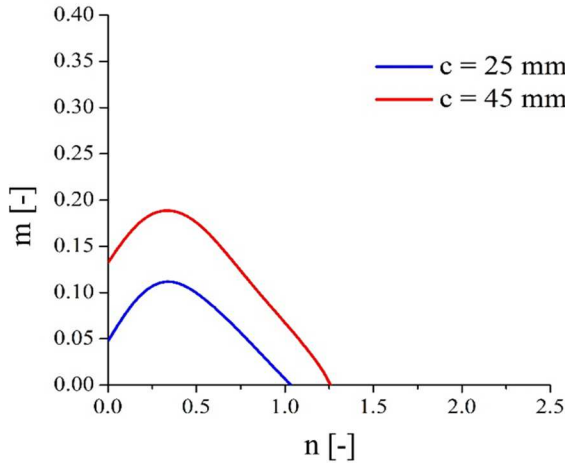


Fig. III.27: Interaction diagrams of columns with different cover thickness in case of an ISO 834 fire and a fire duration of 120 min

Fig. III.27 indicates the influence of the cover thickness. It is obvious that the moment capacity in case of $c = 45$ mm is much larger than that in case of $c = 25$ mm in case of a fire duration of 120 min. Therefore, it is a very important step to determine the cover thickness of columns when the fire resistance design is required. Further, it is noticed that the axial compression ratio corresponding to the peak moment keeps approximately the same in case of different cover thicknesses.

III.5.6. Influence of the slenderness ratio on the effective cross-sectional capacity when considering second-order effects

Finally, the second-order effects are taken into account. Besides the full cross-sectional capacity, different lengths of the column (300 mm × 300 mm) are considered, i.e. 1 meter, 2 meters and 3 meters in case of a fire duration of 120 min. The interaction curves are presented in Fig. III.28.

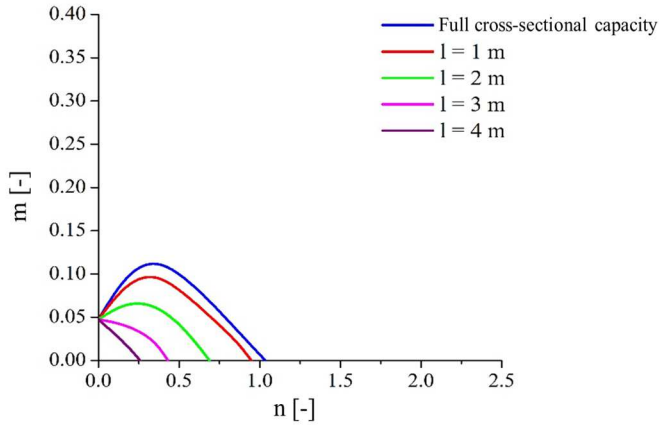


Fig. III.28: Interaction diagrams of columns with different slenderness ratios in case of an ISO 834 fire and a fire duration of 120 min

It is observed that the moment capacity as well as the load capacity decreases with increasing length (and increasing slenderness ratio). The load capacity in case of the 3 m column is less than half of full cross-sectional capacity. Furthermore, the value of the axial compression ratio corresponding to the peak moment decreases with increasing slenderness ratio. This value decreases to 0 when the length of the column reaches 3 meters in the case investigated.

III.6. Conclusions

A cross-sectional calculation tool was presented in this chapter. Comparing with experimental data, this tool is first validated for predicting interaction curves, deflections as well as the fire resistance of columns in case of fire.

Based on the parametric study on the influence of fire durations, dimensions, reinforcement ratios, axial compression ratios and eccentricities, concrete cover thickness and slenderness ratios, the following conclusions can be made:

- (1) The fire duration has a significant influence on the capacity of columns. With respect to an ISO 834 standard fire, the capacity decreases with increasing fire duration.

(2) For the column with the same reinforcement ratio and the same cover thickness, the larger the cross-sectional size is, the better fire resistance it has. The axial compression ratio corresponding to the peak moment is about the same in case of the same fire condition.

(3) The load capacity as well as the axial compression ratio corresponding to the peak moment decreases with decreasing concrete characteristic compressive strength (increasing reinforcement ratio).

(4) The value of the axial compression ratio corresponding to the peak moment is influenced by the fire duration, the reinforcement ratio and the slenderness ratio of columns. The effects of cross-sectional column size and cover thickness are not so significant.

(5) The cover thickness has a significant influence on the fire resistance of columns.

(6) The fire resistance decreases significantly with increasing length (slenderness ratio) of columns. Therefore, the second-order effects should be considered to be very important for the fire resistance design of columns.

CHAPTER IV

DESIGN OF REINFORCED CONCRETE COLUMNS EXPOSED TO FIRE IN CASE OF UNIAXIAL BENDING USING TABULATED DATA

Most of the results in this chapter have been published in Wang L. J., Caspee R., Van Coile R. & Taerwe L. "Extension of tabulated design parameters for rectangular columns exposed to fire taking into account second-order effects and various fire models." *Structural Concrete*, 16(1), 17–35, 2015.

The developed calculation tool has been introduced and validated in the previous chapter. In this chapter, the influence of different fire scenarios, number of exposed faces as well as fire durations are investigated in case of uniaxial bending. Three types of fire curves are considered, i.e. an ISO 834 standard fire, a hydrocarbon fire and natural fires as defined in Eurocode 2 (2004) are discussed. Biaxial bending is not considered here, but will be the subject of **chapter VI**.

IV.1. Influence of the fire exposed faces on the temperature distribution

As a first step of the calculation, the heat transfer is studied based on a cross-sectional analysis. Again, the lower limit of the thermal conductivity, a concrete moisture content of 1.5% and a concrete density of 2300 kg/m³ are considered. As shown in section III.2 for the temperature distribution of a square cross-section exposed at all faces, the same calculation for a circular cross-section is first analysed. Then, a square cross-sectional column with different exposed faces such as one-face exposure, two-faces exposure, three-faces exposure and four-faces exposure is investigated. Furthermore, interaction curves are calculated considering different exposed faces. Finally, the temperature distribution of this square cross-section is investigated considering different thermal conductivity curves (the upper limit and the lower limit). Interaction curves of the cross-section are discussed adopting limits of the thermal conductivity.

IV.1.1. Circular cross-section

A column with a circular cross-section and a radius of 150 mm, a concrete moisture content of 1.5% and a concrete density of 2300 kg/m³ is chosen to be compared with the temperature distributions given in Eurocode 2 (2004). The temperature distributions of the cross-section in case of an ISO 834 standard fire for fire durations of 30 min, 60 min, 90 min and 120 min are shown in Fig. IV.1.

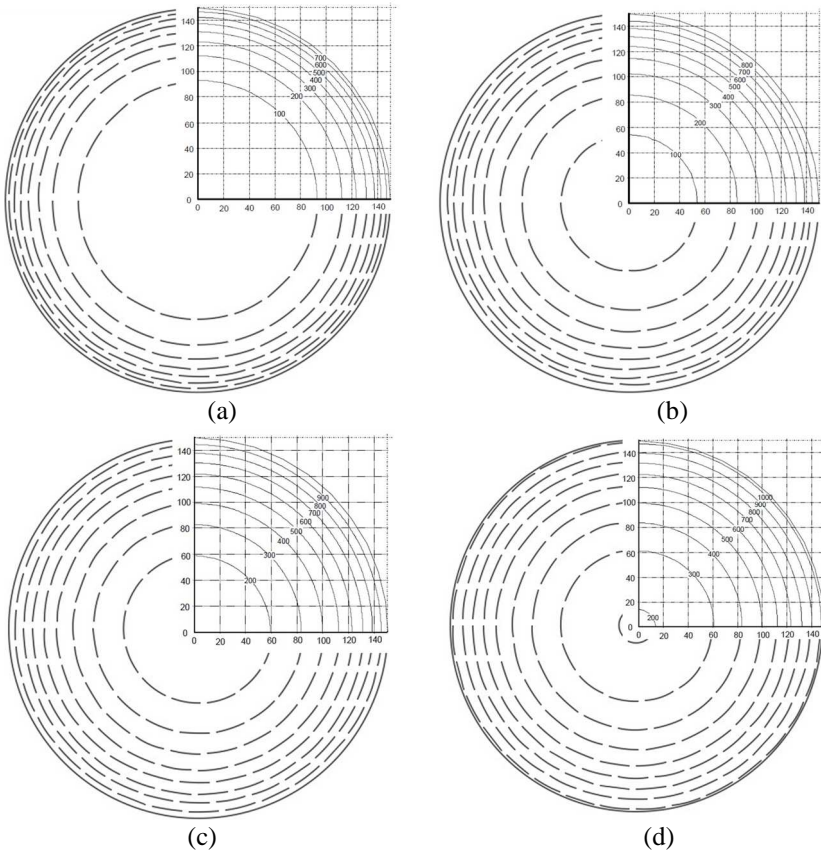


Fig. IV.1: Comparison of the temperature distribution calculated using the proposed methodology implemented in a Matlab routine (dashed line), with graphs given in EN 1992-1-2 (solid line) in case of an ISO 834 fire with fire durations of 30 min (a), 60 min (b), 90 min (c), 120 min (d)

IV.1.2. Rectangular cross-section

So far, it has been proven that the proposed calculation tool could be used for both a rectangular cross-section and a circular cross-section. In order to investigate the influence of different exposed faces, a square column is considered. A cross-section of 300 mm × 300 mm, the same as in Fig. III.6, with a concrete moisture content of 1.5% and a concrete density of 2300 kg/m³ is discussed in case of an ISO 834 standard fire. In Fig. IV.2, the temperature distributions for one sided exposure (a), two adjacent sides exposure (b), two opposite sides exposure (c), three sides exposure (d) and four sides exposure (e) are given in case of a fire duration of 120 minutes.

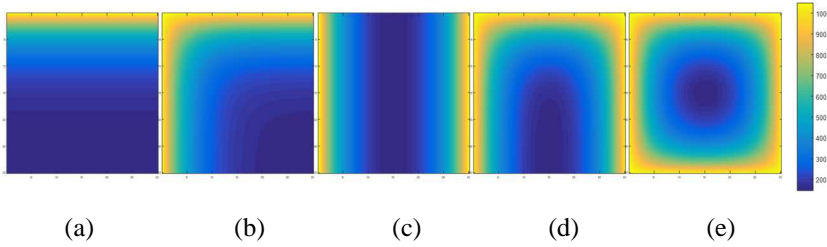


Fig. IV.2: Temperature distributions calculated using the proposed methodology in case of one sided exposure (a), two adjacent sides exposure (b), two opposite sides exposure (c), three sides exposure (d) and four sides exposure (e) under an ISO 834 fire with a duration of 120 min (values in °C)

The material properties used for the consequent structural analysis are: 20°C concrete compressive strength $f_{ck} = 55$ MPa, reinforcement yield strength $f_y = 500$ MPa and Young's modulus of steel $E_s = 2 \times 10^5$ N/mm². Based on the temperature distributions obtained in Fig. IV.2, the interaction curves for these five cases are presented in Fig. IV.3, with $n = \frac{N_c + N_s}{0.7(A_c f_{cd} + A_s f_{yd})}$ and $m = \frac{M_c + M_s}{0.7(A_c f_{cd} + A_s f_{yd})h}$, where N_c , M_c , N_s , M_s are the maximum axial forces and bending moments respectively for concrete and reinforcement, b is the width and h is the height of the cross-section.

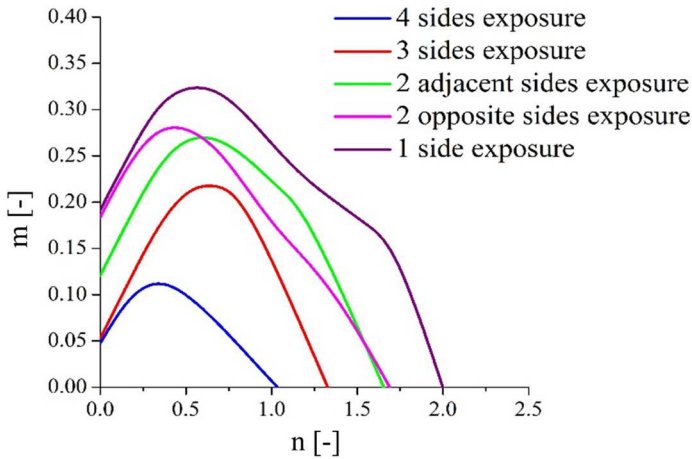


Fig. IV.3: Interaction curves obtained with the proposed methodology in case of different fire exposures

It is seen that the moment capacity decreases with increasing number of exposure faces for a given axial load. Hence, as a conservative consideration for the fire

resistance design, interaction curves of columns in case of 4 sides exposed to an ISO 834 standard fire are proposed for columns exposed on more than one side.

Considering the upper limit and the lower limit of the thermal conductivity provided by Eurocode 2 (2004), the temperature distributions in case of an ISO 834 fire and a fire duration of 120 minutes are shown in Fig. IV.4 (for the same case study as before).

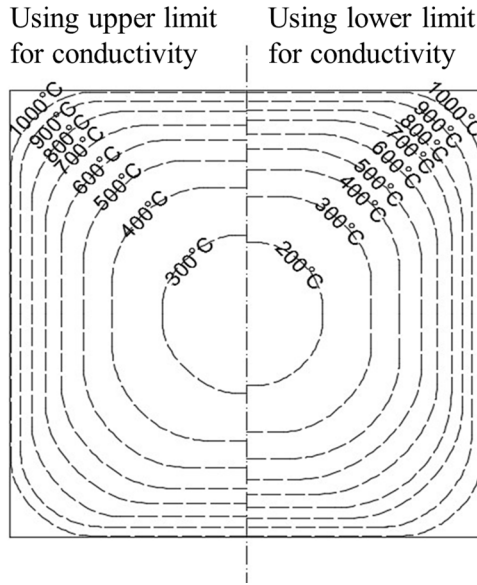


Fig. IV.4: Temperature distributions in case of an ISO 834 fire and a fire duration of 120 minutes taking into account the upper limit (left) and the lower limit (right) of the thermal conductivity

It is observed that the heat transfers much faster when the upper limit of the thermal conductivity is adopted. The difference of the temperature in the core of the cross-section could be around 100°C after 120 minutes of a standard fire exposure.

Finally, based on the calculated temperature distributions shown in Fig. IV.4, the corresponding interaction curves are obtained and given in Fig. IV.5.

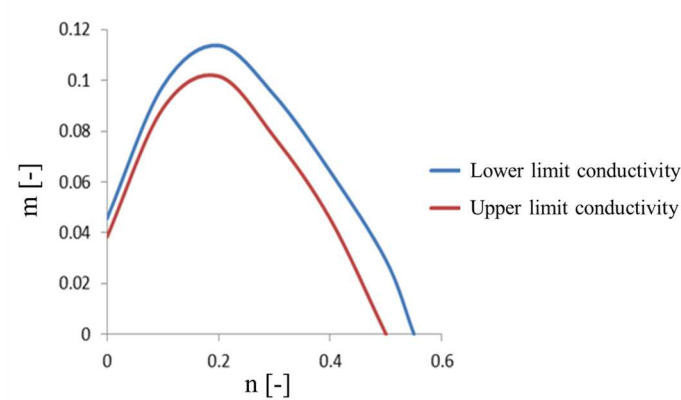


Fig. IV.5 Interaction curves of columns in case of an ISO 834 fire and a fire duration of 120 minutes taking into account the upper limit and the lower limit of the thermal conductivity

It is seen that the thermal conductivity has a more significant influence on the interaction curves in case of high axial loads. The difference in bending moment capacity in case of an ISO 834 fire with a fire duration of 120 minutes amounts to 29% between adopting the upper limit and the lower limit. Hence, it is important to make it clear which curve is adopted for the thermal conductivity when the structural fire analysis is required.

IV.2. Comparison of calculated ISO834 standard fire resistance times of rectangular concrete columns with EN 1992-1-2 tabulated values for different slenderness ratios and eccentricities

With respect to fire resistance of columns in braced structures, EN 1992-1-2 (Eurocode 2, 2004) provides tables with the minimum required cross-section and concrete cover for different slenderness ratios and ISO 834 standard fire durations. In order to compare with EN 1992-1-2 (Eurocode 2, 2004), the same input data has been used for the numerical method described above. In EN 1992-1-2 (Eurocode 2, 2004), the moisture content of concrete for all the tabulated tables is 1.5% and this value is further adopted for all the fire calculations in this investigation. It is worth mentioning that explosive spalling is unlikely to occur when the moisture content of concrete is less than 3% (Eurocode 2, 2004) (*fib* Bulletins 38, 2007). Hence, explosive spalling is not taken into account for all the cases in this paper. The effect of imperfections is considered as an eccentricity $e_i = l_0/400$ as mentioned

in EN 1992-1-1 (Eurocode, 2004), where l_0 is the effective length of the column. Other parameters, like the reinforcement ratio ($\omega = \frac{A_s f_{yd}}{A_c f_{cd}}$) and load eccentricity (e) are varied over the different tables, i.e. $\omega = 0.1, 0.5, 1.0$; $e = 0.025b, 0.25b, 0.5b$ (or $0.025h, 0.25h, 0.5h$). Tables with allowable parameter combinations in case of an ISO 834 fire with fire durations of 30 min, 60 min, 90 min and 120 min are illustrated (Tables IV.1 to IV.9), with $n = \frac{N_c + N_s}{0.7(A_c f_{cd} + A_s f_{yd})}$ as proposed in EN 1992-1-2 (Eurocode 2, 2004), where A_c is the cross sectional area of concrete, A_s is the cross sectional area of reinforcing bars, f_{cd} is the design value of concrete compressive strength, f_{yd} is the design yield stress of reinforcement, N_c , N_s are maximum axial forces respectively for concrete and reinforcement, b is the width of the column and h is the height of the cross-section.

It is worth mentioning that columns in braced structures with a width up to 600 mm are investigated in order to make a comparison with Eurocode 2 (2004). For those which demand a width greater than 600 mm, a particular assessment for buckling is required (Eurocode 2, 2004).

Table IV.1: Minimum dimensions and concrete covers for reinforced concrete columns with rectangular section (ISO 834). Mechanical reinforcement ratio $\omega = 0.1$. Low first order moment: $e = 0.025b$ with $e \geq 10$ mm

Fire resistance	λ	Minimum dimensions [mm] : Column width b_{min} [mm]/axis distance a [mm]													
		Columns exposed on more than one side													
		n=0.15			n=0.3			n=0.5			n=0.7				
		standard fire		hydrocarbon fire		standard fire		hydrocarbon fire		standard fire		hydrocarbon fire			
		Numerical calculation	Eurocode 2	Numerical calculation	Eurocode 2	Numerical calculation	Eurocode 2	Numerical calculation	Eurocode 2	Numerical calculation	Eurocode 2	Numerical calculation	Eurocode 2		
R30	30	150/25		150/25		150/25		150/25		200/25		150/25		200/25	
	40	150/25		150/25		150/25		150/25		200/25		150/30:200/25	150/25	250/25	
	50	150/25		150/25		150/25		200/25	150/30:200/25	150/25		250/25	200/25	300/35:350/25	
	60	150/25		150/25		150/25		250/35:300/25	200/25	300/50:350/25		300/30:350/25	250/25	350/50:400/25	
	70	150/25		200/25	200/25	150/25		300/35:350/25	300/50:350/25	250/25	350/50:550/25	350/50:450/25	300/25	500/50:550/25	
	80	150/25		200/25	250/25	200/25		350/50:600/35	350/50:500/25	250/30:300/25	500/50:600/45	450/50:600/25	350/25	550/60:600/45	
R60	30	150/25		200/25		150/25		200/25		200/25		200/40:250/25	200/25	200/30:250/25	250/50:300/25
	40	150/25		200/25		150/30:200/25	150/25	200/40:250/25	200/30:250/25	200/25	250/50:300/25	250/40:300/25	250/25	350/25	
	50	150/25		200/40:250/25	200/30:250/25	200/25		250/50:350/25	250/50:300/25	250/25	350/50:400/25	350/35:400/25	300/25	450/25	
	60	150/30:200/25	150/25	200/40:300/25	250/40:350/25	200/40:250/25		350/50:500/25	350/50:400/25	250/40:300/25	500/50:550/25	500/40:550/25	350/30:400/25	550/60:600/25	
	70	200/25		250/50:350/25	350/50:400/25	250/30:300/25		500/50:600/45	500/60:600/25	300/40:350/25	600/60	550/40:600/60	450/35:550/25	600/80	
	80	200/25	200/30:250/25	350/50:550/25	500/60:600/45	250/40:300/25		550/60	550/60:600/60	400/30:450/25	①	①	550/60:600/35	①	
R90	30	150/25		200/25		200/25		250/25		200/50:250/25		250/50:300/25	250/40:300/25	250/30:300/25	350/25
	40	200/25	150/35:200/25	250/25	200/35:250/25	200/30:250/25		250/50:300/25	250/50:300/25	250/25	350/25	300/50:350/25	300/25	400/25	
	50	200/35:250/25	200/25	250/50:350/25	250/40:350/25	250/25		300/50:400/25	300/50:450/25	300/25	450/25	450/50:500/25	350/50:400/25	550/25	
	60	200/35:300/25	200/35:250/25	250/50:500/25	350/50:550/25	250/40:300/25		500/50:600/25	500/60:550/25	350/35:400/25	600/80	600/60	450/50:550/25	①	
	70	250/50:400/25	250/25	350/50:550/25	500/60:600/45	300/35:350/25		600/80	550/60:600/80	400/45:550/25	①	①	600/40	①	
	80	350/50:500/25	250/30:300/25	550/60	550/60:600/60	350/35:400/25		600/80	①	550/40:600/25	①	①	①	①	
R120	30	200/25		250/25		250/25		250/50:300/25	250/25		300/25	300/50:350/25	300/45:350/25	400/35:450/25	
	40	250/25		300/25	250/40:300/25	250/25		300/50:350/25	350/25	300/25	350/25	400/50:450/25	400/25	500/35:550/25	
	50	250/40:350/25	250/25	300/50:350/25	350/50:400/25	300/25		400/50:500/25	500/25	350/50:400/25	550/40:600/25	550/40:600/25	450/50:500/25	600/25	
	60	250/50:400/25	250/25	350/50:600/25	500/60:600/25	350/25		550/60	600/25	450/40:500/25	①	600/80	550/50	①	
	70	350/50:500/25	250/50:300/25	500/50:600/35	600/60	400/25		600/80	600/80	500/60:550/25	①	①	①	①	
	80	500/25	300/25	600/80	600/80	450/40:500/25		①	①	600/45	①	①	①	①	

*① Requires a width larger than 600 mm.

Table IV.2: Minimum dimensions and concrete covers for reinforced concrete columns with rectangular section (ISO 834). Mechanical reinforcement ratio $\omega = 0.1$. Moderate first order moment: $e = 0.25b$ with $e \leq 100$ mm

Fire resistance	λ	Minimum dimensions [mm] : Column width b_{min} [mm]/axis distance a [mm]											
		Columns exposed on more than one side											
		n=0.15		n=0.3				n=0.5		n=0.7			
		standard fire		hydrocarbon fire		standard fire		hydrocarbon fire		standard fire		hydrocarbon fire	
		Numerical calculation	Eurocode 2	Numerical calculation	Numerical calculation	Eurocode 2	Numerical calculation	Numerical calculation	Eurocode 2	Numerical calculation	Numerical calculation	Eurocode 2	Numerical calculation
R30	30	150/25		150/25	150/25		200/25		200/30:250/25		300/35:400/25		500/25
	40	150/25		200/25	200/25	150/30:200/25	300/25		350/35:400/25	300/25	400/50:500/25		500/25
	50	150/25		200/40:250/25	300/25	200/40:250/25	400/35:500/25		450/50:500/25	350/40:500/25	550/40:600/45		550/25
	60	150/25		250/35:350/25	400/50:450/25	300/25	500/50:600/35		550/40:600/25	550/25	600/30		600/30
	70	200/25		300/50:500/25	500/40:600/25	350/40:500/25	550/60:600/45		①	550/30:600/25	①		①
	80	300/30:400/25	250/25	500/35:600/35	600/45	550/25	①		①		①		①
R60	30	150/25	150/30:200/25	200/40:300/25	250/25	200/40:300/25	300/35:400/25		350/50:400/25	300/40:500/25	400/50:550/25		500/25
	40	200/25	200/30:250/25	250/50:350/25	300/50:400/25	300/35:350/25	400/50:600/35		500/25	450/50:550/25	550/60:600/80		550/40:600/25
	50	200/35:300/25	200/40:300/25	300/50:600/35	450/50:500/25	350/45:550/25	550/60:600/45		550/60:600/25	550/30:600/30	①		600/55
	60	300/50:500/25	250/35:400/25	400/50:600/35	550/60:600/25	450/50:550/25	600/80		①	600/35	①		①
	70	400/50:500/25	300/40:500/25	550/60:600/45	600/80	550/30:600/25	①		①	600/80	①		①
	80	500/40:600/45	400/40:550/25	550/60:600/80	①	600/30	①		①		①		①
R90	30	200/35:300/25	200/40:250/25	250/50:400/25	300/50:400/25	300/40:400/25	350/50:550/25		450/50:500/25	500/50:550/25	500/50:600/45		550/60:600/45
	40	250/40:400/25	250/40:350/25	300/50:600/35	400/50:600/25	350/50:550/25	500/50:600/45		550/60:600/45	550/35:600/25	①		600/50
	50	350/50:500/25	300/40:500/25	400/50:600/45	550/60:600/45	500/60:550/25	600/80		①	600/40	①		①
	60	400/50:600/45	300/50:550/25	550/60:600/80	600/80	550/45:600/25	①		①	①	①		①
	70	550/60:600/45	400/50:550/25	600/80	①	600/45	①		①	①	①		①
	80	550/60:600/60	500/60:600/25	①	①		①		①		①		①
R120	30	250/50:450/25	250/50:350/25	300/50:350/25	400/50:500/25	400/50:550/25	500/50:600/35		500/60:600/25	550/25	550/60:600/80		600/60
	40	300/50:500/25		400/50:600/45	500/60:600/25	500/50:550/25	550/60:600/80		600/80	550/55:600/25	①		①
	50	450/50:550/25	400/50:550/25	550/60:600/80	600/60	550/50:600/25	①		①	600/60	①		①
	60	500/60:600/45	500/50:550/25	600/80	600/80	550/55:600/50	①		①	①	①		①
	70	550/60:600/80	500/60:600/25	①	①	600/60	①		①	①	①		①
	80	600/80	550/50:600/25	①	①		①		①		①		①

*① Requires a width larger than 600 mm.

Table IV.3: Minimum dimensions and concrete covers for reinforced concrete columns with rectangular section (ISO 834). Mechanical reinforcement ratio $\omega = 0.1$. High first order moment: $e = 0.5b$ with $e \leq 200$ mm

Fire resistance	λ	Minimum dimensions [mm] : Column width b_{min} [mm]/axis distance a [mm]											
		Columns exposed on more than one side											
		n=0.15			n=0.3			n=0.5			n=0.7		
		standard fire		hydrocarbon fire	standard fire		hydrocarbon fire	standard fire		hydrocarbon fire	standard fire		hydrocarbon fire
	Numerical calculation	Eurocode 2	Numerical calculation	Numerical calculation	Eurocode 2	Numerical calculation	Numerical calculation	Eurocode 2	Numerical calculation	Numerical calculation	Eurocode 2	Numerical calculation	
R30	30	150/25		250/35:300/25	450/25	400/40:550/25	500/25	550/40:600/25	550/25	Ⓛ	Ⓛ	Ⓛ	
	40	200/25		300/35:400/25	500/40:550/25	550/25	550/60	Ⓛ	550/35:600/30	Ⓛ	Ⓛ	Ⓛ	
	50	300/30:400/25	250/30:300/25	400/35:500/25	600/25	550/30:600/25	Ⓛ	Ⓛ	Ⓛ	Ⓛ	Ⓛ	Ⓛ	
	60	400/50:450/25	300/40:550/25	500/50:600/35	Ⓛ	600/50	Ⓛ	Ⓛ	Ⓛ	Ⓛ	Ⓛ	Ⓛ	
	70	500/40:550/25	400/40:550/25	550/60:600/45	Ⓛ	Ⓛ	Ⓛ	Ⓛ	Ⓛ	Ⓛ	Ⓛ	Ⓛ	
	80	550/40:600/25	550/25	Ⓛ	Ⓛ	Ⓛ	Ⓛ	Ⓛ	Ⓛ	Ⓛ	Ⓛ	Ⓛ	
R60	30	300/30:400/25	300/35:500/25	350/50:550/25	550/25	500/50:550/25	550/40	Ⓛ	550/50:600/40	Ⓛ	Ⓛ	Ⓛ	
	40	400/50:550/25	350/40:550/25	500/35:600/35	600/25	550/40:600/30	Ⓛ	Ⓛ	Ⓛ	Ⓛ	Ⓛ	Ⓛ	
	50	550/25	450/50:550/25	550/60:600/45	Ⓛ	550/50:600/40	Ⓛ	Ⓛ	Ⓛ	Ⓛ	Ⓛ	Ⓛ	
	60	550/40:600/25	550/30	Ⓛ	Ⓛ	600/80	Ⓛ	Ⓛ	Ⓛ	Ⓛ	Ⓛ	Ⓛ	
	70	600/60	550/35	Ⓛ	Ⓛ	Ⓛ	Ⓛ	Ⓛ	Ⓛ	Ⓛ	Ⓛ	Ⓛ	
	80	Ⓛ	550/40	Ⓛ	Ⓛ	Ⓛ	Ⓛ	Ⓛ	Ⓛ	Ⓛ	Ⓛ	Ⓛ	
R90	30	350/50:550/25		400/50:600/45	550/60:600/45	550/45:600/40	Ⓛ	Ⓛ	600/80	Ⓛ	Ⓛ	Ⓛ	
	40	450/50:600/45	500/60:600/30	550/60:600/80	Ⓛ	550/60:600/50	Ⓛ	Ⓛ	Ⓛ	Ⓛ	Ⓛ	Ⓛ	
	50	550/60:600/45	550/40	600/80	Ⓛ	600/80	Ⓛ	Ⓛ	Ⓛ	Ⓛ	Ⓛ	Ⓛ	
	60	550/60:600/60	550/50:600/45	Ⓛ	Ⓛ	Ⓛ	Ⓛ	Ⓛ	Ⓛ	Ⓛ	Ⓛ	Ⓛ	
	70	Ⓛ	550/60:600/50	Ⓛ	Ⓛ	Ⓛ	Ⓛ	Ⓛ	Ⓛ	Ⓛ	Ⓛ	Ⓛ	
	80	Ⓛ	600/70	Ⓛ	Ⓛ	Ⓛ	Ⓛ	Ⓛ	Ⓛ	Ⓛ	Ⓛ	Ⓛ	
R120	30	450/50:600/25	550/40:600/30	500/50:600/80	600/60	550/50	Ⓛ	Ⓛ	Ⓛ	Ⓛ	Ⓛ	Ⓛ	
	40	500/60:600/45	550/50:600/45	550/60:600/80	Ⓛ	600/70	Ⓛ	Ⓛ	Ⓛ	Ⓛ	Ⓛ	Ⓛ	
	50	550/60:600/60	550/55:600/50	Ⓛ	Ⓛ	Ⓛ	Ⓛ	Ⓛ	Ⓛ	Ⓛ	Ⓛ	Ⓛ	
	60	600/80	550/60:600/50	Ⓛ	Ⓛ	Ⓛ	Ⓛ	Ⓛ	Ⓛ	Ⓛ	Ⓛ	Ⓛ	
	70	Ⓛ	600/70	Ⓛ	Ⓛ	Ⓛ	Ⓛ	Ⓛ	Ⓛ	Ⓛ	Ⓛ	Ⓛ	
	80	Ⓛ	Ⓛ	Ⓛ	Ⓛ	Ⓛ	Ⓛ	Ⓛ	Ⓛ	Ⓛ	Ⓛ	Ⓛ	

*Ⓛ Requires a width larger than 600 mm.

Table IV.4: Minimum dimensions and concrete covers for reinforced concrete columns with rectangular section (ISO 834). Mechanical reinforcement ratio $\omega = 0.5$. Low first order moment: $e = 0.025b$ with $e \geq 10$ mm

Fire resistance	λ	Minimum dimensions [mm] : Column width b_{min} [mm]/axis distance a [mm]																							
		Columns exposed on more than one side																							
		n=0.15			n=0.3			n=0.5			n=0.7														
		standard fire		hydrocarbon fire	standard fire		hydrocarbon fire	standard fire		hydrocarbon fire	standard fire		hydrocarbon fire												
	Numerical calculation	Eurocode 2	Numerical calculation	Numerical calculation	Eurocode 2	Numerical calculation	Numerical calculation	Eurocode 2	Numerical calculation	Numerical calculation	Eurocode 2	Numerical calculation													
R30	30	150/25		150/25		150/25		150/25		150/25		200/25													
	40	150/25		150/25		150/25		150/25		200/25		200/25													
	50	150/25		150/25		150/25		150/25		200/25		250/25													
	60	150/25		150/25		150/25		150/25		250/25		300/35:400/25													
	70	150/25		150/25		150/25		200/25		300/35:350/25		350/50:450/25													
	80	150/25		150/25		150/25		200/35:250/25		250/30:300/25		400/50:600/40													
R60	30	150/25		150/25		150/40:200/25		150/25		150/30:200/25		200/35:250/25		250/35:300/25											
	40	150/25		200/25		150/25		200/35:250/25		200/25		250/35:300/25		300/35:400/25											
	50	150/25		200/25		150/35:200/25		200/35:250/25		200/30:250/25		200/40:250/25		250/50:350/25		300/30:350/25									
	60	150/25		200/35:250/25		200/25		200/30:250/25		250/35:300/25		250/40:350/25		250/30:300/25		350/50:450/25									
	70	150/25		200/35:250/25		200/25		200/35:250/25		250/50:350/25		350/40:450/25		250/40:350/25		400/50:600/40									
	80	150/25		150/35:200/25		200/35:250/25		250/25		250/30:300/25		300/35:400/25		350/40:550/35		300/40:500/25									
R90	30	150/25		200/25		200/25		150/40:200/25		200/35:300/25		200/30:250/25		200/40:250/25		250/50:300/25		250/35:300/25		250/40:300/25		300/50:400/25			
	40	150/25		200/35:250/25		200/25		200/35:250/25		250/35:300/25		250/30:300/25		300/35:400/25		300/40:400/25		350/50:500/25		350/50:500/25		350/50:500/25			
	50	150/40:200/25		200/35:300/25		200/30:250/25		200/45:250/25		250/50:400/25		300/40:400/25		250/45:350/25		350/50:500/25		350/40:550/25		350/45:550/25		600/40			
	60	200/25		250/35:300/25		250/30:300/25		250/35:300/25		300/35:450/25		350/40:500/25		300/45:400/25		600/40		550/50:600/45		400/50:550/25		600/60			
	70	200/25		200/35:250/25		250/35:350/25		300/30:400/25		250/45:350/25		300/50:550/25		350/40:600/45		350/45:600/25		600/60		600/60		550/50:600/45		600/80	
	80	200/30:250/25		200/45:250/25		250/50:400/25		300/35:400/25		250/50:400/25		350/50:600/40		600/60		400/50:600/35		600/80		①		600/60		①	
R120	30	200/25		150/35:200/25		200/35:250/25		200/25		200/40:250/25		250/35:300/25		250/30:300/25		250/25		250/50:350/25		300/40:400/25		250/45:350/25		250/50:500/25	
	40	200/25		200/35:250/25		250/35:300/25		250/30:300/25		250/25		250/50:350/25		300/40:400/25		300/45:350/25		350/50:450/25		400/50:500/25		400/55:500/25		450/50:550/25	
	50	200/30:250/25		200/40:250/25		250/50:350/25		250/40:350/25		250/45:300/25		300/50:450/25		350/40:500/25		350/45:450/25		400/50:600/40		500/50:600/45		450/50:600/25		600/60	
	60	200/30:300/25		200/50:250/25		250/50:450/25		300/40:400/25		300/45:350/25		300/50:600/40		500/50:550/50		400/50:550/25		600/60		600/80		500/60:600/35		①	
	70	250/30:350/25		250/35:300/25		250/50:450/25		350/40:550/25		350/45:450/25		400/50:600/40		600/60		500/50:600/40		600/80		①		600/45		①	
	80	250/40:400/25		250/45:300/25		250/50:600/40		350/40:600/45		400/50:550/25		450/50:600/60		600/80		500/60:600/45		①		①		600/60		①	

*① Requires a width larger than 600 mm.

Table IV.5: Minimum dimensions and concrete covers for reinforced concrete columns with rectangular section (ISO 834). Mechanical reinforcement ratio $\omega = 0.5$. Moderate first order moment: $e = 0.25b$ with $e \leq 100$ mm

Fire resistance	λ	Minimum dimensions [mm] : Column width b_{min} [mm]/axis distance a [mm]											
		Columns exposed on more than one side											
		n=0.15			n=0.3			n=0.5			n=0.7		
		standard fire		hydrocarbon fire	standard fire		hydrocarbon fire	standard fire		hydrocarbon fire	standard fire		hydrocarbon fire
	Numerical calculation	Eurocode 2	Numerical calculation	Numerical calculation	Eurocode 2	Numerical calculation	Numerical calculation	Eurocode 2	Numerical calculation	Numerical calculation	Eurocode 2	Numerical calculation	
R30	30	150/25		150/25	150/25		150/25	150/25		200/25	200/25	200/30:250/25	300/25
	40	150/25		150/25	150/25		150/25	200/25		250/25	250/25	300/45:350/25	400/35:450/25
	50	150/25		150/25	150/25		150/25	200/25		200/25	200/30:250/25	300/25	450/35:500/25
	60	150/25		150/25	150/25		150/25	200/25		200/25	200/30:300/25	350/50:450/25	600/40
	70	150/25		150/25	150/35:200/25		250/35:300/25	350/40:450/25		350/30:400/25	450/35:550/25	550/35:600/30	①
	80	150/25		200/25	200/25		200/30:250/25	300/50:400/25		400/35:500/25	400/40:500/25	600/40	①
R60	30	150/25		150/40:200/25	150/25	150/35:200/25	200/35:250/25		250/25	250/35:350/25	300/35:350/25	350/30:400/25	450/35:500/25
	40	150/25		200/25	200/25	200/30:300/25	250/35:300/25		300/25	300/35:500/25	350/35:450/25	450/35:500/25	450/50:600/30
	50	150/25	150/30:200/25	200/35:250/25	200/25	200/40:350/25	250/50:300/25		350/40:500/25	300/45:550/25	550/25	500/50:600/25	600/60
	60	150/25	150/35:200/25	200/35:300/25	250/30:300/25	250/40:500/25	300/25		500/35:550/25	400/45:600/30	600/40	600/45	①
	70	200/25	200/30:300/25	250/35:300/25	300/40:400/25	300/40:500/25	400/50:550/25		550/50:600/45	500/40:600/35	600/60	①	600/80
	80	200/25	200/35:300/25	250/35:400/25	350/40:450/25	350/40:600/25	450/50:600/40		600/60	550/55:600/40	①	①	①
R90	30	150/35:200/25		200/35:300/25	200/30:250/25	200/45:300/25	250/50:400/25		300/40:400/25	300/45:550/25	350/50:450/25	450/35:500/25	500/50:600/40
	40	200/25	200/35:250/25	250/35:300/25	250/30:300/25	250/45:500/25	300/50:450/25		350/40:450/25	350/50:600/25	450/50:600/40	550/50:600/45	600/60
	50	200/30:250/25	200/40:300/25	250/50:400/25	300/30:400/25	300/45:550/25	350/50:500/25		500/35:600/25	500/50:600/35	600/40	600/80	600/55
	60	200/30:300/25	200/50:400/25	250/50:450/25	350/40:450/25	350/50:600/25	450/50:600/40		600/45	500/55:550/45	600/60	①	①
	70	250/35:350/25	300/35:500/25	300/50:450/25	350/40:550/35	400/50:600/35	600/40		600/80	600/50	①	①	①
	80	250/40:400/25	300/40:600/25	300/50:600/25	500/50:600/45	500/55:600/40	600/60		①	600/80	①	①	①
R120	30	200/30:250/25	200/45:300/25	250/35:300/25	250/40:350/25	300/45:550/25	300/50:450/25		350/40:450/25	450/50:600/25	400/50:600/40	500/50:600/45	500/60:600/50
	40	200/30:300/25	200/50:350/25	250/50:400/25	300/40:450/25	350/50:550/25	350/50:550/25		550/50:600/45	500/50:600/40	600/40	600/60	600/55
	50	250/35:350/25	250/45:450/25	250/50:450/25	350/40:550/25	450/50:600/25	400/50:600/40		550/50:600/45	500/55:550/45	600/60	①	600/80
	60	300/40:450/25	300/50:500/25	300/50:600/40	350/40:600/45	500/45:600/40	600/60		600/80	550/60:600/60	①	①	①
	70	300/40:450/25	350/50:550/25	350/50:600/40	550/50:600/45	500/50:550/45	600/60		①	600/75	①	①	①
	80	350/40:600/25	400/50:600/25	400/50:600/40	600/60	500/55:600/40	600/80		①	①	①	①	①

*① Requires a width larger than 600 mm.

Table IV.6: Minimum dimensions and concrete covers for reinforced concrete columns with rectangular section (ISO 834). Mechanical reinforcement ratio $\omega = 0.5$. High first order moment: $e = 0.5b$ with $e \leq 200$ mm

Fire resistance	λ	Minimum dimensions [mm] : Column width b_{min} [mm]/axis distance a [mm]											
		Columns exposed on more than one side											
		n=0.15			n=0.3			n=0.5			n=0.7		
		standard fire		hydrocarbon fire	standard fire		hydrocarbon fire	standard fire		hydrocarbon fire	standard fire		hydrocarbon fire
	Numerical calculation	Eurocode 2	Numerical calculation	Numerical calculation	Eurocode 2	Numerical calculation	Numerical calculation	Eurocode 2	Numerical calculation	Numerical calculation	Eurocode 2	Numerical calculation	
R30	30	150/25		150/25	150/25		200/25	250/25	250/35:300/25	400/25	500/25	500/40:550/25	550/25
	40	150/25		150/25	150/30:200/25		250/25	350/40:400/25	300/35:450/25	450/25	550/25	550/30	600/40
	50	150/25		150/25	200/25 200/30:250/25		300/25	450/25	400/40:500/25	550/25	600/45	550/50:600/40	①
	60	150/25		200/25	200/35:250/25		350/35:400/25	500/35:550/25	450/50:550/25	600/40	①		①
	70	150/25		200/25	300/30:350/25 250/40:400/25		450/35:500/25	550/35:600/25	500/40:600/30	①	①		①
	80	150/25		200/35:250/25	400/35:450/25 300/40:500/25		450/35:550/25	①	550/50:600/40	①	①		①
R60	30	150/25	150/30:200/25	200/35:250/25	200/30:250/25 200/40:450/25		300/35:400/25	450/35:500/25	450/50:550/30	450/50:500/25	550/50:600/40		600/60
	40	150/25	150/35:200/25	200/35:300/25	250/30:300/25 250/40:500/25		350/35:400/25	500/25	500/40:550/35	600/40	①	600/60	①
	50	200/25	200/35:300/25	250/35:300/25	350/25 300/45:550/25		400/50:500/25	550/50:600/45	500/55:550/40	600/60	①		①
	60	200/25	200/40:500/25	250/35:350/25	400/35:500/25 400/40:600/30		450/50:600/30	600/80	550/50:600/45	①	①		①
	70	200/30:250/25	200/40:550/25	300/35:400/25	500/35:550/25 500/40:550/35		600/40	①	600/60	①	①		①
	80	250/30:300/25	250/40:600/25	350/35:500/25	500/50:600/45 500/45:600/35		600/60	①		①	①		①
R90	30	200/30:250/25	200/40:450/25	250/35:400/25	300/30:400/25 300/50:500/25		350/50:450/25	500/35:550/25	500/55:600/40	600/40	①	600/80	①
	40	200/30:300/25	200/50:500/25	250/50:400/25	350/35:450/25 350/50:550/35		400/50:550/25	550/50:600/45	550/60:600/50	600/60	①		①
	50	300/25	250/45:550/25	250/50:450/25	450/35:500/25 500/45:550/40		600/40	600/80	600/60	①	①		①
	60	250/35:400/25	250/50:550/30	300/50:500/25	500/50:550/35 500/50:550/45		600/60	①	600/80	①	①		①
	70	300/40:450/25	300/50:550/35	350/50:600/40	550/50:600/45		600/80	①		①	①		①
	80	400/35:450/25	350/50:600/35	400/50:600/40	600/80 550/60:600/50		①	①		①	①		①
R120	30	250/35:350/25	250/50:550/25	250/50:450/25	350/40:450/25 500/50:550/40		400/50:600/40	550/50:600/45	550/50	600/60	①		①
	40	300/40:400/25	300/50:600/25	300/50:500/25	350/40:600/25 500/55:550/45		450/50:600/40	600/60	550/60:600/55	①	①		①
	50	300/40:450/25	400/50:550/35	300/50:600/40	500/50:600/45 500/60:600/45		600/60	①	600/80	①	①		①
	60	350/40:500/25	450/50:600/40	350/50:600/40	600/45 550/50		600/60	①		①	①		①
	70	350/40:600/45	500/50:550/45	450/50:600/40	600/80 550/60:600/55		①	①		①	①		①
	80	350/40:600/45	550/50:600/45	450/50:600/40	① 600/70		①	①		①	①		①

*① Requires a width larger than 600 mm.

Table IV.7: Minimum dimensions and concrete covers for reinforced concrete columns with rectangular section (ISO 834). Mechanical reinforcement ratio $\omega = 1.0$. Low first order moment: $e = 0.025b$ with $e \geq 10$ mm

Fire resistance	λ	Minimum dimensions [mm] : Column width b_{min} [mm]/axis distance a [mm]											
		Columns exposed on more than one side											
		n=0.15			n=0.3			n=0.5			n=0.7		
		standard fire		hydrocarbon fire	standard fire		hydrocarbon fire	standard fire		hydrocarbon fire	standard fire		hydrocarbon fire
	Numerical calculation	Eurocode 2	Numerical calculation	Numerical calculation	Eurocode 2	Numerical calculation	Numerical calculation	Eurocode 2	Numerical calculation	Numerical calculation	Eurocode 2	Numerical calculation	
R30	30	150/25	150/25	150/25	150/25	150/25	150/25	150/25	150/25	150/25	150/25	200/25	
	40	150/25	150/25	150/25	150/25	150/25	150/25	150/25	150/25	150/25	150/25	200/25	
	50	150/25	150/25	150/25	150/25	150/25	150/25	150/25	200/25	200/25	150/30:200/25	250/25	
	60	150/25	150/25	150/25	150/25	150/25	150/25	150/25	200/40:250/25	200/25	200/30:250/25	300/35:350/25	
	70	150/25	150/25	150/25	150/25	150/25	200/25	150/30:200/25	250/35:300/25	250/35:350/25	250/25	350/50:450/25	
	80	150/25	150/25	150/25	150/25	200/25	200/25	200/30:250/25	300/35:350/25	300/35:350/25	250/30:300/25	350/50:550/25	
R60	30	150/25	150/25	150/25	150/25	150/40:200/25	150/25	150/25	200/40:250/25	200/25	200/40:300/25	250/35:300/25	
	40	150/25	150/25	150/25	150/25	200/25	200/25	200/30:250/25	200/40:300/25	250/25	250/35:350/25	300/35:400/25	
	50	150/25	150/40:200/25	150/25	150/30:200/25	200/40:250/25	200/30:250/25	200/40:250/25	250/50:350/25	300/25	250/40:350/25	350/50:450/25	
	60	150/25	150/40:200/25	150/30:200/25	150/40:250/25	200/40:300/25	250/35:300/25	300/35:450/25	350/40:450/25	300/40:600/25	400/50:600/45	400/50:600/45	
	70	150/25	200/25	200/25	200/35:250/25	250/35:300/25	300/35:400/25	250/40:400/25	350/50:500/25	400/50:600/45	350/40:450/35	500/50:600/45	
	80	150/25	200/40:250/25	200/30:250/25	200/40:300/25	250/35:400/25	300/50:450/25	300/40:550/25	400/50:600/45	450/50:600/45	350/45:450/40	600/60	
R90	30	150/25	150/25	200/25	200/25	200/40:250/25	200/40:250/25	200/40:250/25	250/50:350/25	250/50:350/25	250/45:600/25	300/50:400/25	
	40	150/25	200/25	200/25	200/35:250/25	250/35:300/25	250/35:300/25	250/35:350/25	250/50:400/25	300/50:400/25	300/45:600/30	350/50:600/25	
	50	150/30:200/25	150/35:200/25	200/40:250/25	200/30:250/25	200/40:250/25	250/50:350/25	250/50:400/25	250/45:400/25	300/50:600/25	400/50:550/25	350/45:600/35	450/50:600/45
	60	200/25	150/40:250/25	200/40:300/25	200/40:250/25	250/55:300/25	250/50:450/25	300/50:450/25	300/45:550/25	400/50:600/45	450/50:600/35	400/50:600/40	600/60
	70	200/25	200/35:250/25	250/35:300/25	250/35:300/25	300/35:300/25	250/50:450/25	400/50:600/35	350/45:600/35	450/50:600/45	600/60	550/50:600/45	600/80
	80	200/30:250/25	200/40:250/25	250/35:400/25	250/50:400/25	300/40:500/25	300/50:600/45	450/50:600/45	350/50:600/40	600/60	600/80	550/65:600/55	①
R120	30	200/25	150/40:200/25	200/25	200/40:250/25	200/45:250/25	250/50:300/25	250/50:350/25	250/45:400/25	300/50:400/25	300/50:400/25	400/40:600/25	350/50:500/25
	40	200/25	200/30:250/25	200/40:250/25	250/35:300/25	250/25	250/50:350/25	250/50:450/25	300/45:400/25	300/50:500/25	400/50:600/25	400/50:600/30	450/50:600/25
	50	200/30:250/25	200/40:250/25	250/35:300/25	250/35:350/25	250/35:300/25	250/50:450/25	300/50:550/25	350/40:550/25	400/50:600/25	450/50:600/45	550/45:600/40	600/25
	60	200/40:300/25	200/45:250/25	250/50:400/25	250/50:400/25	250/45:400/25	300/50:600/25	400/50:600/35	400/50:600/25	450/50:600/25	600/60	550/60:600/50	600/80
	70	250/35:300/25	250/25	250/50:450/25	300/50:450/25	350/35:450/25	300/50:600/25	500/50:600/45	550/40:600/35	600/25	600/80	600/70	①
	80	250/35:400/25	250/35:300/25	250/50:450/25	300/50:600/35	350/40:550/25	350/50:600/25	600/60	550/50:600/45	600/80	①	①	①

*① Requires a width larger than 600 mm.

Table IV.8: Minimum dimensions and concrete covers for reinforced concrete columns with rectangular section (ISO 834). Mechanical reinforcement ratio $\omega = 1.0$. Moderate first order moment: $e = 0.25b$ with $e \leq 100$ mm

Fire resistance	λ	Minimum dimensions [mm] : Column width b_{min} [mm]/axis distance a [mm]													
		Columns exposed on more than one side													
		n=0.15			n=0.3			n=0.5			n=0.7				
		standard fire		hydrocarbon fire	standard fire		hydrocarbon fire	standard fire		hydrocarbon fire	standard fire		hydrocarbon fire		
	Numerical calculation	Eurocode 2	Numerical calculation	Numerical calculation	Eurocode 2	Numerical calculation	Numerical calculation	Eurocode 2	Numerical calculation	Numerical calculation	Eurocode 2	Numerical calculation			
R30	30	150/25		150/25	150/25		150/25		150/25		200/25	200/25	200/30:300/25	300/25	
	40	150/25		150/25	150/25		150/25		150/25		250/25	250/25	250/35:300/25	250/30:450/25	350/50:400/25
	50	150/25		150/25	150/25		150/25		200/25		250/25	250/25	350/40:400/25	300/35:500/25	450/50:500/25
	60	150/25		150/25	150/25		200/25		250/25	200/30:250/25	300/50:400/25	450/25	400/40:550/25	500/50:600/25	550/50:600/25
	70	150/25		150/25	150/25		200/40:250/25		300/25	250/35:300/25	400/50:450/25	500/50:550/25	500/35:600/30	550/50:600/30	550/50:600/30
	80	150/25		150/25	200/25		150/30:250/25	250/25		350/40:400/25	300/35:500/25	450/50:550/25	600/35	500/60:600/35	①
R60	30	150/25		150/40:200/25	150/25	150/30:200/25	200/40:250/25		200/25	200/40:400/25	250/50:350/25	300/35:350/25	300/50:600/30	450/25	450/25
	40	150/25		150/40:200/25	150/30:200/25	150/40:250/25	200/40:300/25		250/35:300/25	250/40:500/25	300/35:400/25	450/25	400/50:600/35	500/50:600/25	500/50:600/25
	50	150/25		200/40:250/25	200/25	200/35:400/25	250/35:300/25		300/25	300/40:600/25	400/50:450/25	500/50:600/25	500/45:600/40	550/50:600/45	550/50:600/45
	60	150/25	150/30:200/25	200/40:250/25	200/30:250/25	200/40:450/25	250/50:400/25		400/50:450/25	400/40:600/30	450/50:600/25	600/45	550/40:600/40	600/80	600/80
	70	150/25	150/35:200/25	200/40:300/25	250/35:300/25	250/40:550/25	300/35:450/25		450/50:550/25	450/45:500/35	550/50:600/45	①	600/60	①	①
	80	150/25	200/30:250/25	200/40:300/25	300/35:350/25	300/40:550/25	350/50:450/25		500/50:600/35	500/50:600/40	600/60	①	600/80	①	①
R90	30	150/30:200/25	200/25	200/40:250/25	200/30:250/25	200/40:300/25	250/35:350/25		250/50:350/25	250/40:550/25	300/50:450/25	450/50:500/25	500/50:600/45	500/50:600/45	500/50:600/45
	40	200/25	200/30:250/25	200/40:300/25	200/40:300/25	200/50:400/25	250/50:400/25		300/50:450/25	300/50:600/35	350/50:600/45	500/50:600/35	500/60:600/50	600/45	600/45
	50	200/25	200/35:300/25	250/35:300/25	250/35:300/25	250/50:550/25	300/50:450/25		450/50:500/25	400/50:600/40	500/50:600/45	600/60	600/55	600/80	600/80
	60	200/30:250/25	200/40:400/25	250/35:400/25	300/35:400/25	300/45:600/25	300/50:600/25		500/50:600/35	500/50:600/45	600/45	①	600/70	①	①
	70	200/40:300/25	200/45:450/25	250/50:450/25	300/50:450/25	300/50:600/35	400/50:600/45		600/60	550/55:600/50	600/80	①	①	①	①
	80	200/40:300/25	200/50:500/25	250/50:450/25	400/50:550/25	400/50:600/35	450/50:600/45		600/80	600/55	①	①	①	①	①
R120	30	200/30:250/25	200/40:250/25	250/35:300/25	250/35:300/25	250/50:400/25	250/50:450/25		300/50:550/25	450/45:600/30	400/50:600/25	500/50:600/35	600/60	550/50:600/25	550/50:600/25
	40	200/40:300/25	200/45:300/25	250/50:400/25	250/50:400/25	300/40:500/25	300/50:500/25		400/50:600/35	500/50:600/35	450/50:600/25	600/45	①	600/25	600/25
	50	250/35:300/25	250/40:400/25	250/50:450/25	300/50:450/25	400/40:550/25	350/50:600/25		550/50:600/45	550/50:600/25	①	①	①	①	①
	60	250/35:400/25	250/50:450/25	250/50:450/25	400/50:600/25	400/50:500/35	400/50:600/25		600/45	600/55	600/25	①	①	①	①
	70	250/50:400/25	300/40:500/25	300/50:600/25	450/50:600/35	500/45:600/35	450/50:600/25		600/80	①	①	①	①	①	①
	80	250/50:450/25	300/50:550/25	300/50:600/25	500/50:600/35	500/60:600/40	550/50:600/25		①	①	①	①	①	①	①

*① Requires a width larger than 600 mm.

Table IV.9: Minimum dimensions and concrete covers for reinforced concrete columns with rectangular section (ISO 834). Mechanical reinforcement ratio $\omega = 1.0$. High first order moment: $e = 0.5b$ with $e \leq 200$ mm

Fire resistance	λ	Minimum dimensions [mm] : Column width b_{min} [mm]/axis distance a [mm]											
		Columns exposed on more than one side											
		n=0.15			n=0.3			n=0.5			n=0.7		
		standard fire		hydrocarbon fire	standard fire		hydrocarbon fire	standard fire		hydrocarbon fire	standard fire		hydrocarbon fire
	Numerical calculation	Eurocode 2	Numerical calculation	Numerical calculation	Eurocode 2	Numerical calculation	Numerical calculation	Eurocode 2	Numerical calculation	Numerical calculation	Eurocode 2	Numerical calculation	
R30	30	150/25		150/25	150/25		150/25	200/25	200/30:300/25	300/25	500/25	500/30:550/25	500/50:550/25
	40	150/25		150/25	150/25		200/25	250/35:300/25	250/30:450/25	350/50:400/25	500/25	500/40:600/30	550/50:600/25
	50	150/25		150/25	150/25	150/30:200/25	250/25	350/40:400/25	300/35:500/25	450/25	550/50:600/25	550/35	600/45
	60	150/25		150/25	200/25	200/30:250/25	250/25	450/25	350/40:500/25	500/50:550/25	①	550/50	①
	70	150/25		150/25	200/30:250/25	200/30:300/25	300/25	500/25	450/50:550/25	550/50:600/25	①		①
	80	150/25		200/25	250/35:300/25	250/30:350/25	350/50:400/25	550/25	500/35:600/30	600/45	①		①
R60	30	150/25		200/25	200/25	200/35:450/25	250/35:300/25	350/25	350/40:600/30	450/25	550/25	550/45:600/40	600/45
	40	150/25	150/30:200/25	200/40:250/25	200/30:250/25	200/40:500/25	300/35:350/25	450/25	450/50:500/35	500/50:550/25	600/45	600/60	①
	50	150/25	150/35:250/25	200/40:300/25	250/35:300/25	250/40:550/25	300/35:400/25	500/50:550/25	500/40:600/35	550/50:600/45	①	600/80	①
	60	200/25	200/30:350/25	200/40:300/25	250/50:300/25	300/40:600/25	350/50:450/25	550/50:600/25	500/50:600/40	600/60	①		①
	70	200/25	250/30:450/25	250/35:300/25	350/40:450/25	350/40:600/30	450/50:550/25	600/45	550/50:600/45	①	①		①
	80	200/25	250/55:500/25	250/35:400/25	450/50:500/25	450/40:500/35	450/50:600/45	①	600/70	①	①		①
R90	30	200/25	200/35:300/25	250/35:300/25	250/35:300/25	250/50:550/25	300/50:450/25	450/25	500/50:600/40	400/50:600/45	600/80	600/70	①
	40	200/30:250/25	200/40:450/25	250/35:400/25	300/35:400/25	300/50:600/30	300/50:450/25	500/50:600/25	500/55:600/45	550/50:600/45	①		①
	50	200/40:300/25	200/45:500/25	250/50:400/25	300/50:450/25	350/50:600/35	400/50:600/25	550/50:600/35	550/50	600/60	①		①
	60	200/40:300/25	200/50:550/25	250/50:450/25	400/50:450/25	450/50:600/40	450/50:600/45	600/80	600/60	①	①		①
	70	250/35:300/25	250/45:600/30	300/50:450/25	450/50:600/25	500/50:600/45	500/50:600/45	①	600/80	①	①		①
	80	250/50:400/25	250/50:500/35	300/50:550/25	500/50:600/35	500/55:600/45	600/45	①		①	①		①
R120	30	250/35:300/25	200/50:450/25	250/50:450/25	300/50:450/25	450/45:600/25	350/50:550/25	450/50:600/45	550/55:600/50	500/50:600/25	①		①
	40	250/35:350/25	250/50:500/25	250/50:450/25	350/40:450/25	500/40:600/30	400/50:600/25	550/50:600/45	600/65	600/25	①		①
	50	250/50:400/25	300/40:550/25	300/50:500/25	400/50:600/25	500/50:600/35	450/50:600/25	600/60	①	①	①		①
	60	250/50:450/25	350/45:550/25	300/50:600/25	450/50:600/35	500/60:600/40	500/50:600/25	①	①	①	①		①
	70	300/50:450/25	450/40:600/30	350/50:600/25	550/50:600/45	550/60:600/50	600/25	①	①	①	①		①
	80	300/50:600/25	450/45:600/30	400/50:600/25	600/60	600/65	600/25	①	①	①	①		①

*① Requires a width larger than 600 mm.

From the tables above and comparing these with the tabulated data provided in Eurocode 2 (2004), it can be seen that the tables from Eurocode 2 (2004) are not safe for the case of a reinforcement ratio of 0.1, as well for a reinforcement ratio of 0.5 when the axial load is large ($n \geq 0.5$). On the other hand, some minimum dimensions are overly conservative in case the reinforcement ratio is 1.0.

Finally, based on Table IV.1 to IV.9, an approximate value can be found on which the design can be based using an interpolation value for a minimum cross-section design in case of columns (the reinforcement ratio being no more than 1.0 and the slenderness ratio being no more than 80 and the fire duration being no more than 2 hours) subjected to an ISO 834 fire. As the calculation tool has been validated, the tabulated data recalculated with the tool is strongly recommended to be used in order to update Eurocode 2 for the fire resistance design of reinforced concrete columns.

IV.3. Extension of the tabulated data for concrete columns exposed to hydrocarbon fires and natural fires

Eurocode 2 (2004) only provides minimum dimensions with respect to an ISO 834 standard fire, but this standard fire does not provide a true indication of how structural members and assemblies will behave in an actual fire or when exposed to a hydrocarbon fire. As resistance to hydrocarbon fires may be required in specific situations and little data is available on the design of concrete columns exposed to hydrocarbon fires, extending the tables from EN 1992-1-2 (2004) with respect to this more severe design fire is important. Hence, the same analytical method is used to determine the required cross-section characteristics for columns exposed to these other fire curves.

Hydrocarbon fires represent the burning of for example gasoline pool fires and are widely used when designing technical facilities and tunnels. Natural fires account for the fire loads, openings and thermal properties of surrounding structures and decrease in intensity once the fuel has been burned.

IV.3.1. Fire resistance of columns subjected to hydrocarbon fires

The hydrocarbon temperature-time curve is given by (Eurocode 2, 2004) and shown in Fig. IV.6:

$$\Theta_g = 20 + 1080 (1 - 0.325 e^{-0.167 t} - 0.675 e^{-2.5 t}) \quad (\text{IV.1})$$

where Θ_g is the gas temperature in the fire compartment [$^{\circ}\text{C}$]

t is the time [min]

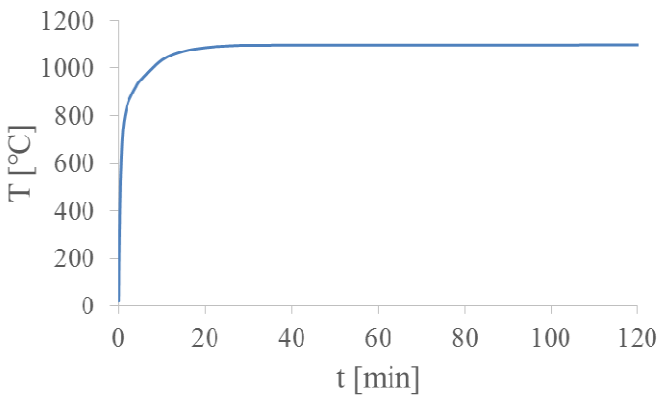


Fig. IV.6 The hydrocarbon fire curve

The same material properties and boundary conditions as in EN 1992-1-2 (Eurocode 2, 2004) are considered in case of this hydrocarbon fire. The minimum required cross-sections of columns at 30 min, 60 min, 90 min and 120 min are shown in the same tables as in case of the ISO 834 standard fire (Table IV.1 to IV.9).

IV.3.2. Fire resistance of columns subjected to natural fires

Unlike a nominal fire curve, a natural fire model takes into account how the environment, density of combustible materials and ventilation will affect the development of the fire. The temperature-time curves in the heating phase are given by (Eurocode 2, 2004):

$$\Theta_g = 20 + 1325 (1 - 0.324 e^{-0.2 t^*} - 0.204 e^{-1.7 t^*} - 0.472 e^{-19 t^*}) \quad (\text{IV.2})$$

where Θ_g is the gas temperature in the fire compartment [°C]

$$t^* = t \times \Gamma \text{ [h]}$$

with t time

$$\Gamma = \left[\frac{0}{b} \right]^2 / \left(\frac{0.04}{1160} \right)^2 \text{ [-]}$$

$$b = \sqrt{(\rho c \lambda)} \text{ with the limits: } 100 \leq b \leq 2200 \text{ [J/m}^2\text{s}^{1/2}\text{K]}$$

ρ density of boundary of enclosure [kg/m³]

c specific heat of boundary of enclosure [J/kgK]

λ thermal conductivity of boundary of enclosure [W/mK]

O opening factor: $O = A_w \sqrt{h_w} / A_t$ with the limits: $0.02 \leq O \leq 0.2$ [m^{1/2}]

A_w total area of vertical openings on all walls [m²]

h_w weighted average of window heights on all walls [m]

A_t total area of enclosure (walls, ceiling and floor, including openings) [m²]

Besides considering standard ISO 834 fires or hydrocarbon fires, the developed calculation analysis can also be used when columns are subjected to natural fires. Interaction curves of columns are derived here for natural fires considered for dwellings and offices. The fire load densities are listed in Table IV.10.

Table IV.10: Occupancy-specific fire load densities [MJ/m²]

Occupancy	Mean	Standard Deviation	80-Percentile
Dwelling	780	234	948
Office	420	126	511

In EN 1992-1-2 (Eurocode 2, 2004), the mean value of the fire load density is provided for the typical occupancy and the characteristic value is proposed to be the 80-percentile of a Gumbel distribution. In this case, the same fire compartment as (Zehfuss, 2007) is adopted for both the case of a dwelling and an office with $A_f = 16 \text{ m}^2$, height $h = 3 \text{ m}$, area of openings $A_w = 8 \text{ m}^2$, total area of enclosing components (including openings) $A_t = 80 \text{ m}^2$ and average height of openings $h_w =$

2.50 m. The temperature-time curves for the dwelling and the office are given in Fig. IV.7 (a) & (b), respectively.

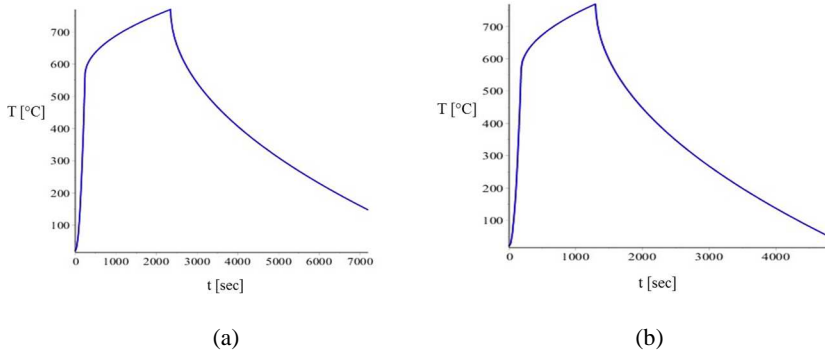


Fig. IV.7: Specific temperature-time curves considered for the analysis: (a) dwelling; (b) office

It is worthwhile to note that these natural fires start to decrease after about 50 min in the dwelling and 30 min in the office.

Next, a square column subjected to these fire conditions is analysed. The cross-section is $300 \text{ mm} \times 300 \text{ mm}$, with one diameter 32 mm reinforcing bar in each corner and a concrete cover of 25 mm; concrete compressive strength $f_{ck} = 55 \text{ MPa}$, reinforcement yield strength $f_y = 500 \text{ MPa}$ and Young's modulus of steel $E_s = 2 \times 10^5 \text{ N/mm}^2$. The reinforcement temperature as a function of the fire exposure time is shown in Figs. IV.8 and IV.9, for the two fire simulations respectively.

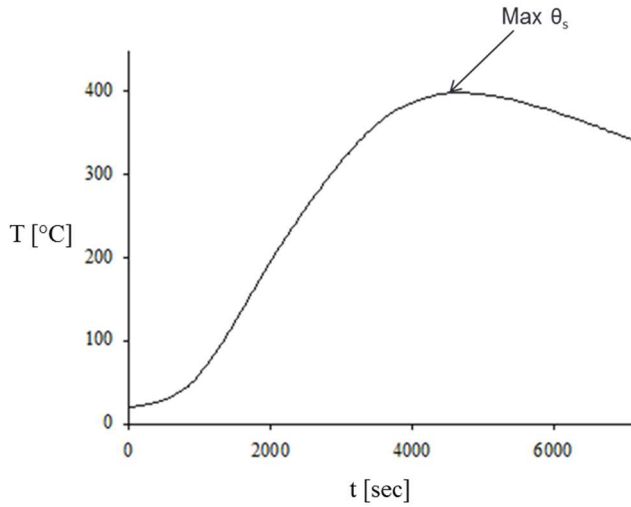


Fig. IV.8: Temperature-time diagram of the reinforcement bars (dwelling)

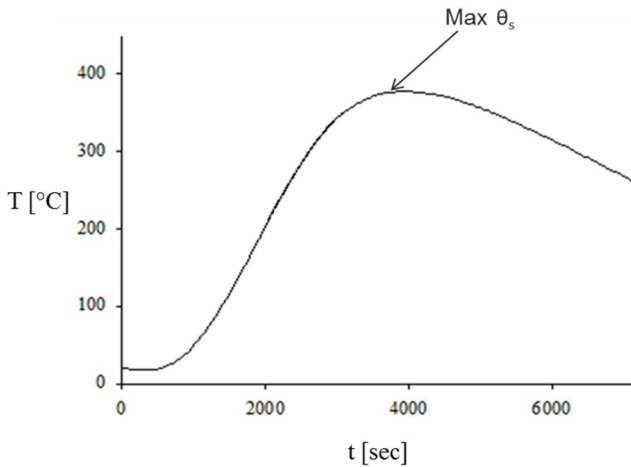


Fig. IV.9: Temperature-time diagram of the reinforcement bars (office)

It can be observed that the reinforcement temperature begins to decrease at 75 min (4500 sec) in the dwelling and 60 min (3600 sec) in the office. Considering plastic damages and strength losses of concrete material, the stress-strain relationship for cooling down is not the same as for increasing fire temperature. However, no specific guidelines are given in Eurocode 2 to calculate the cooling down branch. In order to solve this problem, an analytical method is proposed. This analytical

approach, on the one hand, supposes that there is no strength recovery of the concrete and adopts the same stress-strain model to calculate the upper limit curve during the cooling down period (considering perfect recovery). On the other hand, it considers that the stress-strain model associated with the maximum local concrete temperature obtained during the fire is maintained. In this way, a lower limit curve can be obtained (considering no recovery). As a result, the real bending moment capacity of columns should be located between these two curves. The current analytical tool, however, has not been validated for the full cooling phase yet. The maximum local concrete temperature is a simplified and conservative way to predict the fire resistance when the fire temperature begins to decrease. Take the dwelling for instance: upper and lower limit curves (Figs. IV.10 and IV.11) in the case of different normal forces are calculated, where M is the bending moment capacity, $n = N_{0Ed,fi} / (0.7(A_c f_{cd} + A_s f_{yd}))$ as proposed in EN 1992-1-2 (Eurocode 2, 2004). It is worth mentioning that an additional reduction of 10% on the residual strength is recommended for the cooling phase when the implicit transient creep strain material model provided in Eurocode 2 (2004) is adopted (EN 1994-1-2, 2005).

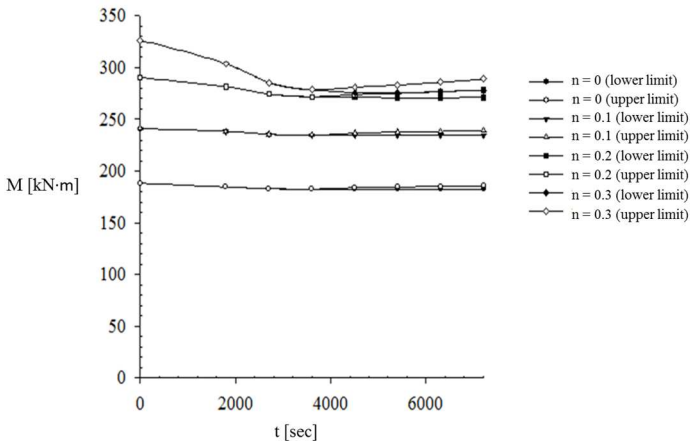


Fig. IV.10: Maximum bending moment of columns during the fire in case of a dwelling ($n \leq 0.3$)

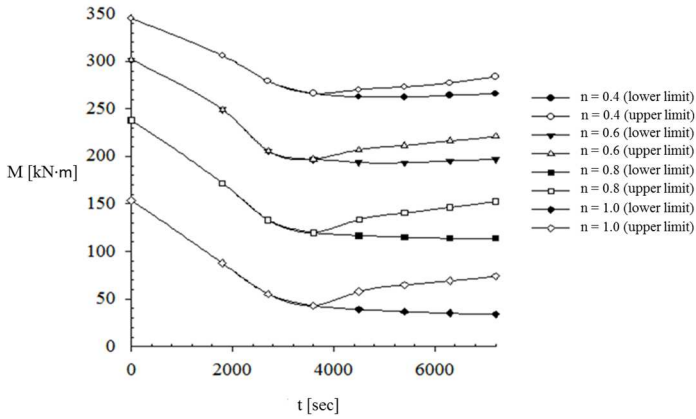


Fig. IV.11: Maximum bending moment of columns during the fire in case of a dwelling ($n > 0.3$)

Fig. IV.10 indicates that the maximum bending moment does not decrease much when the normal force is low (n is less than 0.3). This is because second-order effects are insignificant in case of axial loads with small eccentricities. As soon as n reaches 0.3, the maximum bending moment decreases significantly when the eccentric load is increasing. It is worth mentioning that the lower limit curve increases again when the reinforcing bars are cooling down. Comparing the curves in Fig. IV.11, it is observed that the lower limit curve does not decrease much further below the most critical point of the upper limit curve. The same analysis has been performed for an office in case of a natural fire and the maximum bending moments in function of fire duration are shown in Table IV.11.

Table IV.11: Maximum bending moment of columns during natural fires in case of an office

n t (min)	0		0.1		0.2		0.3		0.4		0.5		0.6		0.7		0.8		0.9		1	
	Perfect recovery	No recovery	Perfect recovery	No recovery	Perfect recovery	No recovery	Perfect recovery	No recovery	Perfect recovery	No recovery	Perfect recovery	No recovery	Perfect recovery	No recovery	Perfect recovery	No recovery	Perfect recovery	No recovery	Perfect recovery	No recovery	Perfect recovery	No recovery
0	188	188	241	241	290	290	326	326	345	345	332	332	301	301	271	271	238	238	199	199	154	154
15	188	188	241	241	290	290	325	325	342	342	331	331	298	298	265	265	229	229	187	187	143	143
30	183	183	237	237	278	278	297	297	297	297	270	270	236	236	197	197	158	158	116	116	73	73
45	182	182	235	234	272	270	283	278	275	266	244	237	200	193	166	156	126	117	86	80	48	41
60				233		269		274		259		227		188		144		112		75		36
75								273		259		227		188		143		111		73		33
90																				72		32

Take the case of $n = 0.3$ for instance, the possible range of the maximum permitted bending moment curve during cooling down is indicated as the shaded area in Fig. IV.12.

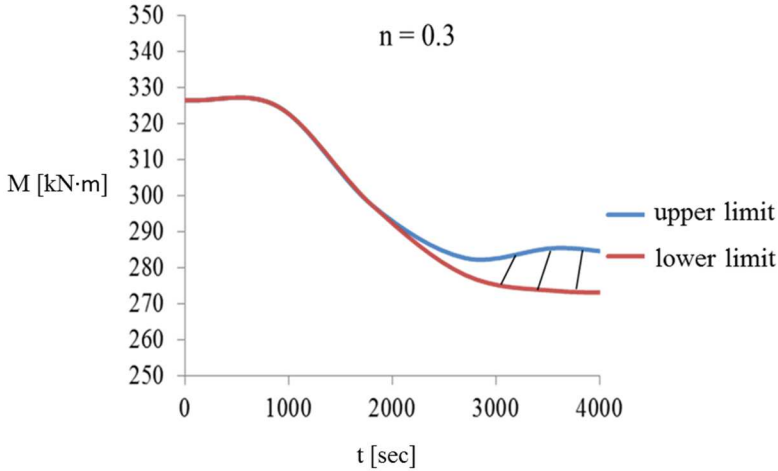


Fig. IV.12: Range of maximum bending moment during a natural fire when $n = 0.3$

Further, the lower limit curve can be adopted to calculate interaction curves of columns for different slenderness ratios. Take the same material properties and the same cross-section as mentioned in Section IV.1.2 for instance, interaction curves based on the lower limit curve at the most critical time for the dwelling and the office are provided in Figs. IV.13 and IV.14, with $n = \frac{N_c + N_s}{0.7(A_c f_{cd} + A_s f_{yd})}$ and $m = \frac{M_c + M_s}{0.7(A_c f_{cd} + A_s f_{yd})h}$, where N_c , M_c , N_s , M_s are maximum axial forces and bending moments respectively for concrete and reinforcement, b is the width of the column and h is the height of the cross-section.

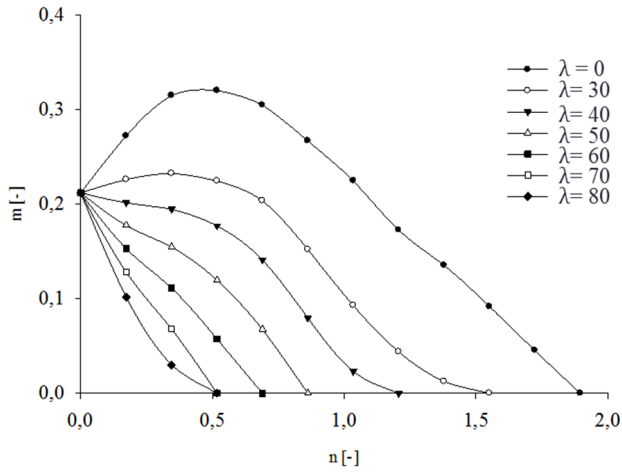


Fig. IV.13: Interaction curves of columns at 75 min of fire (dwelling)

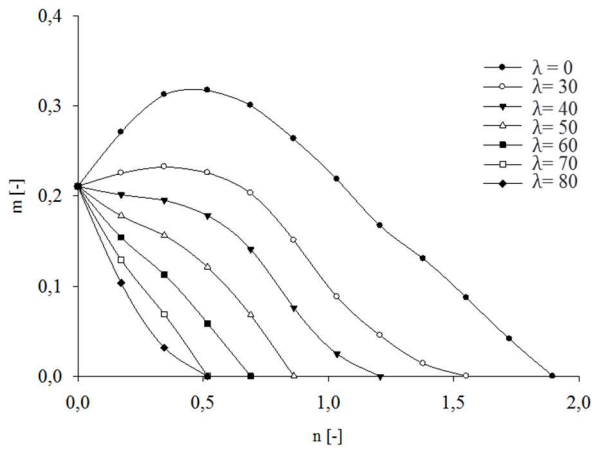


Fig. IV.14: Interaction curves of columns at 60 min of fire (office)

Finally, natural fires with a fire load density which ranges from 200 MJ/m² to 1000 MJ/m² are investigated. Minimum required dimensions of columns for different slenderness ratios and different n values are provided in Table IV.12 for the case of a reinforcement ratio $\omega = 0.5$ and eccentricity $e = 0.025b$ with $e \geq 10$ mm, in

Table IV.13 for the case of $\omega = 0.5$ and $e = 0.25b$ with $e \leq 100$ mm and in Table IV.14 for the case of $\omega = 0.5$ and $e = 0.5b$ with $e \leq 200$ mm.

Table IV.12: Minimum dimensions and concrete covers for reinforced concrete columns; rectangular section. Mechanical reinforcement ratio $\omega = 0.5$. Low first order moment: $e = 0.025b$ with $e \geq 10$ mm (natural fires)

Fire load densities [MJ/m ²]	λ	Minimum dimensions [mm] : Column width b_{min} [mm]/axis distance a [mm]			
		Columns exposed on more than one side			
		$n = 0.15$	$n = 0.3$	$n = 0.5$	$n = 0.7$
200	30	150/25	150/25	150/25	150/25
	40	150/25	150/25	150/25	150/25
	50	150/25	150/25	150/25	150/25
	60	150/25	150/25	150/25	150/25
	70	150/25	150/25	150/25	200/25
	80	150/25	150/25	200/25	300/25
400	30	150/25	150/25	150/25	150/25
	40	150/25	150/25	150/25	150/25
	50	150/25	150/25	150/25	200/25
	60	150/25	150/25	150/25	250/25
	70	150/25	150/25	200/25	300/25
	80	150/25	150/25	300/25	350/25
600	30	150/25	150/25	150/25	150/25
	40	150/25	150/25	150/25	150/25
	50	150/25	150/25	150/25	200/25
	60	150/25	150/25	200/25	300/25
	70	150/25	150/25	250/25	350/25
	80	150/25	150/25	300/25	550/25
800	30	150/25	150/25	150/25	150/25
	40	150/25	150/25	150/25	200/25
	50	150/25	150/25	150/25	250/25
	60	150/25	150/25	200/25	300/25
	70	150/25	150/25	300/25	400/25
	80	150/25	200/25	350/25	①
1000	30	150/25	150/25	150/25	150/25
	40	150/25	150/25	150/25	200/25
	50	150/25	150/25	200/25	250/25
	60	150/25	150/25	250/25	350/25
	70	150/25	200/25	300/25	500/25
	80	150/25	250/25	400/25	①

*① Requires a width larger than 600 mm.

Table IV.13: Minimum dimensions and concrete covers for reinforced concrete columns; rectangular section. Mechanical reinforcement ratio $\omega = 0.5$. Moderate first order moment: $e = 0.25b$ with $e \leq 100$ mm (natural fires)

Fire load densities [MJ/m ²]	λ	Minimum dimensions [mm] : Column width b_{min} [mm]/axis distance a [mm]			
		Columns exposed on more than one side			
		n = 0.15	n = 0.3	n = 0.5	n = 0.7
200	30	150/25	150/25	150/25	150/25
	40	150/25	150/25	150/25	200/25
	50	150/25	150/25	150/25	300/25
	60	150/25	150/25	200/25	400/25
	70	150/25	150/25	300/25	500/25
	80	150/25	150/25	450/25	600/25
400	30	150/25	150/25	150/25	200/25
	40	150/25	150/25	150/25	250/25
	50	150/25	150/25	200/25	400/25
	60	150/25	150/25	250/25	500/25
	70	150/25	150/25	450/25	①
	80	150/25	250/25	500/25	①
600	30	150/25	150/25	150/25	250/25
	40	150/25	150/25	200/25	300/25
	50	150/25	150/25	250/25	450/25
	60	150/25	150/25	400/25	600/25
	70	150/25	200/25	500/25	①
	80	150/25	300/25	①	①
800	30	150/25	150/25	150/25	250/25
	40	150/25	150/25	200/25	400/25
	50	150/25	150/25	300/25	500/25
	60	150/25	200/25	450/25	①
	70	150/25	250/25	550/25	①
	80	150/25	300/25	①	①
1000	30	150/25	150/25	200/25	300/25
	40	150/25	150/25	250/25	450/25
	50	150/25	200/25	300/25	550/25
	60	150/25	250/25	450/25	①
	70	150/25	300/25	①	①
	80	150/25	400/25	①	①

*① Requires a width larger than 600 mm.

Table IV.14: Minimum dimensions and concrete covers for reinforced concrete columns; rectangular section. Mechanical reinforcement ratio $\omega = 0.5$. High first order moment: $e = 0.5b$ with $e \leq 200$ mm (natural fires)

Fire load densities [MJ/m ²]	λ	Minimum dimensions [mm] : Column width b_{min} [mm]/axis distance a [mm]			
		Columns exposed on more than one side			
		$n = 0.15$	$n = 0.3$	$n = 0.5$	$n = 0.7$
200	30	150/25	150/25	200/25	450/25
	40	150/25	150/25	300/25	500/25
	50	150/25	150/25	400/25	550/25
	60	150/25	200/25	450/25	600/25
	70	150/25	250/25	550/25	①
	80	150/25	300/25	①	①
400	30	150/25	150/25	300/25	500/25
	40	150/25	150/25	400/25	550/25
	50	150/25	200/25	450/25	①
	60	150/25	250/25	550/25	①
	70	150/25	350/25	①	①
	80	150/25	400/25	①	①
600	30	150/25	150/25	350/25	500/25
	40	150/25	200/25	500/25	600/25
	50	150/25	250/25	500/25	①
	60	150/25	350/25	600/25	①
	70	150/25	450/25	①	①
	80	150/25	500/25	①	①
800	30	150/25	150/25	350/25	550/25
	40	150/25	200/25	450/25	①
	50	150/25	300/25	550/25	①
	60	150/25	350/25	①	①
	70	150/25	450/25	①	①
	80	200/25	550/25	①	①
1000	30	150/25	200/25	350/25	550/25
	40	150/25	250/25	500/25	①
	50	150/25	300/25	600/25	①
	60	150/25	450/25	①	①
	70	200/25	500/25	①	①
	80	250/25	600/25	①	①

*① Requires a width larger than 600 mm.

Tables IV.12 to IV.14 illustrate the minimum required dimensions of columns exposed to natural fires. It can be noticed that a conservative minimum required dimension $250 \text{ mm} \times 250 \text{ mm}$ corresponding to a maximum slenderness ratios of 80 and a fire load density of 1000 MJ/m^2 can be suggested for all fire densities above in case of $n=0.3$ when the first order moment is low. However, the minimum required dimension is increasing quickly with increasing normal force due to the high first order moment. As it is shown in Table IV.14, a width higher than 600 mm is required when the slenderness ratio is more than 50 and the fire load density is 400 MJ/m^2 in case of $n = 0.7$. It is worth noting that only the parameters provided in Zehfuss (2007) are discussed herein considering different fire load densities. However, the calculation tool can be easily adopted for any parametric fire.

IV.4. Conclusions

In this chapter, the minimum dimensions of columns in case of ISO 834 standard fire are determined and some comparisons with experimental results are provided in order to validate the obtained calculation tool. It is found that Eurocode provisions on the one hand are not safe for the case of a reinforcement ratio equal to 0.1 as well as a reinforcement ratio equal to 0.5 when the axial load is large. On the other hand, tabulated data is found to be too conservative for high reinforcement ratios ($\omega = 1.0$), which results in inefficient and uneconomical solutions for practice. Considering an economical aspect as well as the safety issue, the tabulated data obtained in the current work provide more precise proposals for the design of concrete columns exposed to fire.

Furthermore, the application area is extended to other fire scenarios. The minimum column dimensions are determined for hydrocarbon fires. Comparing the results for the hydrocarbon fire with the tables obtained for the ISO 834 standard fire, it is noted that fire resistance to the hydrocarbon fire may result in very stringent requirements.

Moreover, some specific examples are given in case of columns subjected to natural fires. Both the upper limit and lower limit curves are introduced to investigate the fire resistance of columns when the fire temperature begins to decrease. The results prove that second-order effects are insignificant when the normal force is low. When the eccentric loads are large, the maximum bending moment of the column firstly decreases continuously during the fire, and then

shows a slight increase during the cooling phase. As a result, this value based on the lower limit curve could be considered when determining minimum dimensions for this specific fire.

With respect to natural fires, the results suggest that the design value for the maximum bending moment first increases with increasing axial load, then decreases when a certain axial load is exceeded. Further, the maximum bending moment shows no apparent reduction due to the natural fire when the axial load is low. Moreover, the bending moment capacity shows a slight increase when the column is cooling down. However, the design bending moment is determined by the minimum value during natural fires. Finally, tabulated values are listed for the determination of minimum required dimensions of columns exposed to natural fires for different fire load densities.

CHAPTER V

EVALUATION OF SIMPLIFIED CALCULATION METHODS FOR SECOND-ORDER EFFECTS IN CASE OF UNIAXIAL BENDING AND AN ISO 834 STANDARD FIRE

Simplified methods provided by code provisions as well as the numerical tool have been presented in previous chapters. The applicability and validity of these simplified methodologies is discussed in the current chapter, using the developed numerical tool.

V.1. Parametric study on applicability of the 500°C isotherm method

Comparing calculations with results available in literature, it is found that the 500°C isotherm method does not always well predict the resistance to bending moments and axial forces. Hence, a parametric study is executed to figure out the applicability range of the 500°C isotherm method.

First, a simply supported column with all the surfaces subjected to the standard fire is chosen as a basic calculation model. The interaction curves obtained by the 500°C isotherm method are compared with numerical results of columns with cross-sections 150 mm × 150 mm, 200 mm × 200 mm and 250 mm × 250 mm. The mechanical reinforcement ratio of all four columns is 0.5. The interaction curves in case of fire durations of 30 min, 60 min and 90 min are shown in Figs. V.1, V.2 and V.3, respectively, considering $n = \frac{N_c + N_s}{0.7(A_c f_{cd} + A_s f_{yd})}$ and $m = \frac{M_c + M_s}{0.7(A_c f_{cd} + A_s f_{yd})h}$, where N_c , M_c , N_s , M_s are design values of normal forces and bending moments respectively for concrete and steel reinforcement, b is the width of the column and h is the height of the cross-section. Note that, taking into account the EN 1992-1-2 provisions, 0.7 was chosen as reduction factor for the design load and included in the dimensionless parameters m and n .

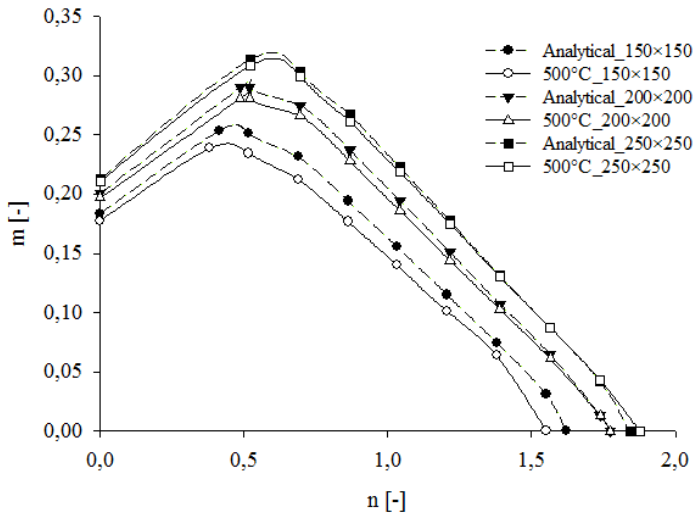


Fig. V.1: Comparison of the 500°C isotherm method (designated ‘500°C’) and the numerical results (designated ‘Analytical’) for interaction curves of columns in case of 30 minutes standard fire

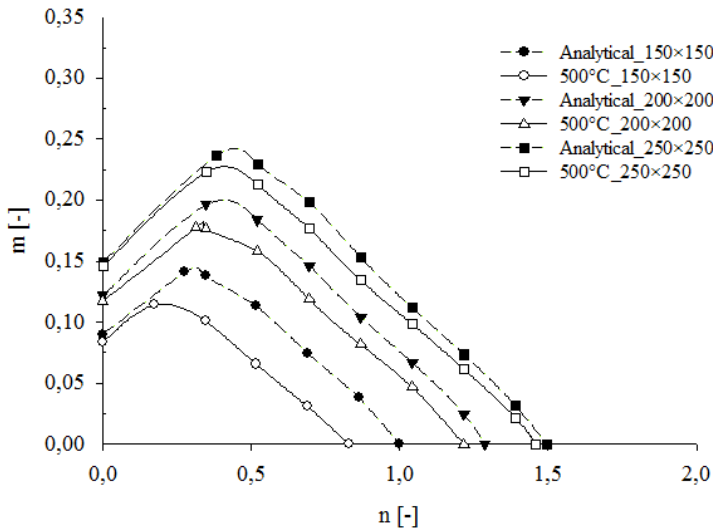


Fig. V.2: Comparison of the 500°C isotherm method (designated ‘500°C’) and the numerical results (designated ‘Analytical’) for interaction curves of columns in case of 60 minutes standard fire

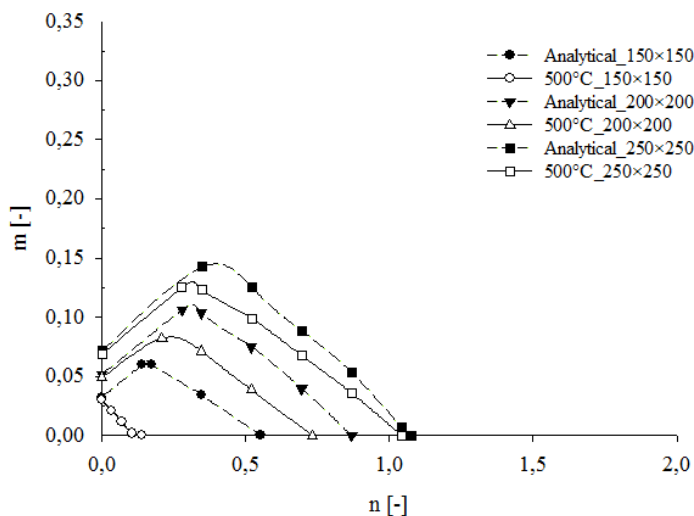


Fig. V.3: Comparison of the 500°C isotherm method (designated ‘500°C’) and the numerical results (designated ‘Analytical’) for interaction curves of columns in case of 90 minutes standard fire

Fig. V.1 indicates that the 500°C isotherm method can predict interaction curves well for all these three cases during the first 30 minutes of fire. In Fig. V.2, it is seen that the differences with the simplified method for the cross-section 150 mm \times 150 mm become apparent at 60 minutes of fire, because the concrete area whose temperature is above 500°C still makes a contribution to the load bearing capacity of the column. However, the approximation of the 500°C isotherm method is at the conservative side. In case of the 90 minutes fire duration shown in Fig. V.3, the 500°C isotherm method is not appropriate for columns with small cross-sections since the temperature of the majority of the concrete section is over 500°C and hence the simplified approach yields over-conservative results.

Further, a column with a cross-section of 200 mm \times 200 mm is investigated in case of a reinforcement ratio of 0.1 and 1.0, respectively. The interactions between respective values of the bending moment and the axial load are illustrated in Table V.1 and Table V.2.

Table V.1: Comparison of interactions between m and n based on the 500°C isotherm method and the full cross-sectional method in case of a reinforcement ratio equal to 0.1

Axial load	Fire duration	Bending moment (500°C isotherm/ full cross-sectional method)
n [-]	(min)	m [-]
0	30	0.06/ 0.07
0.2	30	0.19/ 0.20
0.4	30	0.20/ 0.21
0.6	30	0.12/ 0.12
0	60	0.03/ 0.03
0.2	60	0.12/ 0.14
0.4	60	0.07/ 0.10
0	90	0.11/ 0.13
0.2	90	0.05/ 0.09

Table V.2: Comparison of interactions between m and n based on the 500°C isotherm method and the full cross-sectional method in case of a reinforcement ratio equal to 1.0

Axial load	Fire duration	Bending moment (500°C isotherm/ full cross-sectional method)
n [-]	(min)	m [-]
0	30	0.27/ 0.28
0.2	30	0.34/ 0.34
0.4	30	0.32/ 0.33
0.6	30	0.25/ 0.26
0	60	0.18/ 0.18
0.2	60	0.21/ 0.23
0.4	60	0.17/ 0.19
0	90	0.07/ 0.08
0.2	90	0.09/ 0.11
0.4	90	0.03/ 0.06

From Tables V.1 and V.2, it is seen that the reinforcement ratio is not a decisive parameter with respect to the performance of the 500°C isotherm method compared

to the fire duration. As a simplified calculation, the 500°C isotherm method could generally predict the fire resistance of columns sufficiently accurate. However, it is not suitable for cases when the fire lasts 90 minutes or more. However, considering the values in these tables, the bending moments calculated with the 500°C isotherm method in case of specific axial loads are approximately half of the values obtained by the numerical method after 90 minutes of fire. Hence, 500°C should not always be chosen as the critical temperature for the columns particularly in the case of small cross-sections combined with a long fire duration as this might yield a very conservative result.

Finally, the critical isotherm value is evaluated and discussed for the concrete columns with respect to an ISO 834 fire at 90 min. Both 550°C and 600°C are taken into account as critical temperatures and then compared with the 500°C isotherm method for a column with reinforcement ratio 0.5 combined with cross-sections 200 mm × 200 mm and 300 mm × 300 mm respectively (Table V.3 and Table V.4).

Table V.3: Comparison of interactions between m and n based on the 500°C/ 550°C/ 600°C isotherm method and the full cross-sectional method in case of an ISO 834 fire at 90 minutes (cross-section 200 mm × 200 mm)

Axial load n [-]	Bending moment (Full cross-sectional method) m [-]	Bending moment (500°C/ 550°C/ 600°C isotherm method) m [-]
0.2	0.1	0.07/ 0.09/ 0.11
0.3	0.07	0.04/ 0.06/ 0.09
0.4	0.04	0/ 0.03/ 0.05

Table V.4: Comparison of interactions between m and n based on the 500°C/ 550°C/ 600°C isotherm method and the full cross-sectional method in case of an ISO 834 fire at 90 minutes (cross-section 300 mm ×300 mm)

Axial load n [-]	Bending moment (Full cross-sectional method) m [-]	Bending moment (500°C/ 550°C/ 600°C isotherm method) m [-]
0.2	0.18	0.16/ 0.16/ 0.18
0.3	0.17	0.15/ 0.15/ 0.17
0.4	0.14	0.11/ 0.11/ 0.13
0.5	0.09	0.08/ 0.08/ 0.10
0.6	0.06	0.05/ 0.05/ 0.07
0.7	0.03	0.01/ 0.01/ 0.03

Table V.3 shows that the full cross-sectional results are located between the isotherm method based on the critical temperature 550°C and 600°C, while the 500 °C method gives very conservative results. Hence, 550°C is suggested to be used as the critical isotherm value for this small cross-sectional column. However, differences between the bending moments obtained with the 500°C isotherm method and the full cross-sectional numerical method (shown in Table V.4) are not so apparent in case of a cross-section of 300 mm ×300 mm. As a result, the 500 °C method could still be used for such a case.

The 500°C isotherm method is proven to be an effective and conservative method to predict fire resistance. However, for some cases like columns with small cross-sections (less than 200 mm × 200 mm) or columns exposed to an ISO 834 standard fire of over 90 minutes, a higher critical isotherm temperature is recommended for the fire resistance design.

V.2. Parametric study on buckling of concrete columns exposed to fire

In EN 1992-1-1 (Eurocode 2, 2004), a simplified method—the stiffness method is introduced. This method presents a calculation model based on an estimated nominal stiffness, which is further adopted to predict the design moment of the cross-section with respect to the bending moment and the axial force. At the same time, a quasi-linear theory of elasticity (KLE) method is illustrated in the Dutch

concrete code NEN 6720 (NEN, 1995). The KLE-method makes it possible to determine the physical nonlinear behaviour for a concrete structure while using the linear theory of elasticity. The nominal stiffness method and the KLE-method in common are both based on an estimation of the stiffness and are proven to be adequate for determining the second-order effects of braced columns at ambient temperature. With respect to fire, a reduced cross-section as well as a relevant stiffness is proposed in EN 1992-1-2 (Eurocode 2, 2004). However, the KLE-method has not been verified at elevated temperatures. Therefore, the applicability of the KLE-method in case of fire still needs to be investigated.

V.2.1. Interaction diagrams at ambient temperature

First, a simply supported column is analysed, having a cross-section 300 mm×300 mm, 4 bars with diameter 32 mm and concrete cover 25 mm; concrete compressive strength $f_c = 55$ MPa; reinforcement yield stress $f_y = 500$ MPa and Young's modulus of steel $E_s = 2 \times 10^5$ N/mm². As it is verified that the numerical method has a good agreement with experimental data (see **chapter III**), this numerical method, but also the stiffness method as well as the KLE-method are adopted to obtain interaction curves of columns for different slenderness ratios, i.e. $\lambda = 35, 70$ and 105, at ambient temperature. The interaction diagrams are shown in Fig. V.4, where $n' = \frac{N_c + N_s}{f_{ck}bh}$ and $m_x = \frac{M_c + M_s}{f_{ck}bh^2}$, N_c, M_c, N_s, M_s are design values of normal forces and bending moments respectively for concrete and steel reinforcement, b is the width of the column and h is the height of the cross-section.

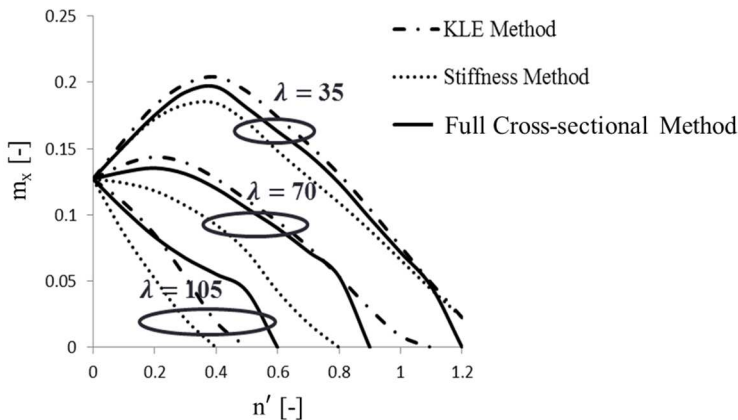


Fig. V.4: Interaction diagrams of columns at ambient temperature for slenderness ratios 35, 70 and 105 adopting the KLE-method, the stiffness method and the developed numerical method

In Fig. V.4, it is observed that at ambient temperature, the difference of the bending moment capacity obtained from these three approaches increases with the slenderness ratio. This difference between the KLE-method and the numerical method is no more than 7.0% in the range of all the permitted axial loads in case of slenderness ratios 35 and 70, while it reaches at maximum 26.2% ($n = 0.3$) in case of the slenderness ratio 105. It is worth pointing out that with the numerical method, the bending moment capacity decreases significantly when the axial load is about to reach the maximum load capacity. This is because the effect of imperfections is taken into account as an initial eccentricity, which leads to a significant bending moment in case of a large axial load. Comparatively, the KLE-method has a good agreement with the numerical method. However, the prediction of the load capacity with the KLE-method is not always on the safe side in case of slenderness ratios 35 and 70, while the results of the stiffness method are too conservative for slender columns.

V.2.2. Interaction diagrams at elevated temperatures

Further, the same columns with slenderness ratios 35, 70 and 105 are used in case of a four-sided exposure to an ISO 834 fire. As the numerical tool has also been verified to be adopted in case of fire (see **chapter III**), the respective values of the bending moment capacity obtained with the KLE-method are compared with results from the numerical calculation in case of fire durations of 30 minutes, 60 minutes and 90 minutes (Table V.5).

Table V.5: Comparison of respective values of the bending moment capacity in case of fire durations of 30 minutes, 60 minutes and 90 minutes with the KLE-method and the numerical method

Fire duration (min)	Slenderness ratio λ [-]	Axial load n [-]	Bending moment m [-]		$\frac{(2)-(1)}{(2)}\%$
			KLE-method (1)	Numerical method (2)	
30	35	0.1	0.14	0.13	-7.7
		0.3	0.15	0.14	-7.1
		0.5	0.11	0.1	-10
		0.7	0.05	0.05	0
		0.9	0.01	0	-
	70	0.1	0.11	0.09	-22.2
		0.2	0.08	0.07	-14.3
		0.3	0.04	0.05	20
	105	0.1	0.05	0.06	16.7
60	35	0.1	0.11	0.1	-10
		0.3	0.09	0.08	-12.5
		0.5	0.03	0.03	0
	70	0.1	0.05	0.05	0
90	35	0.1	0.06	0.05	-20
		0.3	0.02	0.02	0

Table V.5 shows that the results obtained with KLE method are basically in agreement with the results calculated with the tool. However, it is not always safe to implement the traditional KLE-method for predicting the stiffness as well as the bending moment capacity of columns in case of fire. This risk occurs mostly when the axial load is rather small and sometimes in case the axial load is about to reach the maximum load capacity. Among the effects of all the parameters, we can see that the differences on the bending moment capacity between the numerical method and the KLE-method increase significantly in function of the fire duration. This is probably because the slope of the moment-curvature diagram, which represents the stiffness (presented in Fig. II.4) after the point of $0.8M_{Ed}$ changes significantly and this value of the slope is not representative for the stiffness in case of fire. Hence, it is necessary to investigate the changes of the stiffness of the column in function of the fire duration and find a safer value which represents the stiffness to evaluate the bending moment of columns in case of fire.

Next, the cross-sectional numerical calculation tool is adopted to find a point of the moment-curvature curve which can represent the stiffness of columns in order to extend the applicability of the KLE-method to the case of an ISO 834 fire. The aforementioned columns of slenderness ratios 35, 70 and 105 are studied in case of fire durations of 0 minutes, 30 minutes, 60 minutes and 90 minutes. The ratio of the bending moment corresponding to the respective value of the stiffness to the bending moment capacity of columns in case of different axial loads as well as different fire durations in case of slenderness ratios 35, 70 and 105 are listed in Table V.6.

Table V.6: Comparison of the ratio of the bending moment corresponding to the respective value of the stiffness to the bending moment capacity in case of fire durations of 0 minutes, 30 minutes, 60 minutes and 90 minutes based on the numerical method

Axial load n [-]	Slenderness ratio [-]									
	$\lambda = 35$				$\lambda = 70$			$\lambda = 105$		
	Fire duration [min]				Fire duration [min]			Fire duration [min]		
	0	30	60	90	0	30	60	0	30	60
0.1	0.99	0.97	0.96	0.93	0.97	0.93	0.79	0.96	0.78	0.32
0.2	0.98	0.94	0.93	0.65	0.96	0.93	0.63	0.84	0.3	-
0.3	0.98	0.95	0.93	-	0.94	0.52	-	0.68	-	-
0.4	0.99	0.97	0.52	-	0.87	0.61	-	0.6	-	-
0.5	0.98	0.93	0.61	-	0.85	0.57	-	0.55	-	-
0.6	0.98	0.93	0.57	-	0.85	-	-	-	-	-
0.7	0.98	0.91	-	-	0.86	-	-	-	-	-
0.8	0.99	0.88	-	-	0.8	-	-	-	-	-
0.9	0.99	-	-	-	-	-	-	-	-	-
1	0.98	-	-	-	-	-	-	-	-	-
1.1	0.97	-	-	-	-	-	-	-	-	-

From Table V.6, it is observed that the ratio of the assumed average bending moment to the bending moment capacity decreases in function of the fire duration as well as in function of the slenderness ratio. An interpolation value can be used for columns with intermediate slenderness ratios in case of an ISO 834 fire of intermediate fire duration. It is worth pointing out that a higher ratio than 0.8 is suggested as a simplification for the stiffness of the column adopted in the KLE-method. Although $0.8M_{Ed}$ is indicated to be less conservative for the KLE-method, the difference on the bending moment (shown in Table V.5) between the KLE-method and the numerical method is less than 10.0% in case of the slenderness ratio 35 and the fire duration 30 minutes, while it is 7.0% at ambient temperature. It means that the slope of the moment-curvature curve between $0.8M_{Ed}$ and M_{Ed} varies very slightly in case the column is not too slender and the fire exposure does not exceed 30 minutes. However, the slope of the moment-curvature diagram at

$0.8M_{Ed}$ cannot always be used as the stiffness of the column considering the evaluation according to Table V.5. Hence, it is suggested to replace 0.8 by the respective coefficient which is larger than 0.8 as presented in Table V.6.

V.2.3. Validation

In order to verify the proposed coefficients shown in Table V.6, a column with a different cross-section $400 \text{ mm} \times 400 \text{ mm}$, but the same reinforcement ratio 0.5 and the slenderness ratio 35 is investigated. The differences on the interaction relationship of columns exposed to an ISO fire 834 with fire durations of 0 minutes, 30 minutes, 60 minutes and 90 minutes are illustrated in Table V.7 adopting the proposed coefficients for the KLE-method in case of the slenderness ratio 35 and these are compared with the results from the numerical method.

Table V.7: Comparison of respective values of the bending moment capacity in case of fire durations of 0 minutes, 30 minutes, 60 minutes and 90 minutes with the KLE-method (using the proposed alternative coefficients) and the numerical method

Fire duration [min]	Axial load n [-]	Bending moment m [-]	
		KLE-method (1)	Numerical method (2)
0	0.1	0.15	0.16
	0.3	0.2	0.2
	0.5	0.19	0.19
	0.7	0.15	0.15
	0.9	0.1	0.1
	1.1	0.05	0.05
30	0.1	0.15	0.15
	0.3	0.17	0.17
	0.5	0.14	0.14
	0.7	0.09	0.09
60	0.1	0.13	0.13
	0.3	0.13	0.13
90	0.1	0.1	0.1

In Table V.7, it is seen that the difference is very small after the correction is used for calculating the stiffness of columns with the KLE-method.

Comparing the KLE-method with the stiffness method and the numerical method at ambient temperature as well as with the numerical method at elevated temperatures, the following conclusions are obtained:

(1) The bending moment capacity predicted with the KLE-method is in good agreement with the results from the numerical method. However, the capacity calculated with the KLE-method is slightly on the unsafe side, while the results obtained with the stiffness method are too conservative.

(2) The stiffness of the column obtained with the slope of the moment-curvature curve for $0.8M_{Ed}$ as prescribed in the Dutch regulations (NEN, 1995) is not available in case of fire. A value corresponding to a higher bending moment is recommended for the assumption of the stiffness in case of fire.

(3) The ratio of the assumed bending moment to the bending moment capacity is given for slenderness ratios 35, 70, 105 in case of fire durations equal to 0 minutes, 30 minutes, 60 minutes and 90 minutes. An interpolated value can be adopted in the range of the slenderness ratio from 0 to 105 and the fire duration from 0 to 90 minutes of an ISO 834 fire exposure. The proposed values have been validated for another case and yield robust results.

V.3. Effect of imperfections

In EN 1992-1-1, an equivalent initial eccentricity is proposed for the imperfection of columns. Based on this simplification, imperfections are incorporated as an initial eccentricity in a first order calculation and are further used to obtain interaction diagrams taking second-order effects into account. Furthermore, EN 1992-1-1 (Eurocode 2, 2004) points out that allowance should be made in the design for uncertainties associated with the prediction of second-order effects. To our knowledge, however, no parametric study has been performed so far in order to investigate the effect of imperfections on columns exposed to fire. Therefore, it is essential to study parameters that influence the effects of imperfections.

First, a simply supported column at ambient temperature is analysed: the cross-section is $300 \text{ mm} \times 300 \text{ mm}$, with one diameter 32 mm reinforcement bar in each corner and concrete cover 25 mm; concrete compressive strength $f_{ck} = 55 \text{ MPa}$, reinforcement yield stress $f_y = 500 \text{ MPa}$ and modulus of elasticity of steel $E_s = 2 \times$

10^5 N/mm^2 . The effect of imperfections on the load capacity of columns for different slenderness ratios is investigated. Fig. V.5 shows the respective values of the load capacity n ($n = \frac{N_c + N_s}{0.7(A_c f_{cd} + A_s f_{yd})}$) of columns for the slenderness ratio (30, 40, 50, 60, 70, 80) in case of different first order moments. Three types of first order moments are studied: a low first order moment ($e = 0.025b$ with $e \geq 10 \text{ mm}$), a moderate first order moment ($e = 0.25b$ with $e \leq 100 \text{ mm}$) and a high first order moment ($e = 0.5b$ with $e \leq 200 \text{ mm}$), where e is the eccentricity and b is the width of the cross-section. In Fig. V.5, the bars present respective values of n in case of different first order effects and the shaded bars show the relative increase due to imperfections.

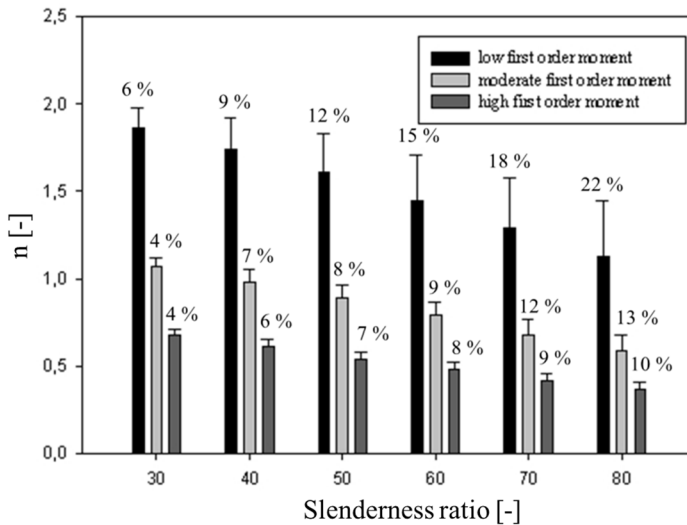


Fig. V.5: The effect of imperfections on the load capacity of columns for different slenderness ratios in case of a low first order moment, a moderate first order moment and a high first order moment (ambient temperature)

From the figure we can see that the influence of imperfections on columns becomes more apparent with increasing slenderness ratio at ambient temperature. It is noticed that this influence increases from 6% (slenderness ratio 30) to 22% (slenderness ratio 80) in case of the low first order moment. It indicates that imperfections cannot be neglected in case of slender columns, especially when combined with a low first order moment at ambient temperature.

Next, an ISO 834 standard fire is adopted to investigate the effect of imperfections in fire conditions. Four different comparisons are made (see Table V.8) each time

considering parameter variations for one of the four parameters, i.e. dimensions of the cross-section, reinforcement ratio, slenderness ratio and fire durations. For all these cases the influence of eccentricities is investigated.

Table V.8: Parametric study on the influence of imperfections (i.e. eccentricities)

Comparison Group No.	Dimensions (mm × mm)	Reinforcement ratio	Slenderness ratio	Fire duration (min)
1	300 mm × 300 mm	0.5	60	0, 30, 60, 90
2	300 mm × 300 mm	0.5	40, 50, 60, 70	60
3	300 mm × 300 mm	0.1, 0.5, 1.0	60	60
4	150 mm × 150 mm	0.5	60	60
	300 mm × 300 mm			
	600 mm × 600 mm			

For the first set of parameters, interaction diagrams ($m = \frac{M_c + M_s}{0.7(A_c f_{cd} + A_s f_{yd})h}$) are shown in Fig. V.6 taking into account different fire durations.

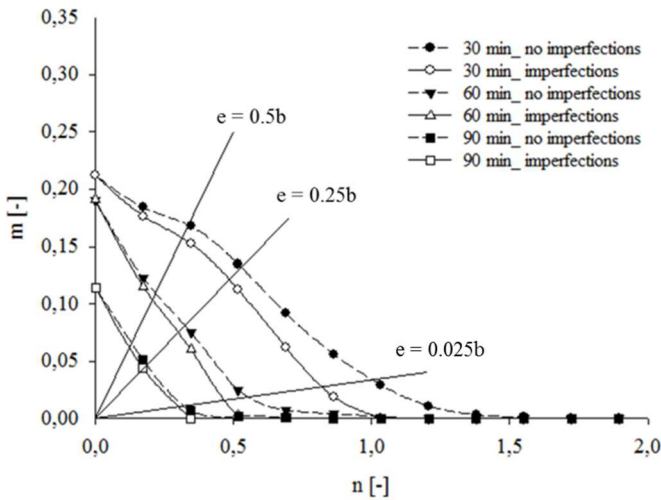


Fig. V.6: Interaction diagrams of a column in case of an ISO 834 fire at 30 min, 60 min and 90 min of fire exposure (Group No. 1)

The effect of imperfections (Fig. V.6), in case of a low first order moment ($e = 0.025b$ with $e \geq 10$ mm), first has a slight increase from 15% (at 0 min) to 20% (at 30 min), and then drops from 20% (at 30 min) to 6% (at 90 min). However, for other cases, the influence of imperfections is getting lower with the temperatures of columns increasing. The imperfections have almost no influence on the interaction curves when the ISO 834 fire lasts 90 minutes.

The second set of parameters presents the effect of the slenderness ratio (Fig. V.7).

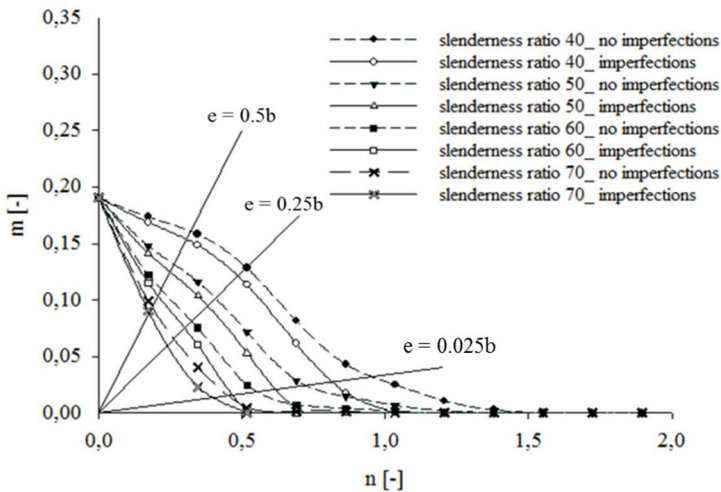


Fig. V.7: Interaction diagrams of columns (slenderness ratios 40, 50, 60, 70) exposed to an ISO 834 fire after 60 min fire exposure (Group No. 2)

Fig. V.7 indicates that the effect of imperfections increases slightly with increasing slenderness ratio. However, no significant additional effect is observed compared to that at ambient temperature.

Fig. V.8 shows the effect of the reinforcement ratio on the influence of imperfections.

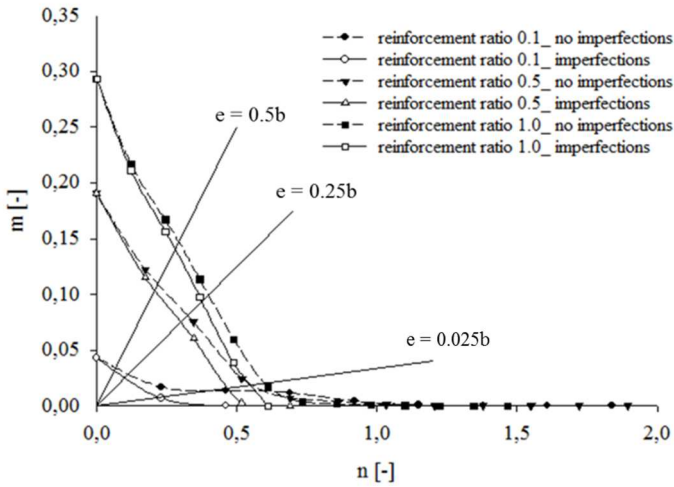


Fig. V.8: Interaction diagrams of columns (reinforcement ratios 0.1, 0.5, 1.0) exposed to an ISO 834 fire after 60 min of fire exposure (Group No. 3)

In Fig. V.8, it is clear that the influence of imperfections on the maximum allowable bending moment under fire exposure decreases with an increasing reinforcement ratio when the first order moment is low ($e = 0.025b$ with $e \geq 10$ mm). However, this observation does not hold in case of a high first order moment ($e = 0.5b$ with $e \leq 200$ mm) for which Fig. V.8 illustrates only a minor influence of the reinforcement ratio. Hence, the reinforcement ratio is not an important parameter of imperfections.

The influence of imperfections for different sizes of the cross-section is quantified in Fig. V.9.

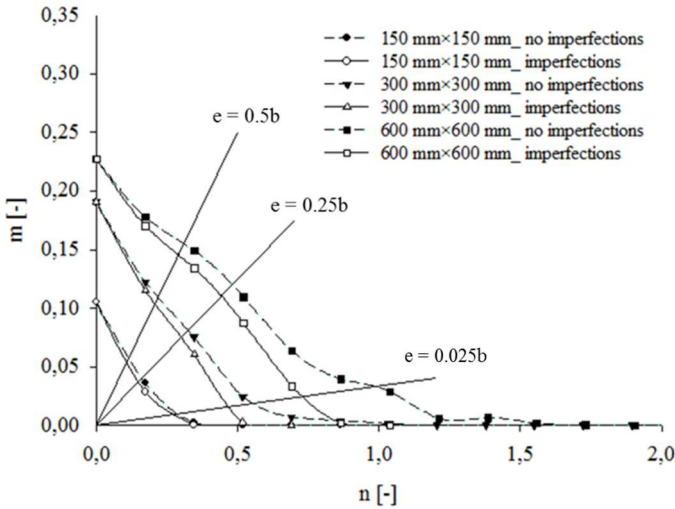


Fig. V.9: Interaction diagrams of columns (cross-section 150 mm×150 mm, 300 mm×300 mm, 600 mm×600 mm) exposed to an ISO 834 fire after 60 min of fire exposure (Group No.4)

Firstly, it is observed that in Fig. V.9 imperfections have more effects on columns with a larger cross-section if other properties are kept the same. Secondly, imperfections are very important when the initial eccentricity is very low or in case of a pure axial load. In the case of the column with cross-section 600 mm×600 mm, the ideal load capacity under compression is more than twice as the one considering imperfections. Hence, it would be quite unsafe to neglect imperfections when performing the fire resistance design of columns.

In general, no matter how the configurations of the columns are and no matter whether the columns are at ambient temperature or exposed to fire, the imperfections have significant effects on the load capacity of columns under compression. Furthermore, the resistance without considering imperfections could be overestimated by a factor 2 compared to the case when considering imperfections at elevated temperatures. Two main reasons can be given for this effect. First, the imperfection is considered as an initial eccentricity, which causes a more significant bending moment under a large axial load. Secondly, the maximum allowable bending moments of columns decrease fast with increasing temperature of columns, but the imperfections are considered to remain the same as at ambient temperature. Therefore, the bending moment caused by imperfections will present an increasing proportion of the total bending moment in case of fire.

Based on the comparison of the results from the parametric studies, the following observations can be made:

(1) Fire duration (temperature)

The effect of imperfections is generally getting smaller in function of the fire duration time because the relative importance is higher compared to the centric loading case. However, this effect cannot be neglected in case of slender columns combined with low first order moments.

(2) Slenderness ratio

The higher the slenderness ratio becomes, the more influence the imperfections have. Nevertheless, due to the second-order effects, this influence decreases in function of the fire duration time.

(3) Eccentricity

The effect of eccentricities in form of a low, moderate and high first order moment was investigated. The results indicate that imperfections have more effects on columns in case of a low first order moment. The reason for this is that the bending moment associated to imperfections has a relatively high influence on the first order moment if the eccentricity is low. To some extent, eccentricity is one of the most important parameters in the study on the effect of imperfections.

(4) Reinforcement ratio

According to Fig. V.8, the reinforcement ratio is only of minor importance for the imperfection study.

(5) Dimensions of the cross-section

The effect of imperfections is more apparent on a bigger cross-section in case of the same slenderness ratio, because the assumed eccentricity ($l_0/400$) for a certain slenderness ratio has a minimal influence if the dimensions of the cross-section are small and the additional bending moment caused by imperfections is negligible.

Hence, with respect to the axial load design under compression, imperfections have to be taken into account. Further, fire durations and eccentricities have important influences on the effect of imperfections. The slenderness ratios as well as dimensions of the cross-section have a significant effect on imperfections in certain cases (as pointed out in the previous).

V.4. Improved curvature approximation based on interaction diagrams

In the *fib* Model Code 2010 (2013), an approximation of the maximum design curvature is presented. The design value of the bending moment is:

$$M_{Ed} = -N_{Ed}e_d \quad (V.1)$$

where N_d is the axial load

e_d is the maximum eccentricity, being the maximum distance between the compression resultant and the deformed axis of the compression member;

$$e_d = e_i + e_{1d} + e_{2d} \quad (V.2)$$

where e_i is the eccentricity due to imperfections, being the greater value of: $e_i = \alpha_i l_0/2$ and $e_i = h/300$; EN 1992-1-1 (Eurocode, 2004) states that $e_i = h/400$ may always be used as a simplification for isolated columns in braced systems; l_0 is the effective length of the compression member; $1/200 \geq \alpha_i = 0.01/\sqrt{l_0} \geq 1/300$ (l_0 in m)

e_{1d} is the first-order eccentricity, $e_{1d} = -\frac{M_{1d}}{N_d}$; M_{1d} is the first-order moment

e_{2d} is the eccentricity due to the deformation of the compression member, $e_{2d} = \frac{\kappa_d l_0^2}{c_0}$; c_0 is the integration factor accounting for the curvature distribution along the member, κ_d is the maximum design curvature:

$$\kappa_d = \frac{\varepsilon_{sd} - \varepsilon'_{sd}}{h - 2c} \quad (V.3)$$

where ε_{sd} , ε'_{sd} are the strains of the reinforcing bars at the top and the bottom layers

h is the height of the cross-section

c is the cover thickness

The maximum design curvature may be obtained with $\varepsilon_{sd} = f_{yd}/E_s$ and $\varepsilon'_{sd} = -f_{yd}/E_s$.

Further, three simplified methods are provided to calculate the integration factor c_0 in the *fib* Model Code 2010 (2013):

The first method is assuming the value of the integration factor as:

$$c_0 = \pi^2 \quad (V.4)$$

which is based on Euler's elastic buckling theory.

Based on Eq. (V.3) for the maximum design curvature of point B shown in Fig. V.10, the second method provides an equation to obtain a more accurate value of the maximum design curvature for any point between A and B:

$$\kappa_d = K_r \cdot \frac{\varepsilon_{sd} - \varepsilon'_{sd}}{h - 2c} = \left(\frac{n_u - n_d}{n_u - n_{bal}} \right) \cdot \frac{\varepsilon_{sd} - \varepsilon'_{sd}}{h - 2c} \quad (V.5)$$

where $K_r = \frac{n_u - n_d}{n_u - n_{bal}}$ is a correction factor depending on the axial load (see Eq. (V.9))

h is the height of the cross-section

c is the cover thickness

$$n_u = 1 + \omega$$

$$\omega = \frac{A_s f_{yd}}{A_c f_{cd}}$$

$$n_d = \frac{N_{Ed}}{A_c f_{cd}}$$

n_{bal} is the value of n at maximum moment resistance; $n_{bal} \approx 0.4$ (point B is shown in Fig. V.10)

Assuming the distance between the reinforcing bars as $0.9h$ and the reinforcement yields at both sides, Eq. (V.5) can be simplified as:

$$\kappa_d = \left(\frac{n_u - n_d}{n_u - n_{bal}} \right) \cdot \frac{\varepsilon_{yd}}{0.45h} \quad (V.6)$$

Eq. (V.6) is based on interpolation adopting a linearized interaction diagram shown in Fig. V.10. It is worth pointing out that at point B, the reinforcement yields at both sides of the column at ambient temperature, so that the curvature is $\kappa = \frac{\varepsilon_{yd}}{0.45h}$. Considering the curvature $\kappa = 0$ at point A, the curvature in point C can be obtained by a linear interpolation from Eq. (V.6).

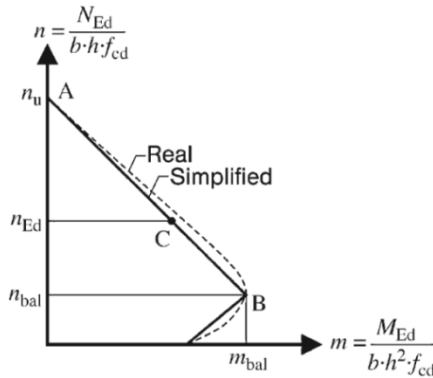


Fig. V.10: Simplified representation of interaction curves

Since the integration factor c_0 is based on the curvature distribution, the first and the second methods both adopt an estimated maximum curvature to determine the value for c_0 . However, with realistic assumptions concerning the distribution of curvature, the third method proposes a more refined value of the integration factor c_0 which can be calculated on the basis of the values of the various integration factors c_i :

$$c_0 = \pi^2 \cdot \frac{N}{N_{cr}} + \frac{\sum_{i=1}^n M_i}{\sum_{i=1}^n c_i} \cdot \left(1 - \frac{N}{N_{cr}} \right) \quad (V.7)$$

where c_i is a coefficient which depends on the distribution of the first-order moment (for instance, $c_i = 8$ for a constant first order moment, $c_i = 9.6$ for a parabolic and 12 for a symmetric triangular distribution etc.)

As a first step of the curvature method, it is essential to figure out the coefficient K_r which is depending on the axial load. In order to determine K_r , the value of n_{bal}

has to be obtained first. In Eurocode 2 (2004), an approximation value 0.4 is adopted for n_{bal} at ambient temperature as a simplification. However, this value might not be suitable in case of fire. Hence, interaction curves of columns exposed to fire in case of different reinforcement ratios are investigated in order to obtain values of n_{bal} at elevated temperatures and further to develop the application of the simplified method to an ISO 834 standard fire.

A column with a cross-section 300 mm × 300 mm and a cover thickness 25 mm is analysed for different reinforcement ratios of 0.1, 0.5 and 1.0 in case of an ISO 834 fire with a duration of 0 min (ambient temperature), 30 min, 60 min and 90 min. Interaction curves of columns at ambient temperature are obtained in Fig. V.11, where $n' = \frac{N_{Ed}}{bhf_c}$, $m_x = \frac{M_{Ed}}{bh^2f_c}$, b is the width of the cross-section, h is the height of the cross-section.

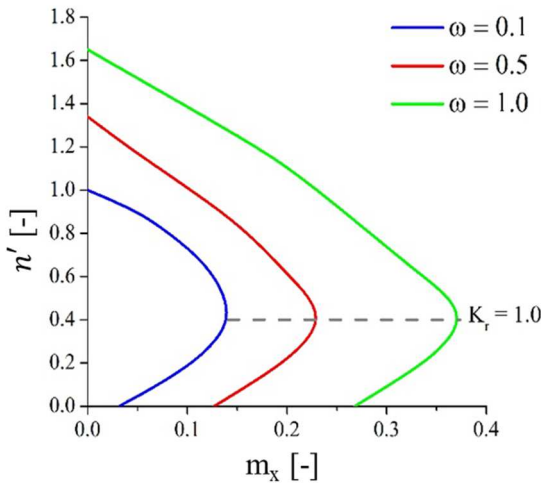


Fig. V.11: Interaction curves of columns at ambient temperature for reinforcement ratios 0.1, 0.5 and 1.0

On the basis of Fig. V.11, it is seen that n_{bal} can be considered as 0.4 also for columns with different reinforcement ratios. Further, interaction curves are presented in Fig. V.12, Fig. V.13 and Fig. V.14 for the same columns, considering $n' = \frac{N_{Ed}}{bhf_c}$ and $m = \frac{M_c + M_s}{0.7(A_c f_{cd} + A_s f_{yd})h}$ as explained in section V.1 that 0.7 as a reduction factor for the design load in case of fire. The figures illustrate the behaviour for a fire duration of 30 min, 60 min and 90 min, respectively.

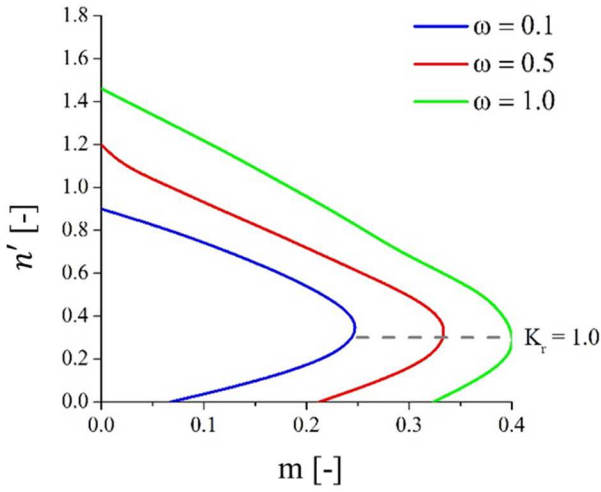


Fig. V.12: Interaction curves of columns for reinforcement ratios of 0.1, 0.5 and 1.0 in case of an ISO 834 fire with a fire duration of 30 minutes

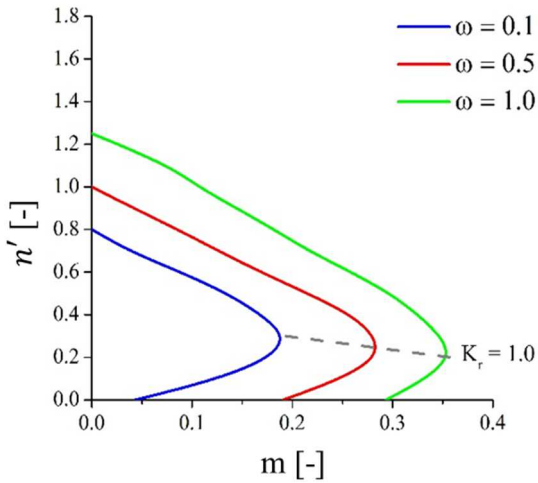


Fig. V.13: Interaction curves of columns for reinforcement ratios of 0.1, 0.5 and 1.0 in case of an ISO 834 fire with a fire duration of 60 minutes

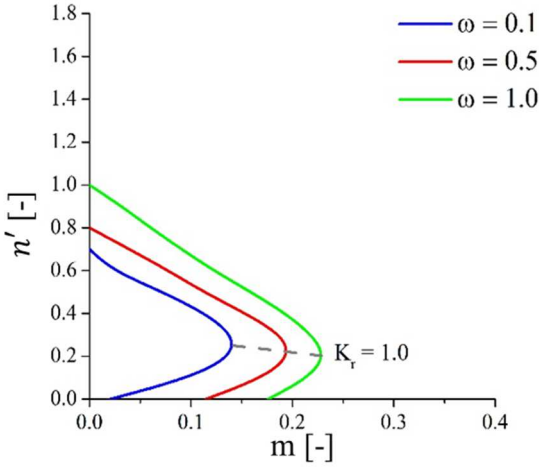


Fig. V.14: Interaction curves of columns for reinforcement ratios of 0.1, 0.5 and 1.0 in case of an ISO 834 fire with a fire duration of 90 minutes

From Fig. V.12 to Fig. V.14, we can see that the value of n_{bal} as well as n' (overall) decreases with fire duration. As a simplification, it is observed that the interaction curves in case of n not less than n_{bal} can still be approximated by a linear relationship.

In order to check the accuracy of the simplified method, the maximum curvature is investigated using the developed numerical tool. First, a column with a cross-section $300 \text{ mm} \times 300 \text{ mm}$, a $\varnothing 32$ bar in each corner and a cover thickness 25 mm is chosen. The column with the same material properties as section III.3 (1) is investigated. The bending moment—curvature diagrams based on the numerical calculation tool at ambient temperature in case of different axial loads are illustrated in Fig. V.15, where $n' = \frac{N_{Ed}}{bh_f c}$, M is the bending moment capacity, χ is the corresponding curvature, point B is the peak point which represents the maximum design curvature and $(\varepsilon_1, \varepsilon_2)$ are strains of the reinforcement at point B.

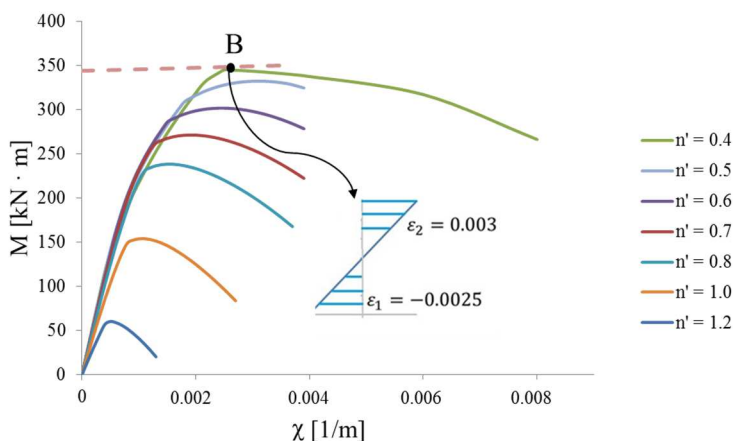


Fig. V.15: The bending moment—curvature diagrams of the column at ambient temperature and the strain distribution at point B at ambient temperature

Fig. V.15 shows the relationship between the bending moment and the curvature in case of different axial loads. It is worth mentioning that at the peak of the curve in case of $n' = 0.4$, the strain of the reinforcing bars in the tensile zone does not equal the limit strain because the reinforcing bars not exactly yield at the both sides in case of $n' = 0.4$. However, as a simplification, $n_{\text{bal}} = 0.4$ may always be used.

Since our numerical calculation method is based on the strain distribution of the cross-section which has the same basis as the second method using Eq. (V.5) or a more simplified formula Eq. (V.6), the comparison is made in order to develop the second method to the application of fire. The values of the curvature obtained with the simplified formula Eq. (V.6), the simplified calculation based on the interaction curves adopting Eq. (V.5) as well as the numerical tool are listed in Table V.9.

Table V.9: Comparisons of the maximum design curvature obtained with the simplified formula, interaction diagrams based calculation and the numerical method

Curvature [1/m] n'	Simplified formula Eq.(V.6) (1)	Simplified formula Eq.(V.5) (2)	Numerical values (3)	$\frac{(3) - (1)}{(3)}$ (%)	$\frac{(3) - (2)}{(3)}$ (%)
0.4	0.019	0.025	0.025	24	0
0.5	0.017	0.023	0.031	45	26
0.6	0.015	0.02	0.025	40	20
0.7	0.013	0.017	0.019	32	11
0.8	0.011	0.014	0.015	27	7
1	0.007	0.009	0.011	36	18
1.2	0.003	0.004	0.005	40	20
1.34	0	0	0	—	—

It is observed that Eq. (V.6) gives very conservative results for the maximum design values. The difference at ambient temperature could reach 45% in this case. Hence, it is not an economical way to use this simplified formula for the design. Comparing with the simplified formula Eq. (V.6), the prediction based on Eq. (V.5) is closer to the numerical values. However, the prediction is still conservative. Therefore, an improved formula is derived for the calculation of the maximum design curvatures (which will be in the following extended to the case of fire).

In order to find a simplified way to determine the maximum design curvature at ambient temperature as well as in case of fire, the strain distribution obtained with the numerical tool is investigated. The aforementioned column which has been investigated at ambient temperature is further adopted in case of an ISO 834 standard fire. Considering the effect of a fire duration of 30 minutes, the interaction curves and the mechanical strain distribution in case of the maximum design curvature are shown in Fig. V.16 and Fig. V.17, where $n' = \frac{N_{Ed}}{bdf_{cd}}$, $m = \frac{M_C + M_S}{0.7(A_c f_{cd} + A_s f_{yd})h}$, and compression is positive.

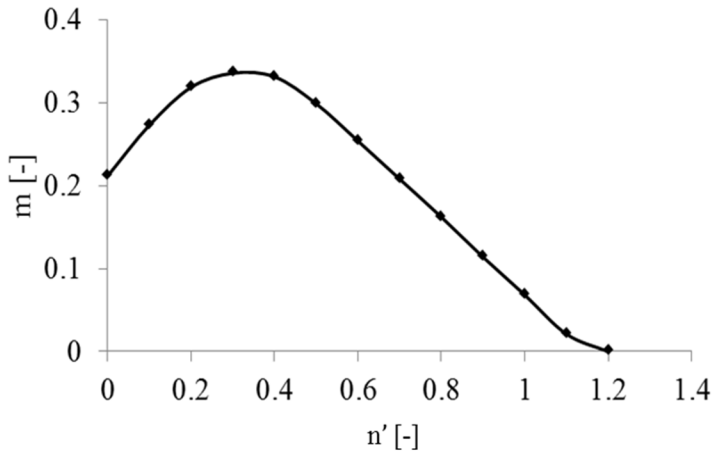


Fig. V.16: The interaction curve of the cross-section in case of an ISO 834 fire of 30 minutes

From Fig. V.16, it is seen that n_{bal} is between 0.3 and 0.4. In order to figure out the applicability of Eq. (V.3), strain distributions along the central axis in case of $n = 0.3, 0.4, 0.5, 0.7$ and 0.9 are illustrated in Fig. V.17.

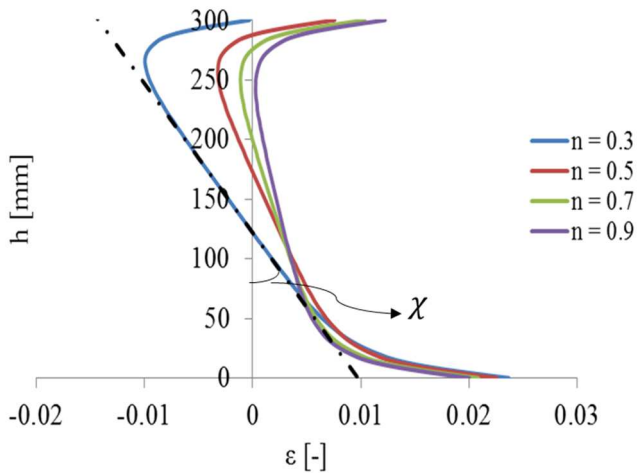


Fig. V.17: The strain distribution of the maximum design curvature of columns exposed to an ISO 834 fire of a duration of 30 minutes in case of the axial load $n = 0.3, 0.4, 0.5, 0.7$ and 0.9

Fig. V.17 shows the strain distribution of the maximum design curvature of columns in case of a fire duration of 30 minutes. It is seen that the strain distribution is nonlinear due to the effect of thermal strain. However, the slope of the strain diagram in the central part of the cross-section tends to be a constant in case of a 30-minutes fire. That means that with respect to the maximum design curvature in case of fire, an assumption of a linear strain distribution for the core of the cross-section is feasible at least for a small fire duration. As a basic calculation principle, the maximum design curvature in case $n \approx 0.4$ where the strain at the centroid of the cross-section equals 0 is used at ambient temperature. Hence, the same calculation condition which is required for n_{bal} is proposed in case of fire. As such, an improved formula, developed from Eq.(V.6), is proposed:

$$\kappa_d = \left(\frac{n_u - n_d}{n_u - n_{bal}} \right) \chi_{bal} \quad (V.8)$$

Taking the curves in Fig. V.13 for instance, the strain distribution along the height h between 50 mm and 250 mm is assumed to be linear, where the temperature is below 100 °C and there is no reduction on the concrete strength. Since the mechanical strain at the centroid of the cross-section approaches 0 in case of $n = 0.4$, the curvature $\chi = 0.055$ 1/m is adopted as χ_{bal} and $n_{bal} = 0.4$.

Next, the same column is investigated in case of a fire duration of 60 minutes, 90 minutes and 120 minutes. Based on the calculation with the numerical tool, $\chi_{bal} = 0.080$ 1/m and $n_{bal} = 0.4$ are obtained in case of the fire duration 60 minutes while $\chi_{bal} = 0.096$ 1/m and $n_{bal} = 0.3$ in case of the fire duration 90 minutes, $\chi_{bal} = 0.094$ 1/m and $n_{bal} = 0.3$ in case of the fire duration 120 minutes. The maximum design curvature obtained with Eq. (V.8) and the numerical values are shown in Table V.10.

Table V.10: Comparisons of the maximum design curvature obtained with Eq.(V.8) and the numerical method in case of fire

Curvature [1/m] n'	Simplified calculation based on Eq. (V.8) (1)				Numerical values (2)				$\frac{(2) - (1)}{(2)}$ (%)			
	Fire duration [min]				Fire duration [min]				Fire duration [min]			
n''	30	60	90	120	30	60	90	120	30	60	90	120
0.3	—	—	0.096	0.094	0.084	0.1	0.096	0.094	—	—	0	0
0.4	0.06	0.078	0.077	0.062	0.06	0.078	0.08	0.066	0	0	4	6
0.5	0.053	0.065	0.058	0.031	0.054	0.07	0.06	0.042	2	7	3	26
0.6	0.045	0.052	0.038	—	0.046	0.06	0.042	—	2	13	10	—
0.7	0.038	0.039	0.019	—	0.038	0.044	0.02	—	0	11	5	—
0.8	0.03	0.026	—	—	0.032	0.032	—	—	6	19	—	—
0.9	0.023	0.013	—	—	0.026	0.018	—	—	12	28	—	—
1	0.015	—	—	—	0.018	—	—	—	17	—	—	—
1.1	0.008	—	—	—	0.008	—	—	—	0	—	—	—

Table V.10 illustrates the maximum design curvature to be used in Eq. (V.8). The results calculated with Eq. (V.8) are more conservative than the ones from the numerical method. However, the difference is quite reasonable and safe enough to predict the deflection due to the second-order effects as well as the bending moment capacity. It is worth pointing out that the critical point B shown in Fig. V.10 is at $n = 0.4$ in case of a fire duration of 30 minutes and 60 minutes while $n = 0.3$ in case of a fire duration of 90 minutes. As a simplification, $n = 0.4$ may always be used in case of fire although the prediction of the maximum design curvature is even more conservative than results calculated based on the curvature at the real critical point B.

In order to verify the applicability of Eq. (V.8), parameters like dimensions, the reinforcement ratio as well as the slenderness ratio are investigated. Three groups of parametric variations are listed in Table V.11.

Table V.11: Parametric study for accessing the validity of Eq. (V.8)

Comparison Group No.	Dimensions	Reinforcement ratio	Slenderness ratio
	(mm × mm)		
1	150 mm × 150 mm	0.5	0
	300 mm × 300 mm		
	500 mm × 500 mm		
2	300 mm × 300 mm	0.1, 0.5, 1.0	0
3	300 mm × 300 mm	0.5	30, 40, 50

In the comparison of these three groups, the maximum design curvatures in case of an ISO 834 fire of a fire duration of 60 minutes are used.

V.4.1. Effect of dimensions

In group 1, three columns of different cross-sections as listed in Table V.11 are analysed. The maximum design curvatures obtained with Eq. (V.8) (designated 1) and the numerical tool (designated 2) in case of a fire duration of 60 minutes are shown in Table V.12.

Table V.12: Comparisons of the maximum design curvature obtained with Eq. (V.8) (1) and the numerical method (2) in case of a fire duration of 60 minutes considering the effect of different cross-sectional dimensions

Curvature [1/m]	Dimensions [mm × mm]								
	150 × 150			300 × 300			500 × 500		
n'	(1)	(2)	$\frac{(2)-(1)}{(2)}$ (%)	(1)	(2)	$\frac{(2)-(1)}{(2)}$ (%)	(1)	(2)	$\frac{(2)-(1)}{(2)}$ (%)
0.3	0.22	0.22	0	—	0.1	—	—	0.06	—
0.4	0.165	0.18	8	0.078	0.078	0	0.039	0.039	0
0.5	0.11	0.14	21	0.065	0.07	7	0.033	0.035	6
0.6	0.055	0.06	8	0.052	0.06	13	0.028	0.03	7
0.7	—	—	—	0.039	0.044	11	0.022	0.025	12
0.8	—	—	—	0.026	0.032	19	0.017	0.018	6
1	—	—	—	—	—	—	0.006	0.009	33

Table V.12 indicates that the results obtained with Eq. (V.8) for all these three columns are close to the numerical values and all are on the safe side. Hence, it follows that the prediction is insignificantly influenced by the column dimensions.

V.4.2. Effect of reinforcement ratio

In group 2, columns of different reinforcement ratios are calculated for the maximum design curvatures obtained with Eq. (V.8) (1) and the numerical tool (2) in case of a fire duration of 60 minutes and compared in Table V.13.

Table V.13: Comparison of the maximum design curvature obtained with Eq. (V.8) (1) and the numerical method (2) in case of a fire duration of 60 minutes considering the effect of different reinforcement ratios

Curvature [1/m]	Reinforcement ratio [-]								
	0.1			0.5			1		
n'	(1)	(2)	$\frac{(2)-(1)}{(2)}$ (%)	(1)	(2)	$\frac{(2)-(1)}{(2)}$ (%)	(1)	(2)	$\frac{(2)-(1)}{(2)}$ (%)
0.3	—	0.1	—	—	0.1	—	—	0.1	—
0.4	0.06	0.06	0	0.078	0.078	0	0.092	0.092	0
0.5	0.042	0.042	0	0.065	0.07	7	0.081	0.081	0
0.6	0.025	0.03	17	0.052	0.06	13	0.07	0.076	8
0.7	0.007	0.014	50	0.039	0.044	11	0.059	0.07	16
0.8	—	—	—	0.026	0.032	19	0.048	0.066	27
1	—	—	—	—	—	—	0.037	0.046	20

From Table V.13, it is seen that only the prediction in case of the reinforcement ratio 0.1 and the axial load 0.7 is too conservative. For other cases, this simplified calculation is in good agreement with the numerical results.

V.4.3. Effect of slenderness ratio

Group 3 presents columns for different slenderness ratios. The maximum design curvatures of the cross-sectional calculation shown in Table V.10 are adopted to calculate the second-order eccentricity for the slenderness ratios 30, 40 and 50. As a result, the second-order deflections calculated with Eq. (V.2) (1) are compared with results from the numerical tool (2) (Table V.14).

Table V.14: Comparisons of design deflections (m) obtained with Eq. (V.2) (1) and the numerical method (2) in case of a fire duration of 60 minutes considering the effect of slenderness ratios

Curvature [1/m]	Slenderness ratio [-]								
	30			40			50		
n'	(1)	(2)	$\frac{(1)-(2)}{(1)}$ (%)	(1)	(2)	$\frac{(1)-(2)}{(1)}$ (%)	(1)	(2)	$\frac{(1)-(2)}{(1)}$ (%)
0.4	0.053	0.044	17	0.095	0.073	23	0.148	0.109	25
0.5	0.044	0.041	7	0.079	0.068	14	0.123	0.1	19
0.6	0.036	0.035	3	0.063	0.056	11	0.099	—	—
0.7	0.027	0.026	4	0.047	—	—	0.074	—	—

Table V.14 indicates that the difference between the simplified equation (V.2) and the numerical method increases with the slenderness ratio in case of the same axial load. This difference reaches a maximum of 25% in case of these three columns. The prediction calculated with Eq. (V.2) is most often in good agreement with the numerical value and is always on the safe side. Hence, it can be concluded that this improved formula can be adequately used in case of fire design.

Comparing the effect of dimensions, the reinforcement ratio as well as the slenderness ratio, it is concluded that only the slenderness ratio has a significant influence on the prediction of the second-order effects with the proposed simplified formula. The difference between the deflections obtained with the simplified method and the numerical values increase in function of the slenderness ratio (in case of the same axial load). However, the simplified formula is proven to be easy-to-use and safe for the prediction of second-order effects in columns exposed to fire.

V.5. Conclusions

In this chapter, the influence of parameters on the simplified methods provided by codes is investigated in case of columns exposed to fire. It is concluded that:

(1) The 500°C isotherm method is proven to be an efficient and easy-to-use method to predict the interaction curves of columns in case of fire. With respect to small cross-sections (less than 200 mm × 200 mm) or columns with exposure times of more than 90 minutes to the standard ISO 834 fire, however, the prediction with this simplified method is very conservative. Hence, for these cases, a higher critical isotherm temperature is recommended for the fire resistance design.

(2) Considering second-order effects, the nominal stiffness method is widely used at ambient temperature. This method, as a simplification, is proven to be safe enough for the design of columns. However, the interaction curves obtained with the nominal stiffness method are too conservative in case of slender columns. The capacity calculated with the KLE-method provided by the Dutch code (NEN, 1995) is slightly on the unsafe side at ambient temperature. However, interaction curves with the KLE-method are closer to the numerical results than those from the nominal stiffness method. Regarding elevated temperatures, the stiffness of the column obtained with the slope of the moment-curvature curve assumed at $0.8M_{Ed}$ in the Dutch prescriptions (NEN, 1995) is not applicable anymore. A value corresponding to a higher bending moment is recommended for the assumption of the stiffness in case of fire.

(3) Imperfections cannot be neglected for slender columns considering second-order effects. Based on the parametric study, fire duration and eccentricity have an important influence on the effect of imperfections. The slenderness ratios as well as dimensions of the cross-section have a significant effect on imperfections under some specific conditions.

(4) The application of the curvature approximation method provided by *fib* Model Code 2010 (2013) is extended to the application of fire based on a parametric study. Furthermore, it is concluded that only the slenderness ratio has a significant influence on the prediction of the second-order effects with the proposed simplified formula. The difference between the deflections obtained with the simplified method and the numerical values increases in function of the slenderness ratio in case of the same axial load. However, the simplified formula is proven to be easy-to-use and safe for the prediction of second-order effects of columns exposed to fire.

CHAPTER VI

SIMPLIFIED METHOD AND PROBABILISTIC ANALYSIS FOR EVALUATING THE BIAXIAL CAPACITY OF RECTANGULAR REINFORCED CONCRETE COLUMNS DURING FIRE

Most of the results in this chapter have been published in Wang L. J., Van Coile R., Caspee R. & Taerwe L. "Simplified method for evaluating the biaxial capacity of rectangular reinforced concrete columns during fire." *Materials and Structures*, 50:37, 2017.

For design situations in case of ambient temperature, both EN1992-1-1 and ACI318 provide guidelines for the design of columns in case of biaxial bending. However, the effect of fire on these columns subjected to biaxial bending is not mentioned in the provisions. It is important to evaluate the mechanical behaviour of columns in case of biaxial bending combined with fire and, hence, to perform additional research in order to provide guidelines for fire resistance design.

VI.1. Introduction

With respect to columns subjected to biaxial bending, previously several experiments have been carried out and a number of analytical methods have been proposed. Bresler (1960) first proposed a design formula for columns subjected both to compression and biaxial bending based on numerical simulations as well as test results. Parme et al. (1966) further developed the formula proposed in (Bresler, 1960) and adapted it to determine the required size for the columns. More recently, Gil-Martín et al. (2010) introduced a model which could determine optimal reinforcement solutions for the design of column reinforcement in case of biaxial bending. However, the applicability of these methods has not been proven in case of fire. As a first important step, Raut and Kodur (2011) presented a macroscopic finite element approach for modeling the fire response of concrete columns under biaxial bending. Recently, Tan and Nguyen (2013, 2014) investigated the effects of symmetrical biaxial bending, restraint ratio and concrete strength on the structural behaviour of reinforced concrete columns at elevated temperatures and proposed a simplified model to determine the thermal-induced restraint forces. Nevertheless, these important studies do not provide guidelines for column design in case of biaxial bending for fire exposure. Hence, there exhibits a contemporary research need to develop an easy-to-use tool is required for the design of columns in such cases.

In this chapter, the applicability of the Bresler approximation during fire exposure is first investigated for concrete columns subjected to biaxial bending using the developed calculation tool. Further, this calculation tool is developed to a case study on biaxial bending for fire exposure taking into account structural uncertainties.

In the first part, the approximate calculation methods (the chord method and the Bresler approximation) used to assess the biaxial bending capacity at ambient

temperature (Bresler, 1960) (Cedolin, 2008) are introduced. Subsequently, the Bresler approximation is studied in case of fire.

A stepwise procedure is applied to evaluate the applicability of the Bresler approximation for fire resistance calculations. First, a cross-sectional calculation tool is presented which has been validated in (CEB/FIP Bulletin 75, 1971) for uniaxial bending in case of fire. In section VI.4, the calculation tool is applied to biaxial bending and validated with experimental data obtained from Tan and Nguyen (2013). Next, the formula proposed by Bresler (1960) is adopted to calculate interaction curves of columns subjected to biaxial bending in case of fire and the developed numerical tool is applied in order to evaluate the performance of the proposed design approach. Furthermore, the influence of parameters such as the column dimension, reinforcement ratio and fire duration are investigated and discussed. Since the calculation tool can be used to obtain interaction curves of columns in case of biaxial bending for fire exposure, finally a probabilistic analysis is discussed considering the reliability of the performance of columns exposed to fire.

VI.2. Basic calculation methods

Due to the load transferred from beams and slabs, columns are commonly subjected to biaxial bending. However, the calculation of interaction curves for biaxial bending in case of concrete structures is quite complicated. Therefore, the ambient design of columns for biaxial bending is usually made based on simplified methods and uniaxial calculations (Cedolin, 2008). Two simplified analytical approaches for ambient temperatures – the chord method and the Bresler approximation (Bresler, 1960) are presented here.

VI.2.1. Chord method

With the so-called chord method, the uniaxial bending resistance along the x-axis and y-axis of the column cross-section are calculated independently and a linear relationship is assumed for biaxial bending:

$$\left[\frac{\mu_x(v, \alpha_\mu)}{\mu_x(v, \alpha_\mu = 0^\circ)} \right] + \left[\frac{\mu_y(v, \alpha_\mu)}{\mu_y(v, \alpha_\mu = 90^\circ)} \right] = 1 \quad (\text{VI.1})$$

where v is the dimensionless axial load and μ_x and μ_y are the dimensionless bending moment capacities along the x and y axis, as defined by (VI.1b), (VI.1c) and (VI.1d) respectively. The parameter α_μ is the angle of the bending axis, with $\alpha_\mu = 0^\circ$ corresponding to the x-axis and $\alpha_\mu = 90^\circ$ to the y-axis.

$$v = \frac{N}{f_{ck}bh} \quad (VI.1b)$$

$$\mu_x = \frac{M_x}{f_{ck}bh^2} \quad (VI.1c)$$

$$\mu_y = \frac{M_y}{f_{ck}b^2h} \quad (VI.1d)$$

In equation (VI.1b) to (VI.1d), N is the design value of the axial load and M_x , M_y are the design values of the bending moments along the x and y axis respectively, f_{ck} is the 20°C characteristic concrete compressive strength, b is the width of the cross-section and h is the total depth of the cross-section (see Fig. VI.2.).

When the uniaxial bending capacities $\mu_x(v, \alpha_\mu = 0^\circ)$ and $\mu_y(v, \alpha_\mu = 90^\circ)$ have been determined, the respective bending capacities for biaxial bending for a bending axis with angle α_μ from the x-axis can be determined through Eq. (VI.1) by $\mu_y(v, \alpha_\mu) = \sin(\alpha_\mu)\mu_y(v)$ and $\mu_x(v, \alpha_\mu) = \cos(\alpha_\mu)\mu_x(v)$.

VI.2.2. Bresler approximation

Bresler (1960) first proposed to use the modified non-dimensional interaction equation (VI.2) where the powers γ_1 and γ_2 are depending on the column dimensions, reinforcement ratio, effective depth and material properties.

$$\left[\frac{\mu_x(v, \alpha_\mu)}{\mu_x(v, \alpha_\mu = 0^\circ)} \right]^{\gamma_1} + \left[\frac{\mu_y(v, \alpha_\mu)}{\mu_y(v, \alpha_\mu = 90^\circ)} \right]^{\gamma_2} = 1 \quad (VI.2)$$

Further, in order to evaluate the validity of the proposed method as well as to determine the relationships for γ_1 and γ_2 , preliminary calculations and tests were carried out by Bresler on values of the failure load and bending moment components for a group of five rectangular columns assuming various values for α_μ (Bresler, 1960). It was found that for a rectangular cross-section, the strength

criteria could be closely approximated by Eq. (VI.2) by assuming an equivalence with a square cross-section (Bresler, 1960) for which $\gamma_1 = \gamma_2 = \gamma$. Hence, a general strength criterion could be defined according to Eq. (VI.3).

$$\left[\frac{\mu_x(v, \alpha_\mu)}{\mu_x(v, \alpha_\mu = 0^\circ)} \right]^{\gamma(v)} + \left[\frac{\mu_y(v, \alpha_\mu)}{\mu_y(v, \alpha_\mu = 90^\circ)} \right]^{\gamma(v)} = 1 \quad (\text{VI.3})$$

In case of biaxial bending, the same axial load N is taken as was the case for uniaxial bending. Hence, the first-order bending moments are given by $M_x = N \cdot e_x(v, \alpha_\mu)$ and $M_y = N \cdot e_y(v, \alpha_\mu)$, where e_x , e_y are the maximum allowable member force eccentricities which are applied to the end of the column (see Fig. VI.2), taking into account second-order effects, Eq. (VI.3) can be expressed as:

$$\left[\frac{e_x(v, \alpha_\mu)}{e_x(v, \alpha_\mu = 0^\circ)} \right]^{\gamma(v)} + \left[\frac{e_y(v, \alpha_\mu)}{e_y(v, \alpha_\mu = 90^\circ)} \right]^{\gamma(v)} = 1 \quad (\text{VI.4})$$

where v is the dimensionless axial load as defined by (VI.1b) and e_x , e_y are the maximum allowable eccentricities for a given v along the x and y axis as defined by (VI.4b) and (VI.4c) respectively.

$$e_x = \frac{M_x}{N} \quad (\text{VI.4b})$$

$$e_y = \frac{M_y}{N} \quad (\text{VI.4c})$$

Again M_x and M_y are corresponding to the design values of bending moments along the x and y axis respectively.

Hence, once the maximum permitted eccentricities for a given axial load are known for uniaxial bending, the maximum permitted eccentricities in case of biaxial bending are obtained by taking $e_x(v, \alpha_\mu) = \cos(\alpha_\mu)e_{\text{tot}}$, $e_y(v, \alpha_\mu) = \sin(\alpha_\mu)e_{\text{tot}}$ into Eq. (VI.4), where e_{tot} is the maximum permitted eccentricity to the centroid in case of biaxial bending (see Fig. VI.2). e_{tot} is depending on the value of $\gamma(v)$.

For the case of square columns where $\mu_x(v, \alpha_\mu = 0^\circ) = \mu_y(v, \alpha_\mu = 90^\circ)$, the exponent $\gamma(v)$ can be determined by the situation related to $\alpha_\mu = 45^\circ$, i.e. Eq. (VI.4) is written as Eq. (VI.5) by replacing $e_y(v, \alpha_\mu = 45^\circ) = e_x(v, \alpha_\mu = 45^\circ)$:

$$\gamma(v) \cdot \ln \left[\frac{e_x(v, \alpha_\mu = 0^\circ)}{e_x(v, \alpha_\mu = 45^\circ)} \right] = \ln 2 \quad (\text{VI.5})$$

where $e_x(v, \alpha_\mu = 0^\circ)$ is the maximum allowable eccentricity in case of uniaxial bending

$e_x(v, \alpha_\mu = 45^\circ)$ is the maximum allowable eccentricity in case of a symmetric load applied along an axis under 45° compared to the x-axis

Numerical methods are usually adopted to validate the Bresler approach. Among all the methods, a cross-sectional calculation is most often used to find out the relationship between the bending moment and the curvature. Cedolin (2008) showed a typical moment interaction diagram with the chord and the Bresler methods and made a comparison with the numerical calculation, as shown in Fig. VI.1. The Bresler method is conservative (i.e. underestimation of the numerical solution). This holds true for all configurations where the material models of EN 1992-1-1 (2004) are adopted (Cedolin, 2008). By way of example, the relationship between dimensionless bending moment capacities along the x and y axis in case of $\alpha_\mu = 30^\circ$ is shown in Fig. VI.1.

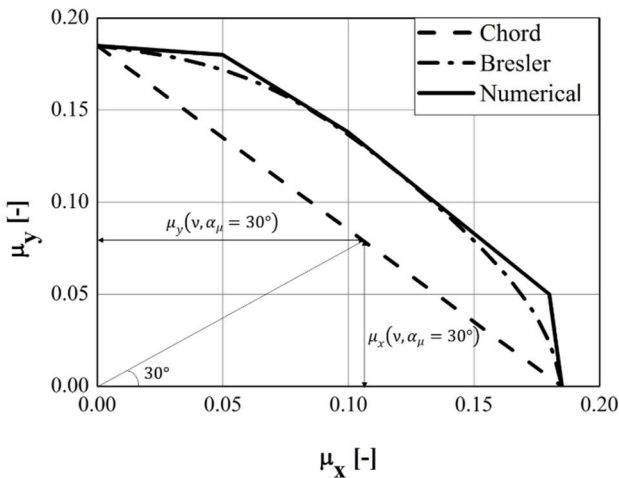


Fig. VI.1: The moment interaction diagram calculated with the exact numerical method, the chord method and the Bresler approximation (Cedolin, 2008)

Furthermore, Fig. VI.1 indicates that results obtained with the Bresler approximation have a good agreement with the numerical calculations. With

reference to EN 1992-1-1 (2004), the Bresler method has been shown to be reliable for all practical ranges of the dimensionless reinforcement ratios ω and dimensionless concrete cover δ (Cedolin, 2008). Hence, the Bresler method has been validated to calculate interaction curves of columns subjected to biaxial bending in ambient temperatures, significantly simplifying the evaluation as only uniaxial calculations are required. In the next sections the application of the Bresler method for fire design is investigated.

VI.3. Assumptions and calculation models for biaxial bending during fire exposure

As a simplified method, the Bresler approximation is provided in Eurocode 2 (2004) for the design of RC columns subjected to biaxial bending under ambient temperature. Herein, the moment resistance of RC columns in case of biaxial bending is based on the design moments of RC columns in case of uniaxial bending about the two principal axes. In order to figure out whether this method can be adopted in case of fire, the same calculation theory is presumed. The fire resistant design of columns subjected to uniaxial bending is a function of the dimensionless normal force parameter v which can be determined by provisions or numerical calculations. The effect of the axial load level is hence incorporated, more specifically through the v -dependent uniaxial bending resistance.

In order to evaluate biaxial bending capacities during fire exposure and to validate the applicability of the Bresler approximation, a calculation model is presented. The model is based on a cross-sectional calculation tool developed in **chapter III** to predict second-order effects of columns exposed to fire, and is based on the same principles as Dwaikat & Kodur (2009, 2011) and Kodur et al. (2013). This calculation tool has a good agreement with the interaction curves calculated in Meda (2002) as well as those simulated in Caldas et al. (2010) for different fire exposures. Furthermore, the calculation tool has been verified with experimental data from Hass (1986) and Dotreppe (1993).

The following assumptions are made: 1) plane sections remain plane; 2) the tensile strength of concrete is not considered; 3) there is no bond-slip between steel reinforcement and concrete; 4) imperfections of columns are considered as a bow imperfection with an initial eccentricity $l_0/400$ (as given by EN 1992-1-1 (2004)).

Further, the stress-strain relationships of concrete and reinforcement bars provided in EN 1992-1-2 (2004) are adopted.

As the first step in the calculation process, the cross-section is discretized into small elements. In the calculation model for the examples described in this chapter, a 1 mm × 1 mm square is chosen as the basic mesh size (Fig. VI.2). The appropriateness of this mesh size for the thermal and structural calculations has been shown for the calculations given in section III.2 and section III.3.

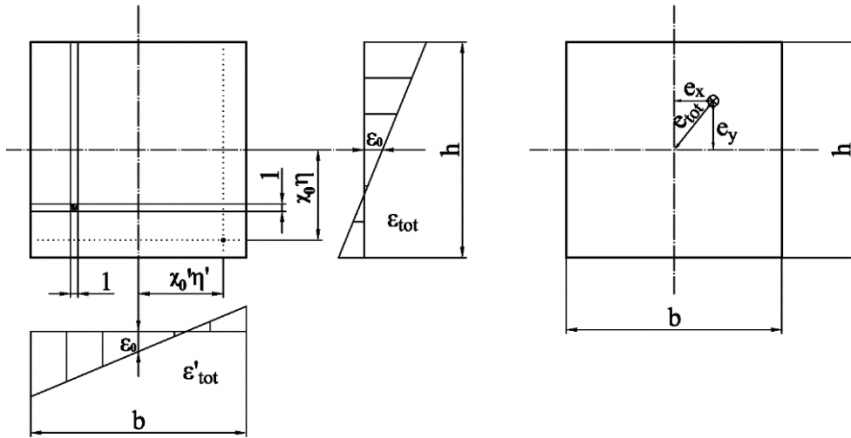


Fig. VI.2: Strain distribution and calculation model

In the calculation procedure, the mechanical strain of the solid point shown in Fig. VI.2 is expressed as follows:

$$\varepsilon_{\text{mech}} = \varepsilon_x + \varepsilon_y - \varepsilon_{\text{th}} = \varepsilon_0 + \chi_0 \eta + \chi_0' \eta' - \varepsilon_{\text{th}} \quad (\text{VI.6})$$

where ε_x is the total strain due to bending along the vertical axis, ε_y is the total strain due to bending along the horizontal axis, ε_{th} is the thermal strain, ε_0 is the strain at the centroid and (χ_0, χ_0') are the curvatures about both axes, (η, η') are the distance from the fiber for which the strain is calculated to the centroid along the vertical axis and the horizontal axis respectively.

In this paper, only symmetrically reinforced square columns with four-sided fire exposure are considered. Furthermore, if the axial load is applied on the diagonal of the cross-section ($\alpha_\mu = 45^\circ$), then $\chi_0 = \chi_0'$ and (VI.6) can be written as:

$$\varepsilon_{\text{mech}} = \varepsilon_0 + \chi_0 (\eta + \eta') - \varepsilon_{\text{th}} \quad (\text{VI.7})$$

The virtual work principle is used to calculate the deflection considering first order effects. Next, second-order bending moments caused by the deflection are calculated with an iterative calculation method as elaborated in section III.3. Subsequently, these are taken into account to calculate the adjusted interaction diagrams when considering the reduced capacity due to second-order effects.

Since for the situation of square columns with an eccentric load on the diagonal of the cross-section both the geometric configuration as the load are symmetric, the bending moment-curvature curves adopted for the x and y axis are the same. Hence, only one bending moment-curvature curve is required for the calculation of deflections in both x and y directions in case of a specific axial load.

VI.4. Validation of the calculation model

In order to verify the calculation method, the results obtained for a specific column with three typical sets of equal biaxial eccentricities, i.e. $e_x = e_y = e = 25$ mm, 40 mm and 60 mm are compared to the experimental data from Tan and Nguyen (2013). Only the three columns from test series “S3” considering symmetric reinforcement and fire are considered here. The concrete of the S3 columns was cast with siliceous aggregates of 20 mm maximum size, silica-based sand and a water/cement ratio of 0.58. The tests were performed 4 months after casting. Each of the specimens has the same geometry: a nominal length of 3.3 m and a cross-section of 300 mm \times 300 mm, 4 reinforcement bars with diameter 25 mm and a concrete cover of 30 mm. The average 20°C concrete compressive strength was measured as $f_c = 29.3$ MPa, the reinforcement yield stress $f_y = 554$ MPa and Young’s modulus of steel $E_s = 201$ GPa. In the test-setup fourteen butt-welded chromel-alumel K-type thermocouples were positioned at the three cross-sections designated as ‘A’, ‘B’ and ‘C’ (shown in Fig. VI.3).

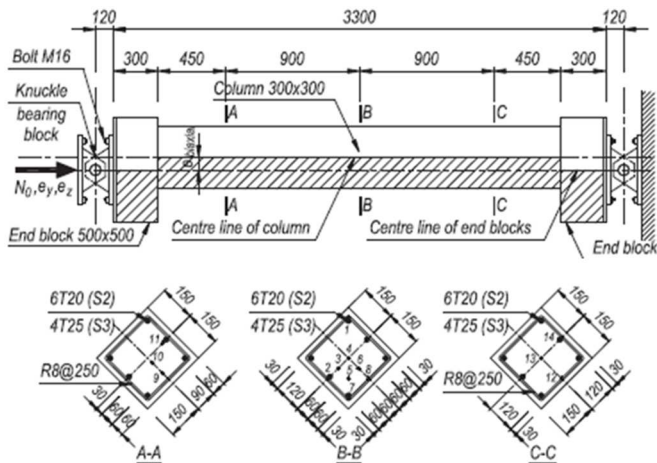


Fig. VI.3: Details of typical test specimen (Tan & Nguyen, 2013)

In the tests from (Tan & Nguyen, 2013), the temperature inside the electric furnace is initially increased at a rate of 5 °C/min up to 200 °C, then held for 85 minutes at 200 °C before being increased further to 800 °C at a constant rate of 10 °C/min. Finally, this constant temperature of 800 °C is maintained until the specimen is deemed to have failed. The time-temperature curves of selected nodes 1 (rebar), 2 (35 mm from a column surface), 4 (center of cross-section) and 5 (90mm from adjacent surfaces) at section ‘B’ are given in Fig. VI.3, together with the temperature obtained with the numerical tool presented above.

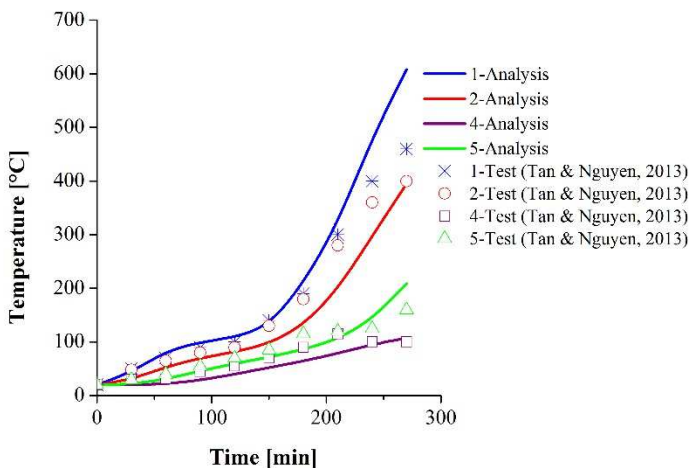


Fig. VI.4: Time-dependent temperature curves of selected nodes (1, 2, 4, 5)

Considering Fig. VI.4, a good agreement is observed between the calculated temperature and the test results, though there are differences on Node 1 and Node 2 after 210 minutes. These differences might be caused by deviations in the setup conditions (loading setup, furnace temperatures, etc.), deviations in the heat transfer (for example the convection coefficient considered), and spalling. As some limited spalling was observed during the test, this is assumed to be the main reason for the differences between the measured and calculated temperatures of the outer layer (Node 1 and Node 2).

The columns mentioned in (Tan & Nguyen, 2013) were tested at 55% of the ambient buckling load for the given eccentricity. This 55% was considered based on EN 1992-1-2 (2004), where a reduction factor is specified for the design load in the fire situation. This reduction factor η_{fi} is used for the design load level as a safe simplification since η_{fi} assumes that the column is fully loaded at normal temperature design. It is worth mentioning that in EN 1992-1-2 (2004), the value of η_{fi} for load combination is given between 0.2 and 0.7.

Adopting the temperatures obtained with the numerical tool (as illustrated above in Fig. VI.4), the mid-height lateral deflection of columns C3-1-25 (S3, axially loaded with 860 kN and an eccentricity of 25 mm), C3-2-40 (S3, axially loaded with 680 kN and an eccentricity of 40 mm) and C3-3-60 (S3, axially loaded with 530 kN and an eccentricity of 60 mm) are presented in Fig. VI.5.

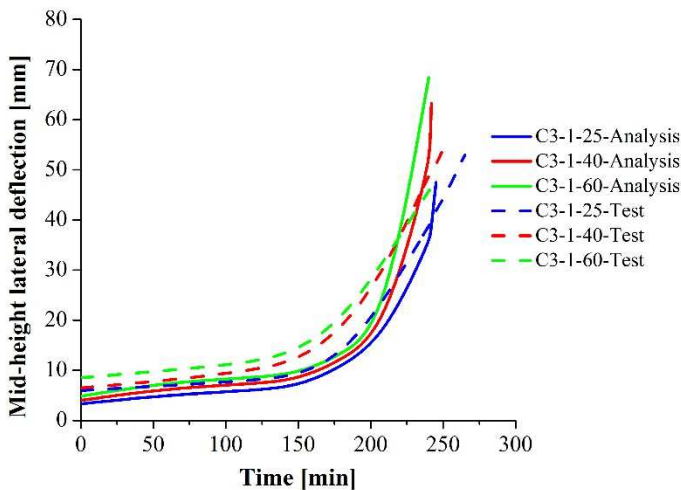


Fig. VI.5: Comparison of the curves of the mid-height lateral deflection of columns with tests from Tan & Nguyen (2013)

In Fig. VI.5, it is seen that the calculated deflections at mid-height increase slowly and are constantly lower than the test measurements before the fire duration of 210 minutes. The differences of the mid-height lateral deflection between the tests and our calculation tool are already observed at the beginning ($t = 0$). This might be attributed to the difference in actual stiffness behaviour at ambient temperature. Furthermore, the difference does not increase significantly during the fire. Hence, spalling is not an explanation of the overall offset. Besides, spalling requires making more hypotheses which are difficult to justify. Currently, there is no generally accepted calculation method for considering spalling. Eurocode 2 (2004) states that explosive spalling is unlikely to occur when the moisture content of concrete is less than 3%. With an assumption of the moisture content of concrete less than 3%, spalling is not specifically considered herein. Due to the actual stiffness behaviour, second-order effects are slightly more pronounced in the test, resulting in larger deflections compared to the numerical model. Note that the deflection grows very fast after 210 minutes due to the reduction in the strength of the reinforcing bars when their temperature exceeds 400 °C. At this point the calculated deflections start to catch up with the observed deflections, and finally all of the three columns fail before the fire duration reaches 250 minutes. The prediction based on the numerical model is close to the experimental data and can be considered as a good estimation of the failure time. Furthermore, this failure time is conservatively assessed by the numerical model. It is concluded that the numerical model gives an acceptable approximation and can be used for parametric studies and for the development of simplified calculation rules, as is the intent of this paper.

It is worth mentioning that the validation of this calculation tool in case of uniaxial bending has been done in section III.4.2 by comparing the results with 15 groups of experimental data (Lie et al., 1984) (Hass, 1986) (Dotreppe and Franssen, 1993). However, with respect to columns subjected to biaxial bending in case of fire, there are not so many experiments available to compare with. The test of Tan and Nguyen (2013) was performed with square cross-sectional columns in case of $e_x = e_y$ ($\alpha_\mu = 45^\circ$). Hence, the results obtained with the calculation tool are only compared with the tests for square columns in case of $e_x = e_y$. Nevertheless, Eq. (VI.6) still remains valid when other angles are considered ($\chi_0 = \chi_0'$ in case of $\alpha_\mu = 45^\circ$) and therefore Eq. (VI.6) is applied in the calculation tool for other angles than 45° . Considering classical assumptions in cross-sectional calculations, there is no reason to expect that a deviating performance of the methodology would be obtained in case of $\alpha_\mu \neq 45^\circ$.

VI.5. Calculation of $\gamma(v)$ and parametric study

To illustrate the concepts introduced above and to determine approximate values for $\gamma(v)$ to be used in structural fire design, a set of parametric studies are performed, first for ambient temperature and subsequently taking into account fire exposure.

As Bresler (1960) has already investigated column dimensions, amount and distribution of steel reinforcement, stress-strain characteristics of steel and concrete, concrete cover and arrangement and size of lateral ties or spiral under ambient temperature, further in this paper only the effects of the reinforcement ratio ω and the angle of the bending axis α are investigated. With respect to fire, the parametric study covers the reinforcement ratio ω , the orientation α of the bending axis, the fire duration t , the column dimensions, the concrete cover and the number of reinforcing bars, which the authors believe to be the most important ones with respect to the fire case. Since Bresler (1960) introduced an approximation based on the study of relatively short columns, a limit ratio of the effective length of column l to the smallest dimension of the cross-section d equal to 10 is chosen for all the columns in the paper. Hence, the effect of the slenderness is not discussed herein.

VI.5.1. Parametric study at ambient temperatures

First, three columns are investigated with the same geometric characteristics—cross-section dimensions of 300 mm \times 300 mm and length of 3 m – but different reinforcement ratios. The properties of material strengths considered as well as the different configurations of the longitudinal reinforcement for these columns are listed in Table VI.1, where the reinforcement ratio $\omega = \frac{A_s f_{yd}}{A_c f_{cd}}$. The parameter $f_{cd} = \alpha_{cc} f_{ck} / \gamma_c$ is the design value of concrete compressive strength with γ_c the partial safety factor and α_{cc} the coefficient taking into account long term effects on the compressive strength and unfavourable effects resulting from the way the load is applied ($\gamma_c = 1.5$ and $\alpha_{cc} = 0.85$ as recommended by Eurocode 2 are adopted). The parameter $f_{yd} = f_{yk} / \gamma_s$ is the design yield stress of the reinforcement with $\gamma_s = 1.15$ as recommended by Eurocode 2. A_c is the cross-sectional area of concrete and A_s is the cross-sectional area of the reinforcement.

Table VI.1: Material strength and geometric properties of investigated columns

No.	20°C characteristic concrete compressive strength f_{ck} (MPa)	20°C characteristic reinforcement yield stress f_y (MPa)	Number of reinforcement bars	Cover thickness (mm)	Reinforcement ratio ω
1	65	500	4 ϕ 16	25	0.1
2	55	500	4 ϕ 32	25	0.5
3	25	500	4 ϕ 32	25	1.1

In Fig. VI.6 results for the coefficient $\gamma(v)$ (at ambient temperatures) obtained with the numerical calculation tool are compared with values of $\gamma(v)$ given in (Cedolin, 2008). As indicated in (Cedolin, 2008) a crude approximation for $\gamma(v)$ in the range $v = 0.3$ until the column failure is 1.10 to 1.50. The numerical results in Fig. VI.6 confirm this approximation. Note that the values of $\gamma(v)$ are much larger than 1.50 when the axial load is small. This is because the reinforcement bars located furthest from the biaxial bending axis bear most of the bending moment, which makes the maximum permitted eccentricity in case of biaxial bending very small.

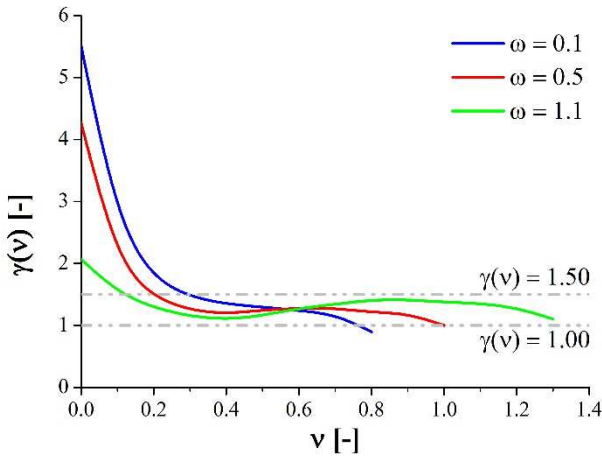


Fig. VI.6: Numerical values of coefficient $\gamma(v)$ at ambient temperature for the investigated columns

Adopting the calculated $\gamma(v)$ presented in Fig. VI.6 and calculating interaction curves in case of uniaxial bending with the numerical tool, Eq. (3) is evaluated for different axial loads. Results for the obtained interaction curves, are illustrated in Fig. VI.7.

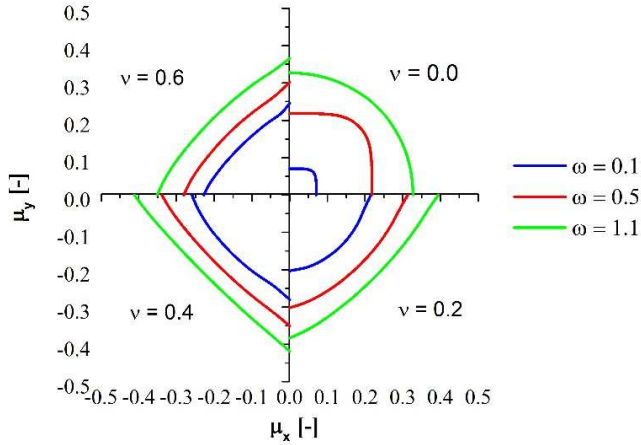


Fig. VI.7: Moment interaction diagrams for values of $v = 0, 0.2, 0.4, 0.6$ at ambient temperature

The diagrams in Fig. VI.7 indicate that the moment capacity of columns at ambient temperature reaches a maximum when v is around 0.4, which agrees with the expression (5.34) provided in EN 1992-1-1 (2004). It is worth pointing out that the interaction diagrams in case of the moderate reinforcement ratios as well as high reinforcement ratios seem to be approximately straight lines when $v = 0.4$. Hence, $\gamma(v) = 1.0$ can be adopted to predict the moment capacity when $v > 0.3$ in case of biaxial bending as an approximate calculation.

Finally, in order to figure out whether the value of $\gamma(v)$ in case of symmetric biaxial bending ($\alpha_\mu = 45^\circ$) could also be used for other biaxial bending types as (Cedolin, 2008) indicates, columns No. 2 and No. 3 (Table VI.1) are investigated for $\alpha_\mu = 60^\circ$, with an eccentric load $v = 0.4$. The difference between the prediction of the Bresler approximation and numerical values on maximum permitted eccentricities in x-axis are compared in Table VI.2, based on the value of $\gamma(v) = 1.18$ and $\gamma(v) = 1.09$ obtained in case of $\alpha_\mu = 45^\circ$ for columns No.2 and No.3 respectively as well as the aforementioned value of $\gamma(v) = 1.00$ as a simplification for both columns.

Table VI.2: Comparison of the Bresler approximation and numerical values on maximum permitted eccentricities in x-axis

No.	$\gamma(v)$	Eccentricity (cm)		Difference (%)
		Bresler approximation	Numerical value	
2	1.18	5.1	5.5	7.3
2	1.00	4.7	5.5	14.5
3	1.09	8.6	9.4	8.5
3	1.00	8.2	9.4	12.8

From Table VI.2, it is seen that results with the Bresler approximation adopting the value of $\gamma(v)$ in case of the symmetric axial load gives good agreements with the obtained numerical values. Moreover, the prediction of Bresler approximation is on the safe side for these two columns. The prediction with $\gamma(v) = 1.0$ is more conservative than adopting the value of $\gamma(v)$ obtained for the symmetric axial load. However, as a simplification, $\gamma(v) = 1.0$ could be adopted in the Bresler approximation to predict the moment capacity in case of $v = 0.4$.

VI.5.2. Parametric study for columns subjected to fire

In order to apply the Bresler approximation to predict the fire resistance of columns, the appropriate power $\gamma(v)$ has to be determined. The range of applicability of specific values of $\gamma(v)$ is determined in the following by performing parameter studies, i.e. by considering the effects of different reinforcement ratios, fire durations, dimensions of the cross-sections, the number of reinforcing bars as well as the angle of the bending axis.

(1) Reinforcement ratios

First, the three columns mentioned in section VI.5.1 are discussed taking into account an ISO 834 standard fire. Fig. VI.8 presents the calculated $\gamma(v)$ relationship in function of v calculated with Eq. (VI.5) in case of fire durations of 30 minutes, 60 minutes and 90 minutes.

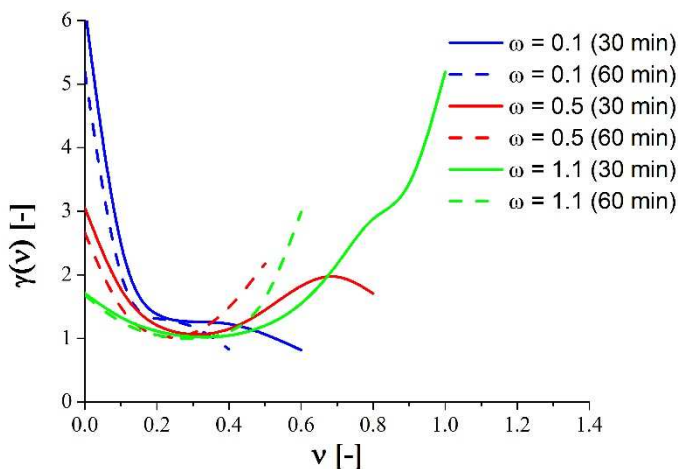


Fig. VI.8: Numerical values of coefficient $\gamma(v)$ for columns with different reinforcement ratios in case of an ISO 834 fire of 30 min, 60 min and 90 min

From the diagrams shown in Fig. VI.6 and Fig. VI.8, it is seen that the lower bound of the range of almost constant values of $\gamma(v)$ shifts to a value of v of about 0.1 in case of fire durations of 30 minutes, 60 minutes and 90 minutes. It is worth mentioning that the curves in case of a reinforcement ratio 1.1 increase significantly in function of fire when v becomes larger than 0.4 in case of fire durations of 30 minutes and 60 minutes as well as when v is larger than 0.3 in case of a fire duration of 90 minutes. As the applied axial load is increasing, the maximum permitted eccentricity is going down quickly. This decrease occurs more significantly in case of biaxial bending, which results in an increase of $\gamma(v)$.

At ambient temperature, the moment interaction curve is largest when $v = 0.4$ (Fig. VI.7). Interaction curves are calculated in case of a fire duration of 30 minutes, 60 minutes and 90 minutes. However, the results show that the value of v corresponding to the largest moment interaction curve decreases with increasing fire duration. Considering the three previously investigated columns for instance, the value v corresponding to the maximum moment contour drops to 0.2 ~ 0.4 in case of a fire duration of 30 minutes and 0 ~ 0.2 in case of fire durations of 60 minutes and 90 minutes. The column with $\omega = 0.1$ cannot bear any moments for $v = 0.4$ in case of 60 minutes ISO 834 standard fire exposure, neither can the column with $\omega = 0.5$ bear any moments for $v = 0.4$ in case of a fire duration of 90 minutes.

(2) Fire duration

In order to investigate the influence of the ISO 834 fire duration, a column with a cross-section of 500 mm × 500 mm, length of 5 meters (same slenderness ratio as columns mentioned in section VI.5.1), cover thickness 25 mm and 4 Ø 32 reinforcement bars ($\omega = 0.3$) is investigated. The results are illustrated in Fig. VI.9.

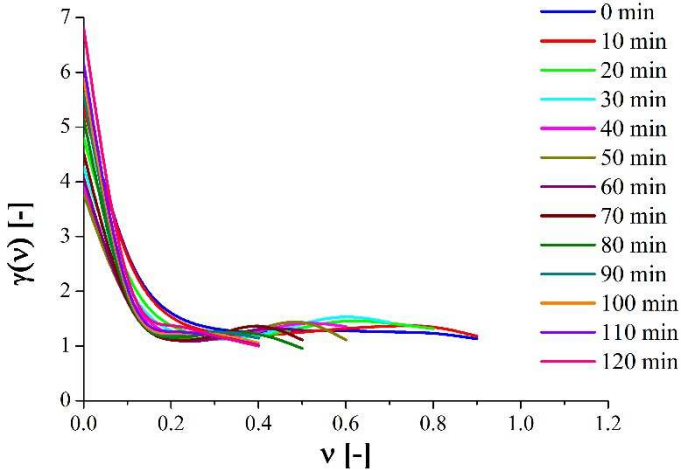


Fig. VI.9: Numerical values of coefficient $\gamma(v)$ for columns with different reinforcement ratios in case of an ISO 834 fire of different fire durations

In order to explain the behaviour observed in Fig. VI.9, consider again $\varepsilon = \frac{e_x(v, \alpha_\mu = 45^\circ)}{e_x(v, \alpha_\mu = 0^\circ)}$ (the ratio of the maximum permitted eccentricity in case of biaxial bending to uniaxial bending). Hence, Eq. (VI.5) could be written as $\gamma(v) \cdot \ln 1/\varepsilon = \ln 2$. If $\gamma(v)$ increases, so will ε . In Fig. VI.9, we can see $\gamma(v)$ firstly decreases with the fire duration ($v = 0.05 \sim 0.15$), which means that the relative loss in the column capacity is more significant in case of biaxial bending than in case of uniaxial bending for small axial loads. Then, the curves begin to increase with an increasing axial load. In the increasing branches of the curves in Fig. VI.9, it is seen that the value of $\gamma(v)$ mainly remains between 1.00 and 2.00, where the upper limit of $\gamma(v)$ is larger than that of $\gamma(v) = 1.50$ at ambient temperature. However, a range of $\gamma(v)$ 1.00 ~ 1.50 can be still recommended when $v = 0.15 \sim 0.4$ during fire. Furthermore, like at ambient temperature, a conservative value of 1.00 can be used for $\gamma(v)$ while a larger value is possible for specific situations (i.e. $v < 0.15$) in case of fire. Finally, the value of $\gamma(v)$ increases and is often followed by a slight decrease when the column is close to failure. This latter phenomenon can be observed clearly after a fire duration of 50 minutes in Fig. VI.9. This can be attributed to the last significant decrease of the maximum permitted eccentricity with an increasing axial

load in case of uniaxial bending with an increasing temperature while the decrease of the maximum permitted eccentricity in case of biaxial bending keeps almost the same.

As Fig. VI.9 indicates that a range 1.00 ~ 1.50 is also recommended for $\gamma(v)$ when v is between 0.15 and 0.40 during fire, the effect of different values $\gamma(v) = 1.00, 1.10$ and 1.50 is shown in Table VI.3, when $v = 0.4$ and the column investigated in Fig. VI.9 is considered.

Table VI.3: Comparison of the maximum permitted eccentricity in case of $\gamma(v) = 1.00, 1.10$ and 1.50 when $v = 0.4$

Fire duration (min)	$\gamma(v)$		Eccentricity (cm)		Difference (%)	
	Actual value ①	Simplified value ②	Actual value ③	Simplified calculation ④	$\gamma(v) \frac{①-②}{①}$	Eccentricity $\frac{③-④}{③}$
0	1.23	1.00	11.0	9.7	18.7	11.8
		1.10	11.0	10.3	10.6	6.4
		1.50	11.0	12.2	-22.0	-10.9
30	1.18	1.00	7.1	6.4	15.3	9.9
		1.10	7.1	6.8	6.8	4.2
		1.50	7.1	8.1	-27.1	-14.1
60	1.36	1.00	3.9	3.3	26.5	15.4
		1.10	3.9	3.5	19.1	10.3
		1.50	3.9	4.1	-10.3	-5.1
90	1.14	1.00	1.8	1.7	12.3	5.6
		1.10	1.8	1.8	3.5	0.0
		1.50	1.8	2.1	-31.6	-16.7
120	1.00	1.00	0.8	0.8	0.0	0.0
		1.10	0.8	0.9	-10.0	-12.5
		1.50	0.8	1	-50.0	-25.0

From Table VI.3, it is seen that the maximum permitted eccentricity is always on the conservative side if $\gamma(v) = 1.00$. On the other hand, it can be inappropriate to use a value of 1.50 for $\gamma(v)$ since it is 14.1%, 16.7% and 25% on the unsafe side when the fire lasts 30 minutes, 90 minutes and 120 minutes, respectively. Furthermore, for the column under consideration (i.e. with $\omega = 0.3$) it makes no significant difference when $\gamma(v) = 1.10$ is adopted. Hence, $\gamma(v) = 1.10$ could be recommended for this type of columns with the slenderness ratio not more than 10 and a reinforcement ratio of 0.3 in case of an ISO 834 fire and $v = 0.4$.

(3) Dimensions

In this section, the effect of different column dimensions are investigated. A column with a cross-section 500 mm × 500 mm, cover thickness 25 mm and 4Ø32 reinforcement bars ($\omega = 0.3$) is compared with a column with a cross-section 300 mm × 300 mm, the same reinforcement ratio 0.3 and the same slenderness ratio 10. The curves of $\gamma(v)$ for these two columns in case of different fire durations are illustrated in Fig. VI.10.

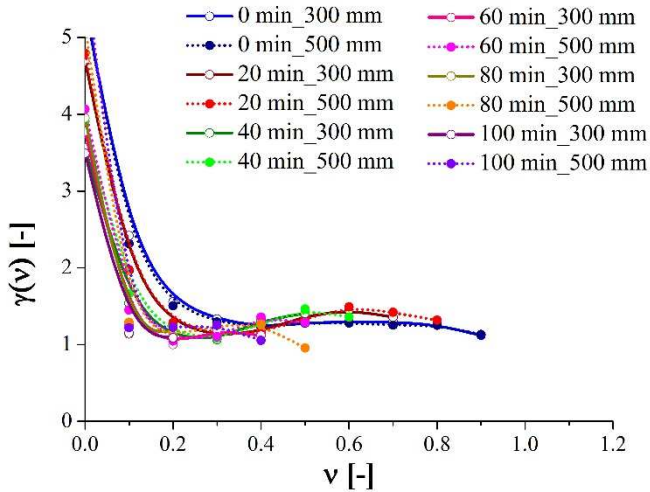


Fig. VI.10: Numerical values of the coefficient $\gamma(v)$ for columns with different dimensions of the cross-section in case of different fire durations

As seen in Fig. VI.10, these two columns have similar values of $\gamma(v)$ for the same fire duration and axial load ratios. Hence, as is the case at ambient temperature (Bresler, 1960), the curves of $\gamma(v)$ could be generalised for short columns exposed to an ISO 834 fire. As long as one considers the maximum allowable capacity for v under pure compression, a $\gamma(v)$ curve can be proposed for the design of square columns with a certain ω and the same number of reinforcing bars.

(4) Numbers of reinforcing bars

Further, also the influence of the number of reinforcing bars is investigated. Two columns with the same cross-section 500 mm × 500 mm, cover thickness 25 mm, length of 5 meters and reinforcement ratio 0.3, but with a different number of reinforcing bars are compared. One is with 4Ø32 (one bar in each corner) and the

other one is with 8Ø25 (one bar in each corner and one bar in the middle of each side).

Table VI.4 illustrates the behaviour of $\gamma(v)$ for these two columns with different configurations of reinforcing bars in case of a fire duration of 0, 30, 60 and 90 minutes.

Table VI.4: Numerical values of coefficient $\gamma(v)$ for columns with a different number of reinforcing bars at ambient temperature, in case of 30 minutes fire, 60 minutes fire and 90 minutes fire

Reinforcing bars 4φ32	v	Fire duration (min)	Reinforcing bars 8φ25
$\gamma(v)$			$\gamma(v)$
5.40	0.0	0	2.27
2.31	0.1		1.80
1.51	0.2		1.63
1.29	0.3		1.48
1.23	0.4		1.38
1.28	0.5		1.37
1.28	0.6		1.43
1.25	0.7		1.37
1.25	0.8		1.37
1.13	0.9		1.28
4.26	0.0	30	1.96
1.80	0.1		1.63
1.20	0.2		1.51
1.08	0.3		1.54
1.18	0.4		1.47
1.41	0.5		1.42
1.59	0.6		1.39
1.43	0.7		1.26
4.07	0.0	60	1.86
1.45	0.1		1.51
1.05	0.2		1.56
1.10	0.3		1.66
1.36	0.4		1.41
1.29	0.5		1.11
1.07	0.6		1.00
5.60	0.0	90	1.76
1.25	0.1		1.67
1.16	0.2		1.89
1.31	0.3		1.59
1.14	0.4		1.00

In Table VI.4, it is observed that the values of $\gamma(v)$ are much larger in case of $4\phi 32$ reinforcing bars when the axial load is very low and these values drop significantly when v reaches 0.1. Furthermore, the values of $\gamma(v)$ of these two columns at ambient temperature change slightly in case of $v = 0.3 \sim 0.8$. However, the values of $\gamma(v)$ in case of $4\phi 32$ reinforcing bars vary significantly with axial loads and fire. The curves in case of $8\phi 25$ reinforcing bars present a limited variability with an increasing axial load and fire duration. It is worth mentioning that the value of $\gamma(v)$ in case of a column with 8 reinforcing bars is falling down to about 1.0 only when the axial load is about to reach the load capacity and the fire effect on the tendency of $\gamma(v)$ is not significant. Although differences are more significant, $\gamma(v) = 1.0$ can be considered to remain applicable (but less conservative results can be obtained from the table).

(5) Concrete cover

Furthermore, the influence of concrete cover is discussed. Two columns are chosen with the same cross-sectional dimensions $300 \text{ mm} \times 300 \text{ mm}$ and length of 3 m and the same material properties as column No. 2 (Table VI.1), but with different cover thicknesses of 25 mm and 45 mm, respectively. Fig. VI.11 shows the calculated $\gamma(v)$ relationship in function of v in case of fire durations of 30 minutes, 60 minutes and 90 minutes.

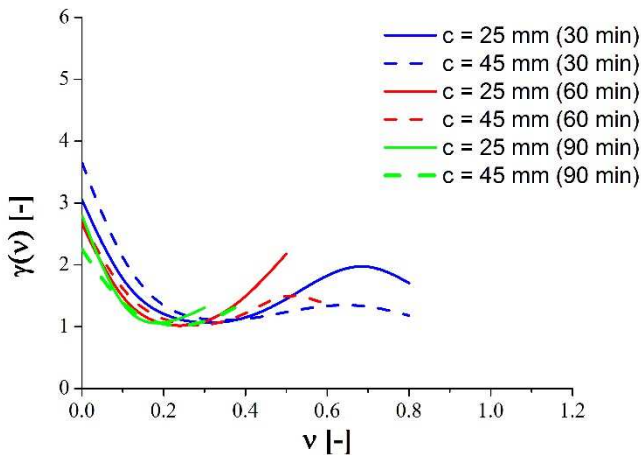


Fig. VI.11: Numerical values of coefficient $\gamma(v)$ for columns with different cover thickness in case of an ISO 834 fire of 30 min, 60 min and 90 min

Fig. VI.11 indicates that the column with a larger cover has larger fire resistance with respect to v . Also, this column with a larger cover presents a limited variability (in terms of $\gamma(v)$) with increasing axial load in case of fire. Further, it is observed that for both columns in case of fire, the value of $\gamma(v)$ is close to 1.0 when the value v is corresponding to the maximum moment contour (see section VI.5.2.(1)).

(6) Angle of the bending axis

Finally, comparisons are done to verify whether the value of $\gamma(v)$ in case of a symmetrically applied eccentric load could also be used for other biaxial bending situations at elevated temperatures. The values of $\gamma(v)$ obtained from columns No. 2 and No. 3 (Table VI.1) with an eccentric load $v = 0.4$ are considered here again with $\alpha_\mu = 60^\circ$ (see Table VI.5). The difference between the Bresler approximation and numerical values with respect to the maximum permitted eccentricities in the direction of the x-axis in case of an ISO 834 fire with duration 30 minutes and 60 minutes is compared in Table VI.5.

Table VI.5: Comparison of the Bresler approximation and numerical values on maximum permitted eccentricities in x-axis in case of fire

No.	Fire duration (min)	$\gamma(v)$	Eccentricity (cm)		Difference (%)
			Bresler approximation	Numerical calculation	
2	30	1.11	3.1	3.4	8.8
2	60	1.44	1.4	1.5	6.7
3	30	1.02	6.0	6.9	13
3	60	1.06	3.7	4.0	7.5

It is seen from Table VI.5 that $\gamma(v)$ proposed in case of the symmetric load can reasonably be adopted for other angles for the bending axis, as is the case for ambient conditions (Parme et al., 1966).

VI.6. Values of $\gamma(v)$ for different reinforcement ratios

From comparisons of an ISO 834 standard fire dependent parametric study, it is found that as in the case for ambient temperature, the reinforcement ratio as well as the number of reinforcing bars have an influence on $\gamma(v)$.

In order to provide comprehensive charts for biaxial bending design, columns subjected to 4-sided standard fire exposure in case of different reinforcement ratios and different reinforcing bars arrangement are investigated. It is verified by

computed values in (Parme et al., 1966) that interpolating the strength of the steel is feasible. Figs. VI.12 to VI.15 list the diagrams of $\gamma(v)$ and v in case of 4 reinforcing bars and the strength of the steel being 500 MPa for the reinforcement ratio 0.1, 0.5, 0.9 and 1.2 at a fire duration of 0 min (ambient temperature), 30 min, 60 min and 90 min.

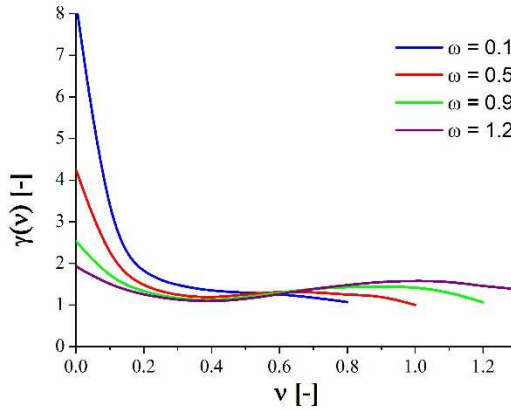


Fig. VI.12: Numerical values of coefficient $\gamma(v)$ for columns with different reinforcement ratios at ambient temperature (4 bars)

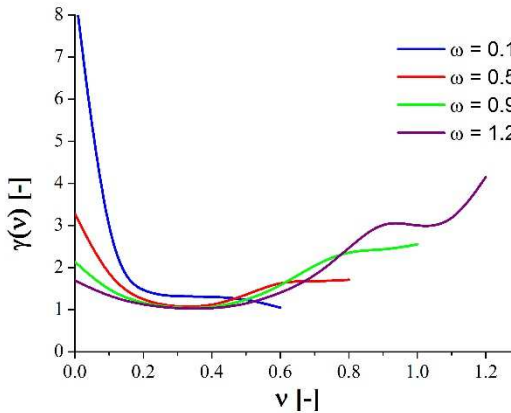


Fig. VI.13: Numerical values of coefficient $\gamma(v)$ for columns with different reinforcement ratios in case of an ISO 834 fire of 30 min (4 bars)

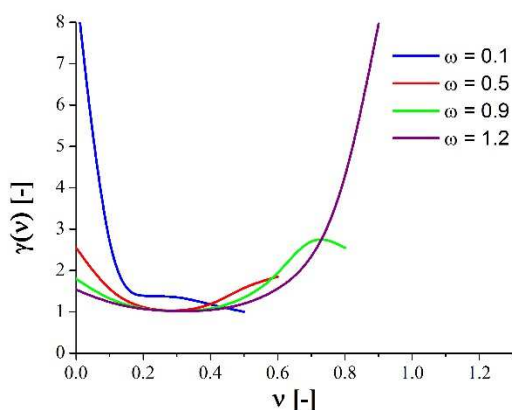


Fig. VI.14: Numerical values of coefficient $\gamma(v)$ for columns with different reinforcement ratios in case of an ISO 834 fire of 60 min (4 bars)

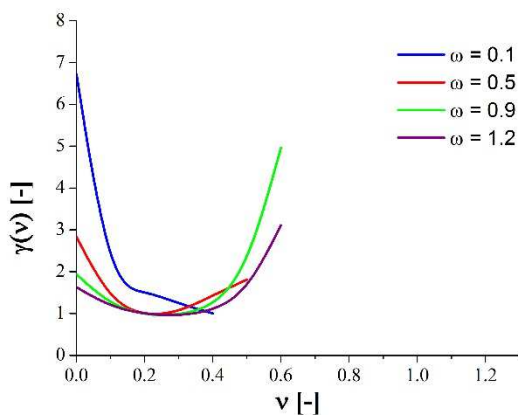


Fig. VI.15: Numerical values of coefficient $\gamma(v)$ for columns with different reinforcement ratios in case of an ISO 834 fire of 90 min (4 bars)

From Fig. VI.12 to Fig. VI.15, it is seen that the values of $\gamma(v)$ in case of steel strength 500 MPa, on the one hand, changes very slightly with fire when $v < 0.4$. Hence, a relevant interpolating curve could be given for the design of any rectangular column of 4 reinforcing bars taking into account biaxial bending combined with a 4-sided fire exposure. On the other hand, these values increase with fire when $v \geq 0.4$ in case of reinforcement ratios of 0.5, 0.9 and 1.2. Therefore, the value of $\gamma(v)$ in case of $v = 0.4$ could be adopted as a conservative design for $v \geq 0.4$ in case of a reinforcement ratio of no less than 0.5. Comparing the influence

of the reinforcement ratio, the lowest value $\gamma(v)$ of 1.0 is observed as a conservative design value of $\gamma(v)$ for columns of a reinforcement ratio between 0.5 and 1.2 in case of the respective value of axial loading v between 0.1 and 0.4 considering an ISO 834 fire duration of no more than 90 minutes.

Further, columns with 8 reinforcing bars respectively located in each corner and the middle of each side are investigated and the curves of $\gamma(v)$ are presented in Figs. VI.16 to VI.19. The results are also reported in Table VI.4.

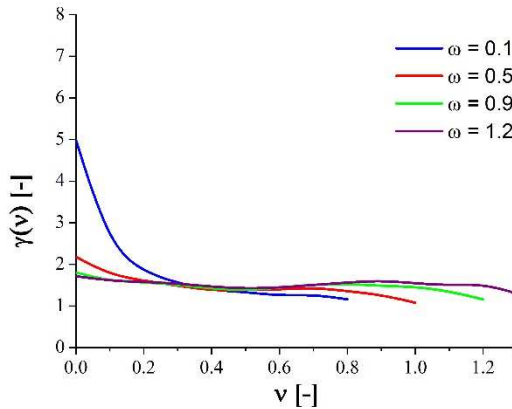


Fig. VI.16: Numerical values of coefficient $\gamma(v)$ for columns with different reinforcement ratios at ambient temperature (8 bars)

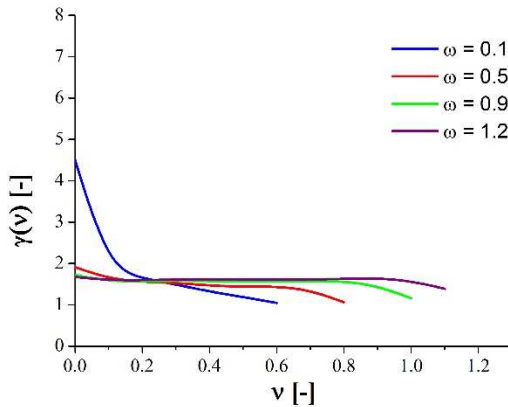


Fig. VI.17: Numerical values of coefficient $\gamma(v)$ for columns with different reinforcement ratios in case of an ISO 834 fire of 30 min (8 bars)

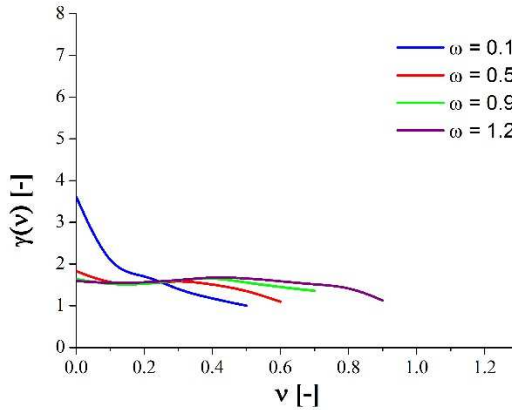


Fig. VI.18: Numerical values of coefficient $\gamma(v)$ for columns with different reinforcement ratios in case of an ISO 834 fire of 60 min (8 bars)

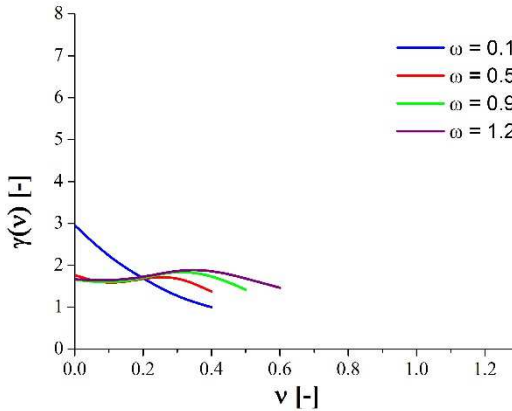


Fig. VI.19: Numerical values of coefficient $\gamma(v)$ for columns with different reinforcement ratios in case of an ISO 834 fire of 90 min (8 bars)

Fig. VI.16 to Fig. VI.19 present the values of $\gamma(v)$ for columns with 8 reinforcing bars in case of different axial loads and fire durations. It is observed that the fire duration as well as the axial load has less significant influence on the values of $\gamma(v)$ than on those in case of 4 reinforcing bars. It is worth pointing out that the value of $\gamma(v)$ shown in Figs. VI.16 to VI.19 changes between 1.05 and 1.75 when v is not less than 0.1 in case of a reinforcement ratio 0.5, 0.9 and 1.2, while it changes comparatively sharply in case of a reinforcement ratio 0.1.

Above all, the calculation tool has been validated with experimental data from Tan & Nguyen (2013) and has been adopted to develop the application of the Bresler approximation to biaxial bending for fire exposure by taking into account a parametric study. However, differences due to initial imperfections on configurations, cover thickness, as well as the common variability in the concrete compressive strength might cause significant differences to interaction diagrams. Therefore, a probabilistic evaluation is required as to evaluate the safety of concrete columns during fire exposure. In the last part of this chapter, a case study is investigated using the developed calculation taking into account the structural uncertainties.

VI.7. Uncertainty quantification of columns subjected to biaxial bending combined with fire in the framework of structural reliability-based design

VI.7.1. Principles of limit states design

Limit state design requires the structure to satisfy two principal criteria (EN 1990, 2002): ultimate limit state (ULS) and serviceability limit state (SLS). The ultimate limit state is reached when the applied stresses actually exceed the strength of the structure or structural elements causing it to fail or collapse (i.e. inadequate strength) while the serviceability limit state is reached when a structure or structural members cannot remain functional for its intended uses during normal use (i.e. deflections, vibrations, etc). As the investigations in this chapter related to structural safety, only ultimate limit states will be investigated further.

In relation to the ultimate limit state, it is required that the resistance R is larger than the load effect E . For practical applications, however, the resistance R and the load effect E are mostly based on (simplified) models. As a result, errors or overestimations might be present when determining R and E . Hence, uncertainties K_R for the resistance effect and K_E for the load effect have to be considered (Ditlevsen & Madsen, 1996). The strength criterion of the ultimate limit state can be represented by the ultimate limit function Z (Eq. (VI.8)), where the strength criterion is met only if $Z \geq 0$.

$$Z = K_R R - K_E E \quad (\text{VI.8})$$

VI.7.2. Reliability index β

EN 1990 (2002) states that in Level II procedures, an alternative measure of reliability is conventionally defined by the reliability index β which is related to P_f by:

$$P_f = \Phi(-\beta) \quad (\text{VI.9})$$

where β is the target reliability index

Target values for the reliability index β for various design situations and for reference periods of 1 year and 50 years, are indicated in Table VI.6. The values of β in Table VI.6 correspond to levels of safety for reliability class RC2 structural members (associated with medium consequences for loss of human life, economic, social or environmental consequences considerable).

Table VI.6: Target reliability index β for Class RC 2 structural members

Limit state	Target reliability index	
	1 year	50 years
Ultimate	4.7	3.8
Fatigue		1.5 to 3.8
Serviceability (irreversible)	2.9	1.5

In the reliability-based design value method, design values need to be defined for all the basic variables. A design is considered to be sufficient if the limit states are not reached when the design values are introduced into the analysis models. In symbolic notation this is expressed as :

$$E_d < R_d \quad (\text{VI.10})$$

where the subscript 'd' refers to design values; E is the action effect and R is the resistance. This is the practical way to ensure that the reliability index β is equal to or larger than the target value.

It is worth mentioning that the design values of action effects E_d and resistances R_d can be defined as follows (EN 1990, 2002):

$$P(E > E_d) = \Phi(+\alpha_E\beta) \quad (\text{VI.11})$$

$$P(R \leq R_d) = \Phi(-\alpha_R\beta) \quad (\text{VI.12})$$

where β is the target reliability index

α_E and α_R are the values of the FORM sensitivity factors. The value of α is negative for unfavourable actions and action effects, and positive for resistances. α_E and α_R may be taken as -0.7 and 0.8, respectively. This gives:

$$P(E > E_d) = \Phi(-0.7\beta) \quad (\text{VI.13})$$

$$P(R \leq R_d) = \Phi(-0.8\beta) \quad (\text{VI.14})$$

VI.7.3. A case study taking into account uncertainties

A probabilistic analysis is performed to investigate the effect of the variability of the basic model parameters. The same cross-section is considered as in the parameter study, with probabilistic models for the basic variables as given in Table VI.7, in accordance with (Holický & Sýkora, 2010) and JCSS (2007). As in (Van Coile, 2015), the reduction factors at elevated temperatures for the concrete compressive strength and the reinforcement yield stress are modelled by a Beta distribution where the mean value is taken as the nominal value given in EN 1992-1-2 (2004).

Table VI.7: Probabilistic models for basic variables, based on (Holický & Sýkora, 2010) and JCSS (2007): property, dimension, distribution, mean value μ , standard deviation σ and coefficient of variation V .

Property	Dim	Dist	μ	σ	V
20°C concrete compressive strength $f_{c,20}$ ($f_{ck} = 55$ MPa)	MPa	LN	$\frac{f_{ck}}{1-2V_{fc}}$	$\mu \cdot V$	0.15
20°C reinforcement yield stress $f_{y,20}$ ($f_{yk} = 500$ MPa)	MPa	LN	$\frac{f_{yk}}{1-2V_{fy}}$	$\mu \cdot V$	0.07
Concrete compressive strength reduction factor $k_{fc}(\theta)$ at temperature θ	-	Beta	EN 1992-1-2	$\mu \cdot V$	(Van Coile, 2015)
Reinforcement yield stress reduction factor $k_{fy}(\theta)$ at temperature θ	-	Beta	EN 1992-1-2	$\mu \cdot V$	(Van Coile, 2015)
Concrete cover c	mm	Beta	25	5	σ/μ
Column width z	mm	DET	Z_{nom}	300	-

Regarding the ultimate limit state and probability of failure of structural members at ambient temperature, a target reliability index $\beta_{t,50}$ of 3.8 is adopted when considering a 50 year reference period (see Table VI.6). Hence, based on Eq. (VII.12), the curve of $(R \leq R_d) = \Phi(-0.8 * 3.8) = 0.12\%$ is used for reliability design at ambient temperature here.

In the present study, 10000 Monte Carlo simulations of the interaction diagram are evaluated. The variability of the obtained first-order interaction diagram can be visualized by the 5, 50, and 95 percentiles. This is applied in Fig. VI.20 as well as the curve of $P(R \leq R_d) = 0.12\%$ for ambient temperature (i.e. prior to fire), in Fig. VI.21 for 30 minutes of ISO 834 standard fire exposure and in Fig. VI.22 for 90 minutes of ISO 834 standard fire exposure. In all the figures, a comparison is made with the interaction diagram obtained when considering characteristic values for the basic parameters (designated as the reference interaction diagram), i.e. f_{ck} for the concrete compressive strength, and f_{yk} for the reinforcement yield stress, with $n = \frac{N_c + N_s}{0.7(A_c f_{cd} + A_s f_{yd})}$ and $m = \frac{M_c + M_s}{0.7(A_c f_{cd} + A_s f_{yd})h}$, where N_c , M_c , N_s , M_s are the maximum axial forces and bending moments respectively for concrete and reinforcement, b is the width of the column and h is the height of the cross-section.

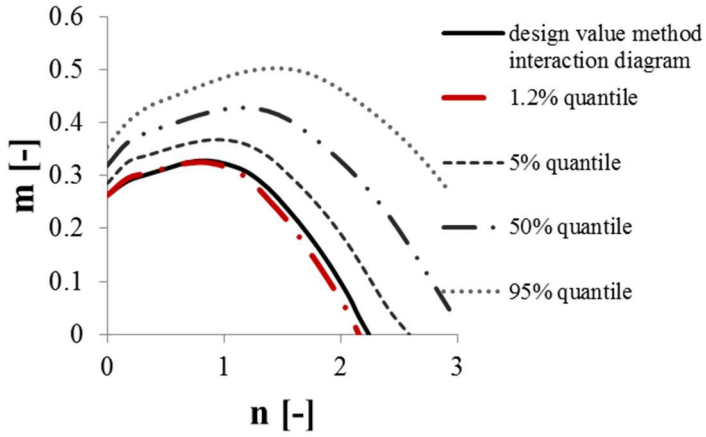


Fig. VI.20: Interaction diagrams of a column at ambient temperature considering a probabilistic analysis according to the variables mentioned in Table VI.7

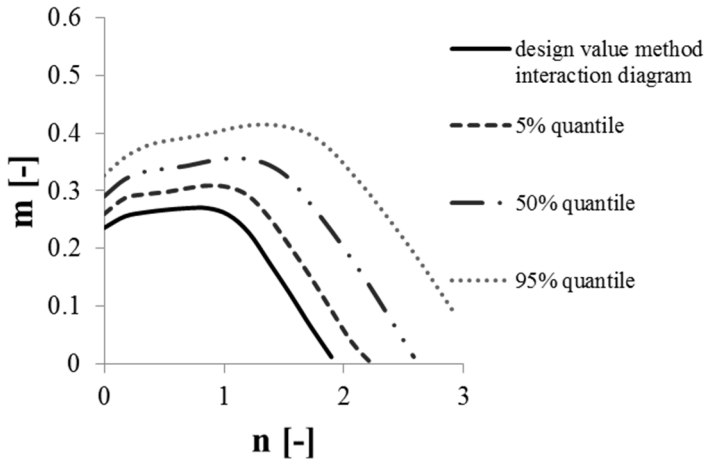


Fig. VI.21: Interaction diagrams of a column exposed to an ISO 834 fire of 30 minutes considering a probabilistic analysis according to the variables mentioned in Table VI.7

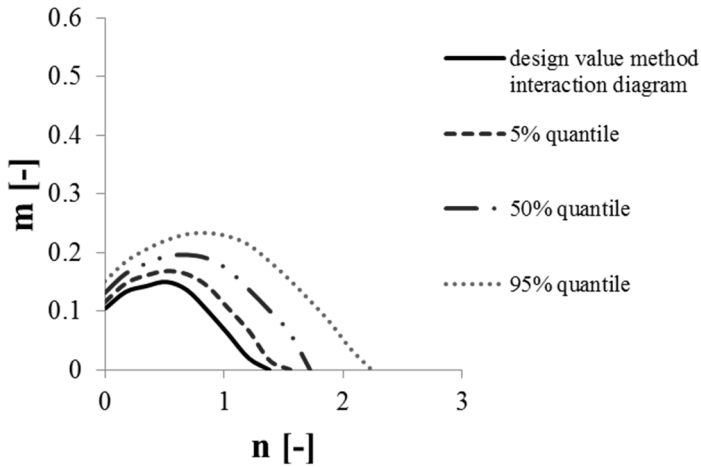


Fig. VI.22: Interaction diagrams of a column exposed to an ISO 834 fire of 90 minutes considering a probabilistic analysis according to the variables mentioned in Table VI.7

Based on the results presented in Fig. VI.20, Fig. VI.21 and Fig. VI.22, it is clear that a very large variability exists with respect to the interaction diagrams for concrete columns subjected to biaxial bending, both at ambient conditions and during fire exposure. The comparison of the percentiles (i.e. 5%, 50% and 95% curves) with the full line representing the nominal calculation in accordance with the normal Eurocode design methodology indicates that the interaction diagram adopting material and mechanical properties provided by Eurocode 2 (2004) is situated below the 5% curve. This is in good agreement with the semi-probabilistic design concept of the Eurocodes where the design value should correspond with a low quantile of the resistance effect. Furthermore, compared to the 1.2% curve in Fig. VI.20, the design value method interaction diagram at ambient temperature is slightly higher only when the respective value of n is more than 0.7. It proves that the design value method interaction diagram obtained with the calculation tool corresponds well with the reliability-based design target related to ultimate limit state and probability of failure of structural members (EN 1990, 2002). However, when calculating the observed quantile of the stochastic interaction diagram which corresponds with the analytical value of the Eurocode design methodology in case of an ISO 834 standard fire, a quantile of 0.20% at 30 minutes (Fig. VI.21) and a quantile of 0.21% at 90 minutes of an ISO 834 fire exposure (Fig. VI.22) are obtained based on the calculation tool.

Further, the second-order effects of columns are taken into account. The interaction diagrams associated to different lengths of columns (3 meters and 4 meters) exposed to fire durations of 30 minutes are presented in Fig. VI.23 and Fig. VI.24, respectively.

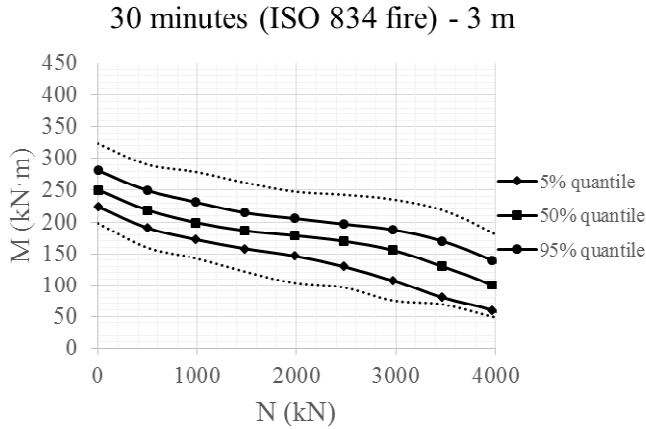


Fig. VI.23: Interaction curves of a column (3 meters long) exposed to an ISO 834 fire of 30 minutes including uncertainties and second-order effects

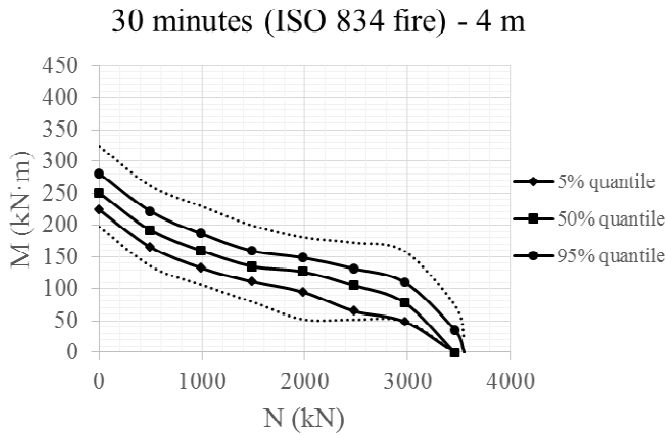


Fig. VI.24: Interaction curves of a column (4 meters long) exposed to an ISO 834 fire of 30 minutes including uncertainties and second-order effects

In Fig. VI.23 and Fig. VI.24, it is observed that the bending moment capacity decreases with increasing axial load. Unlike interaction diagrams of the cross-section shown in Fig. VI.21 and Fig. VI.22, the range of the moment capacity varies slightly with increasing axial load. Further, the 4 meters long column fails around 3500 kN while the 3 meters long column could bear more than 4000 kN axial load.

The similar interaction curves of these columns in case of a 90 minute standard fire exposure for a column length of 3 meters, and 4 meters are shown in Fig. VI.25 and Fig. VI.26, respectively.

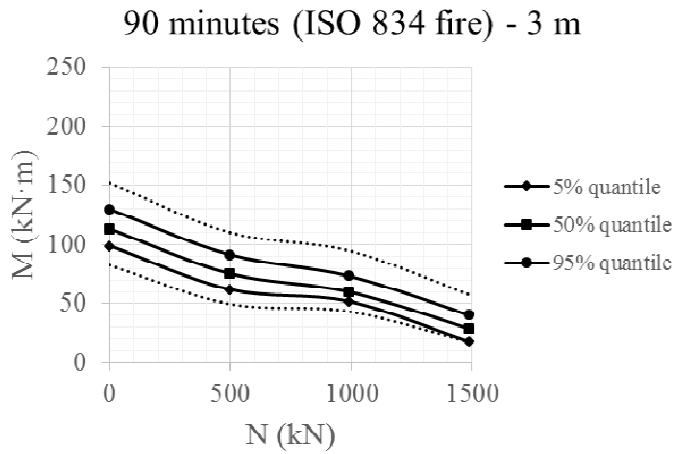


Fig. VI.25: Interaction curves of a column (3 meters long) exposed to an ISO 834 fire of 90 minutes including uncertainties and second-order effects

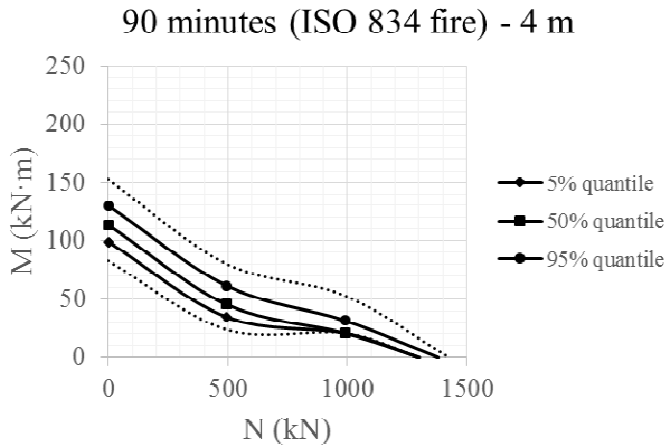


Fig. VI.26: Interaction curves of a column (4 meters long) exposed to an ISO 834 fire of 90 minutes including uncertainties and second-order effects

The same phenomenon is observed as in case of 30 minutes fire exposure, i.e. the bending moment capacity keeps decreasing with increasing axial load for both of the columns in case of a fire duration of 90 minutes. For both of the columns, the moment capacity firstly drops significantly below an axial load of 500 kN. Then, the decrease reduces between an axial load of 500 kN and 1000 kN. Finally, the moment capacity decreases significantly until the columns fail. This decrease on the moment capacity is more significant than that in case of a 30 minutes fire exposure.

Finally, considering different axial loads, the 5% quantile, 50% quantile and 95% quantile maximum permitted eccentricities for the investigated columns of 3 meters and 4 meters lengths are determined in case of fire durations of 30 minutes and 90 minutes. The results are provided in Table VI.8 and Table VI.9, respectively.

Table VI.8: The 5% quantile, 50% quantile and 95% quantile maximum permitted eccentricities for the investigated columns in case of a fire duration of 30 minutes

Case	Maximum permitted eccentricity (mm)														
	N = 495 kN			N = 990 kN			N = 1485 kN			N = 1980 kN			N = 2475 kN		
quantile length (m)	5%	50%	95%	5%	50%	95%	5%	50%	95%	5%	50%	95%	5%	50%	95%
3	38.2	43.9	50.1	17.1	19.8	23.1	10.3	12.2	14.1	7.1	8.7	10.1	4.9	6.6	7.6
4	33.1	38.5	44.4	13.1	15.8	18.5	7.1	8.7	10.3	4.4	6.0	7.1	2.2	3.8	4.9

Table VI.9: The 5% quantile, 50% quantile and 95% quantile maximum permitted eccentricities for the investigated columns in case of a fire duration of 90 minutes

Case	Maximum permitted eccentricity (mm)								
	N = 495 kN			N = 990 kN			N = 1485 kN		
quantile length (m)	5%	50%	95%	5%	50%	95%	5%	50%	95%
3	12.2	14.9	18.2	4.9	5.7	7.1	1.2	2.0	2.7
4	6.6	8.7	12.0	1.7	1.7	2.8	—	—	—

VI.8. Conclusions

Bresler (1960) and Parme et al. (1966) proposed verified curves for biaxial bending design constants at ambient temperature. The current research extends the applicable range of the Bresler method to fire exposure. After a parametric study on the values of $\gamma(v)$, it is concluded that:

(1) $\gamma(v) = 1.0$ is an acceptable approximate value when the relative axial force $v > 0.4$ at ambient temperature. As a conservative consideration, this value 1.0 can be adopted for all the axial forces at ambient temperature.

(2) Due to the reduction of the material strength as well as the stiffness of columns in case of fire, the load capacity of columns decreases with fire. $\gamma(v)$ is mainly situated between 1.00 ~ 2.00 at elevated temperatures. However, as at ambient temperature, a range of 1.00 ~ 1.50 is also recommended for $\gamma(v)$ in case of fire when $v = 0.15 \sim 0.4$. Furthermore, a conservative value 1.00 can be used for $\gamma(v)$ while a larger value is only possible for specific situations in case of fire, for which some guidance however can be found in the results reported in this chapter.

(3) Based on parametric studies at ambient temperature as well as in case of fire, $\gamma(v) = 1.0$ can be applicable for other column dimensions, reinforcement arrangements and reinforcement ratios as a conservative simplification. However, as mentioned this work also presents less conservative results for several specific situations.

Furthermore, based on the evaluation of the developed calculation tool taking into account uncertainties, it is concluded that:

(1) Comparing the design value method interaction diagram with the probabilistic evaluation at ambient temperature, it is seen that they are in good agreement. Although there is no explicit target reliability available for the case of fire, the tool is an important step to evaluate the Eurocode reliability performance during fire.

(2) The second-order effects are more pronounced with increasing fire duration and with increasing slenderness ratio. Taking into account the uncertainties associated with the column characteristics, the results show that the range of the cross-sectional moment capacity changes significantly for different axial loads while the

standard deviation of the moment capacity of columns varies less significantly when second-order effects are considered.

CHAPTER VII

GENERAL DISCUSSIONS , CONCLUSIONS & FUTURE RESEARCH

VII.1. General discussions

With respect to concrete columns exposed to fire, guidelines for the fire resistance design are provided by Eurocode 2 (2004). However, the design values for concrete columns given in Eurocode 2 (2004) are proven to be not always on the safe side comparing with experimental data. In order to enable a quantitative analysis, an efficient and easy-to-use calculation tool is required. For such a purpose, a cross-sectional calculation method has been developed to investigate the behaviour of concrete columns exposed to fire taking into account second-order effects. Based on our work which is presented in this book, advantages, drawbacks as well as the application of the calculation tool are discussed.

VII.1.1. Eurocode-based and easy-to-use calculation tool for the temperature distribution of concrete columns

The calculation tool includes two main parts, i.e. a thermal analysis and structural analysis. For the thermal analysis, the temperature calculation is based on Fourier's law for conduction, Newton's law for convection and Stefan-Boltzmann's law for radiation (**chapter III**). Furthermore, the thermal conductivity, the specific heat as well as the density are all based on either theoretic or experimental results provided by Eurocode 2 (2004). Hence, it is believed that the basis of the calculation tool for the thermal analysis has a sound basis. Moreover, the temperature distributions obtained with the tool in case of an ISO 834 standard fire for different fire durations are verified with those provided by Eurocode 2 (2004). Finally, based on the same method, the calculation tool can be implemented for columns of different dimensions and the most common cross-sectional shapes (rectangular, circle) in case of all types of fire.

The cross-sectional calculation tool for thermal analysis is easy-to-use, efficient and applicable a wide range of applications. Take a rectangular concrete column for instance, the calculation tool can be adopted not only for four-face heated exposure, but also for any set of heated face exposures. As a result, the temperature distribution can be obtained if the parameters such as fire curves, dimensions of columns, mesh sizes, the type of aggregates, moisture contents and concrete densities are given.

With respect to parametric studies, the calculation tool is not only limited to a specific column configuration or a standard fire but it can also be adopted for columns with different properties and in case of standard fires as well as parametric fires. For example, analyses based on parametric fires such as hydrocarbon fires and natural fires are presented in **chapter IV**. Furthermore, the mesh sizes, the type of aggregates, moisture contents as well as concrete densities are required to obtain the temperature distribution of columns. For these parameters, the relevant equations given in Eurocode 2 (2004) are adopted. Considering the mesh of the cross-section, it has an influence on the accuracy of the temperature distribution. A 1 mm×1 mm square was selected as a basic calculation element for all the calculations. Comparing the calculated results with the temperature distributions provided by Eurocode 2 (2004) in case of different fire durations, it shows that they are in good agreement. It is worth mentioning that there is no generally accepted calculation method for considering spalling at the moment. However, Eurocode 2 (2004) states that explosive spalling is unlikely to occur when the moisture content of concrete is less than 3%. With an assumption of the moisture content of concrete less than 3%, spalling is not specifically considered in the calculation tool (Wang et al., 2015).

Based on the tool, the temperature distribution of cross-sections (rectangular, circle) in case of an ISO 834 fire for different fire exposures are presented in **chapter III** and **chapter IV**. Further, the temperature differences adopting different thermal conductivity curves (the upper limit and the lower limit curves) are shown in **chapter IV**. Finally, the application of the tool is expanded to hydrocarbon fires and natural fires (**chapter IV**).

With respect to the consecutive second-order calculations, the cross-sections of columns are assumed to be uniform along the length of the column. Non-uniformed heating along the length of the column is not considered herein. However, this could be an interesting topic for the further research.

VII.1.2. Efficient tool to improve the current simplified methods

In order to obtain the fire resistance of concrete columns in an easy way, simplified methods are provided in the standards. For example, simplified cross-sectional calculations can be used to determine the ultimate load-bearing cross-sectional capacity and to compare the capacity with the relevant combination of actions (Eurocode 2, 2004). For such a purpose, two alternative methods are provided by Eurocode 2 (2004), i.e. the 500°C isotherm method and the zone method. The

interaction curves obtained with the 500°C isotherm method and the numerical calculation tool are compared in **chapter V**. It is observed that the 500°C isotherm method can generally predict the fire resistance of columns. However, it is not suitable when the fire lasts 90 minutes or more in case of an ISO 834 standard fire. Hence, a parametric study has been performed with the calculation tool and a higher isotherm temperature is recommended for the fire resistance design.

The 500°C isotherm method and the zone method concern the ultimate load-bearing capacity at the cross-sectional level. However, second-order effects of concrete columns have an important effect in case of fire. Regarding second-order effects, the most used simplified methods—the curvature method and the stiffness method—are introduced in **chapter II**. However, these two methods provided by Eurocode 2 (2004) are not explicitly explained to be used in case of fire. Hence, the developed calculation tool was applied to investigate the interaction diagrams of concrete columns during fire and assess the applicability of the simplified methods. In **chapter V**, the results are compared with those obtained with the stiffness method and KLE method (NEN, 1995), respectively. Comparing with the numerical simulations, the stiffness method is too conservative in case of fire while the KLE method is slightly on the unsafe side. Suggestions are given to improve these simplified methods.

In addition, Eurocode 2 (2004) suggests to consider imperfections as an initial eccentricity. Based on the calculation tool, a parametric study on the effect of imperfections is discussed in **chapter V**. It is concluded that no matter whether the columns are at ambient temperature or exposed to fire, the imperfections have significant effects on the load capacity of columns under compression. Furthermore, the resistance without considering imperfections could be overestimated by a factor 2 compared to the case when considering imperfections at elevated temperatures. Hence, it is important to take imperfections into account.

Above all, the most used simplified methods provided by standards are discussed and compared with the numerical results. Based on the comparisons, suggestions are given for these simplified methods in order to have better results for the fire resistance design of concrete columns.

VII.1.3. Extension of tabulated design guidelines for rectangular columns exposed to fire

In EN 1992-1-2 (2004), tabulated data is provided for assessing columns in braced structures with a width up to 600 mm and a slenderness ratio up to 80 for a standard fire exposure. However, the guidelines are not always on the safe side comparing with experimental results from the Technical University of Braunschweig (Hass, 1986). Hence, these tabulated values have been investigated.

The numerical calculation tool is firstly verified with experimental data in **chapter III**. Then, the tabulated tables are recalculated considering the same columns with a width up to 600 mm and a slenderness ratio up to 80 in case of an ISO834 standard fire. Furthermore, more tables are established in case of hydrocarbon fires and natural fires (**chapter IV**).

Based on the recalculated and extended tabulated data, a minimum dimension, a minimum slenderness ratio as well as a minimum concrete cover thickness can be obtained for the fire design if the type of fire and the fire duration are given. It is worth mentioning that these tables are suitable for the most common columns in case of a standard fire and a hydrocarbon fire. However, due to the fact that a simplification on the stress-strain relationship is assumed for the cooling down branch in case of natural fires, a range instead of a design value is given. Besides, as the natural fire curves depend on the fire density, the opening factor, time, etc., an interpolation is not very appropriate for such cases.

VII.1.4. Design of concrete columns subjected to biaxial bending in case of fire

Simplified methods provided by standards are discussed in the first five chapters. However, these methods are mainly used for columns exposed to uniaxial bending at ambient temperature and in case of fire. In EN1992-1-1 and ACI318, a simplified method for the design of columns is provided for evaluating the structural capacity in case of biaxial bending. This so-called Bresler approximation was originally proposed by Bresler (1960). Based on a parametric study with the calculation tool, the Bresler approximation is discussed in **chapter VI**. Suggestions are given for adopting this formula to analyse columns exposed to biaxial bending in case of fire. Hence, the application of this method is extended to be used in case of fire.

Currently, the Bresler approximation is only investigated in case of an ISO 834 standard fire in the thesis. The numerical calculation tool, however, can also be

used for parametric fires. Although the examples which are given in **chapter VI** are mostly for columns with a square cross-section in case of a symmetrical biaxial load ($\alpha_{\mu} = 45^{\circ}$), the angle of the bending axis is discussed in the last part of the chapter. It is proven that $\gamma(v)$ proposed in case of the symmetric load can reasonably be adopted for other angles for the bending axis, as is the case for ambient conditions (Parme et al., 1966). Columns subjected to different fire exposures are not discussed herein, although the basic calculation method is the same.

VII.1.5. Probabilistic analysis of biaxial bending of columns in case of fire

Commonly the design value of the load capacity of concrete columns in case of fire is obtained from a single calculation if all the geometrical and material properties are considered. However, when one or more of the material or geometrical properties, or the actions on the structure are of a stochastic nature, the response of the structure cannot be determined with certainty (Benjamin & Cornell, 1970). So they are on structural members. Hence, a probabilistic analysis is needed in order to quantify the structural reliability performance.

The calculation tool was extended with probabilistic models for evaluating interaction diagrams of columns in case of fire. The curves of a most common used cross-section are presented in **chapter VI**. Based on the calculation, the influence of the length limit of columns, the applied axial load and the maximum permitted eccentricity in case of an ISO 834 fire is discussed.

In the thesis, only one typical cross-section was investigated for the time being due to the fact that the probabilistic calculations performed are time-consuming. In the future, the influence of more parameters should be investigated.

VII.2. Conclusions

Chapter I gives a brief introduction on the development of the research of concrete structures and the behaviour of concrete structures in case of fire. The literature research covers the subjects of material properties, mechanical properties, spalling, fire type, simplified methods, experiments as well as analytical methods. Based on the literature study, contemporary research challenges with respect to the fire resistance design in case of concrete columns exposed to fire are identified. In

conclusion, the most urgent work is to find an easy-to-use tool to investigate interaction curves of columns in case of fire. Therefore, the thesis presents a numerical calculation tool to accommodate for this.

Further in **chapter II**, simplified methods are explained and discussed. An example is given comparing the general method, the stiffness method and the curvature method. It is shown that both the stiffness method and the curvature method show a rather wide scatter when compared to the general method. However, the curvature method predicts comparatively reasonable results for low to moderate slenderness, although the prediction is too conservative in case of high slenderness ratios. Finally, second-order effects are considered adopting the equivalent stiffness. It is concluded that simplified methods may be adopted to predict interaction curves of columns in case of ambient temperature and fire. However, these predictions are sometimes either unsafe or too conservative.

In order to find an efficient way to obtain interaction curves of columns exposed to fire, **chapter III** presents a cross-section based calculation tool. Comparing with experimental data, this tool is proven to be applicable for predicting interaction curves, deflections as well as the fire resistance of columns in case of fire. Based on a parametric study with the calculation tool, the influence of the fire duration, the dimensions, the reinforcement ratio, the axial compression ratio, the eccentricity, the concrete cover thickness as well as the slenderness ratio on the capacity of columns is investigated. It is concluded that the fire duration, the cover thickness as well as the slenderness ratio have significant influences on the behaviour of columns in case of fire. It is worth mentioning that the fire resistance decreases sharply with increasing length (slenderness ratio) of columns. Therefore, second-order effects should be considered as very important for the fire resistance calculation of columns.

In **chapter IV**, different fire scenarios are discussed. First, the minimum dimensions of columns in case of ISO 834 standard fire are recalculated and some comparisons with experimental results are provided in order to validate the obtained calculation tool. It is found that, on the one hand, Eurocode provisions are not safe for the case of a reinforcement ratio equal to 0.1 or reinforcement ratio of 0.5 when the axial load is large. On the other hand, tabulated data is found to be too conservative for high reinforcement ratios ($\omega = 1.0$), which results in inefficient and uneconomical solutions for practice. Furthermore, hydrocarbon fires and natural fires are investigated. Comparing the results for the hydrocarbon fire with

the tables obtained for the ISO 834 standard fire, it is noted that fire resistance to the hydrocarbon fire may result in very stringent requirements. Finally, with respect to natural fires, the results prove that second-order effects are insignificant when the normal force is low. When the eccentric loads are large enough, the maximum bending moment of the column firstly decreases continuously during the fire, and then shows a slight increase at a certain point during the cooling phase.

The interaction curves obtained with the simplified methods are compared with those from the calculation tool and presented in **chapter V**. It is concluded that these simplified methods are efficient to predict the fire resistance of columns. First, the 500°C isotherm method is suitable for small cross-sections (less than 200 mm × 200 mm) or columns with exposure times of more than 90 minutes to the standard ISO 834 fire. Secondly, the nominal stiffness method is proven to be safe for the design of columns. However, the interaction curves obtained with the nominal stiffness method are too conservative in case of slender columns. On the contrary, the capacity calculated with the KLE-method provided by the Dutch code (NEN, 1995) is slightly on the unsafe side. Thirdly, imperfections cannot be neglected for slender columns considering second-order effects. Based on the parametric study, fire durations and eccentricities have important influences on the effect of imperfections. The slenderness ratios as well as dimensions of the cross-section have a significant effect on the effect of imperfections. Finally, regarding to the curvature approximation, only the slenderness ratio has a significant influence on the prediction of the second-order effects with the proposed simplified formula.

Chapter VI extends the application of the Bresler approximation from ambient temperature to fire. After a parametric study on the values of $\gamma(v)$, it is seen that $\gamma(v)$ is mainly situated between 1.00 ~ 2.00 at elevated temperatures. However, as at ambient temperature, a range of 1.00 ~ 1.50 is also recommended for $\gamma(v)$ in case of fire when $v = 0.15 \sim 0.4$. Furthermore, a conservative value 1.00 can be used for $\gamma(v)$ while a larger value is only possible for specific situations in case of fire. Based on parametric studies at ambient temperature as well as in case of fire, $\gamma(v) = 1.0$ can be applicable for other column dimensions, reinforcement arrangements and reinforcement ratios as a conservative simplification. Finally, a probabilistic study is discussed. The second-order effects are taken into account to investigate the influence of the column length, the applied axial load and the maximum permitted eccentricity in case of an ISO 834 fire. As the Monte Carlo simulation procedure developed is computationally expensive at this stage, only

one of the most common cases, i.e. a cross-section of 300 mm × 300 mm, is investigated.

Above all, the numerical tool presented herein is proven to be a valid, easy-to-use and efficient tool. Most importantly, it easily enables quantitative analyses and provides references to compare with experiments and simulations for the fire resistance of concrete columns. Furthermore, a calculation tool such as elaborated herein enables practicing engineers to achieve more accurate results than those obtained with the simplified methods.

VII.3. Future work

Regarding the fire safety of concrete columns, this dissertation provides proposals for the fire resistance design for both uniaxial bending and biaxial bending. The current work, on the one hand, is validated with experimental data and the current simplified methods. On the other hand, it extends the currently available simplified methods which were adopted at ambient temperature to be used in case of fire and it provides proposals for the methods which were used in case of fire to be more efficiently and more accurately used for fire resistance design. At the moment, the calculation tool developed can be easily adopted for the fire resistance design of concrete structural members. This tool could be further developed into a web based application. In future research, this tool can also be further developed to be used in a Direct Stiffness Method for the analysis of multi-span frames.

VII.3.1. Generalization of conclusions by more simulations

A large number of simulations have been done in this dissertation in order to obtain validated proof for the fire design proposals and also give more general and convincing conclusions. Further, a generalization of conclusions can possibly be obtained by performing more calculations, for example evaluating the behaviour of the fire resistance of columns by changing the range of different parameters.

VII.3.2. Analysis of super columns subjected to fire

With respect to the design of high-rise buildings, often super columns are applied. These types of columns are commonly using high-performance concrete and a large number of reinforcement bars or steel profiles which are more significantly affected in case of fire. Furthermore, the calculation of these super columns is more

complicated and requires several adaptations of the calculation tool. Evaluating the behaviour of these columns in case of fire is a topic of great importance.

VII.3.3. Investigation of concrete column spalling

With respect to concrete columns subjected to fire, spalling is one of the most discussed topics. Although a number of calculation tools have been introduced in literature, there exists no generally accepted calculation method to describe practically the phenomenon of spalling. Apparently, spalling is very difficult to simulate but important for fundamental research. The effects of spalling on the performance of columns can be very significant for columns with a moisture content more than 3%.

VII.3.4. Optimizing calculation for concrete columns taking into account uncertainties

Based on the evaluation of the fire performance of concrete columns, a probabilistic analysis is taken into account and presented in **chapter VI**. At the moment, it consumes a lot of time to finish a single set of calculations. Optimizing these probabilistic calculations is required in order to allow for more calculations in order to determine the safety level of columns exposed to fire.

VII.3.5. Post-fire strength assessment of fire damaged concrete columns

Concrete columns can still bear some loads after fire exposure. It is possible to evaluate whether the fire damaged concrete columns can still be kept in the structure and what is its remaining lifetime.

VII.3.6. Investigation on real-life fires

The heat flux is a very complicated phenomenon. To the best of the author's knowledge, there barely exists any simple models which can accurately capture effects of the heat flux of real-life fires on concrete members. Therefore, most often an engineering approach is applied to investigate the real-life fire. In this thesis, such assumptions are made to simplify the heat flux for the structural analysis, i.e. by simplifying the fire to a temperature-time curve, assuming the entire compartment is filled with fire gases of uniform temperature, etc. However, the gas temperatures which can be measured in the experiments and real cases could also be adopted in the model in order to investigate the differences between the assumed idealized fires and the real-life fires.

VII.3.7. Investigation on the total amount of heat transferred into the material

In this thesis, the interaction curves of concrete columns are based on the temperature-time curves, and hence the obtained fire resistance of columns is given in function of the fire duration. In future research, it can also be considered to provide the results in terms of the total amount of heat transferred into the material. As such, one can investigate the consequence of using different temperature-time curves or different materials and properties, considering the same total amount of heat transferred.

REFERENCES

Abrams M. S. "Behaviour of inorganic materials in fire." *ASTM special publication 685, symposium on design of buildings for fire safety, Boston (MA), 1978.*

Achenbach M., Morgenthal G. "Extension of the zone method of Eurocode 2 for reinforced concrete columns subjected to standard fire." *Journal of Structural Fire Engineering, 2015.*

ACI 318-11: Building Code Requirements for Structural Concrete and Commentary, *American Concrete Institute, 2011.*

ACI Committee 318-71, "Building Code Requirements for Reinforced Concrete." (ACI 318-71), *American Concrete Institute, Detroit, 1971.*

Albrecht C., Hosser, D. "Risk-informed framework for performance-based structural fire protection according to the eurocode fire parts." *Proc. of the 12th Interflam Conference, Nottingham, 2010 ,(5-7/07), 1031-1042.*

Anderberg Y. "Analytical fire design of reinforced concrete structures based on real fire characteristics." *CEB/FIP 8th Congress Proceedings, Part 1, London 1978.*

Anderberg Y. "Mechanical Properties of Reinforcing Steel at Elevated Temperatures," *Tekniska Meddelande, Sweden, 36, 1978.*

Anderberg Y. "Modelling steel behaviour." *Fire Safety Journal, 13(1), 17–26, 1988.*

Anderberg Y., Thelandersson S. "Stress and deformation characteristics of concrete at high temperatures: 2. Experimental investigation and material behavior model." *Lund Institute of Technology, 1976.*

Annerel E. "Assessment of the residual strength of concrete structures after fire exposure." *Ph.D. thesis, Ghent University, 2010.*

Archer R.R. and Lardner T. J. "An introduction to the mechanics of solids." *Auckland: Mc Graw-Hill, 1978.*

Ayyub B. M., Mc Cuen R. H. "Probability, statistics, and reliability for engineers and scientists." *2nd Ed., Chapman Hall/CRC, Boca Raton, Fla, 2003.*

Bailey C. G. "Holistic behaviour of concrete buildings in fire." *Structures and Buildings*, 152(3): 199–212, 2002.

Bamonte P., Meda A. "Towards a simplified approach for the sectional analysis of R/C members in fire." *Proceedings of the 2nd International Congress Keep Concrete Attractive, Naples, Italy*, June 5–8, 2005.

Bazant Z. P., Chern J. C. "Stress-induced thermal and shrinkage strains in concrete." *Journal of Engineering Mechanics*, 113(10):1493-1511, 1987.

BBK 94, Boverkets handbok om betongkonstruktioner, BBK 94, Band 1, Konstruktion., *Boverket, Stockholm*, 185 pp, 1995.

Becque J., and Rasmussen K.J.R. "Experimental investigation of the interaction of local and overall buckling of stainless steel I-columns,." *Research Report No R887, School of Civil Engineering, University of Sydney*, 2007.

Benmarce A., Guenfoud M. "Experimental behaviour of high-strength concrete columns in fire." *Mag.Concr.Res.* 57(5):283–287, 2005.

Bisby L. A., Gales J., Maluk C. "A contemporary review of large-scale non-standard structural fire testing." *Fire Science Reviews*, 2(1), 2013.

Bresler B. "Design criteria for reinforced columns under axial load and biaxial bending." *ACI Journal Proceedings*, 57(11):481-490, 1960.

Bousias S. N., Verzelletti G., Fardis M. N. and Magonette G. "RC columns in cyclic biaxial bending and axial load." *10th World Conference on Earthquake Engineering, Madrid*, 3041-3046, 1992.

CEB/FIP Bulletin 123. "Manual of buckling." December 1977.

CEB/FIP Bulletin 239. "Non-linear analysis." May 1997.

Caldas R. B., Sousa Jr. J. B. M., Fakurya R. H. "Interaction diagrams for reinforced 36 concrete sections subjected to fire." *Eng. Struct.*, 32(9):2832–2838, 2010.

Cedolin L., Cusatis G., Eccheli S. & Roveda M. "Capacity of rectangular cross sections under biaxially eccentric loads." *ACI Structural Journal*, 2008, 105(2), 215–224.

CEN. "EN 1992-1-1: Design of concrete structures - Part 1-1: General rules and rules for buildings.", *European Committee for Standardization, Brussels, Belgium*, 2004.

CEN. "EN 1992-1-2: Design of concrete structures - Part 1-2: General rules - Structural fire design.", *European Committee for Standardization, Brussels, Belgium*, 2004.

CEN. "EN 1994-1-2: Design of composite steel and concrete structures - Part 1-2: General rules - Structural fire design.", *European Committee for Standardization, Brussels, Belgium*, 2005.

Cheng F, Kodur V. K. R. & Wang T. "Stress-Strain curves for high strength concrete at elevated temperatures." *Journal of Materials in Civil Engineering*, January/ February 2004.

Chudyba K., Seręga S. "Structural fire design methods for reinforced concrete members." *Technical Transactions, iss. 6. Civil Engineering, iss. 1-CE, s. 15-36*, 2013.

Claeson C. "Structural behaviour of reinforced high strength concrete columns." *Chalmers Technical University, Sweden*, 1998.

Chen W. F., Shoraka M. T. "Tangent stiffness method for biaxial bending of reinforced concrete columns." *Fritz Engineering Laboratory Report No. 389.1, Lehigh University, Bethlehem, Pa.*, October 1972.

Cooke G. M. E. "An introduction to the mechanical properties of structural steel at elevated temperatures." *Fire Safety Journal*, 13:45-54, 1988.

Crook R. N. "The elevated temperature properties of reinforced concrete." *Ph. D. Thesis, University of Aston*, 1980.

Cyllok M., Achenbach M. "Anwendung der Zonenmethode für brandbeanspruchte Stahlbetonstützen." *Beton- und Stahlbetonbau 104*, pp. 813-822, 2009.

Dimia M. S., Guenfoud M., Gernay T., Franssen J. M. "Collapse of concrete columns during and after the cooling phase of a fire." *Journal of Fire Protection Engineering*, 21(4):245-263, 2011.

Dotreppe J. C., Franssen J. M., Bruls A., Baus R., Vandeveldel P., Minne R., Van Nieuwenburg D., Lambotte H. "Experimental research on the determination of the main parameters affecting the behavior of reinforced concrete columns under fire conditions." *Magazine of concrete research 49*, pp. 117- 127, 1996.

Dotreppe J.C, Franssen J.M. "Dimensionnement des colonnes en béton armé en considérant le problème de la résistance au feu", *External Report*, 1993.

Dotreppe J. C., Franssen J. M., Vanderzeypen Y. "Calculation method for design of reinforced concrete columns under fire conditions.", *ACI Structural Journal*, 96(1), 9-18, 1999.

Drysdale D. "An introduction to fire dynamics.", *Wiley Press*, 1999.

Elghazouli A. Y., Cashell K. A., Izzudin B. A. "Experimental evaluation of the mechanical properties of steel reinforcement at elevated temperature." *Fire Safety Journal*, 44:909-919, 2009.

Eurocode 2 – Commentary – *European Concrete Platform ASBL*, June 2008.

Fédération International du Béton (fib). Model code for concrete structures 2010, *Ernst & Sohn*, Berlin, 2013.

fib Bulletin 16. Design examples for the FIP recommendations "Practical design of structural concrete." *fib*, Lausanne, January 2002.

fib Bulletins No. 38: "Fire design of concrete structures – materials, structures and modeling", *State-of-art Report*, 2007.

fib Bulletins No. 46: "Fire design of concrete structures - structural behaviour and assessment", *State-of-art Report*, 2008.

fib Model Code for Concrete Structures 2010, Ernst & Sohn, 2013.

Franssen J. M., Dotreppe J. C. "Fire tests and calculation methods for circular concrete columns." *Fire Technology*, 39:89-97, 2003.

Gernay T., Dimia M. S. "Structural behavior of concrete columns under natural fires including cooling down phase." *Proceedings of The International Conference on Recent Advances in Nonlinear Models-Structural Concrete Applications. RAGRAF*, 2011.

Gernay T., Franssen J. M. "Consideration of Transient Creep in the Eurocode Constitutive Model for Concrete in the Fire situation." *Proceedings of the Sixth International Conference Structures in Fire*, pp. 784-791, 2010.

Harmathy T. Z. "Thermal properties of concrete at elevated temperatures." *ASTM Journal of Materials*, vol. 5, no. 1, pp. 47-74, 1970.

Haß R., Klingsch W., "Parameterunteruntersuchungen zum Brandverhalten von Stahlbetonstützen – Versuche und theoretische Begleitung." *In Sonderforschungsbereich 148 - Brandverhalten von Bauteilen – Arbeitsbericht 1978-1980, Teil I. Technische Universität Braunschweig*, pp. 91-111, 1980.

Haß R. "Zur praxisgerechten brandschutztechnischen Beurteilung von Stützen aus Stahl und Beton." *Ph.D. Thesis, Technische Universität Braunschweig*, 1986.

Hertz K. "Design of fire exposed concrete structures." Report 160, *Technical University of Denmark, Institute of Building Design, Lyngby*, 1981.

Karlsson B., Quintiere J. "Enclosure fire dynamics." *CRC Press*, 1999.

Karmazinova M., Melcher J. "Initial imperfections of steel and steel-concrete circular columns." *Recent Advances in Continuum Mechanics, Hydrology and Ecology*, 2013, 36-41.

Khoury G. A., Grainger B. N., Sullivan P. J. E. "Strain of concrete during first heating to 600°C under load." *Mag Concrete Res* 37(133):195-215, 1985.

Klingsch W, Haksever A, Walter R. "Brandversuche an Stahlbetonstützen, Versuchsergebnisse und Numerische Analyse." Sonderforschungsbereich 148, *Brandverhalten von Bauteilen, Arbeitsbericht, 1975-1977, teil I, T.U. Braunschweig*, July 1977.

Kodur V. K. R. "Fire resistance design guidelines for high strength concrete columns." *National Research Council of Canada, Institute for Research in Construction, NRCC 46116, Ottawa, Ont, Canada*, pp. 11, 2003.

Kodur V. K. R., Franssen J.M. "Structures in Fire." *Proceedings of the Sixth International Conference, Lancaster, Pennsylvania*, 2010.

Kodur V. K. R., Phan L. "Critical factors governing the fire performance of high strength concrete systems." *Fire Safety Journal*, 42, 482-488, 2007.

Kodur V. K. R. "Properties of concrete at elevated temperatures." *ISRN Civil Engineering*, 2014.

Kodur V. K. R., Raut N. "A simplified approach for predicting fire resistance of reinforced concrete columns under biaxial bending." *Eng Struct*, 41, 428-443, 2012.

Kodur V. K. R., Sultan M. A. "Effect of temperature on thermal properties of high-strength concrete." *Journal of Materials in Civil Engineering*, vol. 15, no. 2, pp. 101-107, 2003.

Kowalski R., Urbański M. "Redistribution of bending moments in multi – span R/C beams and slabs subjected to fire." *Technical Transactions, Civil Engineering Issue 1-B (6)* 2013, 115-138.

Lie T. T., Celikkol B. "Method to calculate the fire resistance of circular reinforced concrete columns." *ACI Materials Journal*, 88(1), 84-91, 1991.

Lie T. T. "Fire and Buildings." *Applied Science Publishers Ltd., London*, 1972.

Lie T. T., Irwin R. J. "Method to calculate the fire resistance of reinforced concrete columns with rectangular cross section.", *ACI Structural Journal*, 90(1), 52-60, 1993.

Lie T. T., Kodur V. K. R. "Fire resistance of steel columns filled with bar-reinforced concrete". *Journal of Structural Engineering*, 1996, 122(1), 30-36.

Lie T. T., Kodur V. K. R. "Thermal properties of fibre reinforced concrete at elevated temperatures." IR 683, IRC, *National Research Council of Canada, Ottawa, Canada*, 1995.

Lie T. T., Kodur V. K. R. "Thermal and mechanical properties of steel-fibre-reinforced concrete at elevated temperatures." *Canadian Journal of Civil Engineering*, vol. 23, no. 2, pp. 511–517, 1996.

Lie T. T., Lin T. D., Allen D. E and Abrams M. S. "Fire resistance of reinforced concrete columns", Division of Building Research, DBR Paper No. 1167, National Research Council of Canada, Ottawa, Canada, February, 1984.

Lie T. T., Rowe T. J. & Lin T. D. "Residual strength of fire-exposed reinforced concrete columns." *ACI Publication SP 92-9*, pp. 153–174, 1986.

Lie T. T. "Structural fire protection: manual of practice." *ASCE manual and reports on Engineering Practice*, No. 78, pp. 241, *American Society of Civil Engineers, New York, NY. Editor*, 1993.

Li L., Purkiss J. A. "Stress–strain constitutive equations of concrete material at elevated temperatures." *Fire Safety Journal*, 40:669–86, 2005.

Li W., Guo Z. H. "Experimental investigation of strength and deformation of concrete at elevated temperature." *Journal of Building Structures*, 14(1):8-16, 1993.

Lin C. H., Chen S. T. & Yang C. A. Repair of fire damaged reinforced concrete columns. *ACI Structure* 92(4): 406–411, 1995.

Lu L. "Numerical analysis of the influence of end restraints on the fire resistance of continuous reinforced concrete beams and slabs." *Ph.D. thesis, Ghent University*, 2015.

Malhotra H. L. "Effect of temperature on the compressive strength of concrete." *Magazine of concrete research*, 8:85-94, 1956.

Marí A., Hellesland J. “When can second-order effects in columns be neglected?” *Research Rep. No. 2003-01, Dept. of Construction Engineering, Univ. Politècnica de Catalunya, Barcelona, Spain, 2003.*

Meda A., Gambarova P.G. “Bonomi M., High-performance concrete in fire-exposed reinforced concrete sections.” *ACI Structural Journal*, 99 (3), May-June 2002.

NEN, "NEN 6720 Technische Grondslagen voor Bouwvoorschriften, Voorschriften Beton TGB 1990 – Constructieve Eisen en Rekenmethoden (VBC 1995)," *Civieltechnisch centrum uitvoering research en regelgeving, Nederlands Normalisatie-instituut, ; Delft, The Netherlands, 1995.*

Ngo T., Fragomeni S., Mendis P. and Ta T. B. “Testing of Normal- and High-Strength Concrete Walls Subjected to Both Standard and Hydrocarbon Fires.” *Structural Journal*, 110(3):503-510, 2013.

Nguyen T. T., Tan K. H. “Thermal-induced restraint forces in reinforced concrete columns subjected to eccentric loads.” *Fire Safety Journal*, 69: 136-146, 2014.

Parme A, Nieves J, Gouwens A. “Capacity of reinforced rectangular columns subject to biaxial bending.” *ACI Journal Proceedings*, 63(9):911-924, 1966.

Purkiss J. A. “Fire Safety Engineering Design of Structures”. *Butterworth-Heinemann, Elsevier, Oxford, UK, 2007.*

Raut N., Kodur V. K. R. “ Response of reinforced concrete columns under fire-induced biaxial bending.” *ACI Structural Journal*, 108(5): 610-619, 2011.

Robinson J. , Fouré F. , and Bourghli M. “Le flambement des poteaux en béton armé chargés avec des excentricités différentes à leurs extrémités.” *Annales I.T.B.T.P.*, 333, 46–74, 1975.

Sadaoui A., Illouli S. and Khennane A. “Effect of restraints on the response of RC columns in a parametric fire.” *Proceedings of FraMCoS-8*, 2013.

Schillinger D., Papadopoulos V., Bischoff M., Papadrakakis M. "Buckling analysis of imperfect I-section beam-columns with stochastic shell finite elements." *Comput Mech.*, 2010, 46, 495–510.

Schneider U. "Verhalten von Beton bei hohen Temperaturen (Behaviour of Concrete at High Temperatures)." Heft 337 des Deutscher Ausschuss für Stahlbeton, Berlin, 1982.

Schneider U. "Properties of materials at high temperatures concrete. *RILEM committee 44 PHT, University of Kassel, Kassel*, June 1985.

Serega S. "A new simplified method for determining fire resistance of reinforced concrete sections." *Proceedings of 6th International Conference Analytical Models and New Concepts in Concrete and Masonry Structures*, 2008.

Tan K. H., Nguyen T. T. "Experimental behaviour of restrained reinforced concrete columns subjected to equal biaxial bending at elevated temperatures." *Engineering Structures*, 56: 823-836, 2013.

Tan K. H., Nguyen T. T. "Structural responses of reinforced concrete columns subjected to uniaxial bending and restraint at elevated temperatures." *Fire Safety Journal*, 60:1-13, 2013.

Ta T. B. "Performance of high strength concrete walls subjected to fire." *Ph.D. thesis*. 2009.

Ta T. B., Ngo T., Mendis P. and Haritos N. "Performance of high strength concrete walls subjected to fire." *Incorporating Sustainable Practice in Mechanics and Structures of Materials*, 513-518, 2011.

Terro M. J. Numerical modeling of the behavior of concrete structures in fire. *ACI Structure Journal*, 95(2):183–93, 1998.

Tomasson B. "High Performance Concrete Design Guide Lines", *Report 5008, Lund, Sweden*, 1998.

Topcu I. B. and Karakurt C. "Properties of reinforced concrete steel rebars exposed to high temperatures." *Research Letters in Materials Science*, 2008.

Van Coile R., Annerel E., Caspee R., Taerwe L. "Full-Probabilistic analysis of concrete beams during fire." *Journal of Structural Fire Engineering*, 165-174, 2013.

Van Coile R., Caspee R., Taerwe L. "Lifetime cost optimization for the structural fire resistance of concrete slabs." *Fire Technology*, June 2013.

Van Coile R. "Reliability-based decision making for concrete elements exposed to fire." *Ph.D. dissertation*, Ghent University, 2015.

Wang L., Caspee R. and Taerwe L. "Development of an Excel-based calculation tool for interaction curves of rectangular concrete columns subjected to fire." *IRF'2013. 4th International Conference on integrity, reliability & failure*. 2013, 49-50.

Wang L., Caspee R. and Taerwe L. "Effect of imperfections on concrete columns subjected to fire taking into account second-order effects." *fib symposium : Concrete - Innovation and Design Proceedings*. 2014, 1-7.

Wang L., Caspee R. and Taerwe L. "Study on the fire resistance of rectangular concrete columns exposed to natural fires." *8th International Conference on Structures in Fire Proceedings*. 2014, 363-370.

Wang L., Caspee R., Van Coile R. & Taerwe L. "Extension of tabulated design parameters for rectangular columns exposed to fire taking into account second-order effects and various fire models." *Structural Concrete*, 16(1), 17-35, 2015.

Westerberg B. "Beräkning av betongpelare med datamaskin (Computerized calculation of concrete columns)." *Nordisk Betong (Journal of the Nordic Concrete Federation)*, 1971:4.

Woolman J., Mottram R. A. The mechanical and physical properties of the British standard En steels (BS 970-1955), Vol. 1, En 1 to En 20, *British Iron and Steel Research Association by the Macmillan Company, New York*, 1964.

Wu B., Li Y. H. "Experimental study on fire performance of axially-restrained NSC and HSC columns." *Struct.Eng.Mech.* 32(5):635-648, 2009.

Youssef M. A., Mofteh M. "General stress–strain relationship for concrete at elevated temperatures." *Engineering Structures*, 29:2618-2634, 2007.

Zehfuss J., Hosser D. "A parametric natural fire model for the structural fire design of multi-storey buildings." *Fire Safety Journal*, 2007, 42, 115–126.

Zilch K., Müller A. "Reitmayer, C. Erweiterte Zonenmethode zur brandschutztechnischen Bemessung von Stahlbetonstützen." *Bauingenieur* 85, pp. 282-287, 2010.

LIST OF PUBLICATIONS

List of journal papers

Wang L., Van Coile R., Caspee R., Taerwe L. “Simplified method for evaluating the biaxial capacity of rectangular reinforced concrete columns during fire.” *Materials and Structures*. 50:37, 2017.

Wang L., Caspee R., Van Coile R., Taerwe L. “Extension of tabulated design parameters for rectangular columns exposed to fire taking into account second-order effects and various fire models.” *Structural Concrete*. 16(1): 17-35, 2015.

List of conference papers

Wang L., Van Coile R., Caspee R., Taerwe L. “A parametric study on concrete columns exposed to biaxial bending at elevated temperatures using a probabilistic analysis.” *fib symposium : High tech concrete- where technology and engineering meet*. Maastricht, The Netherlands. p.1-7, 2017 (in press).

Van Coile R., Balomenos G., Pandey M., Caspee R., Criel P., Wang L. and Alfred S. “Computationally efficient estimation of the probability density function for the load bearing capacity of concrete columns exposed to fire.” *Proceedings of the 2016 International Symposium of the International Association for Life-Cycle Civil Engineering*. Delft, The Netherlands. p.1-8, 2016.

Wang L., Van Coile R., Caspee R., Taerwe L. “A probabilistic study on concrete columns exposed to biaxial bending at elevated temperatures.” *9th International Conference on Structures in Fire*, Princeton, USA. p.942-948, 2016.

Wang L., Caspee R., Taerwe L. “A parametric study on buckling of R/C columns exposed to fire.” *Applications of Structural Fire Engineering*, Dubrovnik, Croatia. p.190-195, 2015.

Wang L., Caspee R., Taerwe L. “Effect of imperfections on concrete columns subjected to fire taking into account second-order effects.” *fib symposium : Concrete - Innovation and Design, Proceedings*. Copenhagen, Denmark. p.1-7, 2015.

Wang L., Caspee R., Taerwe L. “A parametric study on the applicability of the 500 °C isotherm method for investigating interaction curves of columns exposed to fire.” *IFireSS – International Fire Safety Symposium*. Coimbra, Portugal. p.195-202, 2015.

Wang L., Caspee R., Taerwe L. "Study on the fire resistance of rectangular concrete columns exposed to natural fires." *8th International Conference on Structures in Fire, Proceedings*. Shanghai, China. p.363-37, 2014.

Wang L., Caspee R., Taerwe L. "Development of an excel-based calculation tool for interaction curves of rectangular concrete columns subjected to fire." *Recent advances in integrity-reliability-failure, Proceedings*. Funchal, Portugal p.1-7, 2013.

